

Flow Analysis of Compound Channels With Wide Flood Plains



Prabir Kumar Mohanty

Flow Analysis of Compound Channels with Wide Flood Plains

*Thesis Submitted to the
Department of Civil Engineering
National Institute of Technology, Rourkela*

for award of the degree

*of
Doctor of Philosophy*

by

Prabir Kumar Mohanty



**Department of Civil Engineering
National Institute of Technology Rourkela
Orissa (India)-769008
December 2013**

DEDICATED TO
MY FAMILY

Certificate

*This is to certify that the thesis entitled “**Flow Analysis of Compound Channels with Wide Flood Plains**” being submitted by Shri Prabir Kumar Mohanty, is a bonafide research carried out by him at Civil Engineering Department, National Institute of Technology, Rourkela, India, under my guidance and supervision. The work incorporated in this thesis has not been, to the best of my knowledge, submitted to any other University or Institute for the award of any degree or diploma.*

Dr. K.K. Khatua
(Thesis Supervisor)

Place: Rourkela

Date:

Declaration

I hereby declare that this submission is my own work and that, to the best of my knowledge and belief, it contains no material previously published or written by another person nor material which to a substantial extent has been accepted for the award of any other degree or diploma of any university or other institute of higher learning, except where due acknowledgement has been made in the text.

(P.K. MOHANTY)

Place: Rourkela

Date:

ACKNOWLEDGEMENT

As I am about to submit this dissertation for the award of Ph.D. degree, I must acknowledge that this has been the most venturesome odyssey of whole of my personal, professional and academic life till date. In the process many hurdles and challenges of monstrous proportion came crashing upon me which nearly derailed my journey. However my unflinching faith in Almighty somehow saw me through those difficult times and safely guided me to my destination.

Oh! Lord, Sri JAGANNATH! Glory to You! You are the ultimate savior! May your blessings always protect us!

Many people and organisations have contributed directly or indirectly in the success of this research programme and it is my earnest duty to express my heartfelt thanks and gratitude to all of them.

At the outset, I must put on record my most sincere gratitude to Hon'ble High Court of Odisha, for adjudicating in my favour, the grant of a study leave which enabled me to embark upon this ambitious voyage. A big thank to National Institute of Technology, Rourkela for selecting me as a research scholar and giving me an opportunity to pursue my academic dream. Govt. of India and Govt. of Odisha are also acknowledged; the former for funding the DST research project wherein I got the opportunity to carry out my research and the latter for relieving me of my regular assignment to pursue the Ph.D. programme in NIT, Rourkela.

My sincere gratitude to Prof. K.K. Khatua, Associate Professor in the department of Civil Engineering of NIT, Rourkela for accepting me as a research scholar and guiding me throughout this research. He has been extremely cooperative, patient and helpful right from the date of submitting the application for Ph.D. programme to NIT, Rourkela till its completion. I fondly cherish all those intense moments which we together had to spend during the course of this research work.

My indebtedness is also due to Prof. Sunil Kumar Sarangi, Director, NIT, Rourkela for extending all sorts of administrative support to my research programme. I am obliged to all the senior faculty members of the Doctoral Scrutiny Committee headed by Prof. N. Roy, Professor and Head of Civil Engg. Department, NIT, RKL for offering constructive criticism for the improvement of my research work. It has been really an

enriching experience to interact with such academic luminaries! My special thanks are also to Prof. K.C. Patra, Prof. M. Panda, Prof. S.P. Singh, Prof. R.K. Jha, Prof. K.C. Biswal and all other faculties and staff of Civil Engg. department for extending all warmth and cooperation during the last four long years. My sincere gratitude goes to the scientists of the 'National Centre for Computational Hydroscience and Engineering', University of Mississippi, USA for providing me technical support in carrying out the simulation studies through the open hydrodynamic software package 'CCHE2D'.

Success of any research project banking heavily upon experimental works is only due to the team of expert manpower assigned to the laboratories. Mr. Kulamani Patra, Senior technical assistant; Mr. Pitambar Rout, ex-laboratory assistant of Hydraulics and Fluid mechanics laboratory and Mr. Harihar Garnayak of Civil Engg. Department are appreciated for their skillful handling of fabrication of all flumes, channels, water tanks, pumps etc. and for ensuring uninterrupted experimentation for this Ph.D. programme. Raja and Upendra, two lab boys have also helped a lot in my experimental assignments. Nimain babu, the caretaker of the hostel I lived in was immensely helpful in making my stay a really comfortable one.

All of my colleagues in the Hydraulics and Fluid Mechanics laboratory and outside have been especially cordial and cooperative with me and I have enjoyed every moment in their company. Mrityunjay, Nirjharini, Sridevi, Saine, Bandita, Janaki, Laxmipriya and Manaswinee and many others of Water resources engineering group and Dr. Ravi Behera from Geotechnical engineering section have helped me a lot and it is only through their unwavering support, I could be able to surmount all challenges in my research work. I thank all of them and wish them all success in life. The list cannot be complete without the mention of two of my colleagues cum friends from my parent organization who also joined NIT, Rourkela for pursuing their Ph.D. course. Mr. P.K. Muduli and Mr. S.K. Nayak are credited for giving me true company in the aftermath of excruciating times spent in the laboratory and in the department. They have been a great source of sustenance during my stay in NIT hostel!

Mr. Mahali (Tulu) has been a dear friend whom I am especially indebted to for providing me all external logistics during the whole of my Ph.D. course. A lot of credit for realization of this dream goes to him for giving me true company in hours of discomfort. Mr. J.N. Dash, Senior Lecturer, Architecture, Government Polytechnic, Bhubaneswar has really helped a lot in creating some drawings through AutoCAD.

Miss Barsha of NIT, Rourkela is also acknowledged for her genuine cooperation in preparation of some other drawings. Many other friends and colleagues are also appreciated for their timely help and encouragement.

My heartfelt gratitude goes out to my revered parents and my in-laws for their blessings and support without which this endeavor would not have borne fruit. Last but not the least, I cannot but help appreciating my lovely wife for taking in her stride the long absence of her husband and for looking after really well our two sons; Abhishek and Tejas and her in-laws during such trying circumstances. My most sincere and affectionate thanks are to my two doting sons who maturely and patiently bore with my long spells of separation during these long four years. I really owe a lot to my whole family for all the sacrifices they have made in providing me enough of time and space to meet the rigours of an intense research work as required in any Ph.D. program!

Prabir Kumar Mohanty

ABSTRACT

This Ph.D. research analyses the flow in straight and meandering compound channels having wide floodplains of large width ratio of value of nearly 12 and main channel aspect ratio of more than 5, which is very significant in the field of river hydraulics. Experiments were conducted in the Fluid Mechanics and Hydraulics laboratory of National Institute of Technology, Rourkela, India by casting smooth and rigid, straight and meandering compound channels inside a tilting flume. The research investigates the distribution of longitudinal velocity; depth averaged velocity for inbank and overbank flow cases in both straight and meandering compound channels. The measurement of the boundary shear stress for those flow conditions was done by Preston tube technique.

As a complementary study to the experimental research undertaken in this work, two numerical hydrodynamic tools viz. Conveyance Estimation System (CES) developed by HR Wallingford, UK and CCHE2D developed by NCCHE, University of Mississippi, US are applied to simulate the overbank flow cases for both straight and meandering compound channels, for large scale EPSRC-FCF experiments and for a natural river. All the important flow parameters are also extracted numerically from the simulation results to study them vis a vis their observed values.

From the study of isovels for straight and meandering compound channels, velocity distribution coefficients are measured and new models are suggested for energy coefficient and momentum coefficient values in straight compound channels and meandering compound channels by validating the developed models with present data and data sets from previous research projects. Integrating the distribution of boundary shear stress over different zones of compound section of straight channel and analyzing them with several data sets of other researchers, new models for subsection shear force are suggested in case of straight compound channels. Using these models, the stage–discharge relations in case of straight compound channels having different width ratios are then developed. These developed models are validated with new experimental data as well as data sets of large scale experimental facility of FCF (Series A), UK; small scale data sets from flume experiments of other past researchers and with some field data of real river flood cases. The flow distribution in straight compound channel is also modeled and validated with data sets from different past studies.

A large number of boundary shear data points are generated for meandering compound channels reported with only stage discharge data in literature by application of numerical tools. The measured boundary shear data of the present meandering compound channel is then analysed with the newly generated boundary shear data sets of other researchers to develop models for subsection shear force in case of meandering compound channels having large width ratio. Finally a new stage-discharge model is suggested for use in case of overbank flow in meandering compound channels under different hydraulic and geometric conditions. The suggested model is also validated with the present data set, data sets from large scale flume experiments for meandering compound channels of FCF (Phase B) & of US Army, Vicksburg, Mississippi, US (1956), data sets from small scale flume experiments of other authors and for a flooded river in meandering reach.

Key Words: Compound channels, Straight, Meandering, Depth averaged velocity, Boundary Shear, CES and CCHE2D.

CONTENTS

LIST OF FIGURES	XII
LIST OF TABLES	XIX
SYMBOLS	XX
ABBREVIATIONS	XXIII
CHAPTER 1 INTRODUCTION	1
1.1 BACKGROUND	1
1.2 AIMS AND OBJECTIVES	5
1.3 ORGANAISATION OF THE THESIS	6
CHAPTER 2 LITERATURE REVIEW	8
2.1 GENERAL	8
2.2 SIMPLE MEANDERING CHANNELS	9
2.3 STRAIGHT COMPOUND CHANNELS	12
2.4 MEANDERING COMPOUND CHANNELS	19
CHAPTER 3 EXPERIMENTAL SETUP AND PROCEDURE	26
3.1 PLAN OF EXPERIMENTAL SETUP	26
3.1.1. Fabrication of Flumes and Accessories	26
3.1.2. Fabrication of Channels	34
3.2 EXPERIMENTAL PROCEDURE	38
3.2.1. Determination of Bed Slope (S)	38
3.2.2. Establishment of Quasi-uniform Flow	39
3.2.3. Measurement of discharge & longitudinal velocity	41
3.2.4. Measurement of Depth averaged velocity	42
3.2.5. Measurement of Boundary Shear	45
CHAPTER 4 EXPERIMENTAL RESULTS	47
4.1 GENERAL	47
4.2 STRAIGHT CHANNEL	47
4.2.1. Stage –discharge curve	47

4.2.2.	Longitudinal velocity	48
4.2.3.	Depth averaged velocity	53
4.2.4.	Boundary Shear stress	56
4.2.4.1.	Inbank cases	56
4.2.4.2.	Overbank cases	58
4.3	MEANDERING CHANNEL	65
4.3.1.	Stage-discharge curve	65
4.3.2.	Longitudinal velocity	66
4.3.3.	Depth averaged velocity	71
4.3.4.	Boundary Shear stress	74
4.3.4.1.	Inbank cases	74
4.3.4.2.	Overbank cases	75
CHAPTER 5	APPLICATION OF NUMERIAL TOOLS	85
5.1	INTRODUCTION	85
5.2	CONVEYANCE ESTIMATION SYSTEM	86
5.2.1.	Development of the model for CES	88
5.2.1.1.	Method description of RANS approach	89
5.2.1.2.	Outline of Steps for Modeling through CES	94
5.3	CCHE2D MODEL	96
5.3.1.	Governing Equations	96
5.3.2.	Turbulence Closure	97
5.3.2.1.	Eddy Viscosity Model	97
5.3.2.2.	Two-dimensional k- ϵ Model	98
5.3.3.	General Procedure	98
5.3.3.1.	Mesh Generation	99
5.3.3.2.	Specification of boundary condition	99
5.3.3.3.	Parameters setting	100
5.3.3.4.	Simulation	100
5.3.3.5.	Results visualization and interpretation	100
5.3.4.	Channel Simulation Results	101
5.3.4.1.	Depth averaged velocity results	110
5.3.4.2.	Boundary shear stress results	113

CHAPTER 6 ANALYSIS AND DISCUSSION	120
6.1 GENERAL	120
6.2 VELOCITY DISTRIBUTION COEFFICIENTS	120
6.2.1. Estimation of α & β	122
6.2.2. Model development for velocity distribution coefficients (α & β) in straight compound channel	124
6.2.3. Model development for velocity distribution coefficients (α & β) in meandering compound channel	127
6.2.4. Discussion	129
6.3 DEVELOPMENT OF STAGE-DISCHARGE MODELS STRAIGHT COMPOUND CHANNEL)	130
6.3.1 DEVELOPMENT OF METHOD (for α upto 6.67)	130
6.3.3.1. The methodology	131
6.3.1.2. The boundary shear model (α upto 6.67)	133
6.3.1.3. Stage- Discharge Results	137
6.3.1.4. Practical Application of the MDCM	138
6.3.1.5. Discussion on MDCM	140
6.3.2. Extended MDCM (EMDCM for $6.67 < \alpha < 12$)	140
6.3.2.1. The methodology	140
6.3.2.2. Development of boundary shear model (for $6.67 < \alpha < 12$)	140
6.3.2.3. Results and Discussion	143
6.3.2.4. Practical Application of EMDCM	144
6.3.3. DEVELOPMENT OF METHOD (For all ranges of α values)	145
6.3.3.1. Background	145
6.3.3.2. The methodology	146
6.3.3.3. Results and Discussion	147
6.4 DEVELOPMENT OF STAGE-DISCHARGE MODELS (MEANDERING COMPOUND CHANNEL)	164
6.4.1. Background	164
6.4.2. Methodology	167
6.4.3. The new boundary shear models	168
6.4.4. Results and Discussion	170

CHAPTER 7 CONCLUSIONS AND SCOPE FOR FUTURE WORK	177
7.1 CONCLUSIONS	177
7.2 SCOPE FOR FUTURE RESEARCH WORK	180
 REFERENCES	 181
APPENDIX	192
PUBLICATIONS BASED ON PRESENT RESEARCH WORK	197
BRIEF BIO-DATA OF THE AUTHOR	199

LIST OF FIGURES

Fig. 1-1	Moscow - Looking over Moskva River to the Cathedral of Christ, the Savior.	2
Fig. 1-2	The flooded River, Yamuna flowing above the danger level in New Delhi	3
Fig. 3-1	Stilling Chamber, Flow Straightener & Point Gauge In U/S Section of Flume	27
Fig. 3-2	Photo of Flume with Straight Compound Channel (Looking U/S)	28
Fig. 3-3	Photo of Straight Channel (Looking From Side)	28
Fig. 3-4	Series of Micro-Pitot Tubes Fitted to the Holder	29
Fig. 3-5	Photo of Straight Channel with Movable Bridge	29
Fig. 3-6	Downstream Volumetric Tank	30
Fig. 3-7	Series of Manometers, Spirit Level & Stop Watch Hung Outside the Flume	30
Fig. 3-8	Overbank Flow Measurement in Straight Channel (Looking From Top)	31
Fig. 3-9	Fabrication of Meandering Compound Channel in Progress	31
Fig. 3-10	Photograph of Bell mouthed Entrance	32
Fig. 3-11	Flooded Meandering Compound Channel	32
Fig. 3-12	Photo of Test Reach at the Third Bend Apex of Meandering Compound Channel	33
Fig. 3-13	Photo of Overbank Flow Experiment in Meandering Compound Channel	33
Fig. 3-14	Experimental Setup of Straight Compound Channel	35
Fig. 3-15	Plan view of Straight Channel (Top) & Flow Section (Side)	35
Fig. 3-16	Experimental Setup of Meandering Compound Channel	36
Fig. 3-17	Plan view of Meandering Channel (Top) & Flow Section (Side)	36
Fig. 3-18	Cross Section of Main Channel	37
Fig. 3-19	Cross Section of Straight Compound Section at Test Reach	37
Fig. 3-20	Cross Section of Compound Meandering Section at Test Reach	37

Fig. 3-21	Geometrical Details of the Sine Generated Curve Used in Meandering Channel	38
Fig. 3-22	Grid Points for Measurement of Boundary Shear & Velocity in Straight Compound Channel	39
Fig. 3-23	Grid Points for Measurement of Boundary Shear & Velocity in Compound Meandering Channel	39
Fig. 3-24	Velocity Profile & Depth Averaged Velocity in Channel	45
Fig. 4-1	Stage-Discharge curve for straight compound channel of NIT, Rourkela	48
Fig. 4-2(a)	Isovels for inbank flow in straight compound channel	49
Fig. 4-2(b)	Isovels for inbank flow in straight compound channel	49
Fig. 4-2(c)	Isovels for inbank flow in straight compound channel	50
Fig. 4-2(d)	Isovels for inbank flow in straight compound channel	50
Fig. 4-2(e)	Isovels for inbank flow in straight compound channel	51
Fig. 4-3(a)	Isovels for overbank flow in straight compound channel	51
Fig. 4-3(b)	Isovels for overbank flow in straight compound channel	52
Fig. 4-3(c)	Isovels for overbank flow in straight compound channel	52
Fig. 4-3(d)	Isovels for overbank flow in straight compound channel	52
Fig. 4-3(e)	Isovels for overbank flow in straight compound channel	53
Fig. 4-3(f)	Isovels for overbank flow in straight compound channel	53
Fig. 4-4(a-e)	Depth averaged velocity distribution in straight compound channel-inbank flow	54
Fig. 4-5(a-f)	Depth averaged velocity distribution in straight compound channel-overbank flow	55
Fig. 4-6(a)	Shear stress distribution for inbank flow in straight channel	56
Fig. 4-6(b)	Shear stress distribution for inbank flow in straight channel	56
Fig. 4-6(c)	Shear stress distribution for inbank flow in straight channel	57
Fig. 4-6(d)	Shear stress distribution for inbank flow in straight channel	57
Fig. 4-6(e)	Shear stress distribution for inbank flow in straight channel	57
Fig. 4-7(a)	Shear stress distribution for overbank flow in straight channel	59
Fig. 4-7(b)	Shear stress distribution for overbank flow in straight channel	60
Fig. 4-7(c)	Shear stress distribution for overbank flow in straight channel	61
Fig. 4-7(d)	Shear stress distribution for overbank flow in straight channel	62
Fig. 4-7(e)	Shear stress distribution for overbank flow in straight channel	63

Fig. 4-7(f)	Shear stress distribution for overbank flow in straight channel	64
Fig. 4-8	Stage-Discharge curve for meandering compound channel of NIT, Rourkela	65
Fig. 4-9(a)	Isovels for inbank flow in meandering channel	66
Fig. 4-9(b)	Isovels for inbank flow in meandering channel	66
Fig. 4-9(c)	Isovels for inbank flow in meandering channel	67
Fig. 4-9(d)	Isovels for inbank flow in meandering channel	67
Fig. 4-9(e)	Isovels for inbank flow in meandering channel	68
Fig. 4-9(f)	Isovels for inbank flow in meandering channel	68
Fig. 4-9(g)	Isovels for inbank flow in meandering channel	68
Fig. 4-9(h)	Isovels for inbank flow in meandering channel	69
Fig. 4-10(a)	Isovels for overbank flow in meandering channel	70
Fig. 4-10(b)	Isovels for overbank flow in meandering channel	70
Fig. 4-10(c)	Isovels for overbank flow in meandering channel	70
Fig. 4-10(d)	Isovels for overbank flow in meandering channel	71
Fig. 4-10(e)	Isovels for overbank flow in meandering channel	71
Fig. 4-11(a-h)	Depth averaged velocity distribution (U_d normalized with U_{av}) for meandering channel- inbank flow	73
Fig. 4-12(a-e)	Depth averaged velocity distribution (U_d normalized with U_{av}) for meandering channel- overbank flow	74
Fig. 4-13(a)	Shear stress distribution for inbank flow in meandering Channel	76
Fig. 4-13(b)	Shear stress distribution for inbank flow in meandering Channel	76
Fig. 4-13(c)	Shear stress distribution for inbank flow in meandering Channel	77
Fig. 4-13(d)	Shear stress distribution for inbank flow in meandering Channel	77
Fig. 4-13(e)	Shear stress distribution for inbank flow in meandering Channel	78
Fig. 4-13(f)	Shear stress distribution for inbank flow in meandering Channel	78
Fig. 4-13(g)	Shear stress distribution for inbank flow in meandering Channel	79

Fig. 4-13(h)	Shear stress distribution for inbank flow in meandering Channel	79
Fig. 4-14(a)	Shear stress distribution for overbank flow in meandering Channel	80
Fig. 4-14(b)	Shear stress distribution for overbank flow in meandering Channel	81
Fig. 4-14(c)	Shear stress distribution for overbank flow in meandering Channel	82
Fig. 4-14(d)	Shear stress distribution for overbank flow in meandering Channel	83
Fig. 4-14(e)	Shear stress distribution for overbank flow in meandering Channel	84
Fig. 5-1	Three Dimensions Of Research in River Hydraulics	86
Fig. 5-2	Channel Discretization for Solution of Depth-Integrated RANS	92
Fig. 5-3	Contributions from Secondary Flow Terms	92
Fig. 5-4	Plan View of NIT Straight Compound Channel Mesh	104
Fig. 5-5	3D View of NIT Straight Compound Channel Mesh	104
Fig. 5-6	Plan View of NIT Meandering Compound Channel Mesh	105
Fig. 5-7	3D View of NIT Meandering Compound Channel Mesh	106
Fig. 5-8	Plan View of FCFA-1 Channel Mesh	106
Fig. 5-9	3D View of FCFA-1 Channel mesh	107
Fig. 5-10	River Severn cross section-geometry at Mont ford bridge site	107
Fig. 5-11	The Physical Model with Mesh for River Severn at Mont ford bridge site	108
Fig. 5-12(i-vi)	Depth Averaged velocity (U_d) normalized with U_{max} for NIT, Straight channel	112
Fig. 5-13(i-viii)	Depth averaged velocity normalized with U_{max} for FCFA-1 Channel	114
Fig. 5-14(i-ii)	Depth averaged velocity (U_d) prediction by CCHE2D for river Severn at Mont ford bridge site	115
Fig. 5-15(i-iii)	Depth averaged velocity (U_d) normalized with U_{max} for NIT, Meandering Channel	116A
Fig. 5-15(iv-v)	Depth averaged velocity (U_d) normalized with U_{max} for NIT, Meandering Channel	116B

Fig. 5-16(i-vi)	Boundary shear stress (τ) normalized with τ_{max} for NIT, Straight channel	117
Fig. 5-17(i-viii)	Boundary shear stress normalized with τ_{max} for FCFA-1 Channel	118
Fig. 5-18(i-v)	Boundary shear stress (τ) normalized with τ_{max} for NIT, Meandering Channel	119
Fig. 6-1	Deviation of α & β from unity in overbank flow cases	124
Fig. 6-2	Variation of α in straight compound channel	125
Fig. 6-3	Variation of β in straight compound channel	125
Fig. 6-4	Variation of Observed and Predicted value of α in straight compound channel	126
Fig. 6-5	Variation of Observed and Predicted value of β in straight compound channel	126
Fig. 6-6	Variation of α in meandering compound channel	127
Fig. 6-7	Variation of β in straight compound channel	128
Fig. 6-8	Variation of Observed and Predicted value of α in meandering compound channel	128
Fig. 6-9	Variation of Observed and Predicted value of β in straight compound channel	129
Fig. 6-10	Common interfaces dividing a compound section into subsections	132
Fig. 6-11	Variation of % error in estimation of $\%S_{fp}$ with β for the FCF channel having large width ratio (α)	134
Fig. 6-12	Variation of % of floodplain shear with % of area of floodplain	135
Fig. 6-13	Scatter plot for observed and modeled value of $\%S_{fp}$	136
Fig. 6-14	Standard error of estimation of $\%S_{fp}$ by various models	137
Fig. 6-15(a-i)	Error percentages between calculated and observed discharges for the test channels of Knight and Demetriou 1983, Khatua (2008), and FCF-Phase-A channels	138
Fig. 6-16	Standard error of estimation of discharge using different methods for different data sets	139
Fig. 6-17	Variation of predicted discharge for river data by different methods with relative overbank flow depth	139
Fig. 6-18	Regression curve for Shear force carried by flood plain with area of floodplain	141

Fig. 6-19(a)	Comparison of models in Wide NIT Channel	142
Fig. 6-19(b)	Comparison of models in FCF A-1 Channel	143
Fig. 6-20	Error percentage of discharge in Wide NIT Channel	144
Fig. 6-21	Error percentage of discharge in FCF Channel	144
Fig. 6-22	Comparison of different methods for natural river data	145
Fig. 6-23(a)	Error percentage in discharge estimation by various methods (NIT, Rourkela wide channel)	152
Fig. 6-23(b)	Error percentage in discharge estimation by various methods (FCF A-1 channel)	152
Fig. 6-23(c)	Error percentage in discharge estimation by various methods (FCF A-2 channel)	153
Fig. 6-23(d)	Error percentage in discharge estimation by various methods (FCF A-3 channel)	153
Fig. 6-23(e)	Error percentage in discharge estimation by various methods (FCF A-8 channel)	154
Fig. 6-23(f)	Error percentage in discharge estimation by various methods (FCF A-10 channel)	154
Fig. 6-23(g)	Error percentage in discharge estimation by various methods (K&D-1 channel)	155
Fig. 6-23(h)	Error percentage in discharge estimation by various methods (K&D-2 channel)	155
Fig. 6-23(i)	Error percentage in discharge estimation by various methods (K&D-3channel)	156
Fig. 6-23(j)	Error percentage in discharge estimation by various methods (M-1 channel)	156
Fig. 6-23(k)	Error percentage in discharge estimation by various methods (M-2channel)	157
Fig. 6-24(a)	Error (%) in discharge estimation for the river Batu	158
Fig. 6-24(b)	Error (%) in discharge estimation for the river Main	159
Fig. 6-24(c)	Error (%) in discharge estimation for the river Severn	159
Fig. 6-25	Series wise RMSE value for the methods	161
Fig. 6-26	Overall RMSE value for the methods	162

Fig. 6-27	Scatter diagram for observed and modeled main channel discharge percentage for different data sets	163
Fig. 6-28	RMSE value for flow distribution by the New Method (NM)	163
Fig. 6-29	Flow Mechanisms in Compound Meandering Channels (Sellin et al. 1993)	165
Fig. 6-30	Regression curve for percentage of Shear force carried by the left flood plain with percentage of area of left floodplain. (Meandering compound channels)	169
Fig. 6-31	Regression curve for percentage of Shear force carried by the flood plain with percentage of area of floodplain. (Meandering compound channels)	169
Fig. 6-32(i-iii)	Error (%) in discharge Estimation for different Data Series for meandering compound channels	174
Fig. 6-32(iv-v)	Error (%) in discharge Estimation for different Data Series for meandering compound channels	175
Fig. 6-33	Scatter plot of predicted and actual discharge for river Baitarani	176
Fig.A-1	Morphological cross-section of River Batu	193
Fig.A-2	The river Main in county Antrim, Northern Ireland	193
Fig.A-3	The River Severn at Montford Bridge site (a) looking upstream from the right bank, (b) looking downstream from the cableway and (c) the cable way at the bridge	194
Fig.A-4	Cross Section of River Baitarani at Anandapur Site, Orissa, India, Inset (Anandapur Site Showing Meandering Reach)	195

List of Tables

Table 3.1	Geometrical Details Of Experimental Channels	40
Table 3.2	Hydraulic Details Of The Experimental Runs	43
Table 3.3(A-B)	Occurance of depth average velocity at the vertical interface for experimental runs (Straight & Meandering compound channel)	44
Table 3.4	Comparision of calculated shear force with energy gradient approach	46
Table 5.1	Summary of Overbank Flow Cases in NIT Channels	103
Table 5.2	Summary of Mesh Details for the Channels	109
Table 5.3	Flow Parameters Set in CCHE2D Numerical Analysis	110
Table 6.1	Values of Energy & Momentum coefficients for straight and meandering channels	123
Table 6.2	Overview of Experimental and Natural river data considered for development and validation purpose of different stage discharge models	150
Table 6.2	Overview of Experimental and Natural river data considered for development and validation purpose of different stage discharge models	151
Table 6.3	Series wise RMS value of error (%) for new method	157
Table 6.4	Overview of Data sets used for development and validation of stage-discharge models for meandering compound channels.	172
Table 6.4	Overview of Data sets used for development and validation of stage-discharge models for meandering compound channels.	173
Table A-1	Geometrical Properties and Surface Conditions of River Batu and River Main.	192
Table A-2	Geometrical and Surface condition details of river Baitarani	196

List of Symbols

α	Width ratio of the compound channel.
β	Depth ratio or relative depth of the compound channel.
α	Energy coefficient of the flow
β	Momentum coefficient of the flow
β'	Coefficient for the influence of lateral bed slope on the bed shear stress in SKM method
γ	Ratio of the floodplain roughness to the main channel roughness.
A	Amplitude of the meandering curve
A	Area of the compound section
δ	Aspect ratio of the main channel $2b/h$
μ	Dynamic viscosity of water
ρ	Density of flowing liquid
g	Acceleration due to gravity
ϵ	The eddy viscosity
λ	The dimensionless eddy viscosity
τ	Point boundary shear stress
τ_z	Zonal boundary shear stress
τ_{mc}	Mean boundary shear stress in main channel per its unit length along the flow direction
τ_{fp}	Mean boundary shear stress in floodplains per its unit length along the flow direction
τ_{lfp}	Mean boundary shear stress in left floodplain in meandering compound channel per its unit length along the flow direction.
τ_{rfp}	Mean boundary shear stress in right floodplain in meandering compound channel per its unit length along the flow direction.
A_{mc}	Area of main channel using vertical interface
A_{fp}	Area of floodplain using vertical interface
$(\%A_{mc})$	% of area of main channel using vertical interface
$(\%A_{fp})$	% of area of floodplain using vertical interface
b	Half bottom width of main channel

B	Half over all width of compound channel
h	Height of main channel up to floodplain bed
H	Total depth of flow in compound channel
R	Hydraulic mean radius of the channel cross section (A/P)
Re	Reynolds number of the flow
Fr	Froude's number of the flow
d	External diameter of the Preston tube
Δp	Difference in static and dynamic pressure of Pitot static tubes.
ν	Kinematic viscosity of water
x^*	Patel's (1965) parameter
y^*	Patel's (1965) parameter
S	Valley slope
r_m	radius of the meander
L	One wave length of the meander channel
$(\%S_{fp})$	Shear force percentages carried by the floodplain perimeter
$(\%S_{mc})$	Shear force percentages carried by the main channel perimeter
S_r	Sinuosity (length along channel center/ straight Valley length)
F^*	Non dimensional discharge coefficient
W	Meander belt width
C	Chezy's channel coefficient
f_{fp}	Resistance coefficient of floodplain sub-area
f	Darcy-Weisbach Friction factor
f_z	Zonal friction factor
f_{mc}	Resistance coefficient of main channel sub-area
f_{fp}	Resistance coefficient of floodplain sub-area
k	Von Karmans constant;
m	An exponent used in Knight & Hamed (1984) formulae
n_{mc}	Manning's roughness factor for main channel
n_{fp}	Manning's roughness factor for floodplain
n	Manning's roughness factor
P	Wetted perimeter of the compound channel section
P_{mc}	Wetted perimeter of the main channel
P_{fp}	Wetted perimeter of the floodplain
R_{mc}	Hydraulic radius of main channel sub-sections

R_{fp}	Hydraulic radius of flood plain sub-sections
Q	Discharge
K	Conveyance
Q_{actual}	Actual discharge
q	The unit flow rate
$\%Q_{mc}$	Percentages of the total discharge carried by the main channel only
U_*	Shear velocity
X_{mc}	Interface length for inclusion in the main channel wetted perimeter
X_{fp}	Length of interface to be subtracted from the wetted perimeter of floodplain
U_{mc}	Mean velocities of the main channel
U_{fp}	Mean velocities of the flood plains
U_d	Depth-averaged streamwise velocity
U_z	The average zonal velocity
U_{av}	Average or Mean cross sectional velocity
V_d	Depth-averaged lateral velocity
τ_b	Bed shear stress
τ_{xx} , τ_{xy} , τ_{yx} , and τ_{yy}	The depth integrated Reynolds stresses in appropriate directions
Γ	Secondary flow term
C_{uv}	A factor which relates the secondary currents to the depth mean velocity

List of Abbreviations

ADO	Average deviation from orthogonality
AAR	Average Aspect ratio
AM	Area Method
CES	Conveyance Estimation System
MDCM	Modified Divided Channel Method
EMDCM	Extended Modified Divided Channel Method
NM	New Method
NIT	National Institute of Technology
FCF	Flood Channel Facility
SKM	Shino Knight Method
DCM	Divided Channel Method
DDM	Diagonal Division Method
HDM	Horizontal Division Method
HDM-1	Horizontal Division Method with length of interface excluded in computation of wetted perimeter.
HDM-1I	Horizontal Division Method with length of interface excluded in computation of wetted perimeter.
RMSE	Root Mean Squared Error
SCM	Single Channel Method
VDM	Vertical Division Method
VDM-1	Vertical Division Method with length of interface excluded in computation of wetted perimeter.
VDM-1I	Vertical Division Method with length of interface included in computation of wetted perimeter of the main channel only.

INTRODUCTION

1.1 BACKGROUND

Rivers being the lifeblood of any civilization have traditionally been regarded as a major natural resource for the growth and the prosperity of the nations or states through which they traverse. The perennial supply of good quantity and quality of water along with a host of other benefits such as fertile and plain landmasses constituting the floodplains suitable for growth of crops and fodder, water connectivity to major cities both intra state and interstate etc. have made the rivers very attractive destination for dense population to settle on their floodplains. Thus so many prosperous cities around the world from the city of London on the Thames to the city of New Delhi on the river Yamuna, to the city of Moscow on the river Moskva (Fig.1-1) etc. have developed alongside river banks.

However during flood times ironically the same rivers are also guilty of destruction of the very life they seem to sustain. Many rivers have wreaked havoc and have simply wiped out vast tracts of habitation, flora & fauna resulting in colossal loss of life and property due to some massive floods in past (Fig.1-2 shows the buildup of high stage for river Yamuna flowing during a recent flood near the city of New Delhi, India). Dense human settlement over the floodplains obstructs the drainage of floodwater thereby even further increasing the depth of inundation and causing more land masses to come under its spate. Although floods are usually associated with high stages in rivers, accurate estimation of magnitude and frequency of floods likely to pass over the river section as well as some proper planning and design of floodplains can to a large extent mitigate the potency of destruction by allowing smooth passage of high discharge without allowing high stage to build up in the flow section. So rivers are naturally or artificially made to inundate their adjacent floodplains thereby lessening the load in the main river and minimizing the effects of devastation.



Fig.1-1 Moscow - Looking over Moskva River to the Cathedral of Christ, the Savior.

(Source: Google Image)

Such river sections which are flanked by one or two adjacent floodplains are commonly addressed as two stage compound channels in river hydraulics vocabulary.

These compound channels are extremely complex from analysis point of view due to the presence of a number of geometrical and physical parameters and hence have attracted the attention of researchers in last half century. Geometrically the main river section is often narrow and deep whereas the floodplains are wide and shallow. Hence the main channel flow are usually much faster as compared to the floodplain flow and due to physical connection between the two adjacent flow sections considerable exchange of momentum takes place which was first demonstrated by Sellin (1964). The path of the river can also be straight in some reaches whereas meandering in other reaches. The primary velocity occurring in streamwise direction is often associated with some amount of secondary currents which are perpendicular to main velocity vector. Flow even in a straight channel is generally associated with spiral motion (Chow, 1956) thereby increasing complexity in its analysis. From practical point of view engineers are often entrusted not only with the task of accurate prediction of stage discharge curve but also finding distribution of velocity and boundary shear stress across the whole compound section for a number of floodplain design measures. Many

developments have since taken place in this field of river engineering resulting in a number of models to predict the stage-discharge relationships or rating curves for compound channels of various geometries and plan forms. Notable among these are the works of Knight & Demetriou (1983) ; Wormleaton et al (1982) ; Lambert & Myers (1988); Shiono & Knight (1988,1991) ; Bousmar & Zech (1999) ; Shiono et al, (1999) ; Ervine et al, (2000) ; Patra & Kar (2000) ; & Khatua (2008) etc.



Fig.1-2 The flooded River,Yamuna flowing above the danger level in New Delhi

(Source: Hindustan Times Dt.19-06-2013)

Compound channels used for investigating flow characteristics are often varied with respect to different geometric and hydraulic parameters. Aspect ratio (δ , where δ =ratio of bottom width and depth of main channel) and width ratio (α , where α = ratio of width of floodplain to width of main channel) are the main geometrical factors while relative depth or depth ratio (β) is the main hydraulic parameter defining the flow condition (where β is the ratio of depth of flow over floodplain to the depth of flow in the main channel). In view of extreme difficulty in obtaining in situ velocity and boundary shear data for a river during flood, researchers in past have resorted to conducting experiments in small scale laboratory channels for developing their models for zonal shear force and hence stage-discharge for the whole compound sections. Researchers such as Knight & Hamed (1984), Patra & Kar (2000), Khatua & Patra (2007) etc. conducted experiments on small scale flumes to develop models predicting

stage-discharge relationships. To augment the channel experiments of individual researchers a dedicated experimental program such as the large scale EPSRC-FCF program at the University of Birmingham constituting compound channels with α values ranging from 1.20 to 6.67 for Phase A series of straight channels (Knight and Sellin, 1987) and a value of 11.11 for Phase B series of meandering channels (Sellin et al. 1993) was used for conducting numerous experiments on channels with different geometric, roughness and hydraulic conditions. It is extremely rare to find any model developed purely from theoretical analysis as the presence of turbulence as the chief mechanism in compound channel flow makes any such attempt only partially successful as some form of empiricism has to be necessarily incorporated through turbulence closure schemes. As a method of analysis, numerical models also have played their part in solving complex hydrodynamics of compound channel flow and often act as handy complementary tools vis a vis analytical and experimental investigations in this area of research.

In many cases of laboratory research, experiments were conducted on compound channels with different geometries and width ratios (α value) and then by measuring the point boundary shear stress (τ) across the compound section, different models were developed representing the relation between the percentages of shear force carried by the flood plains with the percentage of area of the floodplains. Then suitable stage-discharge models were developed from the models of shear force obtained previously, using some form of divided channel method (DCM). However it was noted that (Khatua, 2008) all these models were only applicable to the compound channels or rivers with α value in the range for which they were developed. Any model which can be applicable in channels with wide ranging geometry and α value will obviously have the advantage over models of limited applicability and hence can gain acceptance in the field. Since a single model which can be applied to compound channels of all geometric, hydraulic and roughness conditions is yet to be developed, so there is always a need to develop models for compound channels having new or untested geometry covering the compound channels of different geometries as encountered in field. Many rivers of Asia and Europe during flood times spread far into their floodplains so that the flow section can be easily assumed as a compound section with width ratio in excess of 11 (Metitivier and Gaudemer, 1999; ADB Project report, 2010 and Thonon et al, 2007). It is nearly impossible to get boundary shear and velocity data

in field condition during flood times in rivers of such gigantic proportion. So against this backdrop the current research is aimed at adding to our ever expanding body of database in the field of both straight and meandering compound channel flow, by conducting flume experiments in laboratory for compound channels having width ratio value up to 12 and then in successive stages developing models for different channel geometries.

1.2 AIM AND OBJECTIVES

This research program has been pursued with the following principal aims:

- To conduct experiments on compound channels of straight and meandering planform with wide floodplains in order to gain insight to the flow physics.
- To develop 1D models for stage-discharge relationship in case of both straight and meandering compound channels.
- To explore the alternate ways and means of solution to the problem of discharge or conveyance estimation in both straight and meandering compound channels through 1D or 2D numerical packages.

Apart from the principal aims as stated above the objectives of the current research work can be enumerated as below:

- To measure and plot the depth averaged velocity distribution curves for both straight and meandering compound channels with wide floodplains ($\alpha \approx 12$).
- To develop models for energy and momentum coefficients (α & β) for compound channels.
- To measure and plot the boundary shear stress distribution curves for both straight and meandering compound channels with wide floodplains ($\alpha \approx 12$).
- To apply the 2D numerical hydrodynamic software tool CCHE2D developed by NCCHE, University of Mississippi, USA to validate the results of FCF channel, present straight wide compound channel, present meandering compound channel as well as some field cases.
- To model sub section shear force percentages of straight and meandering compound flow sections.

- To use database of both small scale flume experiments of previous researchers and large scale experiments (EPSRC-FCF Program) to develop new models of conveyance estimation for compound channels with floodplains having α value up to 6.67.
- To use 1D package such as CES-AES developed by HR, Wallingford for both estimating the conveyance or discharge in compound channels and then compare the result with newly developed models.
- To develop new models for conveyance estimation and hence stage-discharge curve for straight compound channels having α value up to 12.
- To develop model for estimation of zonal flow in case of straight compound channels.
- To develop model for conveyance estimation and hence stage-discharge curve for meandering compound channels.
- To validate the developed models with data sets of other researchers and with some field data.
-

1.3 ORGANISATION OF THE THESIS

This thesis has been organized into 7 broad sections or chapters with each section again being subdivided into a few subsections. Section 1 is the ‘INTRODUCTION’ chapter which gives a brief background of the compound channel flow problems and issues, the knowledge gaps and aims and objectives of the current research undertaken.

Section 2 named as ‘LITERATURE REVIEW’ casts a glance over the previous relevant researches in this field. It helps to organize one’s knowledge and thoughts by collecting and collating the huge body of the database as well as the know-how developed by previous researchers while also identifying the issues and challenges facing the research.

Section 3 named as ‘EXPERIMENTAL SETUP AND PROCEDURE’ clearly details all experimental plans and programs, setting up of experiments, methodologies and procedures adopted.

Section 4 ‘EXPERIMENTAL RESULTS’ deals with the outcomes of the experiments conducted. It shows the results of velocity distribution, depth averaged velocity and

boundary shear stress distribution across the whole compound section for both straight and meandering compound channels under a variety of flow conditions.

Section 5 termed as ‘APPLICATION OF NUMERICAL TOOLS’ deals with two very prominent tools used for flow modeling in river engineering. The first one is the conveyance estimation tool ‘CES-AES’, a 1D package developed by joint agency/DEFRA Research program on flood defense with contributions from the Scottish executive and the Northern Ireland Rivers Agency, HR Wallingford and the Environmental agency, UK and widely recommended for use throughout Europe for reliable prediction of conveyance or discharge in flooded channels or streams. The chapter describes all salient features regarding the package. Similarly the second part of the chapter deals with different features regarding hydrodynamic modeling software package developed by the National Center for Computational Hydro-science and Engineering (NCCHE) University of Mississippi, USA, alternatively referred to as ‘CCHE2D’. The latter being a 2dimensional package is based on shallow water equations (SWEs) which solve the depth averaged form of Navier-Stokes (N-S) equations for predicting velocity and boundary shear stress over the entire flow domain.

Section 6 named ‘ANALYSIS AND DISCUSSION’ deals with the development of various models for energy and momentum coefficients, shear force carried by subsections, stage- discharge relationships for compound channels of various geometries etc. The chapter also analyses the results of some well-known previous models to estimate stage-discharge for present experimental channels as well as some small scale and large scale flume experiments of past research projects and some field data of real flooded rivers as available in literature. Error analysis is also done for the previous models and for the new developed models to draw a comparison among all the competing models so as to validate the new models against wide ranging data sets for establishing the latters’ efficacy.

Section 7 ‘CONCLUSION AND SCOPE FOR FUTURE WORK’ is the last chapter in this thesis which in a nutshell points out all relevant conclusions that can be inferred from this research work. The chapter also throws light on the vast scope and possibilities as available in this field to all future researchers.

LITERATURE REVIEW

2.1 GENERAL

The past research findings from the corner stone for the future investigation. Just as a relay race where the race is continued from the preceding runner to the successor, research in the field of science and technology is a continuum where research findings and information of the past are shared with the next generation in form of published literature. So a detailed literature survey is prerequisite to any meaningful and fruitful research in any subject. The present work is no exception and hence a focused and intensive review of literature was carried out covering various aspects concerning the straight and meandering compound channels. The following sections outline the research carried out in past in the field of flow in compound channels of both straight and meandering plan forms. A section specially covering only simple meandering channels has also been included in order to bring out the contrast in nature and characteristics of flow and other parameters in the channel with in bank flow vis a vis overbank flow occurring in compound channels. The literature survey was undertaken keeping in view the aim and objectives of the present research. So effort was made to identify and study the works of past researchers concerning various aspects e.g. the distribution of velocity and boundary shear stress in channels of various geometries and planforms, the energy loss mechanisms associated with straight and meandering compound channel flows, models to predict depth averaged velocity, boundary shear and finally stage-discharge relationships for different cases etc. In this regard works based on analytical, experimental and numerical approach were systematically studied to gain awareness of the issues and challenges present in the area while appreciating the research undertaken by the scientists and investigators of past as well as recent era. Although the literature survey reported herein has been made extensive but no claim is made about its exhaustive nature. Important and updated information as available till the writing of this dissertation could only be included while leaving out some other

works. Meander and straight compound channel flows have been the subject of active research for a fairly long time. It is always better to understand the nature of flow in simple meander channels and straight compound channels before attempting to learn about the flow mechanisms in a compound meandering channel as the complexities go on compounding in that order due to the appearance of more and more flow mechanisms in the scene.

2.2 SIMPLE MEANDERING CHANNELS

The following important studies concerning the flow in meandering channels are mentioned for they provide insight to the nature and characteristics of flow and associated mechanisms occurring in a simple meandering channel where the course of river or flume keeps on changing along its path.

The Soil Conservation Service (1963) proposed a method to account for meander losses by adjusting the basic value of Manning's n using sinuosity of the channel only. The adjusted value of Manning's n was proposed for three different ranges of sinuosity.

Toebe and Sooky (1967) conducted experiments in a small laboratory channel with sinuosity 1.09. From the experimental results they concluded that energy loss per unit length for meandering channel was up to 2.5 times as large as those for a uniform channel of same width and for the same hydraulic radius and discharge. They proposed an adjustment to the roughness f as a function of hydraulic radius below a critical value of the Froude number.

Chang (1983) investigated energy expenditure in curved or meandering channels and derived an analytical model for obtaining the energy gradient, based on fully developed secondary circulation. By making simplifying assumptions he was able to simplify the model for wide rectangular sections.

Johannesson and Parker (1989a) presented an analytical model for calculating lateral distribution of depth averaged primary flow velocity in meandering rivers. Using an approximate "moment method" they accounted for the secondary flow in the convective transport of primary flow momentum, yielding satisfactory results of the redistribution of primary flow velocity.

Knight, Yuan and Fares (1992) reported the experimental data of SERC-FCF concerning boundary shear stress distributions in meandering channels throughout the path of one complete wave length. They also reported the experimental data on surface topography, velocity vectors, and turbulence for the two types of meandering channels of sinuosity 1.374 and 2.043 respectively. They examined the effects of secondary currents, channel sinuosity, and cross section geometry on the value of boundary shear in meandering channels and presented a momentum-force balance for the flow.

James (1994) reviewed the various methods for bend loss in meandering channel proposed by different investigators. He tested the results of the methods using the data of FCF, trapezoidal channel of Willets, at the University of Aberdeen, and the trapezoidal channels measured by the U.S. Army Corps of Engineers at the Waterways Experiment Station, Vicksburg. He proposed some new methods accounting for additional resistance due to bend by suitable modifications of previous methods. His modified methods predicted well the stage discharge relationships for meandering channels.

Nalder (1997) analysed different distinct features of meandering channel flow and also reviewed some equations relating meander length to the discharge, as well as some models of three dimensional flows. The author also presented a curvilinear version of the de Saint-Venant equations leading to new equations for long waves in curved channels.

da Silva (1999) expressed the friction factor of rough turbulent meandering flows as the function of sinuosity and position (which is determined by, among other factors, the local channel curvature). She validated the expression by the laboratory data for two meandering channels of different sinuosity. The expression was found to yield the computed vertically averaged flows that are in agreement with the flow pictures measured for both large and small values of sinuosity.

Shiono, Muto, Knight and Hyde (1999) presented the experimental data of secondary flow and turbulence using two components Laser- Doppler Anemometer for both straight and meandering channels to understand the flow mechanism in meandering channels. They developed turbulence models and studied the behavior of secondary flow and centrifugal forces for both in-bank and over-bank flow conditions. They

investigated the energy loss due to boundary friction, secondary flow, turbulence, expansion and contraction in meandering channels.

Duan (2004) compared the flow analysis in mildly and sharply curved or meandering channels through the use of depth averaged 2-D model and full 3-D model and concluded that the latter is more capable than the former in capturing the flow fields in meandering channels. The author also found that a 2D model could be more preferable because of being computationally cost-effective for parametric trade-off analyses needed by policy and management planning as well as preliminary design applications. Finally the author advocated that the 1D, 2D and 3D numerical models should be integrated when applied to practical engineering projects to achieve the state-of-the-art results and cost effectiveness.

Zarrati, Tamai and Jin (2005) developed a depth averaged model for predicting water surface profiles for meandering channels. They applied the model to three meandering channels (two simple and one compound) data. The model was found to predict well the water surface profile and velocity distribution for simple channels and also for the main channel of compound meandering channel.

Gyr (2010) through a topological view of meandering phenomenon tried to find answers to two paradoxes involving flow in meandering channels. The author explained through this approach the reason for higher discharge and sediment transport rate in a meandering channel compared to a straight channel. By analysing the origin and maintenance of meanders through development of secondary cells he reasoned that through a drag reducing mechanism occurring in rollers of secondary cells via less friction in the walls actually a meandering channel in field carries more discharge and hence higher transportation of sediments.

Stoesser, Ruether and Olsen (2010) applied two Computational Fluid Dynamics (CFD) codes to analyze turbulent flow in meandering channels. The first CFD code solved the steady Reynolds-Averaged Navier–Stokes equations (RANS) using an isotropic turbulence closure while the second code was based on the concept of Large Eddy Simulation (LES). Both the models confirmed the presence of an outer bank secondary cell in addition to primary helical flow in a meandering channel. They also showed that, though LES models was expected to predict bed shear stress along the wetted perimeter

with greater accuracy than RANS model but in practice outputs from both the models agreed with each other well and also agreed well with experimental data.

Khatua, Patra, Nayak and Sahoo (2013) proposed a discharge predictive method for meandering channels taking into account the variation of roughness with depth of flow. The performance of the model was evaluated by comparing with several other models of different researchers.

2.3 STRAIGHT COMPOUND CHANNELS

A river section along with floodplains attached to one or both sides constitute a compound section. In normal times i.e. during periods of low flow the water flows within the banks of river and the section carrying the flow is termed as simple section. However during flood times the river overtops its banks and flow essentially occurs in a compound section. When the path of rivers in a reach is straight but flow occurs both in main channel and floodplains then such cases can be grouped under straight compound channel flow. The flow in such a channel is often associated with a number of mechanisms such as significant planform and streamwise vortices with organized coherent structures rotating about horizontal or vertical axes. Hence it has caught the attention of researchers and engineers alike. Obtaining velocity and other data in a flooded river is not only difficult but also is fraught with risk. So field analysis of such flows though not impossible but is rare. Hence major research on straight compound channels have been conducted through laboratory experiments or through numerical studies. Wherever possible the theories or models developed through such studies have been validated with limited field data by various other researchers.

Sellin (1964) confirmed the presence of the "kinematics effect" after a series of laboratory studies and presented photographic evidence of the presence of vortices at the junction region of main channel and flood plain. He studied the channel velocities and discharge under both interacting and isolated conditions by introducing a thin impermeable film at the junction. Under isolated condition, velocity in the main channel was observed to be more than interacting condition.

Zheleznyakov (1965) was probably the first to investigate the interaction between the main channel and the adjoining floodplains. He demonstrated under laboratory conditions the effect of momentum transfer mechanism, which was responsible for decreasing the overall rate of discharge for floodplain depths just above the bank full level. As the floodplain depth increased, the importance of the phenomena diminished. He also carried out field experiments, which confirmed the significance of the momentum transfer phenomenon in the calculation of overall discharge. The relative 'drag' and 'pull' between the faster moving main channel flow and slower moving floodplain flow gave rise to the momentum transfer mechanism, which he termed as "kinematics effect".

Ghosh and Jena (1973) and Ghosh and Meheta (1974) reported studies on boundary shear distribution in straight two stage channels for both smooth and rough boundaries. They related the sharing of the total drag force by different segments of the channel section to the depth of flow and roughness concentration.

Yen and Overton (1973) used isovel plots to locate the interface plane of zero shear. The data showed that the angle of inclination to the horizontal of the interface plane increased with depth of flow over floodplain.

Myers and Elswy (1975) studied the effect of interaction mechanism and shear stress distribution in channels of complex sections. In comparison to the values under isolated condition, the results showed a decrease up to 22 percent in channel shear and increase up to 260 percent in floodplain shear. This indicated the possible regions of erosion and scour of the channel and flow distribution in alluvial compound sections.

Rajaratnam and Ahmadi (1979) studied the flow interaction between straight main channel and symmetrical floodplain with smooth boundaries. The results demonstrated the transport of longitudinal momentum from main channel to flood plain. Due to flow interaction, the bed shear in floodplain near the junction with main channel increased considerably and that in the main channel decreased. The effect of interaction reduced as the flow depth in the floodplain increased.

Wormleaton, Alen, and Hadjipanous (1982) undertook a series of laboratory tests in straight channels with symmetrical floodplains and used "divide channel" method for the assessment of discharge. From the measurement of boundary shear, apparent shear

stress at the vertical, horizontal, and diagonal interface plains originating from the main channel-floodplain junction could be evaluated. An apparent shear stress ratio was proposed which was found to be a useful yardstick in selecting the best method of dividing the channel for calculating discharge. It was found that under general circumstances, the horizontal and diagonal interface method of channel separation gave better discharge results than the vertical interface plain of division at low depths of flow in the floodplains.

Knight and Demetriou (1983) conducted experiments in straight symmetrical compound channels to understand the discharge characteristics, boundary shear stress and boundary shear force distributions in the section. They presented equations for calculating the percentage of shear force carried by floodplain and also the proportions of total flow in various sub-areas of compound section in terms of two dimensionless channel parameters. For vertical interface between main channel and floodplain the apparent shear force was found to be more at low depths of flow and also for high floodplain widths. On account of interaction of flow between floodplain and main channel, it was found that the division of flow between the sub-areas of the compound channel did not follow the simple linear proportion to their respective areas.

Knight and Hamed (1984) extended the work of Knight and Demetriou (1983) to rough floodplains. The floodplains were roughened progressively in six steps to study the influence of different roughness between floodplain and main channel to the process of lateral momentum transfer. Using four dimensionless channel parameters, they presented equations for the shear force percentages carried by floodplains and the apparent shear force in vertical, horizontal, diagonal, and bisector interface plains. The apparent shear force results and discharge data provided the strength and weakness of these four commonly adopted design methods used to predict the discharge capacity of the compound channel.

Wormleaton and Hadjipanous (1985) studied flow distribution in compound channels and showed that even though a calculation method may give satisfactory results of overall discharge in a compound channel, the distribution of flow between floodplain and main channel may be badly modeled. In general, the floodplain flow was found to be underestimated and the main channel flow overestimated.

Myers (1987) presented theoretical considerations of ratios of main channel velocity and discharge to the floodplain values in compound channel. These ratios followed a straight-line relationship with flow depth and were independent of bed slope but dependent on channel geometry only. Equations describing these relationships for smooth compound channel geometry were presented. The findings showed that at low depths, the conventional methods always overestimated the full cross sectional carrying capacity and underestimated at large depths, while floodplain flow capacity was always underestimated at all depths. He underlined the need for methods of compound channel analysis that accurately model proportions of flow in floodplain and main channel as well as full cross-sectional discharge capacity.

Stephenson and Kolovopoulos (1990) discussed four different methods of subdivision of compound channels on the basis of consideration of shear stress between floodplain and main channel to evaluate a method of discharge calculation. Based on the published data, they concluded that their 'area method' was the most promising alternative of discharge computation and that Prinos-Townsend (1984) equation gave better results for apparent shear stress at floodplain and main channel interface. They incorporated channels with fairly wide range of bed roughness and floodplain widths in their computations.

Shiono and Knight (1988, 1991) studied the flow of water in straight open channels with complex cross section. They derived an analytical model for predicting depth averaged velocity and boundary shear stress first for channels of trapezoidal shape and then for any shape by discretizing the channel boundary in to linear elements. For this they developed the mathematical equations governing the shear layer between a river channel and its floodplains basing on a dimensionless eddy viscosity model. The effects of bed-generated turbulence, lateral shear turbulence and secondary flows were considered in their model. They were able to quantify the influence of Reynolds stresses and secondary flows on eddy viscosity.

Ackers (1992, 1993 a & b) deduced a design formula for straight two stage channels by taking into account the interaction effects between floodplain and main channel. A parameter representing the coherence between the hydraulic condition of floodplain and main channel zones was proposed. The formulations were tested in large-scale experimental channels covering a wide range of geometry.

Myers and Lyness (1997) studied the behavior of two key discharge ratios, namely total to bank full discharge and main channel to floodplain discharge in compound channels for smooth and homogeneously roughened channels of various scales. The total to bank full discharge ratio was shown to be independent of bed slope and scale and was function of cross section geometry only. The other ratio was also independent of bed slope and scale but was influenced by the lateral floodplain bed slope. They evaluated the coefficients and exponents in the equations relating to flow ratios to flow depths.

Pang (1998) conducted experiments on compound channel in straight reaches under isolated and interacting conditions. It was found that the distribution of discharge between the main channel and floodplain was in accordance with the flow energy loss, which can be expressed in the form of flow resistance coefficient. In general, Manning's roughness coefficient n not only denoted the characteristics of channel roughness, but also influenced the energy loss in the flow. The value of n with the same surface in the main channel and floodplain possessed different values when the water depth in the section varied.

Bousmar and Zech (1999) presented a theoretical 1D model of compound channel flow known as the exchange-discharge model (EDM) which is suitable for stage-discharge computation as well as practical water-profile simulations. The momentum transfer is estimated as the product of velocity gradient at the interface by the mass discharge exchanged through this interface resulting from the turbulence. Similarly, the turbulent exchange discharge is estimated by a model analogous to the mixing length model including a proportionality factor χ that is found to be reasonably constant. They summarized that the model predicts well the stage-discharge both for the experimental data and natural data. They applied their models successfully for flow prediction in a prototype River Sambre in Belgium.

Thrnton, Abt, Morris and Fischenich (2000) performed series of eight experiments in a physical model of a compound channel to quantify the apparent shear stress at the interface between main channel and both vegetated and unvegetated floodplain. They analyzed the data by using a turbulence-based method to calculate the apparent shear stress as a function of the fluctuation in channel velocities. They presented an empirical relationship for the estimation of the apparent shear stress at the main channel-floodplain interface which was found to be the function of the bed shear stress, average

velocity, flow depth, and the blockage caused by floodplain vegetation. They also presented an empirical relationship to incorporate a quantitative measure of the density of vegetation within a floodplain.

Myers, Lyness and Cassells (2001) presented the experimental results of both fixed and mobile main channel boundaries together with two types of flood plain roughness compound channel using FCF data. On the basis of mathematical modeling, they proposed the velocity and discharge ratio relationships which was helpful for discharge assessment in over-bank flows and compared their results well with the data from a prototype natural compound river channel. They found that the ratios of main channel to floodplain average velocities and discharge plot logarithmically for the laboratory data, and linearity with the natural river data. The “divided channel method”(DCM) of discharge estimation overestimated the discharge in all cases and exhibited reasonable accuracy when applied to laboratory data with smooth floodplains, but showed significant errors up to 35% for rough floodplain data, and up to 27% for river data. The single channel method (SCM) significantly underestimated compound discharge for all cases for low flow depths, but became more accurate at larger depths for the smooth boundary laboratory data as well as the river data.

Atabay and Knight (2002) presented some stage discharge relationship of symmetrical compound channel section using the experimental results of the Flood Channel Facility (FCF). They examined the influence of flood plain width and main channel aspect ratio to the stage discharge relationship. They derived simple empirical relationships between stage and total discharge, and stage and zonal discharge for uniform roughness and varying flood plain width ratio. The broad effects on the stage –discharge relationship due to flood plain width ratio were examined.

Ozbek and Cebe (2003) used limited experimental results from the FCF at Wallingford, for computing apparent shear stress and discharge in symmetrical compound channels with varying floodplain widths. They considered three assumed interface planes (vertical, horizontal, and diagonal) between the main channel and the floodplain sub-sections for computation of apparent shear stresses across the interfaces. They evaluated the discharge values for each sub-section and for the whole cross-section. They showed that the performance of these computation methods depend on their ability to accurately predict apparent shear stress. The diagonal and horizontal division

methods provided better results than the vertical division method, with the diagonal method giving the most satisfactory results.

Tominaga and Knight (2004) conducted numerical simulation to understand the secondary flow effect on the lateral momentum transfer with a standard $k-\epsilon$ model linked artificially with a given secondary flow. This simulation reproduced the typical linear distribution of momentum transfer term. The simulated secondary flow decreased the bed shear in main channel and increased the flood plain shear.

Proust, Riviere, Bousmar, Paquier, Zech and Morel (2006) investigated experimentally the flow in a asymmetrically compound channel transition reach in an abrupt floodplain contraction (mean angle 22°). They compared three 1D models and one 2D simulation to their experimental data to know whether the models, developed for straight and slightly converging channels, are equally valid to their geometry. They showed that the error on the level of water is moderated due to lateral mass transfer but increased error of discharge distribution in the sub-areas. They suggested for further work to understand the phenomena of severe mass transfers in non-prismatic compound channels.

Khatua (2008) conducted experiments in straight compound channel having width ratio (α , where α is the ratio of width of floodplains to bottom width of main channel) of 3.67 and developed new model for boundary shear distribution. The author also presented model for discharge estimation in compound channels having homogeneously roughened main channels and floodplains.

Tang and Knight (2008) developed a method to predict depth-averaged velocity and bed shear stress for overbank flows in straight rectangular two-stage channels. Their model was an analytical solution to the depth-integrated Navier–Stokes equation which included the effects of bed friction, lateral turbulence, and secondary flows. A novel boundary condition at the internal wall between the main channel and the adjoined floodplain was proposed by them. The analytical solution using the novel boundary condition gave good prediction of both lateral velocity distribution and bed shear stress when compared with experimental data for different aspect ratios.

Moreta and Martin-Vide (2010) studied the interaction between main channel and floodplains in terms of apparent shear stress which resulted in a dimensionally sound

expression. Their model was based on the square of velocity gradient between main channel and floodplain and also apparent friction coefficient. The model developed by them was validated for its general applicability over both small scale flume data and large scale FCF data for smooth and rough floodplains.

Beaman (2010) in his Ph.D. research undertook numerical modeling for inbank and overbank flows concerning channels under various geometric and hydraulic conditions e.g. depth and width ratios etc. Through Large Eddy Simulation technique he successfully derived the values of three calibration constants f , λ & Γ of Shiono & Knight (SKM) method (1988) for application in the numerical model Conveyance Estimation System (CES) which has recently been adopted by the Environment Agency (EA) for England and Wales for estimation of river conveyance across Europe.

Khatua, Patra and Jha (2010) based on experimental research on rectangular compound channels studied the effects of apparent shear stress along the assumed interfaces originating from the junction of main channel and the floodplain. Thus they correctly found the magnitude of such apparent stress for the appropriate interface plain for quantifying the proportionate boundary shear carried by flow subsections and hence correct stage discharge relationship for the entire compound section.

Conway, O' Sullivan and Lambert (2012) presented an improved approach for applying three-dimensional (3D) computational fluid dynamics (CFD) models to estimate uniform flow stage–discharge relationships and velocity distributions in straight compound channels. They proposed an approach representing an advance on standard discharge estimating methods by using a 3D CFD model with $k-\epsilon$ turbulence closure in a predictive capacity where a flow together with physically realistic resistance coefficients are specified. Their approach is further validated against benchmark experimental data obtained from the largescale UK Flood Channel Facility and is compared with predictions from divided channel methods.

2.4 MEANDERING COMPOUND CHANNELS

There are limited reports available in literature concerning the flow, velocity, shear stress and energy distribution in meandering compound sections.

A study by United States Water Ways Experimental Station (1956) related the channel and floodplain conveyance to geometry and flow depth, concerning, in particular, the significance of the ratios of channel width to floodplain width and meander belt width to floodplain width in the meandering two stage channels.

Toebe and Sooky (1967) were probably the first to investigate under laboratory conditions the hydraulics of meandering rivers with floodplains. They attempted to relate the energy loss of the observed internal flow structure associated with interaction between channel and floodplain flows. The significance of helicoidal channel flow and shear at the horizontal interface between main channel and floodplain flows were investigated. It was found that energy loss in compound meandering channel was more than the sum of simple meandering and uniform channel carrying the same total discharge and same wetted perimeter. The interaction loss increased with decreasing mean velocities and exhibited a maximum when the depth of flow over the floodplain was less. For the purpose of analysis, a horizontal fluid boundary located at the level of main channel bank full stage was proposed as the best alternative to divide the compound channel into hydraulic homogeneous sections. Helicoidal currents in meander floodplain geometry were observed to be different and more pronounced than those occurring in a meander channel carrying in bank flow. It was reported that Reynold's number (R_e) and Froude number (F_r) had significant influence on the meandering channel flow.

Ghosh and Kar (1975) reported the evaluation of interaction effect and the distribution of boundary shear stress in meander channel with floodplain. Using the relationship proposed by Toebe and Sooky (1967) they evaluated the interaction effect by a parameter. The interaction loss increased up to a certain floodplain depth and there after it decreased. They concluded that the channel geometry and roughness distribution did not have any influence on the interaction loss.

Ervine and Ellis (1987) carried out experimental investigation for the different sources of losses of energy in the meandering compound channel. They divided the compound channel into three sub areas, namely (i) the main channel below the horizontal interface from the junction, (ii) the meander belt above the interface, and (iii) the area outside the meander belt of the flood plain. They identified the different sources of losses of energy in each sub-area and proposed a discharge estimation method.

Kiely (1989), McKeogh and Kiely (1989) studied the discharges, velocities, and turbulence characteristics for a meandering and straight main channel with floodplains in small laboratory flumes. Kiely observed that (1) the longitudinal turbulence intensities were higher in magnitude for meandering channels than straight channels, (2) the maximum turbulence intensity was observed to occur on the floodplains, adjacent to the downstream interface of the crossover sections and at the inner bend of the main channel, (3) turbulence transfer from the floodplain to the main channel was observed in straight and meandering channels, and (4) floodplains of meander channels may convey more flow than the floodplains of straight channels, and (5) the flow is approximately parallel to the floodplain valley slope for higher depth ratios.

Ervine, Willetts, Sellin and Lorena (1993) reported the influence of parameters like sinuosity, boundary roughness, main channel aspect ratio, width of meander belt, flow depth above bank full level, and cross sectional shape of main channel affecting the conveyance in the meandering channel. They quantified the effect of each parameter through a non-dimensional discharge coefficient and reported the possible scale effects in modelling such flows.

Sellin, Ervine and Willetts (1993) studied the influence of channel geometry, floodplain widths and roughness on the stage-discharge relationship. They found that the interaction mechanism associated with over bank flow in straight channels had very little influence on meandering two stage channels. For compound channel with smooth boundary, the loss of energy at various flow depths was expressed in terms of the variation of Manning's n and Darcy-Weisbach friction factor f . They suggested that considerably more work is needed to establish a sufficiently robust calculation method to reflect adequately the range of circumstances found in the field. The influence of floodplain roughness, main channel cross section, and sinuosity on the flow structures required further studies.

Greenhill and Sellin (1993) presented a method to design compound meandering channels based on the Manning–Strickler equation and found that the method predicted successfully the stage–discharge relationship for the tests carried out using FCF at UK and the data of other research projects. They suggested that their work be tested against field measurements.

Willetts and Hardwick (1993) reported the measurement of stage–discharge relationship and observation of velocity fields in small laboratory two stage channels. It was found that the zones of interaction between the channel and floodplain flows occupied the whole or at least very large portion of the main channel. The water, which approached the channel by way of floodplain, penetrated to its full depth and there was a vigorous exchange of water between the inner channel and floodplain in and beyond the downstream half of each bend. This led to consequent circulation in the channel in the whole section. The energy dissipation mechanism of the trapezoidal section was found to be quite different from the rectangular section and they suggested for further study in this respect. They also suggested for further investigation to quantify the influence of floodplain roughness on flow parameters.

Wark and James (1994) developed a procedure to calculate conveyance in meandering channels with over bank flow based on the horizontal division of the cross section. It represented a significant change to the current practice of using vertical division of separating the floodplain from main channel. The non-friction energy losses were shown to be less important as the floodplain was roughened. The bed friction remained the most significant source of energy loss in the channels with over bank flow. The work was tested against the field data collected from the river Roding at Abridge in Essex and found to predict the measured stage–discharge relations reasonably well.

Shiono, Al-Romaih and Knight (1999) reported the effect of bed slope and sinuosity on discharge of two stage meandering channel. Basing on dimensional analysis, an equation for the conveyance capacity was derived, which was subsequently used to obtain the stage-discharge relationship for meandering channel with over bank flow. It was found that the channel discharge increased with an increase in bed slope and it decreased with increase in sinuosity for the same channel.

Shiono, Muto, Knight and Hyde (1999) presented the secondary flow and turbulence data using two components Laser- Doppler anemometer. They developed the turbulence models, and studied the behaviour of secondary flow for both in bank and over bank flow conditions. They divided the channel into three sub areas, namely (i) the main channel below the horizontal interface (ii) the meander belt above the interfaces and (iii) the area outside the meander belt of the flood plain. They investigated the energy losses for compound meandering channels resulting from boundary friction,

secondary flow, turbulence, expansion and contraction. They reported that the energy loss at the horizontal interface due to shear layer, the energy loss due to bed friction and energy loss due to secondary flow in lower main channel have the significant contribution to the shallow over-bank flow. They also concluded that the energy loss due to expansion and contraction in meander belt have the significant contribution to the high over-bank flow.

Ervine, Babaeyan-Koopaei and Sellin (2000) presented a practical method to predict depth-averaged velocity and shear stress for straight and meandering over bank flows. They also presented an analytical solution to the depth-integrated turbulent form of the Navier-Stokes equation that includes lateral shear and secondary flows in addition to bed friction. They applied this analytical solution to a number of channels, at model, and field scales, and compared with other available methods such as that of Shiono and Knight and the lateral distribution method (LDM).

Patra and Kar (2000) reported the test results concerning the boundary shear stress, shear force, and discharge characteristics of compound meandering river sections composed of a rectangular main channel and one or two floodplains disposed off to its sides. They used five dimensionless channel parameters to form equations representing the total shear force percentage carried by floodplains. A set of smooth and rough sections were studied with aspect ratio varying from 2 to 5. Apparent shear forces on the assumed vertical, diagonal, and horizontal interface plains were found to be different from zero at low depths of flow and changed sign with increase in depth over floodplain. They proposed a variable-inclined interface for which apparent shear force was calculated as zero. They presented empirical equations predicting proportion of discharge carried by the main channel and floodplain.

Morvan, Pender, Wright, and Ervine (2003) investigated the velocity field in meandering compound channels with over bank flow using the Flood Channel Facility (FCF) data, and simulated the flow field using computational fluid dynamics. They predicted the velocities, secondary velocities and the helical motion of the water flowing within the main channel and compared their results with the experimental data.

Patra, Kar and Bhattacharya (2004) reported the test results concerning the flow and velocity distribution in meandering compound river sections. Using power law they presented equations concerning the three-dimensional variation of longitudinal,

transverse, and vertical velocity in the main channel and floodplain of meandering compound sections in terms of channel parameters. The results of formulations compared well with their respective experimental channel data obtained from a series of symmetrical and unsymmetrical test channels with smooth and rough surfaces. They also verified the formulations against the natural river and other meandering compound channel data.

Khatua (2008) presented the research findings from experiments conducted on two rectangular compound meandering channels; one with mild sinuosity and the other with high sinuosity. Out of these two the low sinuous channel was having width ratio of 4.81 and the other one was having width ratio of 16.08. The author derived and proposed a no. of relations for length of interaction between the main channel flow and flood plain flow.

Jing, Guo, Li and Zhang (2009) applied a 3D numerical turbulence model to simulate turbulent flows in a 60° compound meandering channel with semi natural cross sections. They also calculated velocity fields, wall shear stress, and Reynolds shear stresses for various input flow conditions. They showed that simulated velocity fields and Reynolds shear stresses were in reasonable good agreement with the U.K.-FCF measurements. Effects of water depth on secondary flow and wall shear stress were also studied.

Moncho-Esteve, Palau-Salvador, Shiono and Muto (2010) studied turbulent flow structures in the experimental channel of Muto and Shiono (1998) by simulating the flow through Large Eddy Simulations (LES). For this they applied an in-house code LESOCC2. The LES could predict successfully complicated flow structures generated at the junction of flood plain and main channel due to the interaction between flows occurring in zones of floodplain and main channel

Al amin, Khan and Islam (2013) studied variation of shear stress in compound meandering channels under different depth and width ratios by conducting laboratory experiments. They measured the variation of shear stress across the compound section through the Prandtl-Von Karman universal velocity Distribution law.

Patra (2013) reviewed different methods for discharge assessment in straight and meandering compound channels. The focus of this work was on the variation of

discharge in compound channels with width ratio and sinuosity. New methods were presented for stage discharge estimation taking the current advancement in research in compound channels.

The review of literature as outlined in previous sections of this chapter suggests that a great many research works have been done in straight compound channels as well as in meandering compound channels. However the developed boundary shear stress and discharge predictions formulae have been mainly applicable to the geometric and hydraulic conditions of the channels for which they have been developed. The main focus of the present research work is to mainly address the following issues which can be discussed point wise as given below. (a) For straight compound channels the widest compound channel from EPSRC-FCF series-A channels has been with a width ratio of 6.67. Also Khatua et al,(2012) have developed a series of equations for predicting boundary shear and discharge for smooth wide compound channels having width ratio up to 6.67. However the large Asiatic channels and some European channels have their floodplains so wide that there is always a need to develop discharge and boundary shear prediction formulae to address the issue of channel design with width ratio in excess of 11.00 which the current work aims to achieve. (b) Though some studies have been done in meandering compound channels giving mathematical equations to satisfactorily predict boundary shear and discharge in meandering compound channels with different geometric ratios but very few methods can accommodate a varied geometric conditions. This issue is addressed in the current work by including a number of data points from a large number of previous research projects for devising the predictive set of equations. The method then is validated with a number of large scale meandering compound channel data; small scale channel data as well as with natural data set of previous studies. (c) The numerical tools viz. 1D-CES and 2D-CCHE2D packages have been extensively applied to different channels in this work mainly to draw a comparative study vis-à-vis the actual experimental values of boundary shear and discharge in channels of different geometry with main emphasis on channels having high width ratio in excess of 11.00.

EXPERIMENTAL SETUP AND PROCEDURE

3.1 PLAN OF EXPERIMENTAL SETUP

The studies reported in this thesis constitute a part of an extensive research project granted & funded by Department of Science & Technology, Government of India carried out under the supervision of my research guide. As per the goal of the said project study was to be carried out on compound channels with same geometry having a trapezoidal main channel and wide floodplains ($\alpha \approx 12$) for varying flow depths to determine the effects of geometry and sinuosity on boundary shear stress distribution and conveyance capacity. Thus it was decided to build one large steel flume with tilting facility inside the Fluid Mechanics and Hydraulics Engineering Laboratory of the Civil Engineering Department. Keeping in view all the requirements of planned experimental programs, necessary design and calculations were made to find the dimensions of the main channel, floodplains, entrance length, number of curves possible inside the flume length for meandering channel along with lengths of straight portions preceding and succeeding it etc.

3.1.1. Fabrication of Flumes and Accessories

The flume was made up of MS bars, plates and angles, fitted with all accessories to measure velocity and boundary shear stress at any point on the flow domain. A gear arrangement over an inclined metallic ramp supported the flume and by suitable movement of the former up or down the ramp necessary bed slope in the flume and hence in the compound channels could be imparted. For feeding water into the channels a large R.C.C. overhead tank was constructed on the upstream side of the flume inside the laboratory. A masonry volumetric tank was built at the downstream end of the flume for calibration purpose. A large underground sump present outside was used for maintaining uninterrupted water supply to the overhead tank. Two centrifugal pumps of 15HP and 10HP capacity respectively, fitted with suction and delivery pipes completed

the recirculating system of water supply to the channels in the flume. A stilling chamber fitted with a regulating head gate and flow straighteners was created in the entrance portion of the flume to reduce turbulence in the flow entering the channel. A sharp crested rectangular notch made up of 5mm thick MS plate was fitted upstream of the bell mouthed entrance to the channel for discharge measurement. On the downstream side a tail gate was fitted to control the depth of flow and to achieve quasi-uniform flow in the channel. Fig.3-1 to Fig.3-13 show photographs of important components of straight and meandering compound channel experimental setups. Figs. 3.14 and 3.16 show the schematic diagrams of overall experimental setup for straight and meandering compound channels respectively.



Fig. 3-1 Stilling Chamber, Flow Straightener & Point Gauge In U/S Section of Flume



Fig. 3-2 Photo of Flume with Straight Compound Channel (Looking U/S)



Fig. 3-3 Photo of Straight Channel (Looking From Side)



Fig. 3-4 Series of Micro-Pitot Tubes Fitted to the Holder

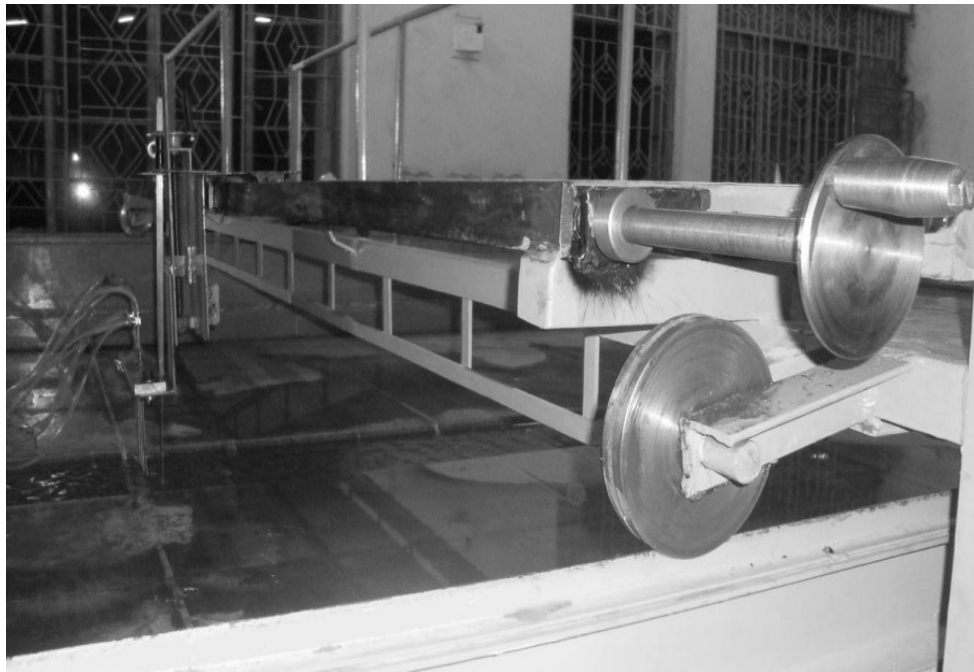


Fig. 3-5 Photo of Straight Channel with Movable Bridge



Fig. 3-6 Downstream Volumetric Tank

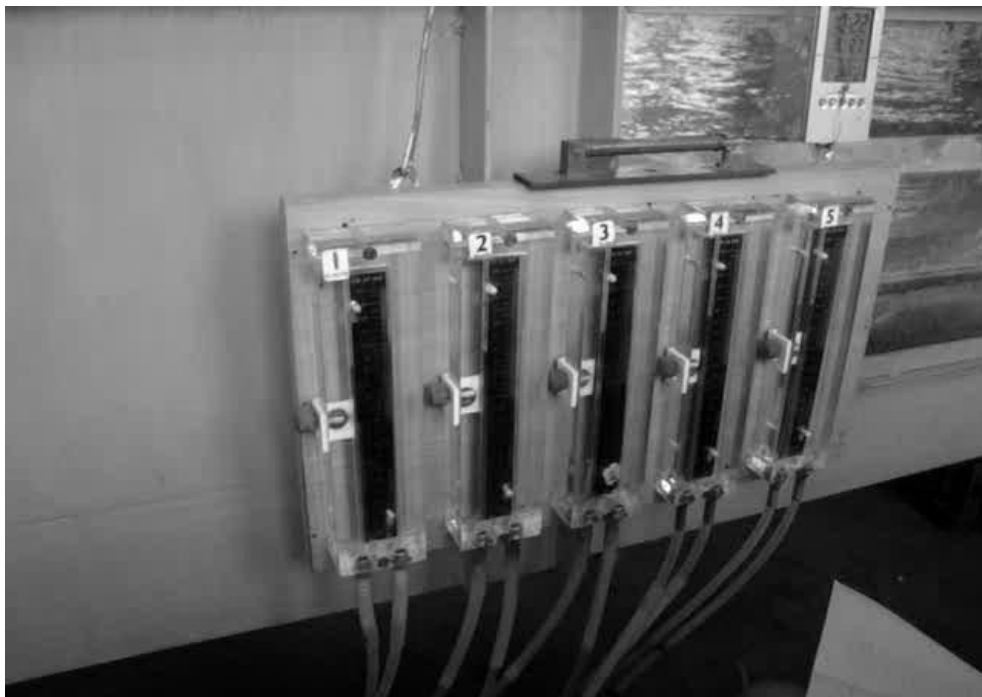


Fig. 3-7 Series of Manometers, Spirit Level & Stop Watch Hung Outside the Flume

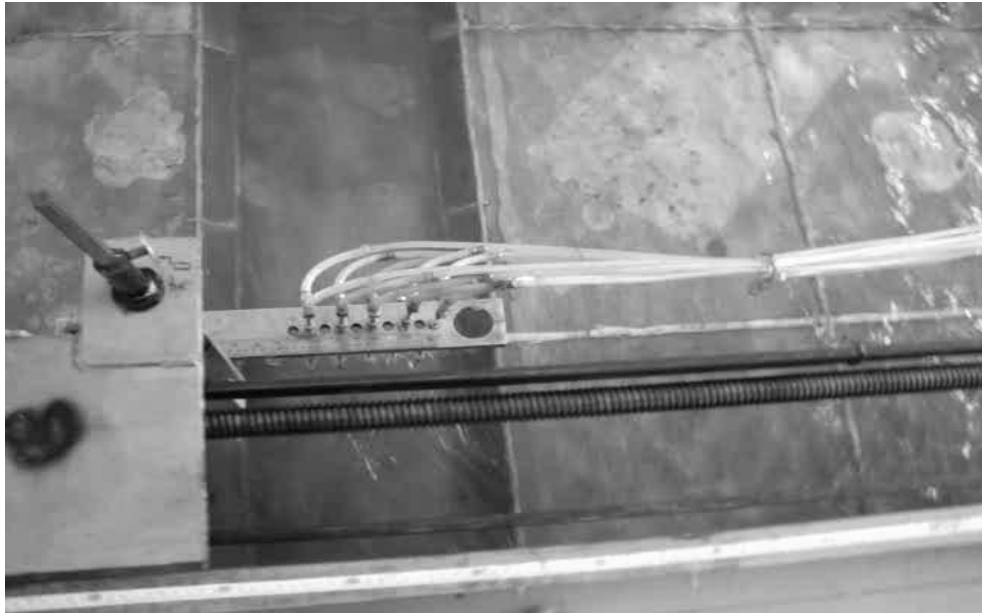


Fig.3-8 Overbank Flow Measurement in Straight Channel (Looking From Top)



Fig.3-9 Fabrication of Meandering Compound Channel in Progress



Fig.3-10 Photograph of Bell mouthed Entrance



Fig.3-11 Flooded Meandering Compound Channel

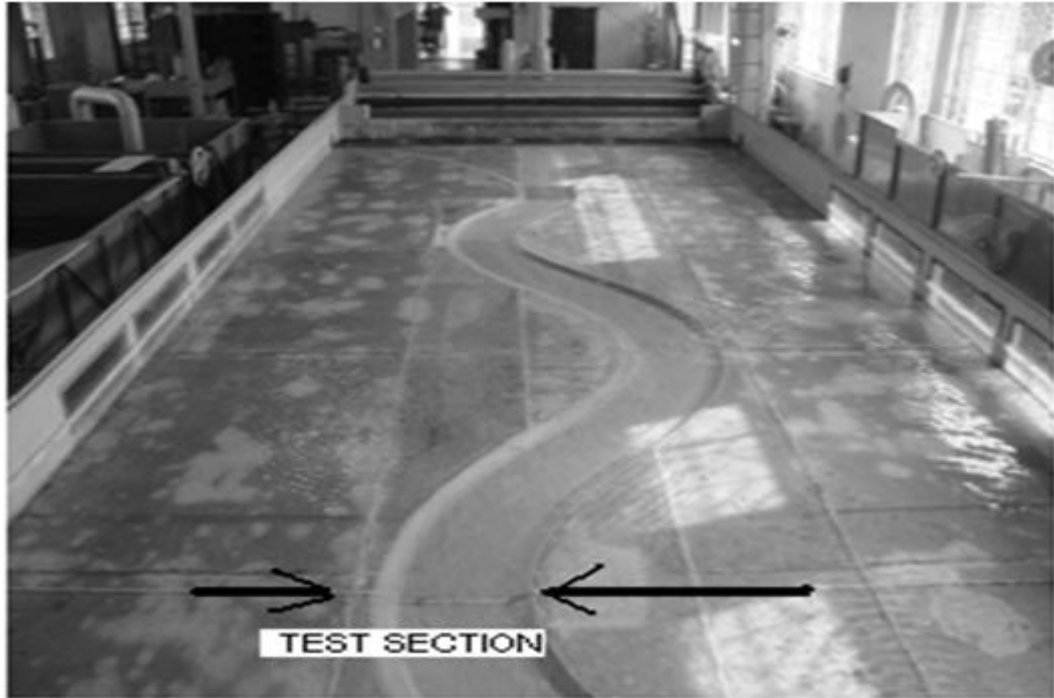


Fig.3-12 Photo of Test Reach at the Third Bend Apex of Meandering Compound Channel

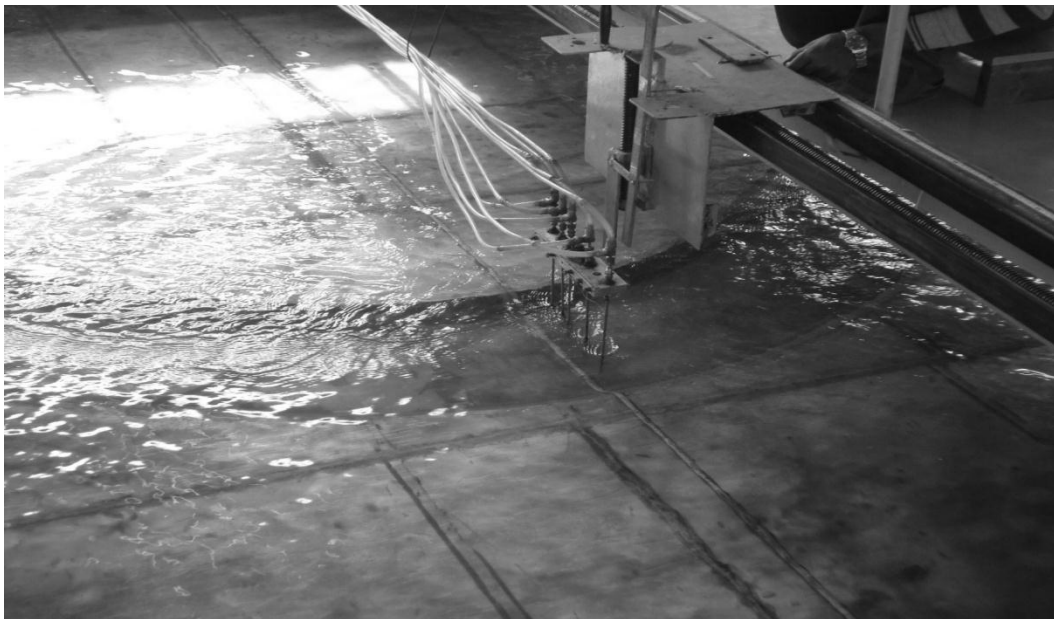


Fig.3-13 Photo of Overbank Flow Experiment in Meandering Compound Channel

3.1.2. Fabrication of Channels

Both the straight compound channel and meandering compound channel have same main channel dimensions and same width of total floodplains. The cross section of the main channel in both cases is trapezoidal in shape with bottom width ($2b$) dimension of 330mm, height (h) of 65 mm and side slope value of 1V:1H. The overall width of floodplains ($2B$) in case of straight channel is 395cm with symmetric floodplain of width (B) lying on either side of center of the main channel. However though total width of left and right floodplains in case of meandering compound channel is still 395cm but due to meandering nature of the channel path, floodplains on left and right are of unequal width.

Flow analysis in straight and meandering compound channels with wide floodplains being the primary aim of the research, experiments were planned to study both type of compound channels keeping the geometry and surface roughness constant. Accordingly only rigid bed channels were designed for both straight and meandering compound channels, by using the Perspex Sheets (6 to 10 mm thick and having Manning's n value=0.01) for creating the desired physical flow domain. The sheets were cut to designed shape and dimensions, glued with chemicals and then were put in position inside the rectangular steel flume built especially for the purpose. The roughness was maintained uniform in main channel and floodplains to investigate the impact of momentum transfer in compound channels due to only the geometrical parameters such as sinuosity, width ratio etc.. For the meandering compound channel, a 40° sine generated curve was chosen as the centerline of the path for the main channel (Sinuosity, $S_r=1.11$ where sinuosity is the ratio of thalweg length to the valley length of the main channel) as sine generated curves closely approximated the shape of real (regular) river meanders (da Silva et al, 2006; Langbein & Leopold, 1966) whereas the floodplains were made to run straight thus mimicking a natural river flanked by unsymmetrical adjoining floodplains on either side. Fig.3.15 shows the dimensions of the main channel and floodplains for the straight compound channel and Fig.3-17 shows the dimensions for the meandering compound channel. The model for the meandering compound channel was built after the experiments were over in straight compound channel.

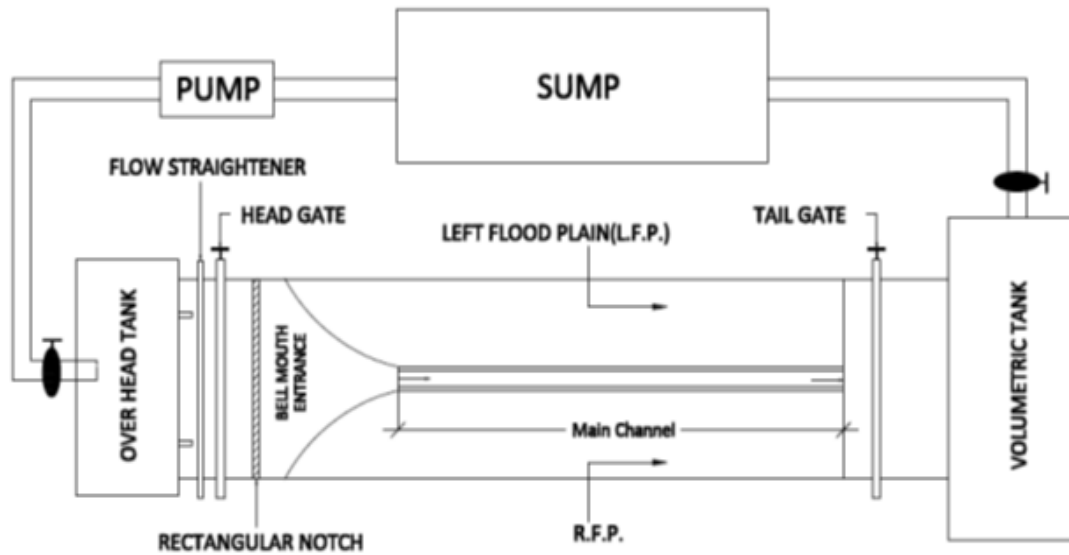


Fig.3-14 Experimental Setup of Straight Compound Channel

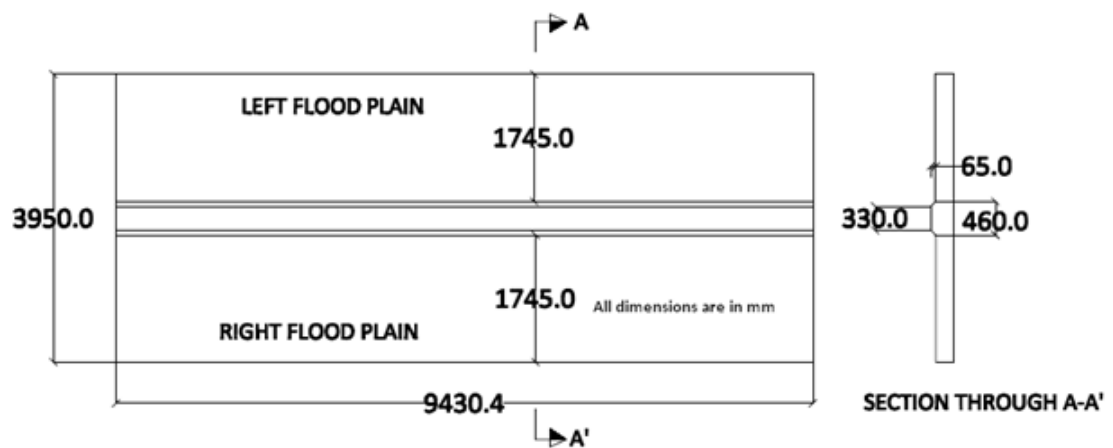


Fig.3-15 Plan view of Straight Channel (Top) & Flow Section (Side)

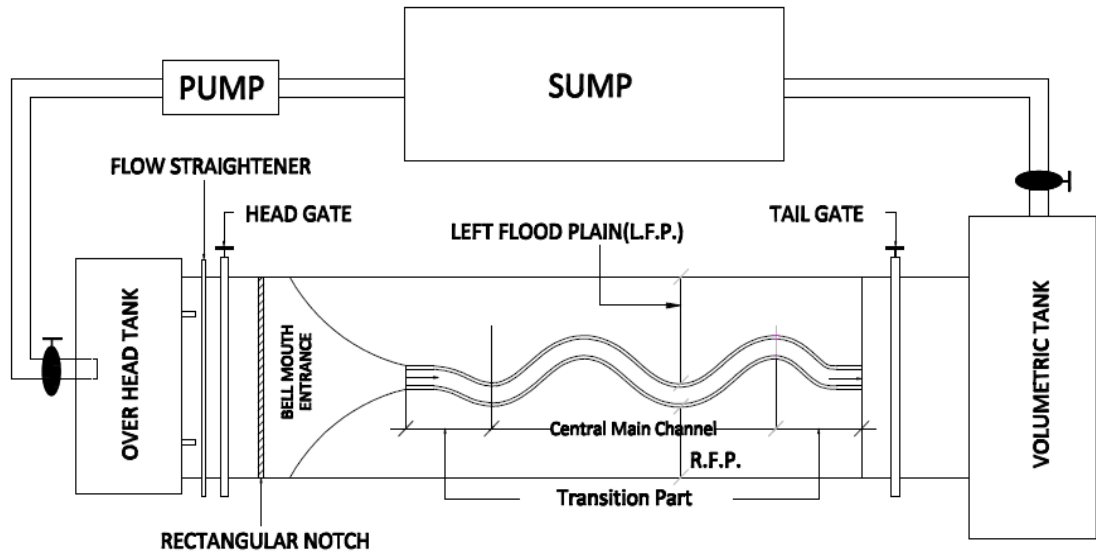


Fig.3-16 Experimental Setup of Meandering Compound Channel

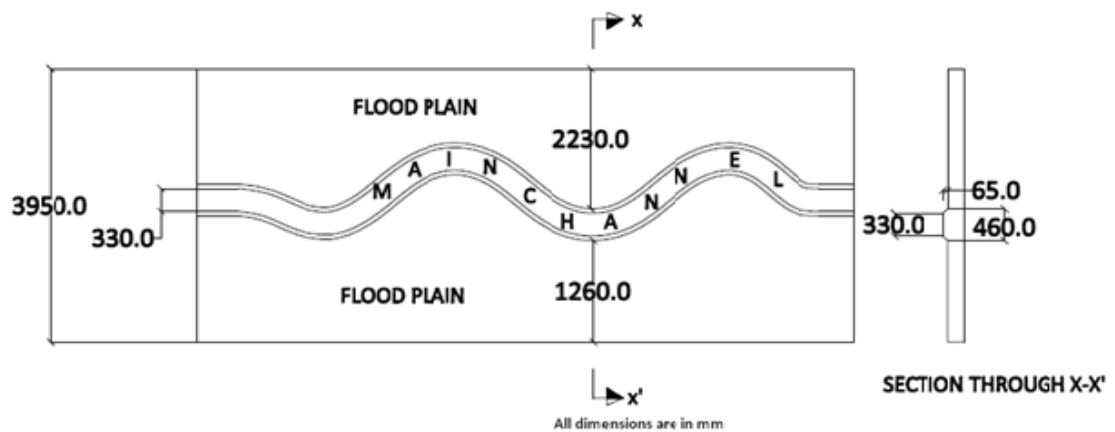


Fig.3-17 Plan view of Meandering Channel (Top) & Flow Section (Side)

Fig. 3-18 shows the trapezoidal section of the main channel whereas Figs.3-19 & 3-20 show the dimensions of left and right floodplains for the straight and meandering compound sections at the test reaches respectively for the channels. The test reach for the straight channel was selected at a length of 8m from the bell mouthed entrance whereas that of meandering compound channel was at the third bend apex from the u/s side of the channel. The geometrical parameters of the sine generated curve used in the meandering channel are as shown in the Fig.3-21 as well as in Table.3-1 along with those of straight compound channel.

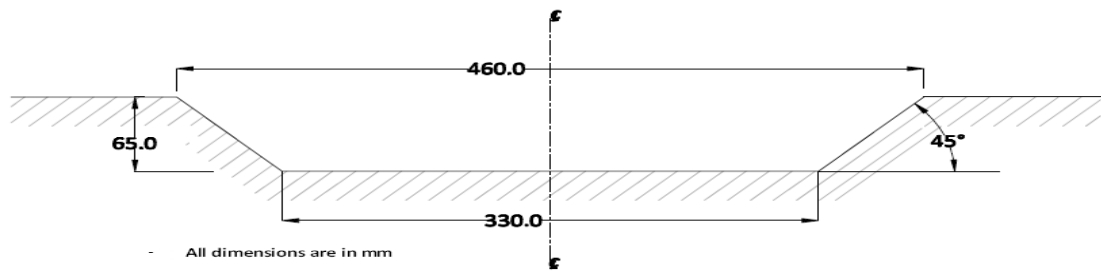


Fig.3-18 Cross Section of Main Channel

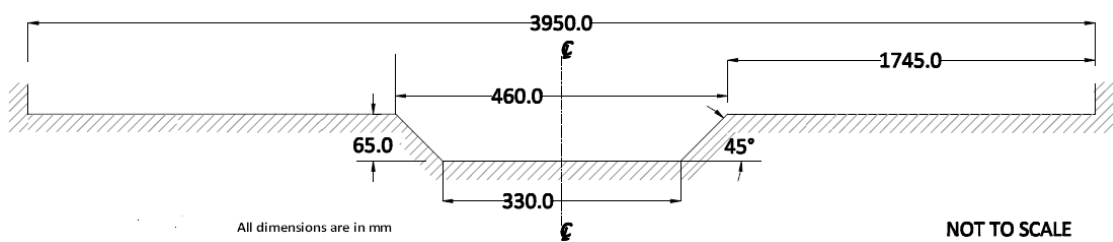


Fig.3-19 Cross Section of Straight Compound Section at Test Reach

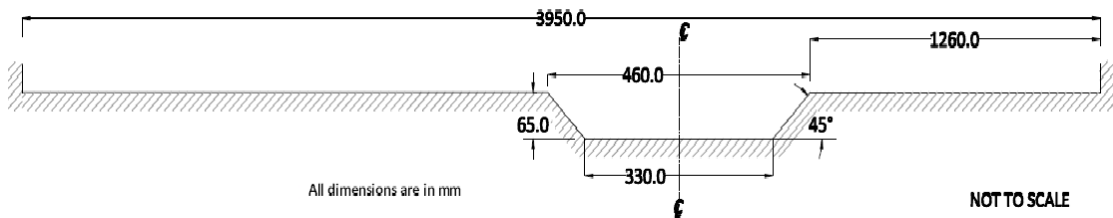


Fig.3-20 Cross Section of Compound Meandering Section at Test Reach

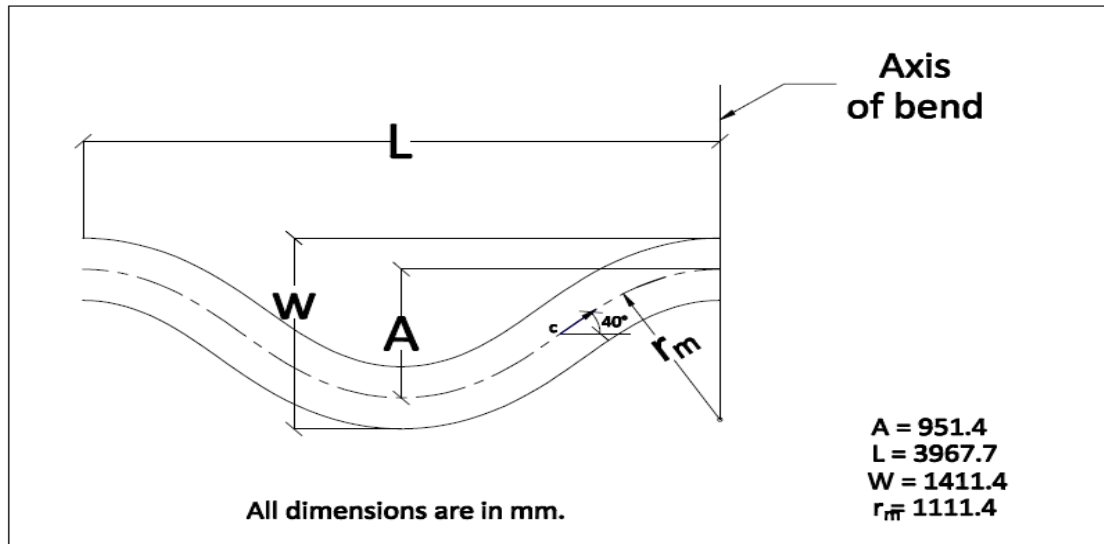


Fig.3-21 Geometrical Details of the Sine Generated Curve Used in Meandering Channel

3.2 EXPERIMENTAL PROCEDURE

3.2.1. Determination of Bed Slope (S)

All the experiments in straight and meandering compound channel were to be done under subcritical flow conditions. Accordingly the flume was given a mild bed slope of value of 0.0011 so that water could flow in the inside channels under gravity. For imparting this desired slope, the flume was tilted by operating the gear mechanism on trial basis. The flume was sealed on the d/s end with sealing putty so that a water tight chamber could be created for impounding water inside the margins of the flume. The traverse bridge with the point gauge (least count 0.1mm) was moved back and forth along the channel length measuring the depth of water at some predetermined points and hence the difference in water surface elevation in a given length, say 1m. By dividing the drop in water surface along two points with their longitudinal distance, the slope could thus be determined. Readings for several such pairs of points on channel bed both on main channel as well as on floodplains with known distance apart were thus taken and mean bed slope was then computed. Thus by changing the inclination of flume on several trials, necessary bed slope could be achieved for the channels and thereafter the gear mechanism was locked in that position to keep the flume and channels inside permanently tilted in a particular slope. The same procedure was

repeated intermittently to check the bed slope for both straight and meandering compound channel.

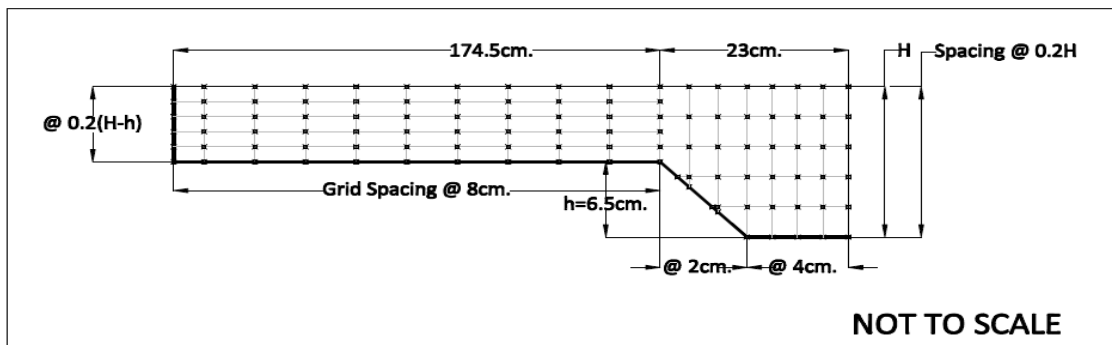


Fig.3-22 Grid Points for Measurement of Boundary Shear & Velocity in Straight Compound Channel

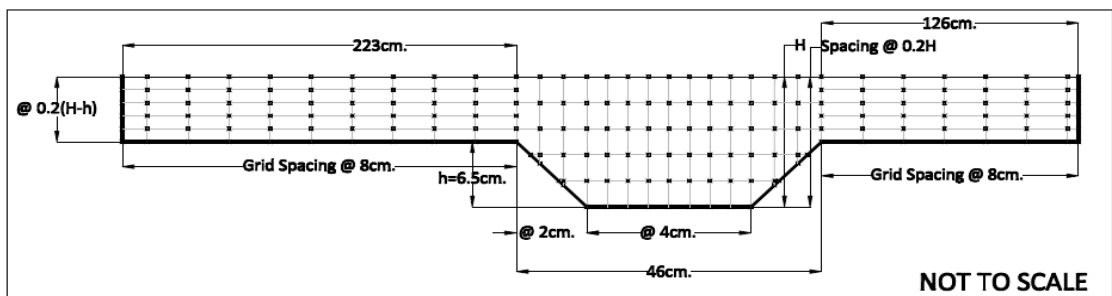


Fig.3-23 Grid Points for Measurement of Boundary Shear & Velocity in Compound Meandering Channel

3.2.2 Establishment of Quasi-Uniform Flow

Ideally open channel flow investigations should be conducted under uniform flow condition where water surface slope or friction slope (S_f) is equal to Bed slope (S) but this condition is quite difficult to achieve practically in the laboratory especially for both straight compound channel and meandering compound channel as pointed out by several previous researchers (Shiono et al. 1999; Terrier, 2010). At best a quasi-uniform flow could be made possible where a maximum discrepancy of 4% in measured longitudinal velocity magnitudes at several points in straight compound channel and a maximum discrepancy of 2% in the value of water surface slope and bed slope at a no. of points on the curved main channel of meandering compound channel were accepted as the criteria for the establishment of the same.

Table.3-1 Geometrical Details of Experimental Channels

Sl.No.	Description	Straight Compound Channel	Meandering Compound Channel
1	Type of main channel	Trapezoidal	Trapezoidal
2	Main channel bottom width (2b)	33cm	33cm
3	Bank full Depth of main channel	65mm	65mm
4	Top width of compound section (2B)	395cm	395cm
5	Side slope of main channel	1V:1H	1V:1H
6	Bed slope of the channel (S)	0.0011	0.0011
7	Sinuosity (S_r)	1.00	1.11
8	Type of floodplains	Symmetrical	Unsymmetrical
9	Roughness criteria	Rigid and smooth main channel & smooth floodplains	Rigid and smooth main channel & smooth floodplains
10	Type of main channel path	Straight	Sine generated curve
11	Crossover angle	-----	40^0
12	Meander belt width (W)	-----	141.14cm
14	Amplitude (A)	-----	95.14cm
15	Wavelength (L)	-----	396.77cm
16	Radius of curvature at bend apex (r_m)	-----	111.14cm
17	Flume size ($l \times b \times h$)	15m \times 4m \times 0.5m	15m \times 4m \times 0.5m

Thus before conducting experiments at each flow depth, water was allowed to run for sufficient time (about 4 to 6 hours) in the flume for achieving the above conditions to ensure the quasi-uniform flow in test channels.

3.2.3 Measurement of discharge & longitudinal velocity

Before beginning the detailed measurements of velocity and boundary shear, the rectangular notch was calibrated with the help of d/s volumetric tank to determine its coefficient of discharge (C_d) so that discharge entering the flume could be found out. The discharge thus measured through the notch was also cross checked for accuracy with the digital flow meter fitted to the pipes carrying supply to the flume.

It was proposed to measure the longitudinal velocity at the test reach (at 8m away from the entry point assuming the flow to be developed) in case of the straight compound channel and at the third bend apex (about 6m from inlet) in case of meandering channel under a number of inbank and overbank flow conditions. It is important to note that at the bend apex in a meandering channel the flow is directed in mean valley direction facilitating direct measurement of flow velocity through Micro-Pitot static tubes. Table 3.2 gives all hydraulic details of the experimental runs for the straight and meandering compound channels. The longitudinal velocity at predetermined points across the cross section at a no. of horizontal layers covering the entire flow depth was measured through a series of Micro-Pitot static tubes (5 nos. fitted to a steel holder) of outside diameter 4.77mm by placing the Pitot tubes normal to the flow direction. For the straight compound channel only half of the cross section was used for measurement of velocity as the compound section was symmetrical about the center of the main channel. The grid of measurement points with horizontal and vertical spacing for straight compound channel is shown in Fig.3-22. Due to very wide floodplains compared to a much narrower main channel the horizontal spacing of points was kept 4cm on the bed of the main channel and 8cm on the floodplain bed to get a proper resolution of velocity vectors. Similarly a spacing of 2cm was adopted along the inclined walls of the main channel and up to 5 layers of equal spacing was maintained (subject to feasibility of complete immersion of Pitot tubes' tips under water at varying relative depth of flow) on the floodplain. In case of the meandering channel the entire flow section at the test reach i.e. the third bend apex was used for taking measurements with the same spacing as adopted previously for the straight channel. The measurement grid for the meandering compound channel is shown in Fig.3-23. A series of five manometers consisting of a pair of piezometers open to atmosphere at one end and joined to the respective static limb (static hole at the bull nosed tip of Pitot tube) and the dynamic limb (holes around the circumference of the submerged tip) of a particular

Pitot tube at the other end through a 5m long transparent PVC tube as shown in Fig.3-7 was used for measurement of static and dynamic pressure at the given points in the flow domain.

Marking the height of water column on each limb and denoting the difference in static and dynamic pressure as Δp , by Bernoulli's equation we have

$$U = \sqrt{\left(\frac{2\Delta p}{\rho}\right)} \quad (3.1)$$

Where U is velocity and ρ is the density of water. Before taking measurements by Pitot static tubes, it was ensured that no air bubble remained anywhere inside the long PVC pipe, in Pitot tube or in the manometer. For this, continuous flow of water from the submerged end of Pitot tube in the channel to the piezometer was maintained for a while after sucking the air out of the system by miniature exhaust pumps. Also for each velocity reading for a particular grid point, the end of the Pitot tube was allowed to remain stationed at that point for at least 5minutes as liquid columns in both the piezometers used to fluctuate preventing accurate measurement of pressure difference for about that period before remaining stable.

3.2.4. Measurement of Depth averaged velocity

The depth-averaged velocity U_d is defined by the equation

$$U_d = \frac{1}{H} \int_0^H U dy \quad (3.2)$$

and shown in Fig.3-24. U_d is a very important parameter along with the boundary shear stress in all compound channel flow studies and needs to be measured with sufficient accuracy to determine its distribution across the flow section with varying relative depth (β) as well as for the estimation of unit discharge. It has been shown by various previous studies that the depth averaged velocity at a particular section in a channel is the point velocity magnitude measured at a flow depth of $0.4H$ (Chaudhry, 2008; Rantz et al,1982) in case of main channel from the channel bottom or at $0.6H$ from water surface. Similarly over floodplains the depth averaged velocity is to be taken as the

Table.3-2 Hydraulic Details of the Experimental Runs

Sl. No.	Description of Items		Straight Compound Channel	Meandering Compound Channel
1	Number of runs for stage-discharge data	Simple channel	Inbank 10nos.	Inbank 10nos.
		Compound channel	Overbank 6 nos.	Overbank 10 nos.
2	Discharge in cm^3/s for detailed measurement	Inbank flow	3850, 4387, 6241, 7155, 7378	578, 3257, 3518, 3876, 4244, 5518, 6355, 6913
		Overbank flow	13543,17482,36396,53546, 60282,106181	17074,27617,47245, 55393,80667
3	Depth of flow in cm for flow discharges of runs at sl.2	Inbank flow	3.00,3.50,5.00,6.20,6.50	1.59,3.3,3.75,4.22, 5.25,5.38,5.72,6.2
		Overbank flow	7.3,7.5,8.8,10.1,10.5,11.5	8.06,8.55,9.5,10.2,11.0
4	Relative depth β		0.110, 0.133, 0.261, 0.356, 0.381, 0.435	0.194, 0.240, 0.316, 0.363, 0.409
5	Nature of surface		Smooth main channel & floodplains	Smooth main channel & floodplains

velocity magnitude of the flow at a point lying at a flow depth of $0.4(H-h)$ where h is the main channel depth. Thus for the straight and meandering channels depth averaged velocities were measured under varying flow depths.

The rule of taking the average velocity at $0.4H$ does not apply strictly in the interface region or junction region of main channel and floodplain as is found out by taking the mean velocity from experimental values for different cases at the junction region and then comparing them with the velocity values occurring at $0.4H$ depth (Pl. see Table 3.3A & 3.3B, page-44). A search of literature was also conducted specifically to find out the issue of average velocity at this junction region but none could be found out. This variation in rule is mainly due to the large variation in velocity vector at the junction region; due to the momentum transfer occurring at the junction; due to lots of vortex formation as well as 3D mixing of the flow etc.

Table.3-3A Occurance of depth average velocity at the vertical interface for experimental runs (straight compound channel)

TOTAL DEPTH OF FLOW in STRAIGHT COMPOUND CHANNEL in cm	DEPTH OF FLOW OVER FLOODPLAIN (H-h) in cm	DEPTH AVERAGE VELOCITY (NON-DIMENSIONALISED)	OCCURANCE OF DEPTH AVERAGE VELOCITY AT THE VERTICAL INTERFACE
7.3	0.8CM	1.4	0.5 (H-h)
7.5	1.0CM	$(1.72+1.78)/2=1.75$	0.5 (H-h)
8.8	2.3CM	$(1.05+1.1+1.15)/3=1.1$	0.52 (H-h)
10.1	3.6CM	$(0.8+0.85+0.9+0.92)/4=0.86$	0.48 (H-h)
10.5	4.0CM	$(0.68+0.66+0.64+0.62+0.6+0.58)/6=.63$	0.55 (H-h)
11.5	5.0CM	$(0.83+0.85+0.9+0.95+0.98)/5=0.90$	0.53 (H-h)

Table.3-3B Occurance of depth average velocity at the vertical interface for experimental runs (meandering compound channel)

Depth of flow (H) in cm IN MEANDERING COMPOUND CHANNEL	DEPTH OF FLOW OVER FLOODPLAIN (H-h) in cm	DEPTH AVERAGE VELOCITY AT VERTICAL LEFT INTERFACE (NON-DIMENSIONALISED)	DEPTH AVERAGE VELOCITY AT VERTICAL RIGHT INTERFACE (NON-DIMENSIONALISED)	OCCURANCE OF DEPTH AVERAGE VELOCITY (AT THE VERTICAL INTERFACE-LEFT)	OCCURANCE OF DEPTH AVERAGE VELOCITY (AT THE VERTICAL INTERFACE-RIGHT)
8.06	1.56	$(3.3+3.4+3.5)/3=3.4$	$(2.6+2.5+2.4)/3=2.5$	0.46 (H-h)	0.53 (H-h)
8.55	2.05	$(3.2+3.3+3.4)/3=3.3$	$(2.6+2.7)/2=2.65$	0.55 (H-h)	0.53 (H-h)
9.5	3	$(3.9+4.0+4.1+4.2+4.3)/5=4.1$	$(2.8+2.9+3+3.1)/4=2.95$	0.54 (H-h)	0.55 (H-h)
10.2	3.7	$(4.0+4.1+4.2+4.3+4.4+4.5+4.6+4.7+4.8+4.9)/10=4.45$	$(3.6+3.7)/2=3.65$	0.54 (H-h)	0.55 (H-h)
11.0	4.5	$(4.6+4.8+5.0+5.2+5.4+5.6+5.8)/7=5.2$	$(4.3+4.2)=4.25$	0.5 (H-h)	0.55 (H-h)

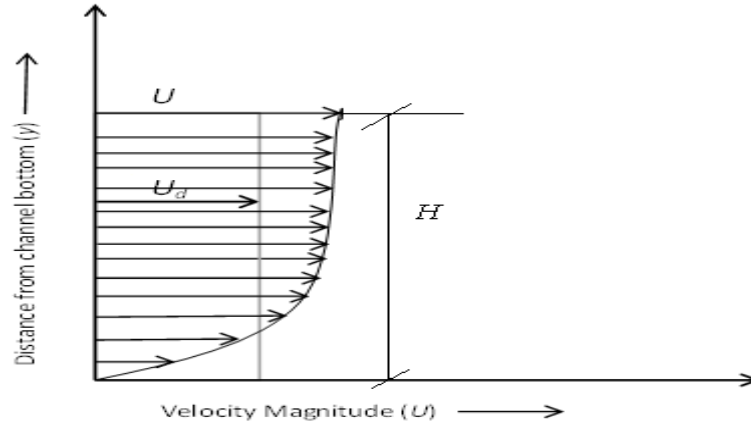


Fig.3-24 Velocity Profile & Depth Averaged Velocity in Channel

3.2.5. Measurement of Boundary Shear

The boundary shear stress (τ) across the wetted perimeter of the flow section constituting the entire compound section of the main channel and the floodplains was measured by Preston tubes. This was done to evaluate or determine the interaction mechanism on the distribution of boundary shear stress across the wetted flow perimeter. The points lying on the channel boundary of the grids (in Figs.3-22 & 3-23) used for straight and meandering compound channel only were used for measurement of skin friction or flow resistance. In other words the readings which were taken previously on the boundary points for velocity measurement were used for computation of boundary shear stress with the help of Patel's method of calibration (Patel, 1965) for Preston tubes. As per Patel (1965) the difference in static and dynamic pressure values (Δp) observed respectively in the static holes and dynamic holes of the Preston tube immersed in the boundary layer of the flowing liquid can be used to measure indirectly the point boundary shear stress over the solid boundary with an accuracy of $\pm 6\%$. For mathematical computations of the boundary shear stress, Patel (1965) suggested a number of relationships which are as follows.

$$y^* = 0.50x^* + 0.037, \quad 0 \leq y^* < 1.50 \quad (3.3)$$

or $0 \leq x^* \leq 2.9$

$$y^* = -0.0060x^{*3} + 0.1437x^{*2} - 0.1381x^* + 0.8287, \quad 1.50 < y^* < 3.50 \quad (3.4)$$

or $2.9 \leq x^* \leq 5.6$

and

$$x^* = y^* + 2\log_{10}(1.95y^* + 4.02), \quad 3.50 < y^* < 5.30 \quad (3.5)$$

or $5.6 \leq x^* \leq 7.6$

with
$$x^* = \log_{10} \left(\frac{(\Delta p)d^2}{4\rho v^2} \right) \quad (3.6)$$

and
$$y^* = \log_{10} \left(\frac{\tau d^2}{4\rho v^2} \right) \quad (3.7)$$

where, d is the external diameter of the Preston tube and v is the kinematic viscosity for the liquid. Accordingly out of the equations (3.3-3.5) the appropriate one was chosen for computing the wall shear stress based on the range of x^* values. After that the shear stress values were integrated over the entire perimeter to calculate the total shear force per unit length normal to flow cross section carried by the compound section. The total shear thus computed was then compared with the resolved component of weight force of the liquid along the stream wise direction to check the accuracy of the measurements and the same was given in Table 3.4. The error percentages are found out to be within $\pm 10\%$.

Table 3.4 : Comparision of calculated shear force with energy gradient approach

Straight compound channel	Relative flow depth(β)	Total shear force from energy gradient approach (N)	Total shear force from Preston tube measurement (N)
1	0.110	0.618	0.574
2	0.133	0.703	0.648
3	0.261	1.257	1.153
4	0.356	1.811	1.648
5	0.381	1.982	1.843
6	0.435	2.408	2.277
Meandering compound channel	Relative flow depth(β)	Total shear force from energy gradient approach (N)	Total shear force from Preston tube measurement (N)
1	0.194	0.942	0.886
2	0.240	1.151	1.083
3	0.316	1.555	1.462
4	0.363	1.854	1.719
5	0.409	2.195	2.110

EXPERIMENTAL RESULTS

4.1 GENERAL

In this section all the results regarding stage-discharge curves, longitudinal velocities, depth averaged velocities; boundary shear distributions etc. from the new experiments conducted in the channels of NIT, Rourkela are presented. As some measurements were taken in inbank conditions (simple channel type) and some others were taken for overbank conditions (compound channel type) for each of the straight and meandering channels, so accordingly separate subsections deal with the results of each type.

4.2 STRAIGHT CHANNEL

4.2.1 Stage –discharge curve

The stage-discharge relationship for the straight compound channel with wide floodplains experiments is presented through the $H \sim Q$ curve in Fig.4-1. The curve is segregated into two segments i.e. the lower portion having a sharp gradient for the inbank flow conditions and the upper part having a mild or moderate gradient typical of overbank flow conditions in a compound channel separated by a dotted horizontal line drawn at the bank full level. The rating curve in the overbank flow cases for the channel is in the form of discharge (Q) varying as a power function of flow depth (H) in the main channel and the same is given as

$$Q = 0.7596H^{0.2361} \quad (4.1)$$

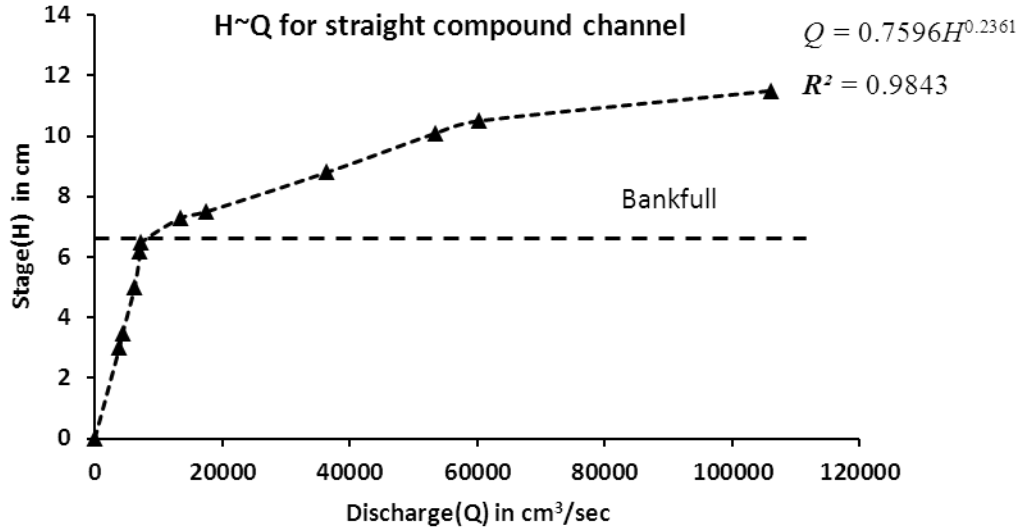


Fig.4-1 Stage-Discharge curve for straight compound channel of NIT, Rourkela

4.2.2 Longitudinal velocity

The streamwise or longitudinal point velocities (U) were measured for different flow depths of inbank and overbank flow at different grid points (shown in Fig.3-22). The velocity magnitude at each point was then normalized with sectional mean velocity (U_{av}) for that flow rate and contour maps or isovels were prepared over the flow section for different in bank and overbank depths. Figs. 4-2 (a-e) shows the isovels for inbank flow cases while Figs. 4-3 (a-f) shows the same for overbank flow cases in straight compound channel. The longitudinal velocity for low inbank cases in straight compound channel is well distributed across the cross section with the difference between the section mean value and maximum value is small. With the rising flow depth, the velocity gradient becomes more. This is due to higher and higher velocity magnitude occurring for the central flow region.

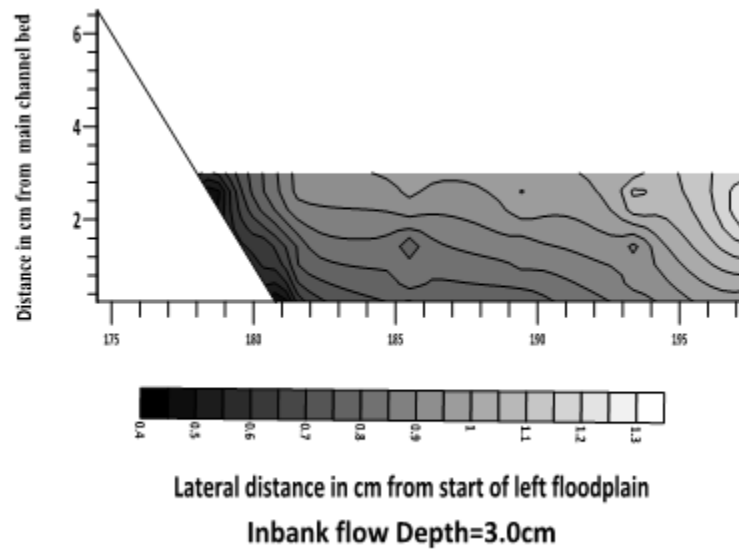


Fig.4-2(a) Isovels for inbank flow in straight compound channel

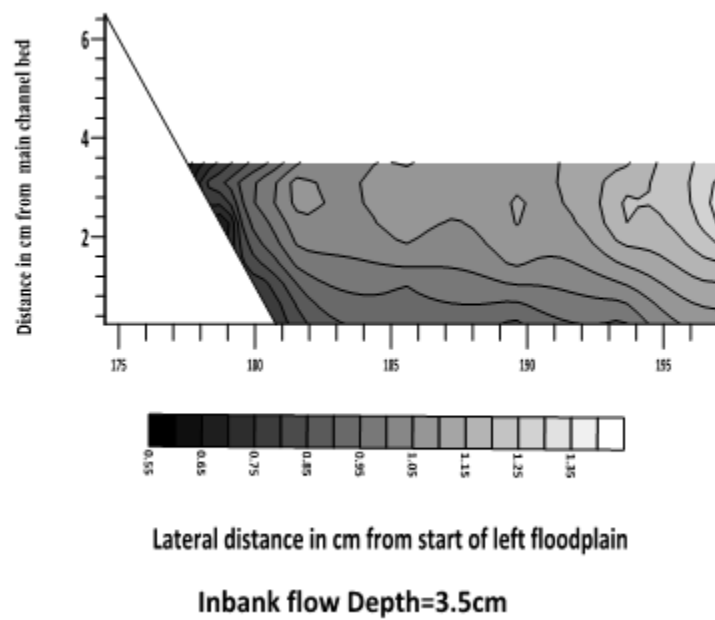


Fig.4-2(b) Isovels for inbank flow in straight compound channel

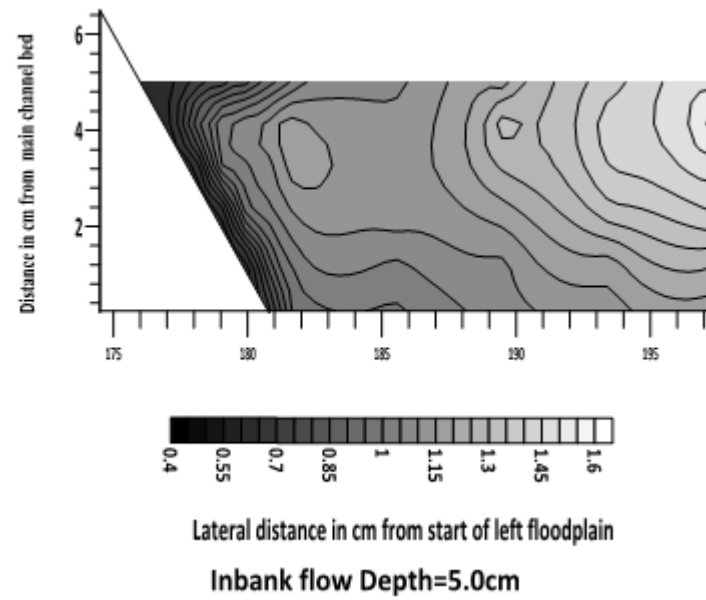


Fig.4-2(c) Isovels for inbank flow in straight compound channel

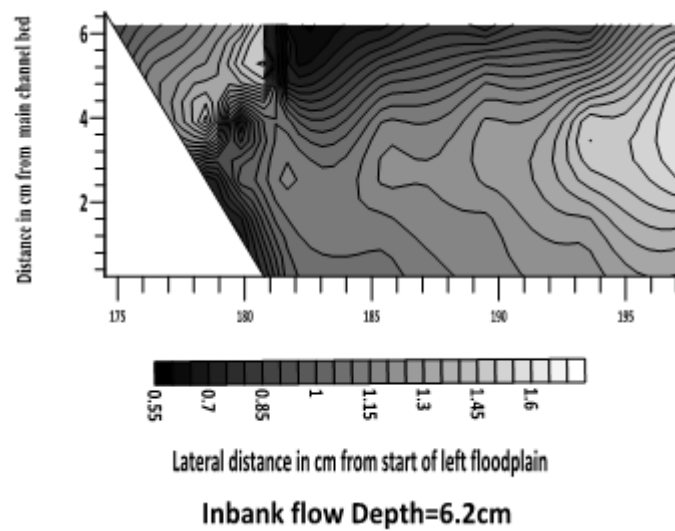


Fig.4-2(d) Isovels for inbank flow in straight compound channel

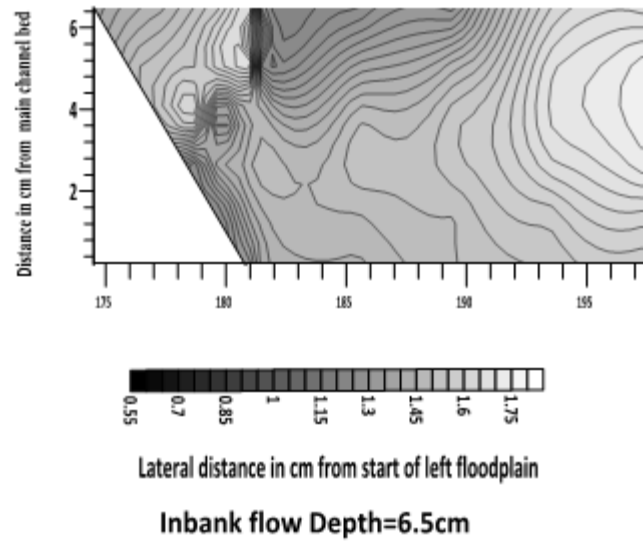


Fig.4-2(e) Isovels for inbank flow in straight compound channel

For overbank cases at low relative depth the main channel flow and floodplain flow is in sharp contrast with each other. The flow in main channel is affected by slow moving floodplain flow due to the sharp difference in velocity magnitudes of the two. The velocity magnitude in central main channel region is much higher as compared to initiation of flow over the floodplains. This interaction effect seems to be more pronounced at low overbank cases of Figs. 4-3 (a-c). The rise in flow depth causes more flow to occur now over the floodplains and the floodplain flow is having almost equal velocity magnitude as compared to the main channel flow velocity as in latter cases of Figs. 4-3 (d-f). The large contribution of flow due to a wide floodplain is less influenced by the comparatively smaller main channel flow.

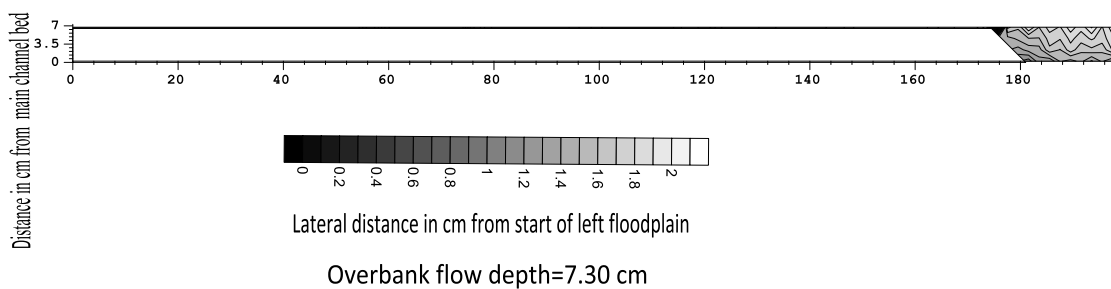


Fig.4-3(a) Isovels for overbank flow in straight compound channel

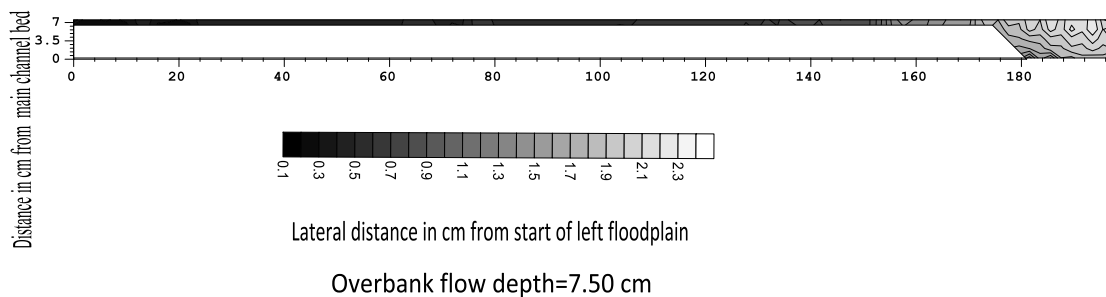


Fig.4-3(b) Isovels for overbank flow in straight compound channel

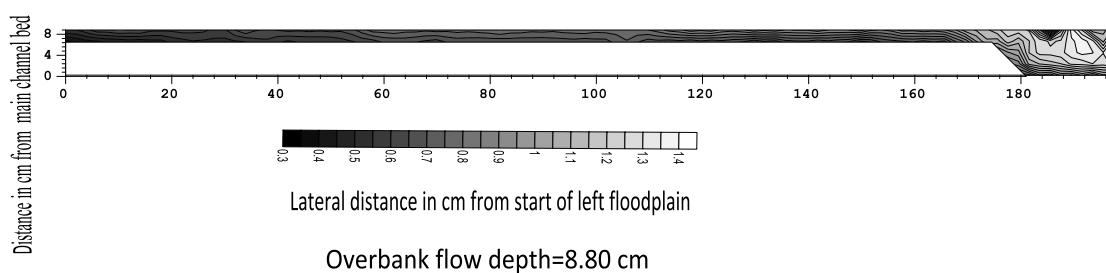


Fig.4-3(c) Isovels for overbank flow in straight compound channel

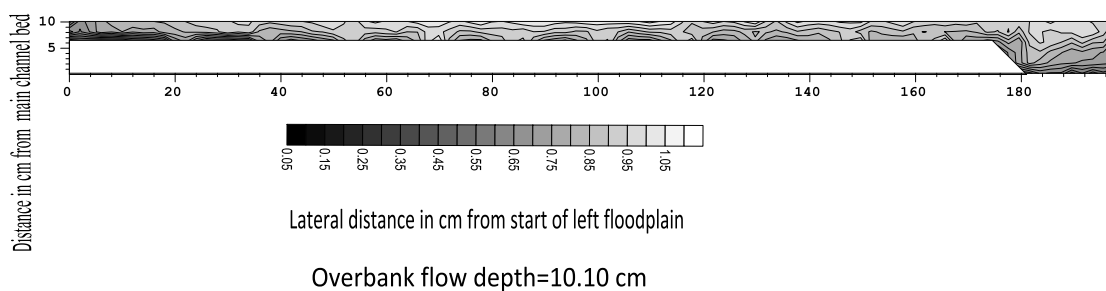


Fig.4-3(d) Isovels for overbank flow in straight compound channel

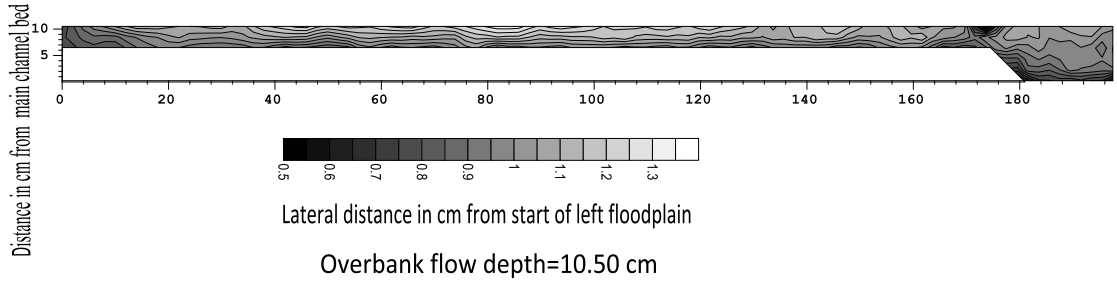


Fig.4-3(e) Isovels for overbank flow in straight compound channel

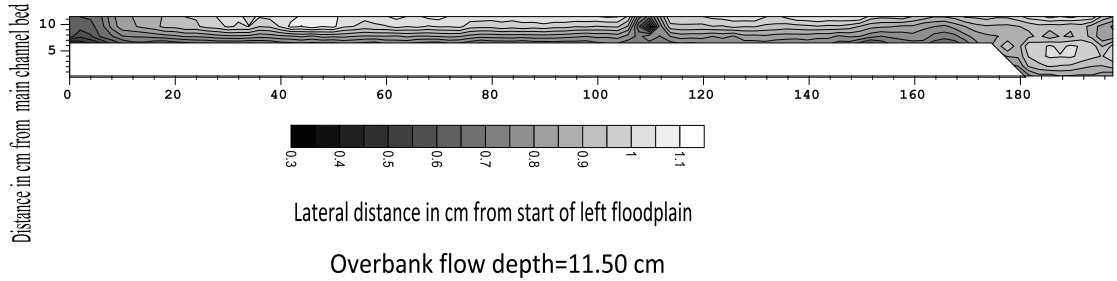


Fig.4-3(f) Isovels for overbank flow in straight compound channel

4.2.3 Depth averaged velocity

The depth averaged velocity (U_d) for all the inbank and overbank cases were also measured for the straight trapezoidal channel. The same are shown normalized with the sectional mean velocities of respective flow cases. For different inbank cases the depth averaged velocity distribution curves are plotted and shown in Figs. 4-4 (a-e) and it is seen that in each case the maximum value occurs above the center of the main channel. The distribution curve rises monotonically from the end of the main channel wall to the center of main channel bed except the case of depth at 3.50 cm as in Fig 4.4(b). For overbank cases (shown in Figs. 4-5 (a-f)) the effect of momentum transfer is seen. The depth averaged velocity curve is at its peak over the central main channel region and it falls sharply at the interface of main channel and floodplains due to intense momentum transfer particularly in low overbank cases (cases a, b & c in Fig. 4-5). As the effect of momentum transfer is less in far regions of the floodplain, so the curve nearly continues as a horizontal line beyond the effects of shear layer. For the latter three cases with higher overbank flows (cases d, e & f in Fig. 4-5) this effect of momentum transfer is not so pronounced and the depth averaged velocity magnitudes are nearly constant over the entire flow domain. This occurs due to very large floodplain flow area overshadowing the comparatively smaller main channel flow in the present wide straight compound channel.

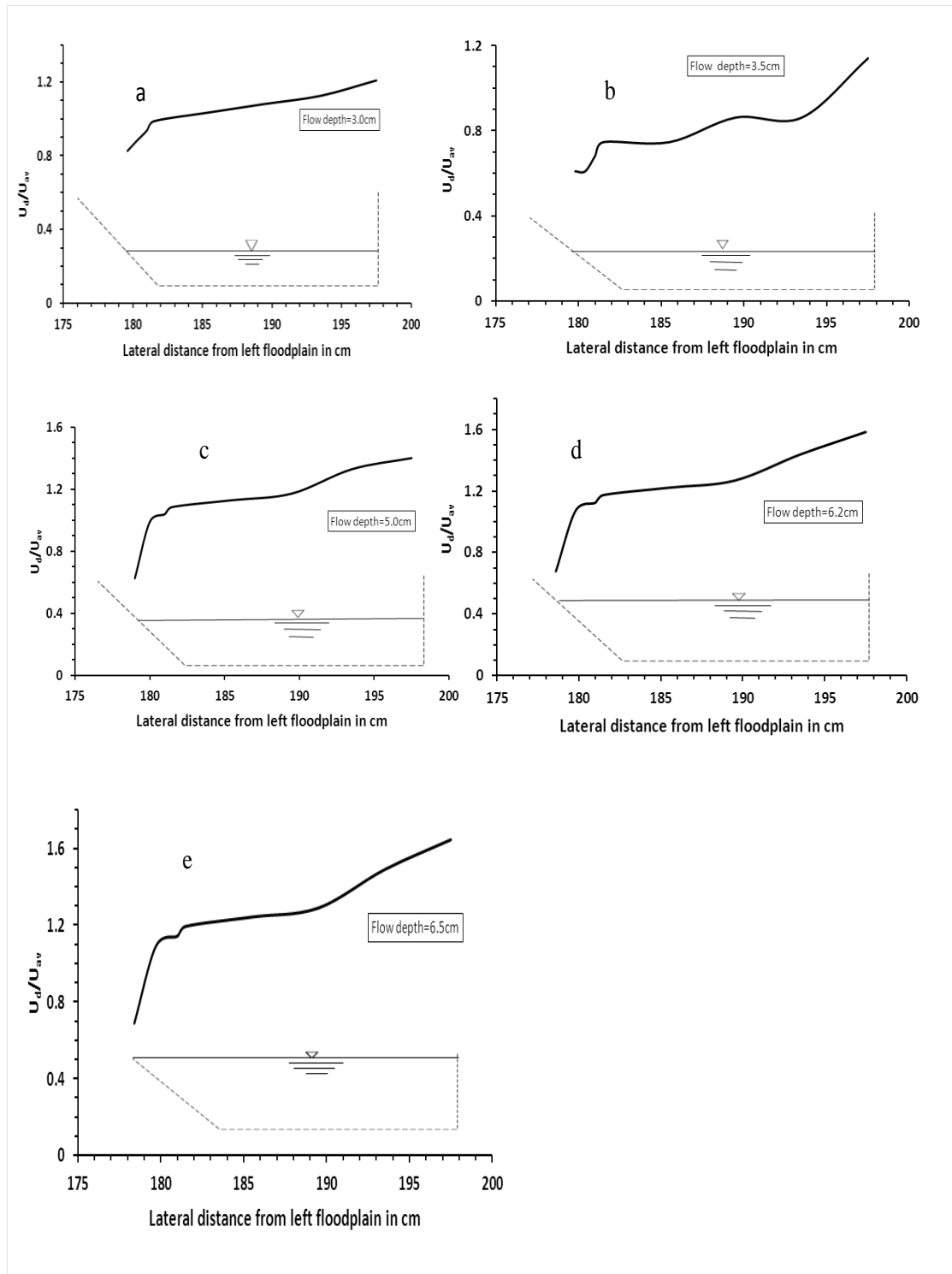


Fig.4-4 (a-e): Depth averaged velocity distribution in straight compound channel-inbank flow.

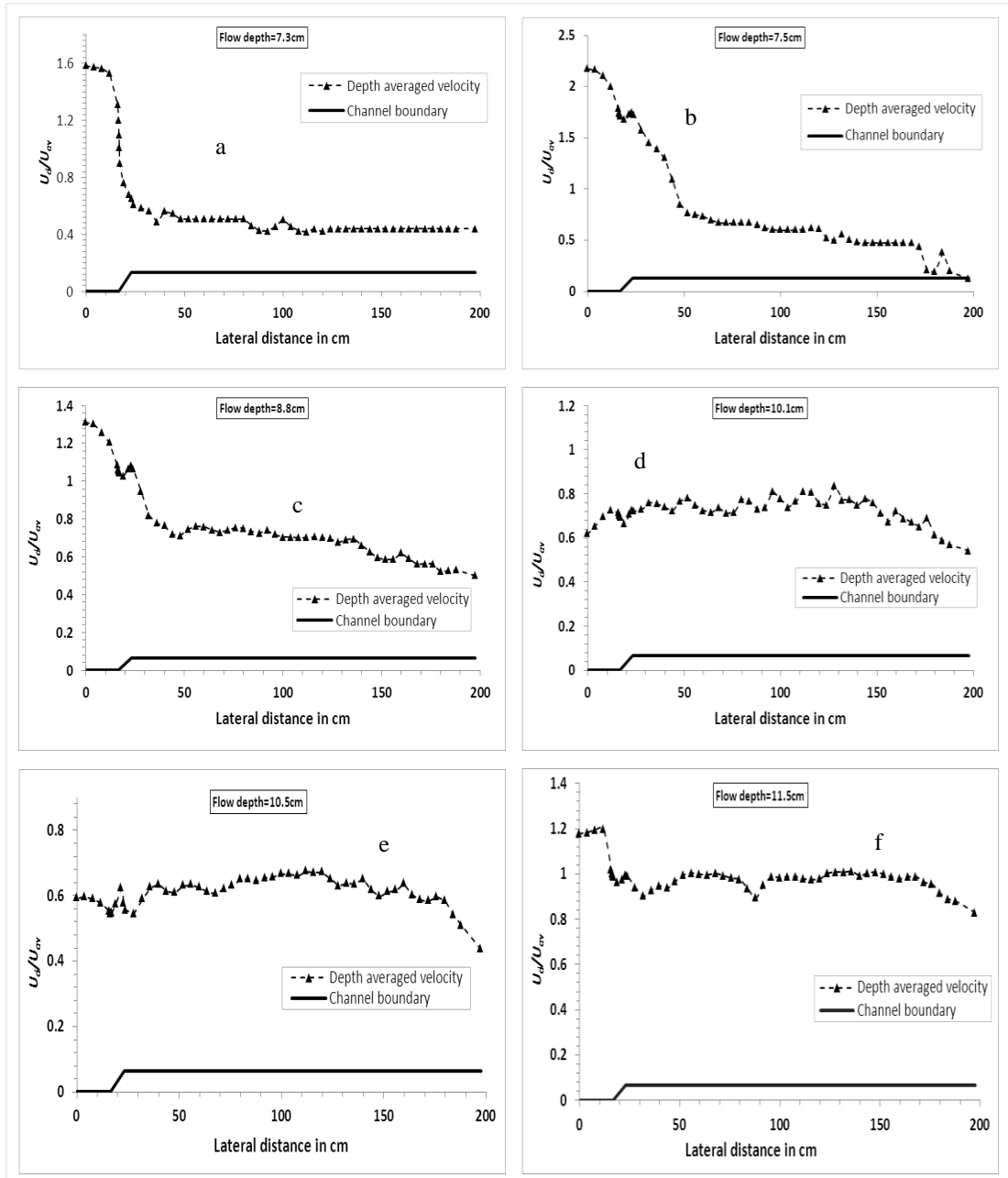


Fig.4-5 (a-f) Depth averaged velocity distribution in straight compound channel-overbank flow.

4.2.4 Boundary Shear stress

4.2.4.1 Inbank cases

The measured point boundary shear stresses (τ) are plotted across the flow domain for inbank flow cases in Figs. 4.6 (a-e). The distribution for inbank cases shows that the maximum value of flow resistance always occurs at the center of main channel bed.

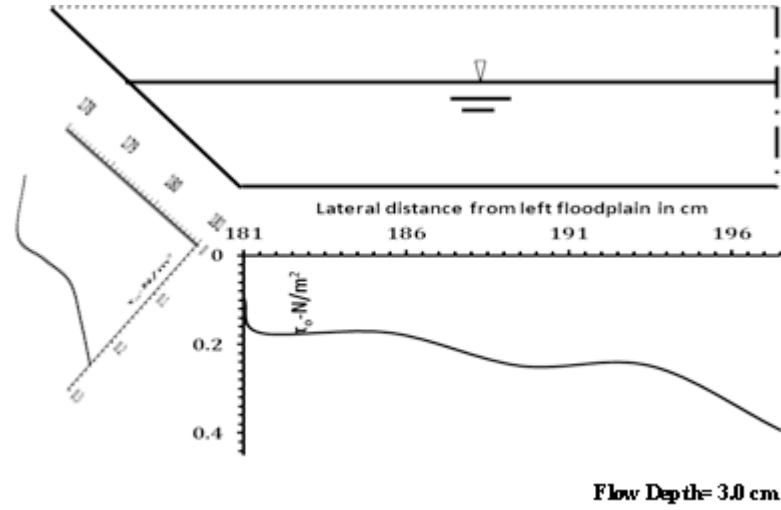


Fig.4-6(a) Shear stress distribution for inbank flow in straight channel

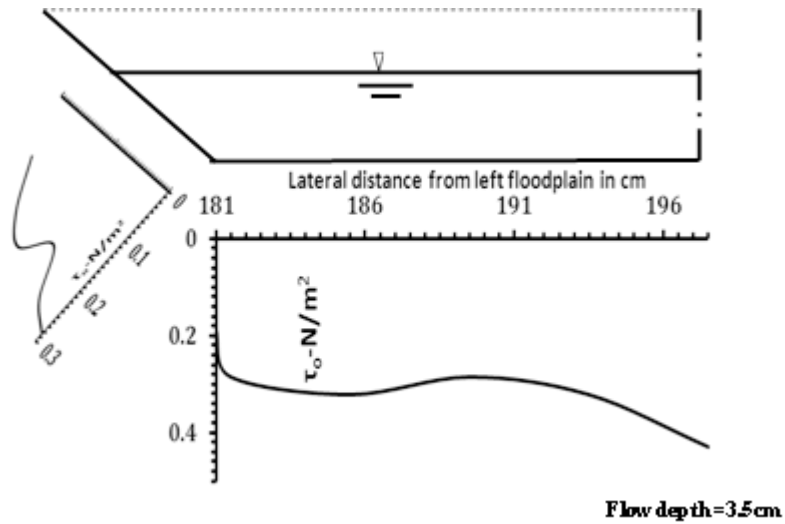


Fig.4-6(b) Shear stress distribution for inbank flow in straight channel

The magnitude of this maximum shear stress is also depth dependent with the former rising with the rising flow depth in the channel.

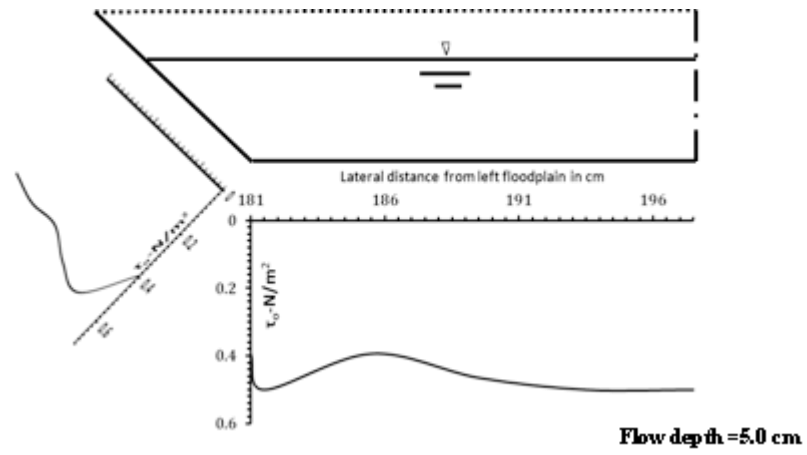


Fig.4-6(c) Shear stress distribution for inbank flow in straight channel

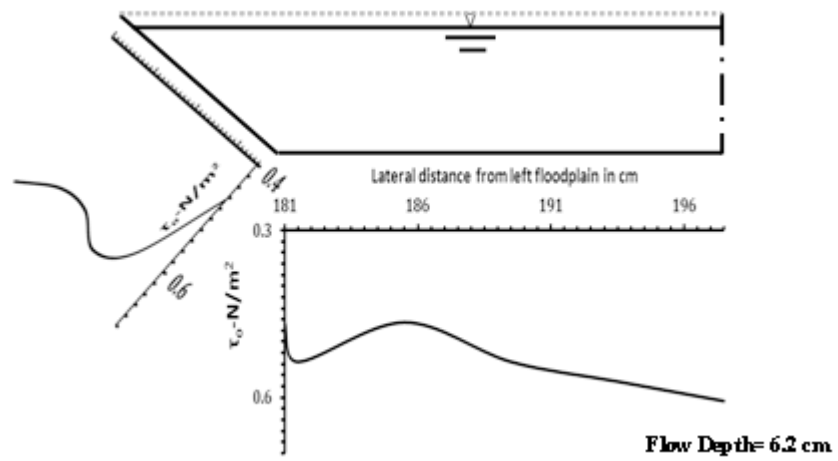


Fig.4-6(d) Shear stress distribution for inbank flow in straight channel

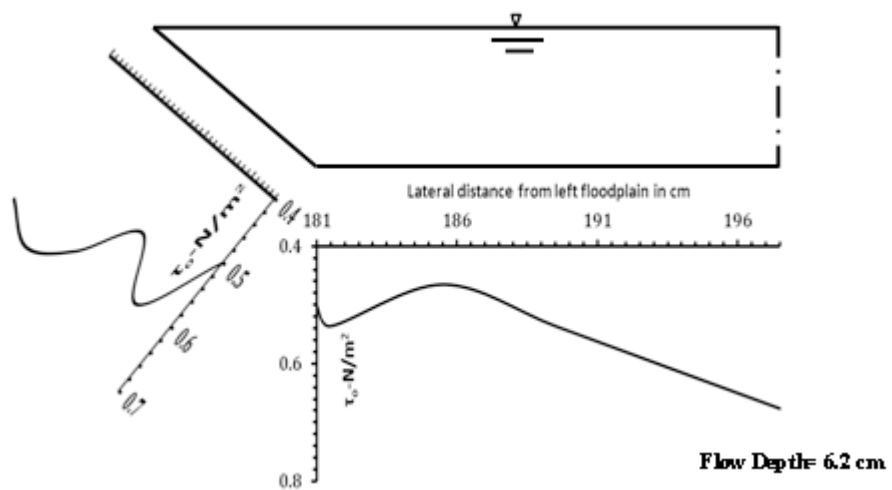


Fig.4-6(e) Shear stress distribution for inbank flow in straight channel

4.2.4.2. Overbank cases

For overbank cases the shear stress distributions are shown in Figs. 4-7 (a-f). The different flow zones such as floodplain wall, floodplain bed, main channel wall and main channel bed are shown highlighted in all these figures. For lowest overbank case (in Fig.4-7 a) it is observed that a no flow zone developed in far end of the floodplain induces zero shear stress. The shear in floodplain bed reaches highest value near the main channel, floodplain interface. The maximum shear stress though occurs at the center of the main channel bed. Gradual rise in shear stress is noticed in the respective flow zones with the rising overbank flow depth. Also the shear layer region where the maximum interaction between slow moving floodplain flow and fast moving main channel flow occurs, is prominent in initial three over bank cases (a, b & c, in Fig.4-7). Thereafter the floodplain flow seem to have encompassed the main channel flow as evident from Fig. 4-7 (d, e & f, cases) due to large shear stress magnitudes generating over the floodplain bed.

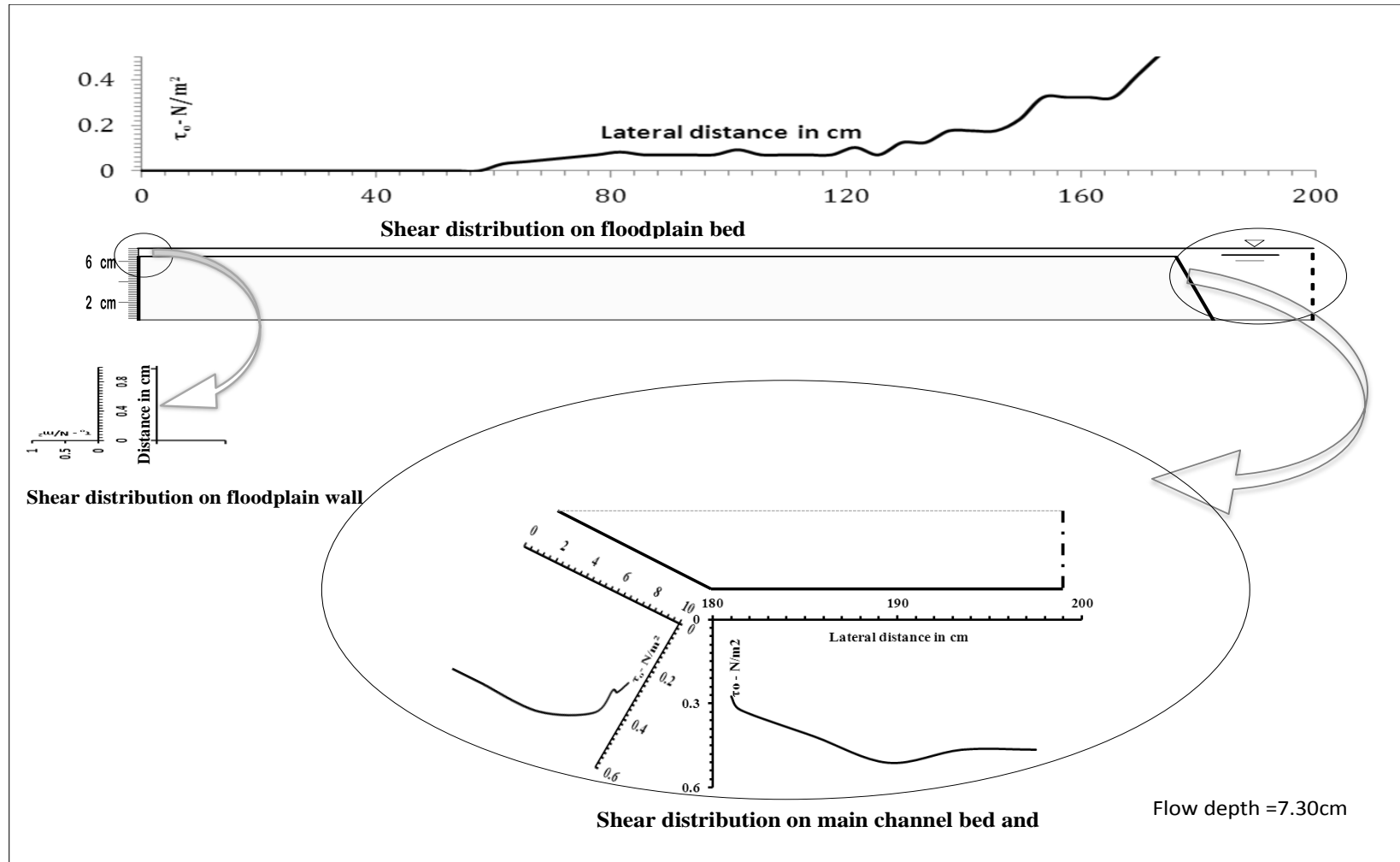


Fig.4-7(a) Shear stress distribution for overbank flow in straight channel

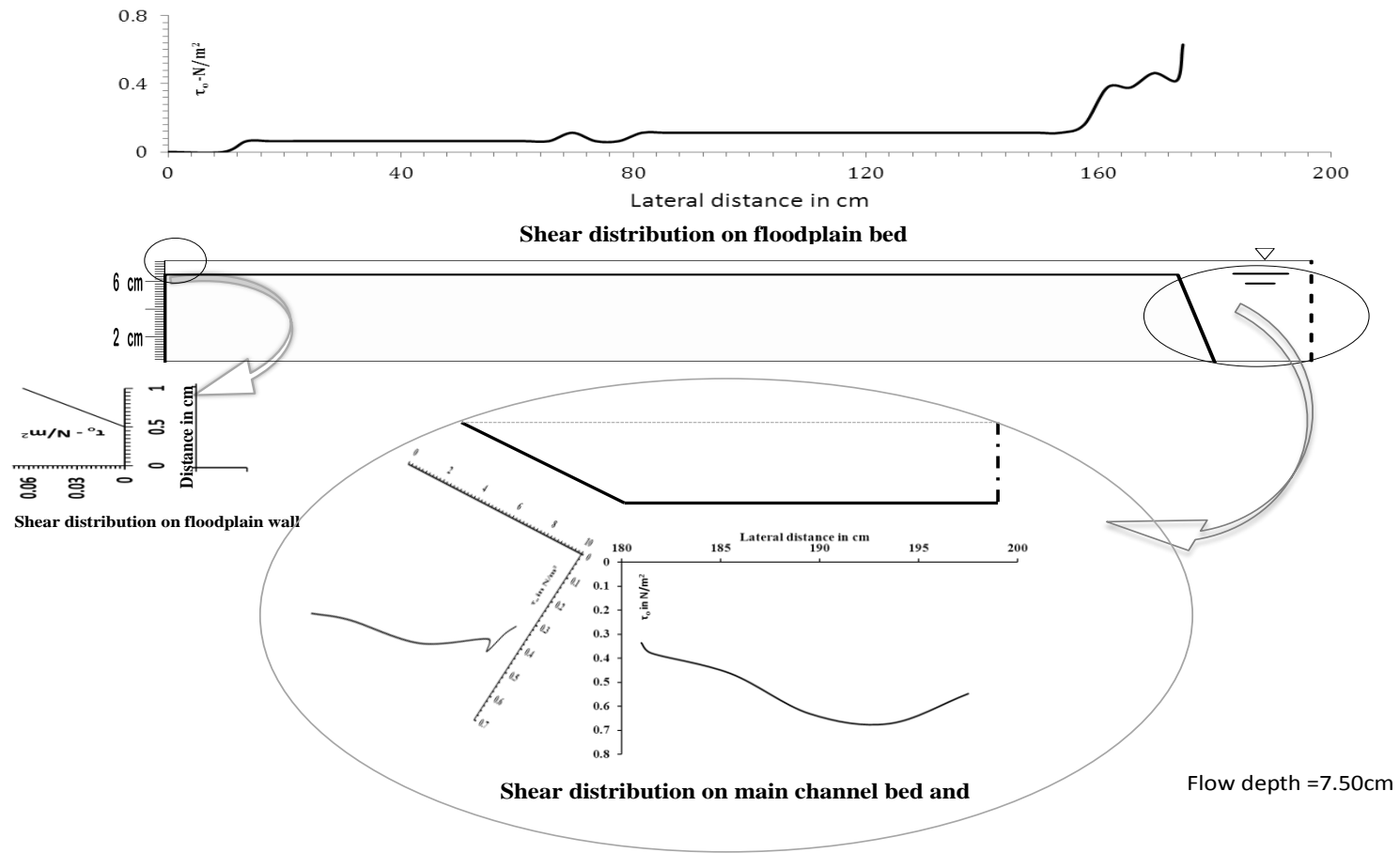


Fig.4-7(b) Shear stress distribution for overbank flow in straight channel

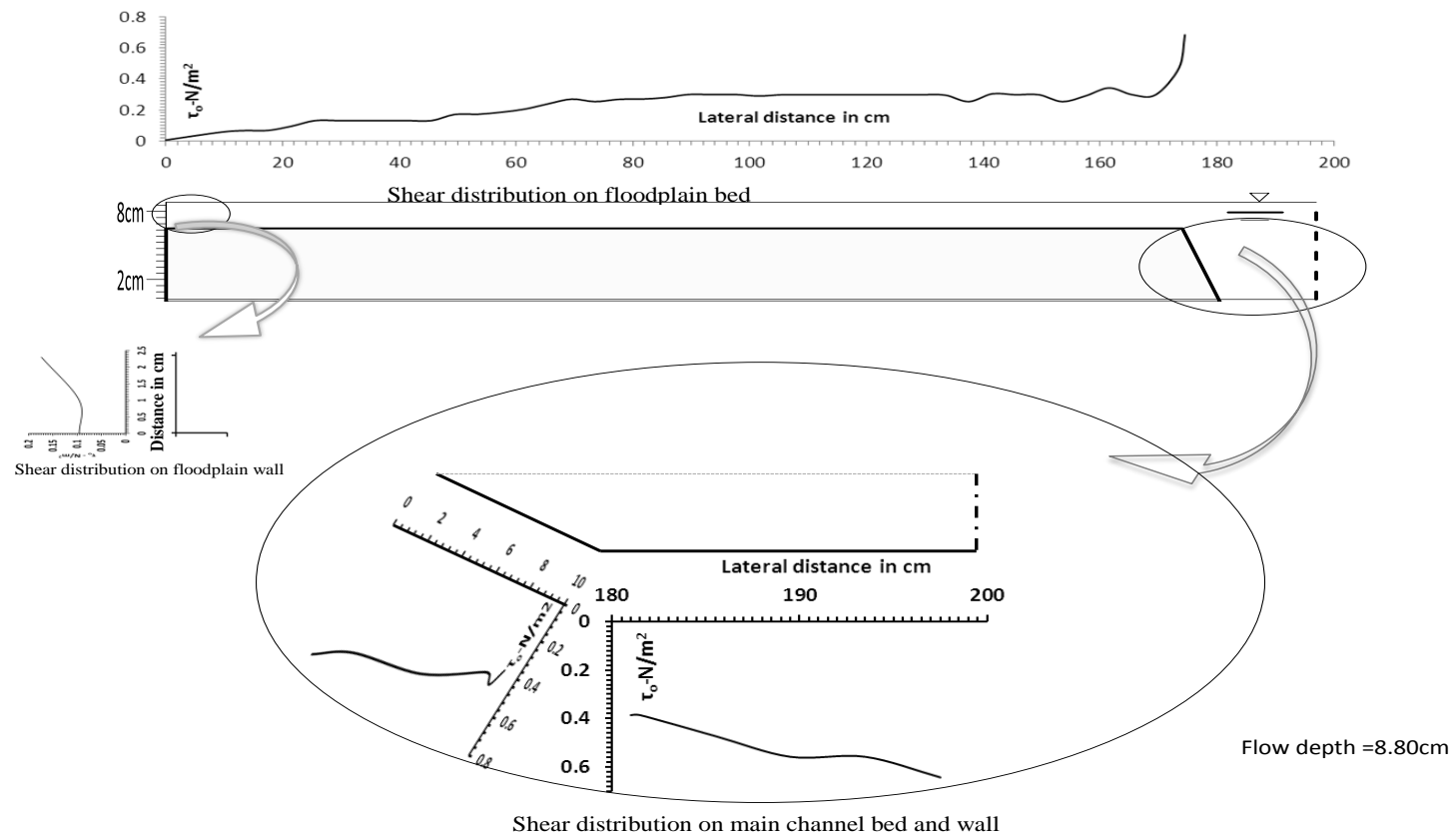


Fig.4-7(c) Shear stress distribution for overbank flow in straight channel

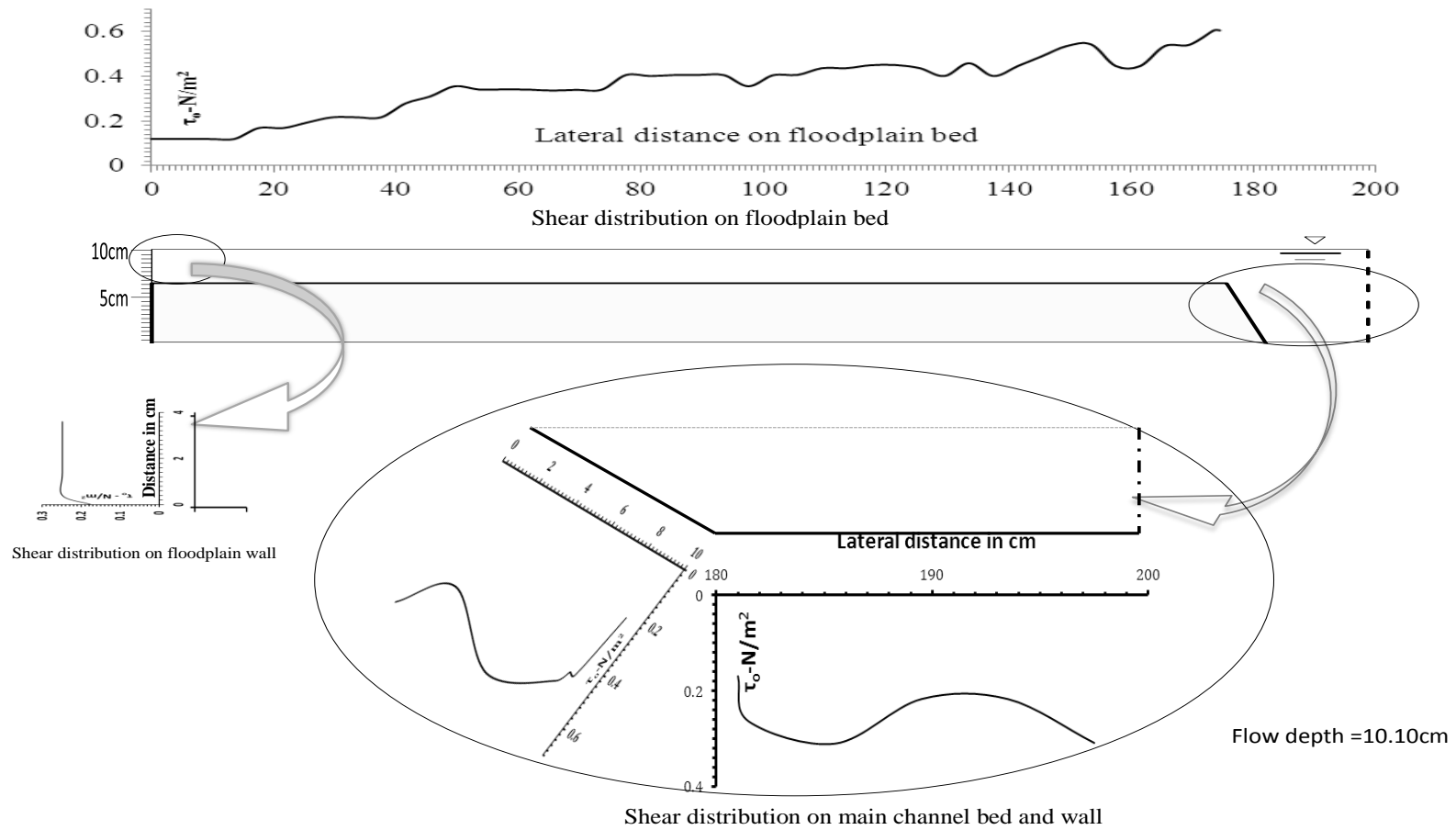


Fig.4-7(d) Shear stress distribution for overbank flow in straight channel

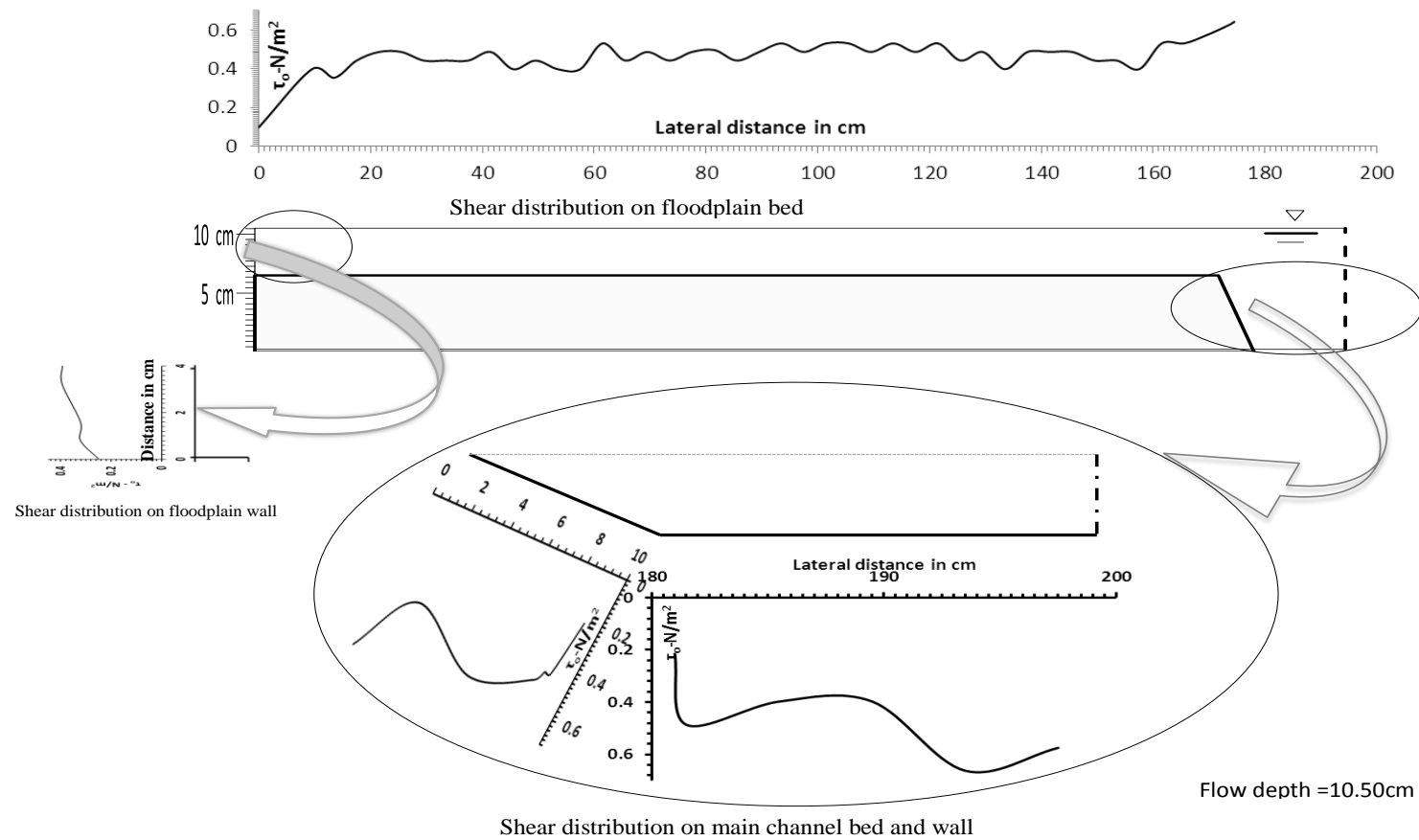


Fig.4-7(e) Shear stress distribution for overbank flow in straight channel

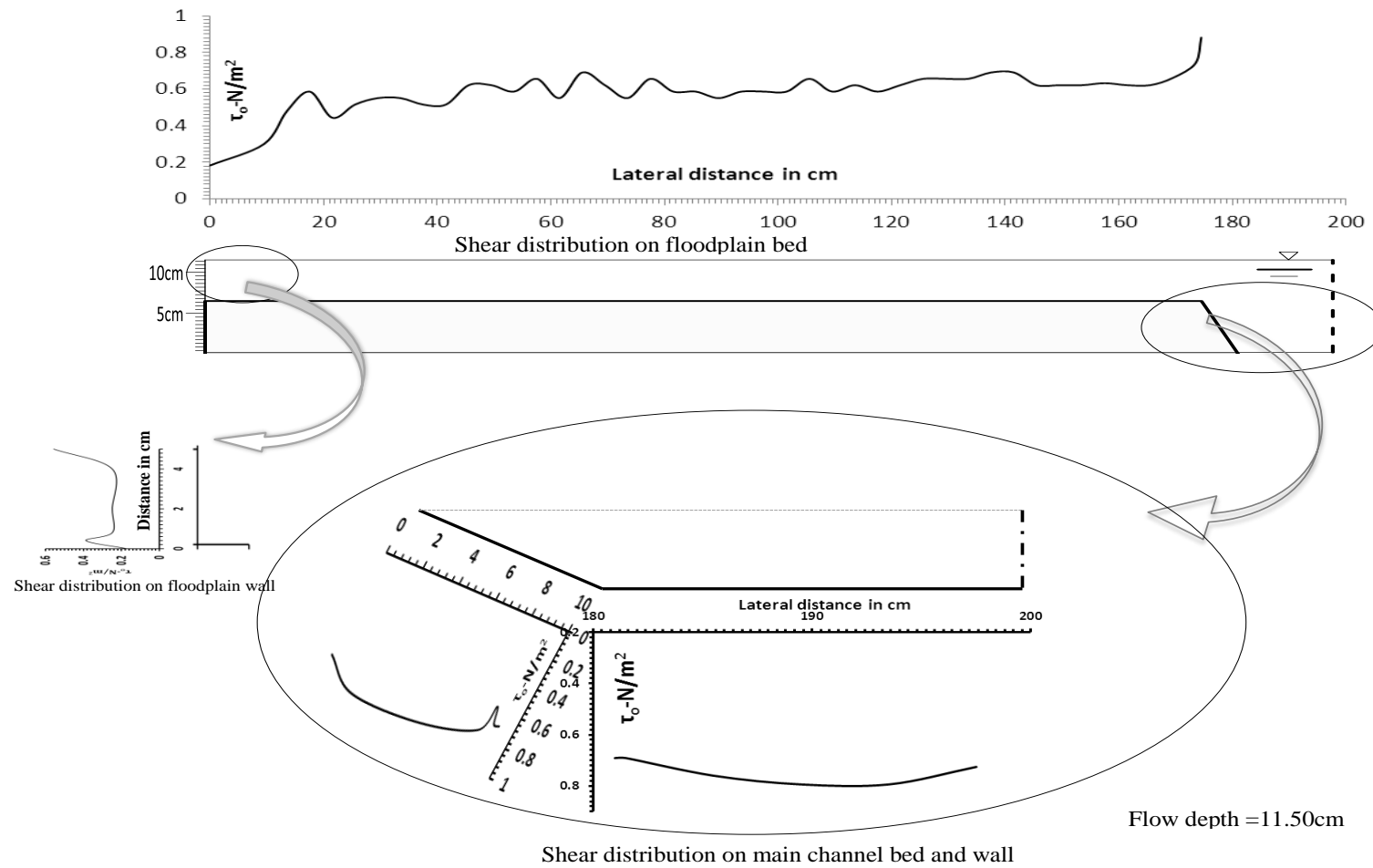


Fig.4-7(f) Shear stress distribution for overbank flow in straight channel

4.3 MEANDERING CHANNEL

4.3.1 Stage-discharge curve

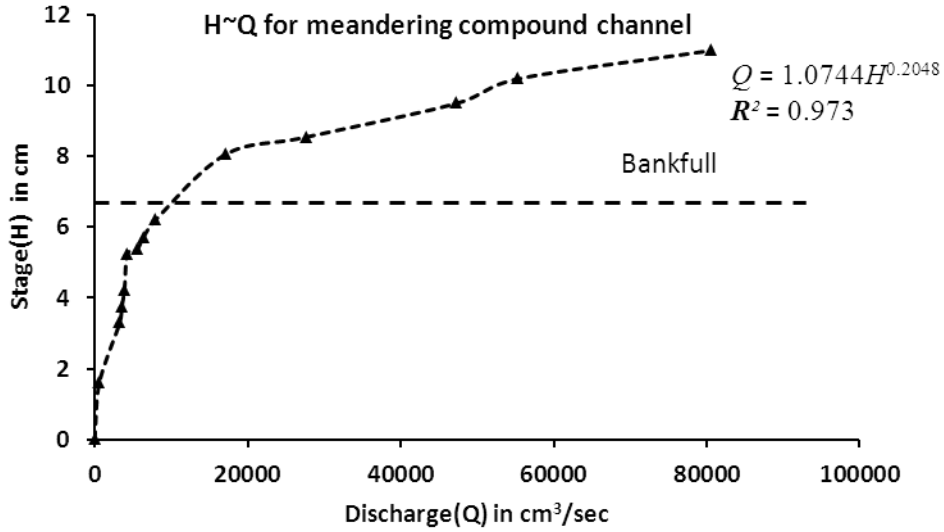


Fig.4- 8 Stage-Discharge curve for meandering compound channel of NIT, Rourkela

The stage-discharge relationship for the meandering compound channel experiments is presented through the $H \sim Q$ curve in Fig.4-8. The curve is segregated into two segments i.e. the lower portion having a sharp gradient for the inbank flow conditions and the upper part having a mild or moderate gradient typical of overbank flow conditions in a compound channel separated by a dotted horizontal line drawn at bank full level. But the curves in inbank zone and out of bank zone are steeper than the respective curves for straight channel cases (please see Fig.4-1) which confirms that a meandering channel having same overall geometrical shape and size as that of a straight channel carries less discharge than the latter. This is due to more energy expenditure by a meandering channel for traversing more distance in curvilinear path than that is for a straight channel which has a shorter straight line path. The rating curve for the overbank flow conditions in this channel is given as

$$Q = 1.0744H^{0.2048} \quad (4.2)$$

As in case of the straight compound channel overbank flow cases, here also the discharge (Q) varies as a power function of the flow depth (H) in the main channel.

4.3.2 Longitudinal velocity

The streamwise or longitudinal point velocities (U) were measured for different inbank and overbank flow cases at different grid points (shown in Fig.3-23). Unlike in case of straight compound channel where the measurement of velocity was done for only half of the compound section due to symmetry, in case of the present meandering channel the velocity measurements were carried out at grid points covering the entire flow domain. The velocity magnitude at each point was then normalized as before with the sectional mean velocity (U_{av}) for that flow rate and contour maps were prepared over the flow section for different flow depths.

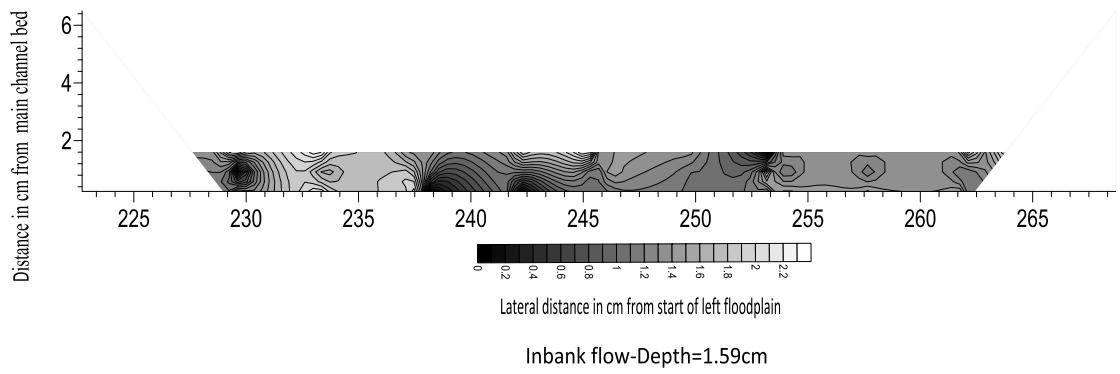


Fig.4-9(a) Isovels for inbank flow in meandering channel

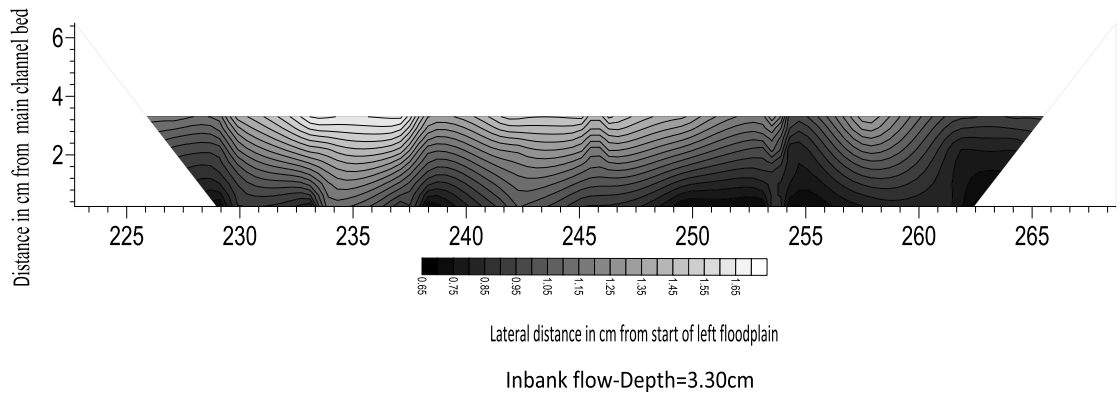


Fig.4-9(b) Isovels for inbank flow in meandering channel

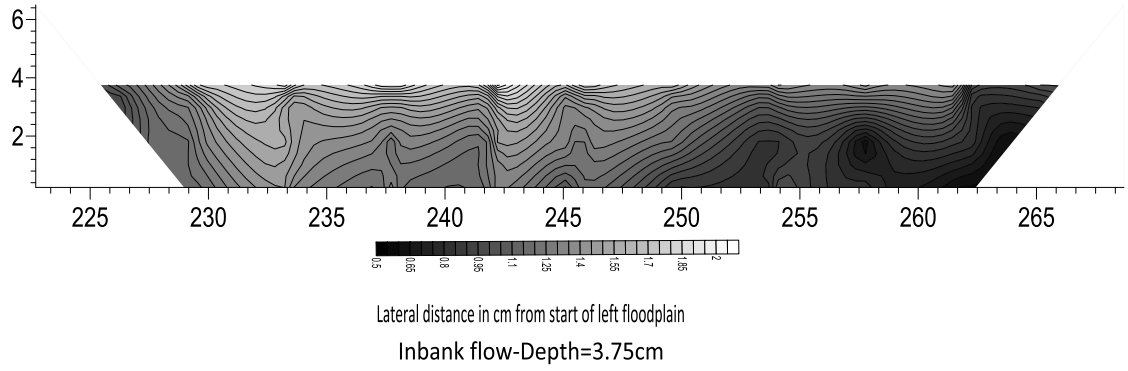


Fig.4-9(c) Isovels for inbank flow in meandering channel

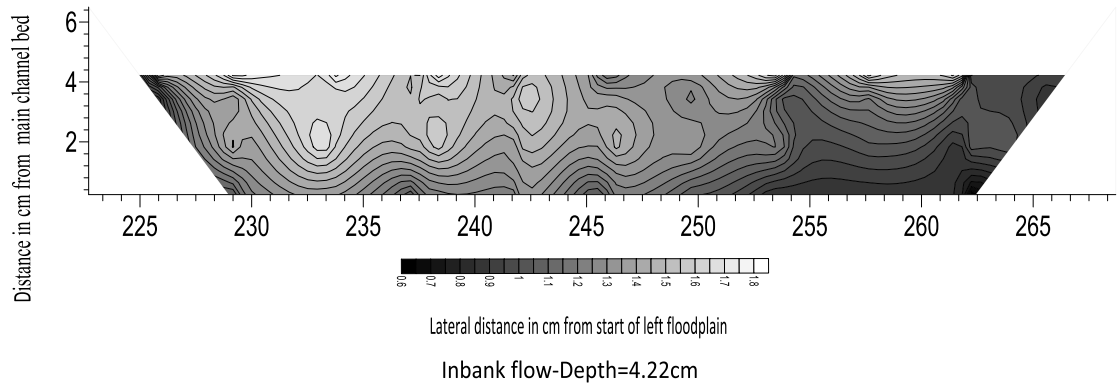


Fig.4-9(d) Isovels for inbank flow in meandering channel

Figs.4-9 (a-h) show the isovels for inbank flow conditions in meandering channel. As the measurement section for the experimental channel happens to be at the bend apex where the path of the main channel turns right (looking from u/s side, see Fig.3-12) so the left sides in all the compound cross sections shown in Figs.4-9 (a-h) are for the inner wall of the bend and the right side is for the outer wall of the bend. The isovels clearly suggest more magnitude of the stream wise velocity in inner wall of the bend as compared to the outer of the bend. However at lower depths (cases a' to d' in Fig.4-9) of flow at subsequent layers there is sharp variation in liquid velocity near the inner side of the bend apex and velocity seem to be more orderly at the outer end. With rise in flow depth this distinct feature ceases to exist

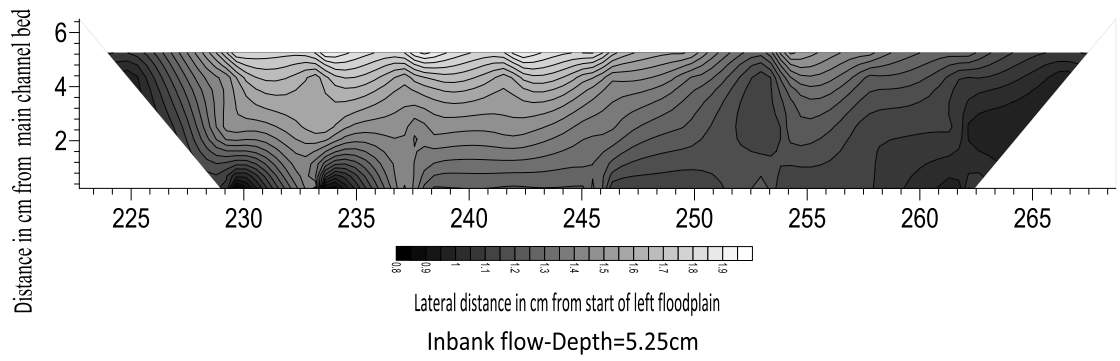


Fig.4-9(e) Isovels for inbank flow in meandering channel

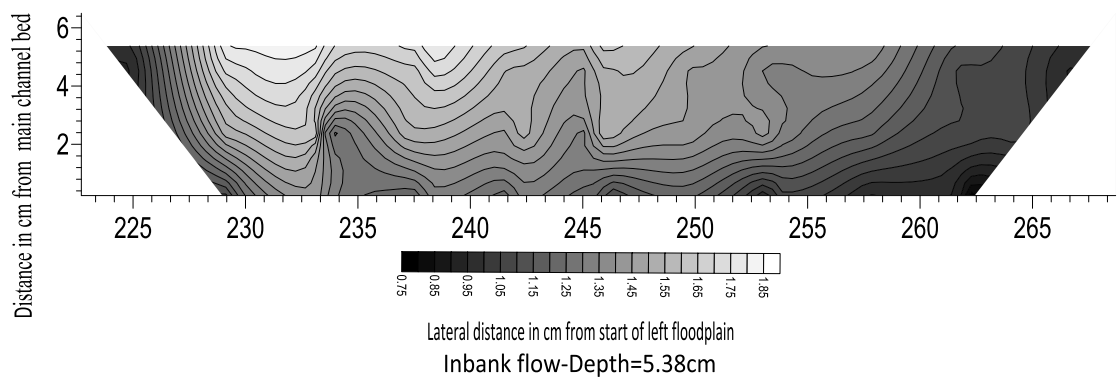


Fig.4-9(f) Isovels for inbank flow in meandering channel

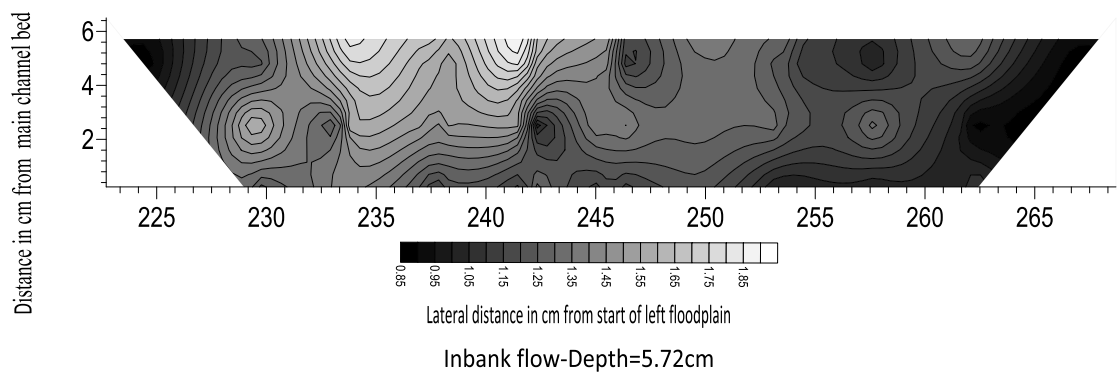


Fig.4-9(g) Isovels for inbank flow in meandering channel

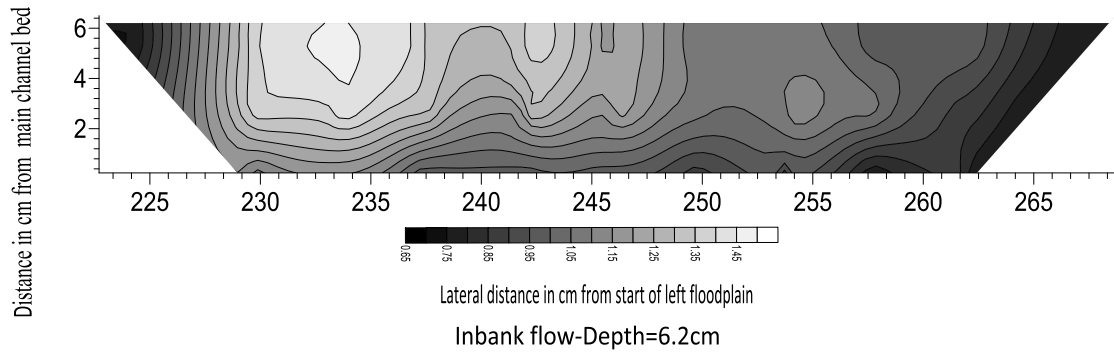


Fig.4-9(h) Isovels for inbank flow in meandering channel

For overbank cases the isovels are shown in Figs. 4-10 (a-e). In the flow cases for low relative depths, due to the vicious interaction among the faster moving main channel flow and the slower moving floodplain flow once again the effect of momentum transfer is noticeable in longitudinal velocity magnitudes. The variation between the magnitudes of the slowest moving liquid as in the far side of the left floodplain and that of inner main channel liquid is evident from the isovels shown in Figs. 4-10 (a & b). The rising flow depth as in other three overbank cases gradually reduces this effect (please see Figs.4-10. c, d & e). Also compared to the first two cases where the main channel flow is influencing the floodplain flow to a large extent, in higher overbank depth cases the floodplain flow is rather less affected due to the main channel flow. The noticeable feature is that large width of floodplains and hence flow area seems to encompass the main channel flow occurring in a smaller area in the present wide meandering compound channel. This is a departure from usual meandering compound channel flow characteristics observed by others (e.g. Ervine et al. 2000).

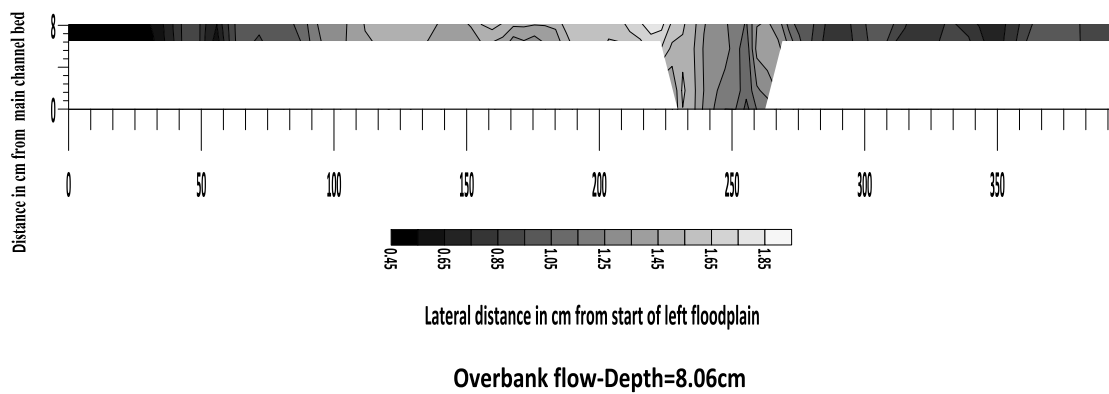


Fig.4-10(a) Isovels for overbank flow in meandering channel

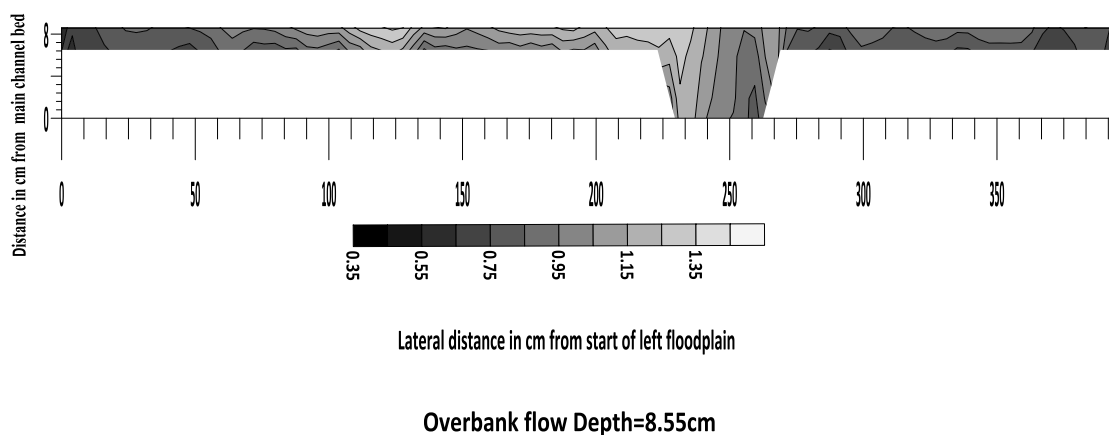


Fig.4-10(b) Isovels for overbank flow in meandering channel

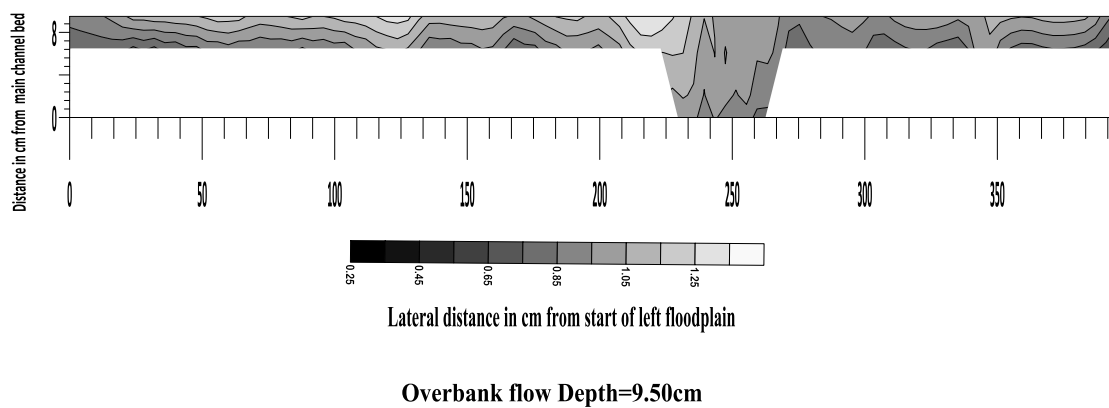


Fig.4-10(c) Isovels for overbank flow in meandering channel

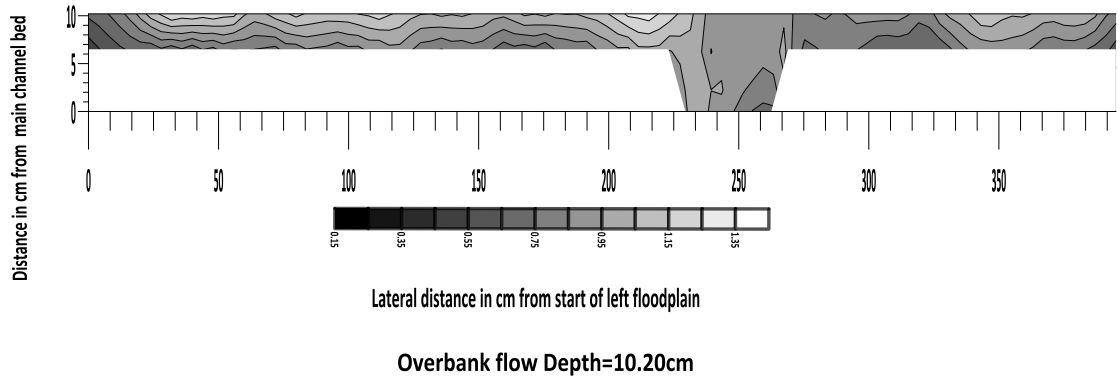


Fig.4-10(d) Isovels for overbank flow in meandering channel

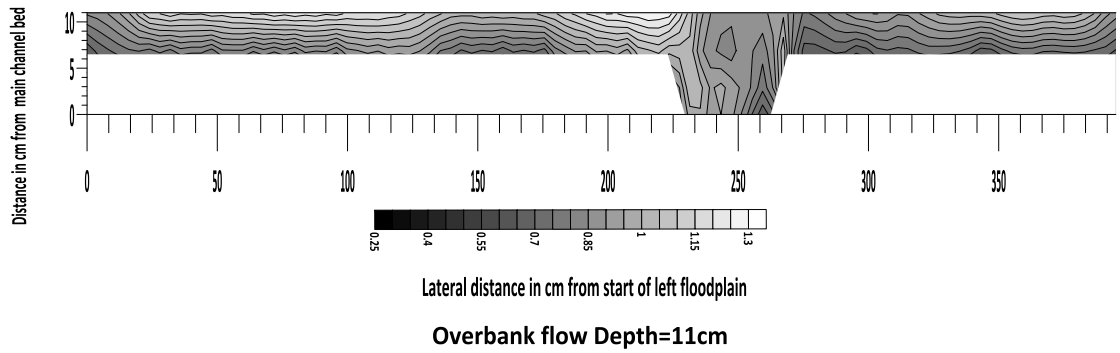


Fig.4-10(e) Isovels for overbank flow in meandering channel

4.3.3 Depth averaged velocity

The depth averaged primary flow velocity (U_d) for all the inbank and overbank cases were also measured for the meandering trapezoidal channel. The same were also normalized with the sectional mean velocities of respective flow cases. For different inbank cases the depth averaged velocity distribution curves are plotted and shown in Figs. 4-11(a-h) and it is seen that in each case the maximum value occurs above the inner wall of the bend apex. The distribution curve has some sharp discontinuities at low flow depths which vanish at higher depths of flow. For overbank cases (shown in Figs. 4-12 (a-e)) the effect of momentum transfer is again seen although with varying degree. The curve rising from far end of the left floodplain has a steep rise near the

inner wall of the bend and then it has sharp fall across the width of only main channel. The magnitude of depth averaged velocity then has a gradual fall towards the end of the right floodplain. This trend is more prominent in first two cases and is very less in highest overbank case (i.e. as in Figs. 4-12e). Also the maximum depth averaged velocity which occurs over the inner wall of the bend is about two times the section mean velocity as in Figs. 4-12(a) and the same is only about 10% more than the section mean velocity in highest overbank case considered i.e. the case in Fig. 4-12(e).

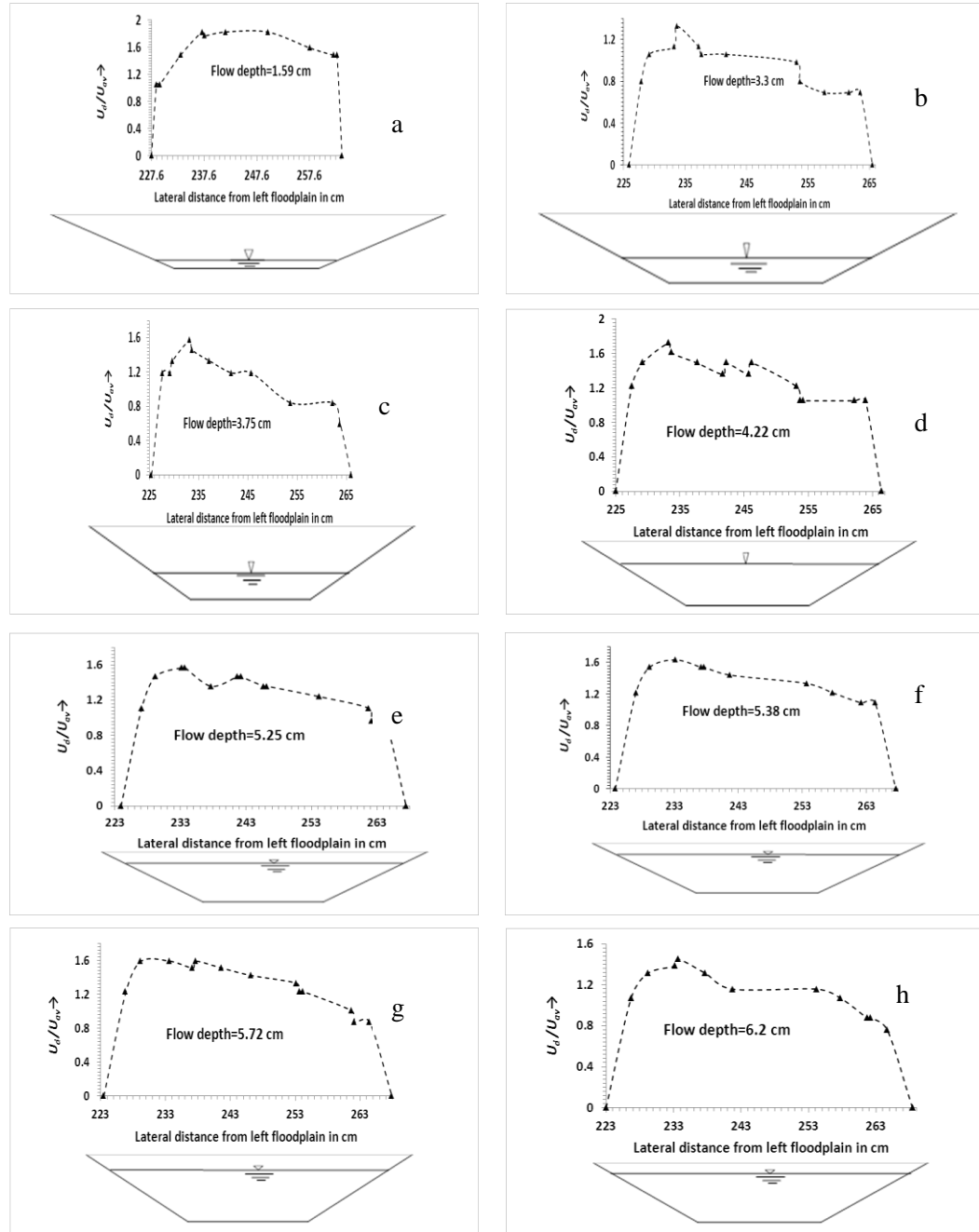


Fig.4-11 (a-h) Depth averaged velocity distribution (U_d normalized with U_{av}) for meandering channel- inbank flow.

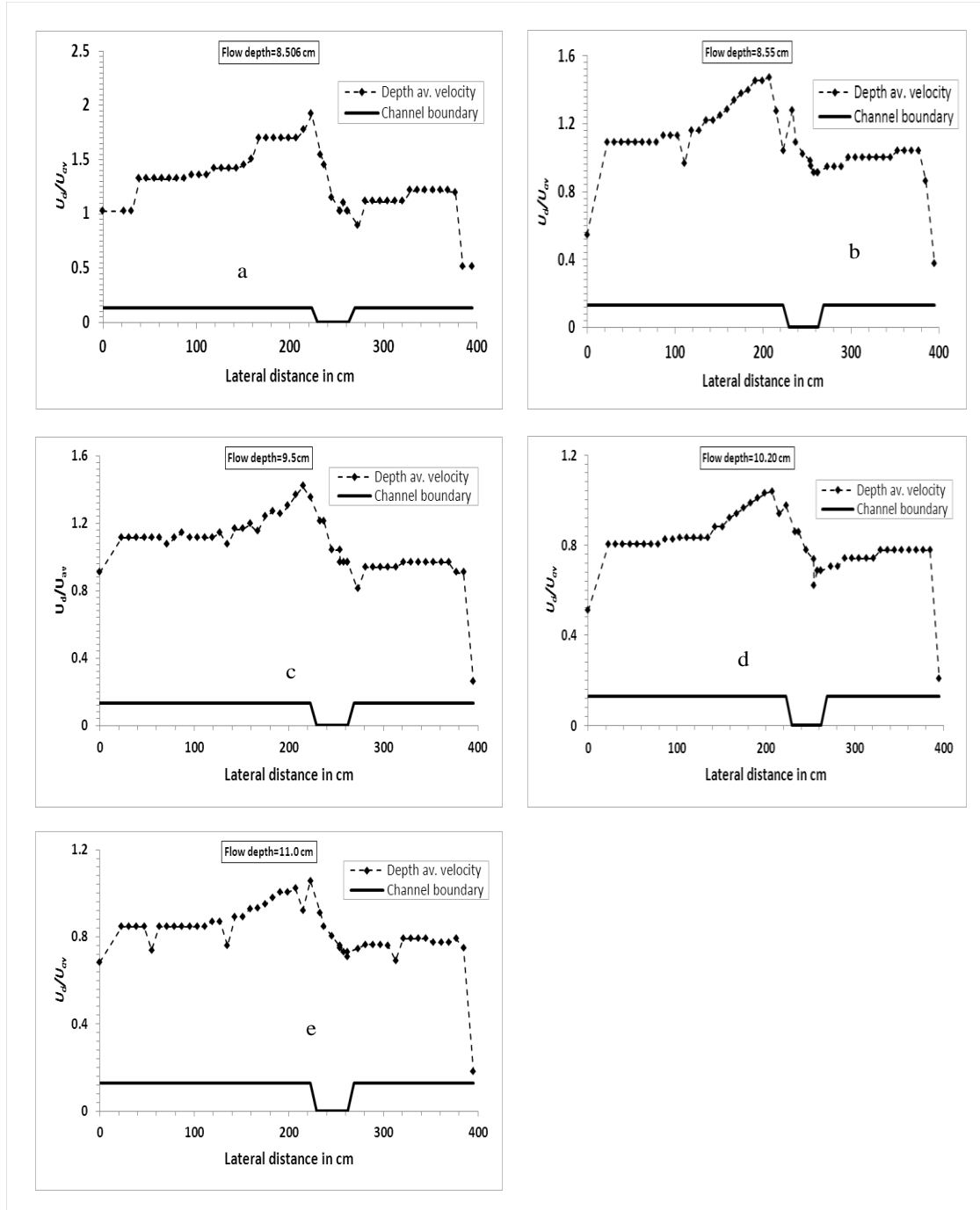


Fig.4-12 (a-e) Depth averaged velocity distribution (U_d normalized with U_{av}) for meandering channel- overbank flow.

4.3.4 Boundary Shear stress

4.3.4.1 Inbank cases

The measured point boundary shear stresses (τ) are plotted across the flow domain for inbank flow cases in Figs. 4.13 (a-h). The distribution for inbank cases shows that the

maximum value of flow resistance always occurs near the inner side of the bend. The shear value rises from the corner of the trapezoidal main channel cross section to some distance along the wall and then gradually falls towards the free surface. The shear stress on the opposite end i.e. on the outer end of the bend is always smaller than the inner side of the bend.

4.3.4.2 Overbank cases

For overbank cases the shear stress distributions are shown in Figs. 4-14 (a-e). The different flow zones such as left floodplain wall, left floodplain bed, main channel wall, main channel bed as well as right floodplain wall and right floodplain bed are shown highlighted in all these figures. Since for the present meandering compound channel at the test reach the meander is a right turning curve so the inner floodplain is the left floodplain with larger width and the right floodplain is the outer one with smaller width. The shear stress value gradually rises from far end of left floodplain towards the main channel with a sharp rise at the junction region only to fall across the width of the main channel. Similarly at the other junction on outer bend the shear stress magnitude falls sharply and then continues with moderate fall towards the outer floodplain end. The main channel wall on the inner side is subjected to maximum shear and the outer wall experiences lower shear stress as compared the inner wall. With rising flow depth however all respective magnitudes increase showing that the shear stress magnitude is dependent on depth of flow in the meandering compound channel. The flow mechanisms in meandering channel being extremely complex (Ervine et al. 2000; Shiono and Muto, 1998) it is very difficult to obtain any fixed pattern in the shear stress variation for all the overbank flow depths considered in present study as evident in different cases (Figs.4-14, a-e).

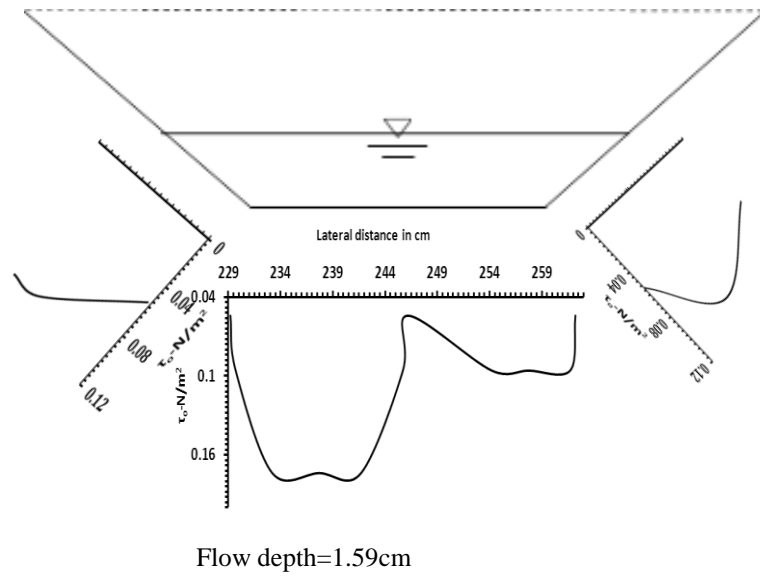


Figure 4-13(a) Shear stress distribution for inbank flow in meandering channel

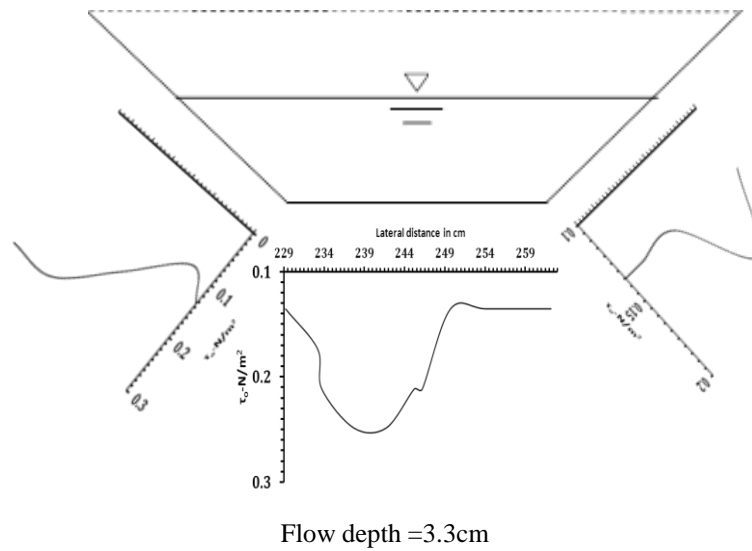


Figure 4-13(b) Shear stress distribution for inbank flow in meandering channel

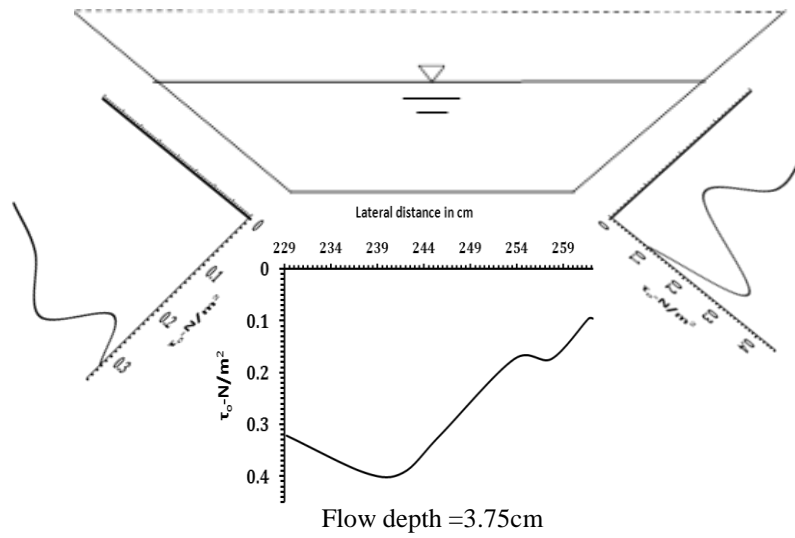


Figure 4-13(c) Shear stress distribution for inbank flow in meandering channel

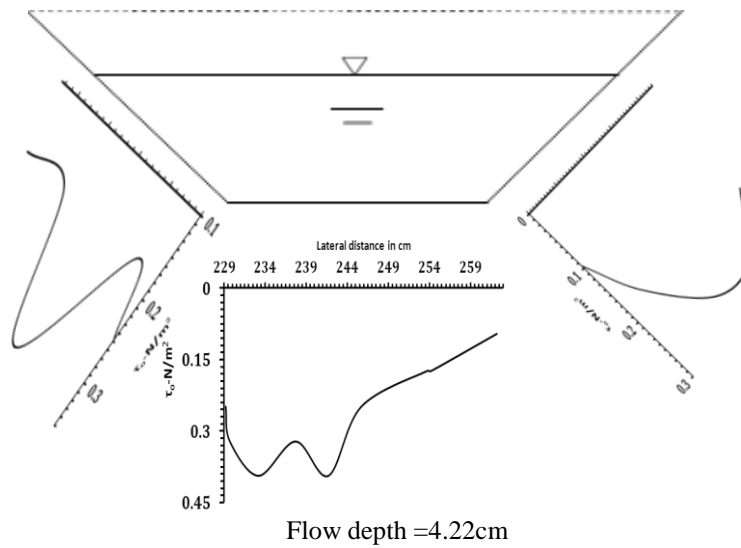


Figure 4-13(d) Shear stress distribution for inbank flow in meandering channel

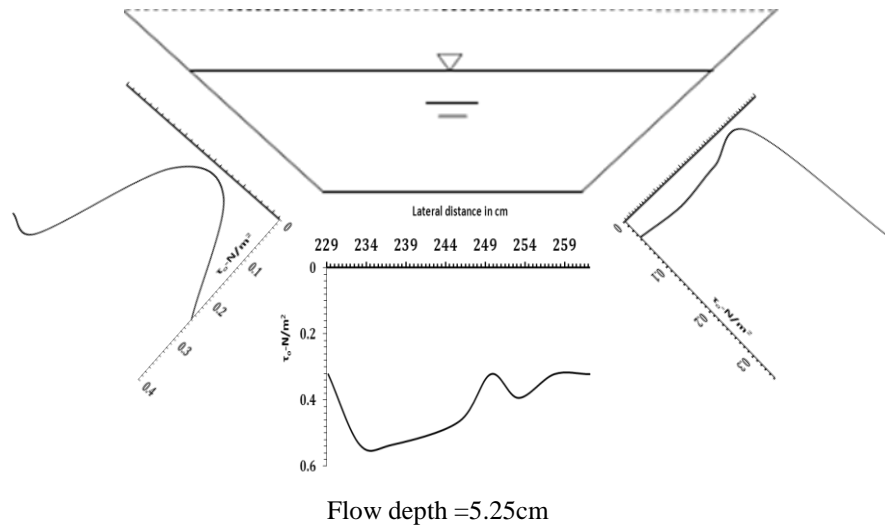


Figure 4-13(e) Shear stress distribution for inbank flow in meandering channel

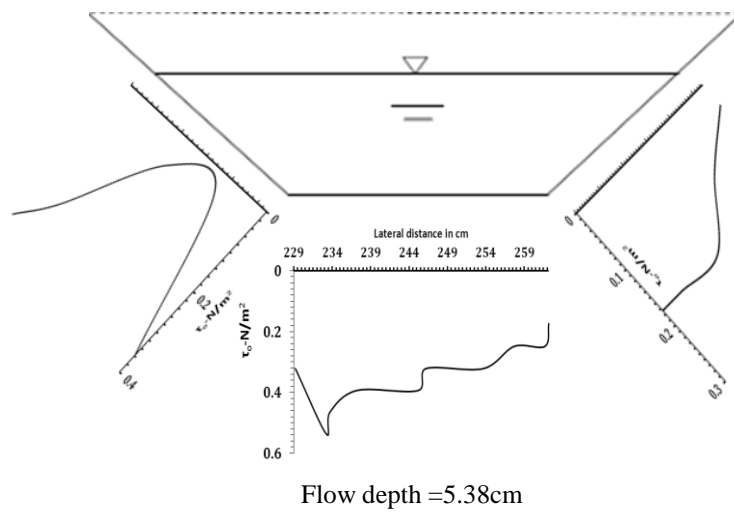


Figure 4-13(f) Shear stress distribution for inbank flow in meandering channel

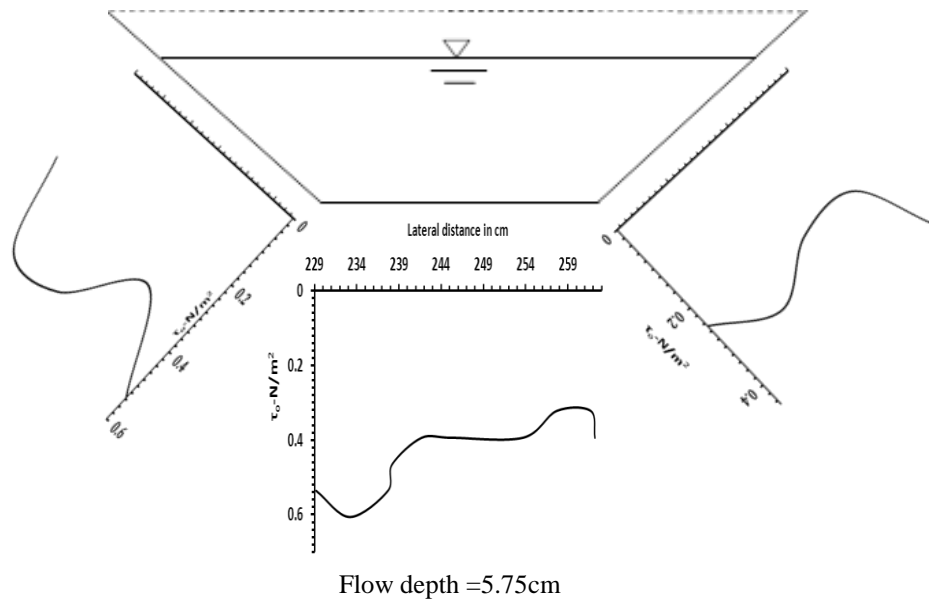


Figure 4-13(g) Shear stress distribution for inbank flow in meandering channel

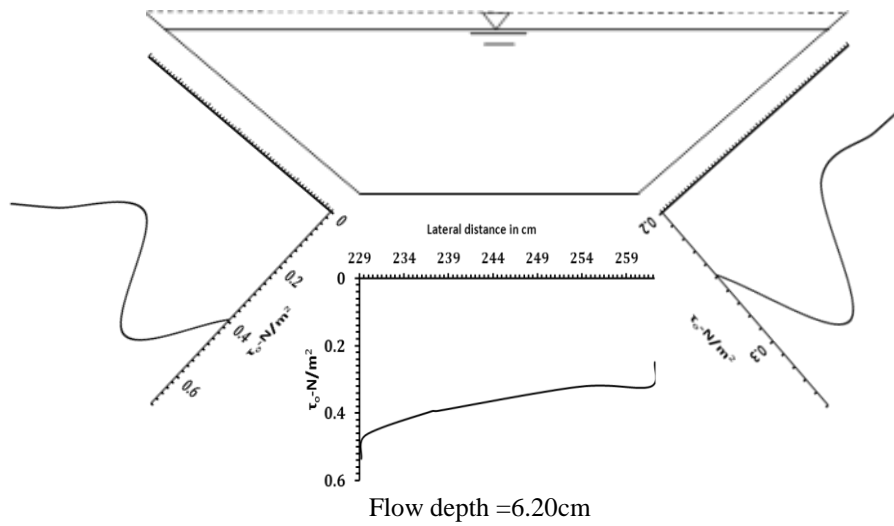


Figure 4-13(h) Shear stress distribution for inbank flow in meandering channel

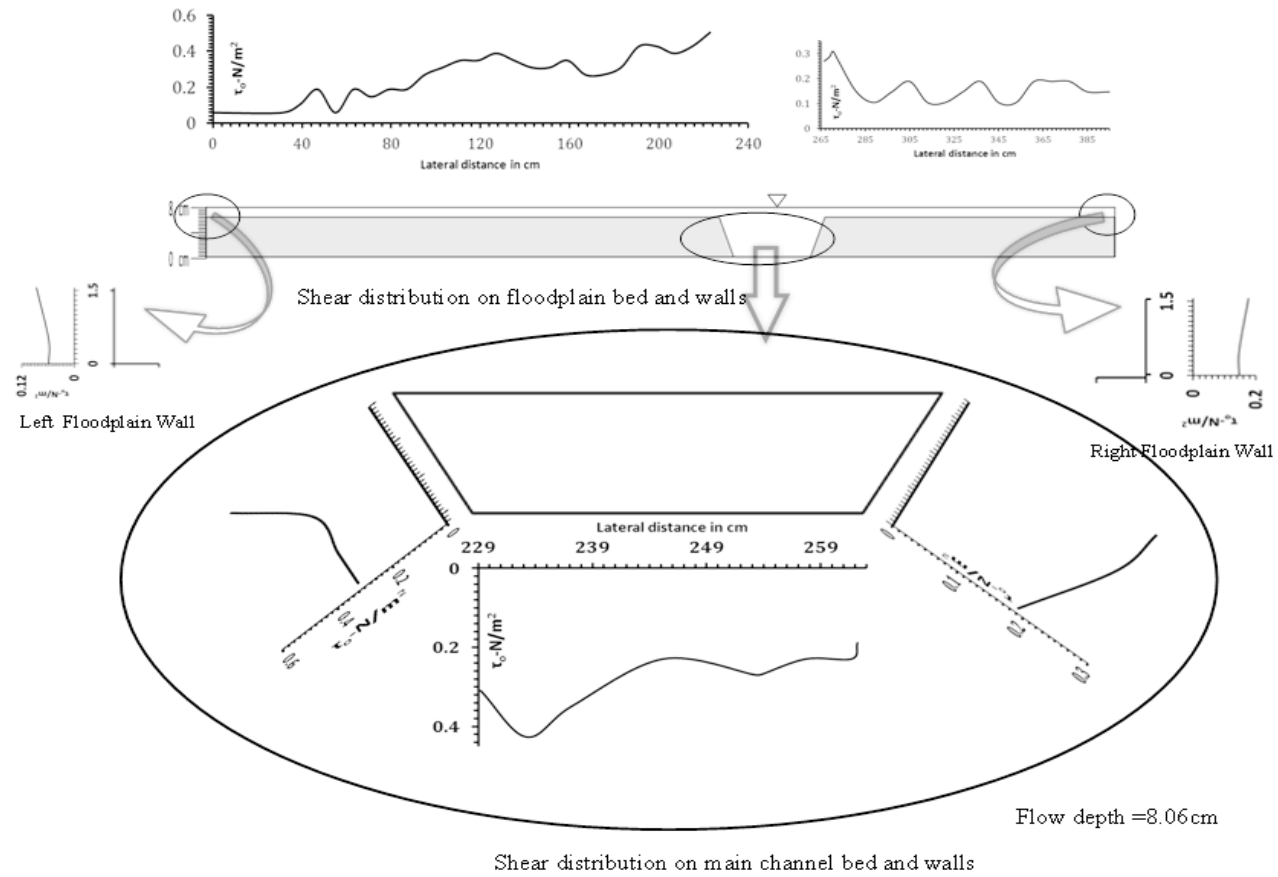


Fig.4-14(a) Shear stress distribution for overbank flow in meandering channel

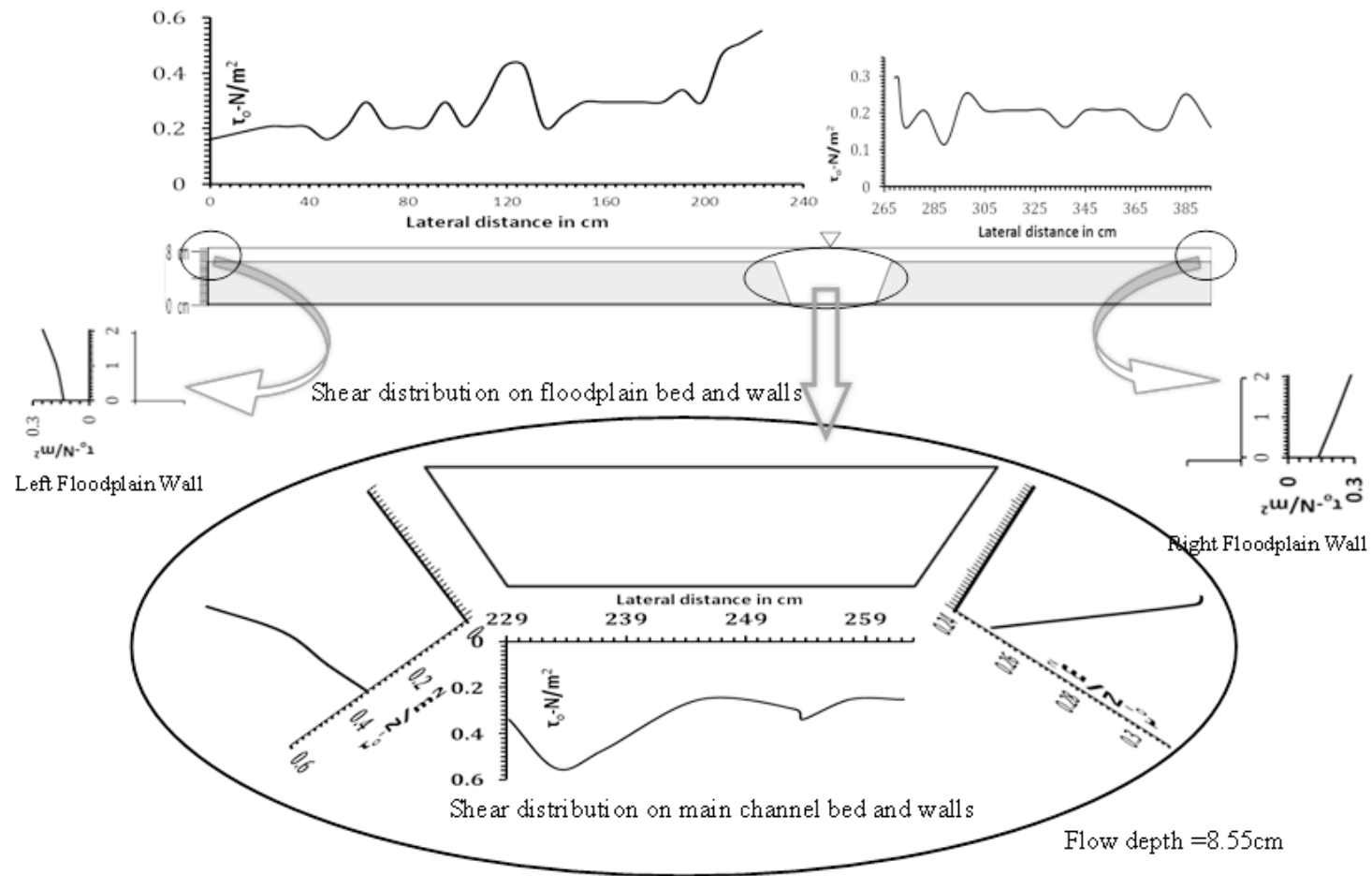


Fig.4-14(b) Shear stress distribution for overbank flow in meandering channel

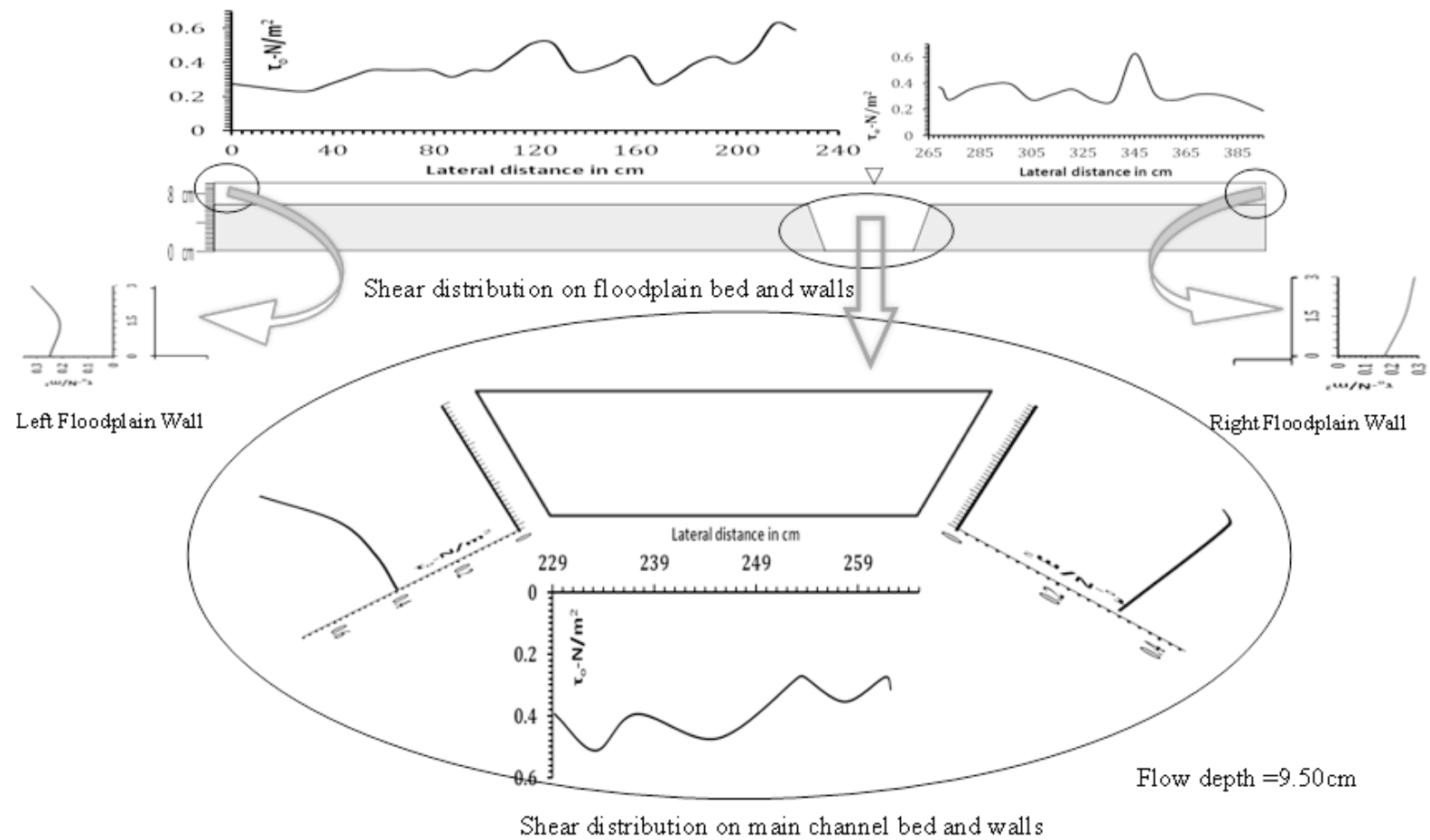


Fig.4-14(c) Shear stress distribution for overbank flow in meandering channel

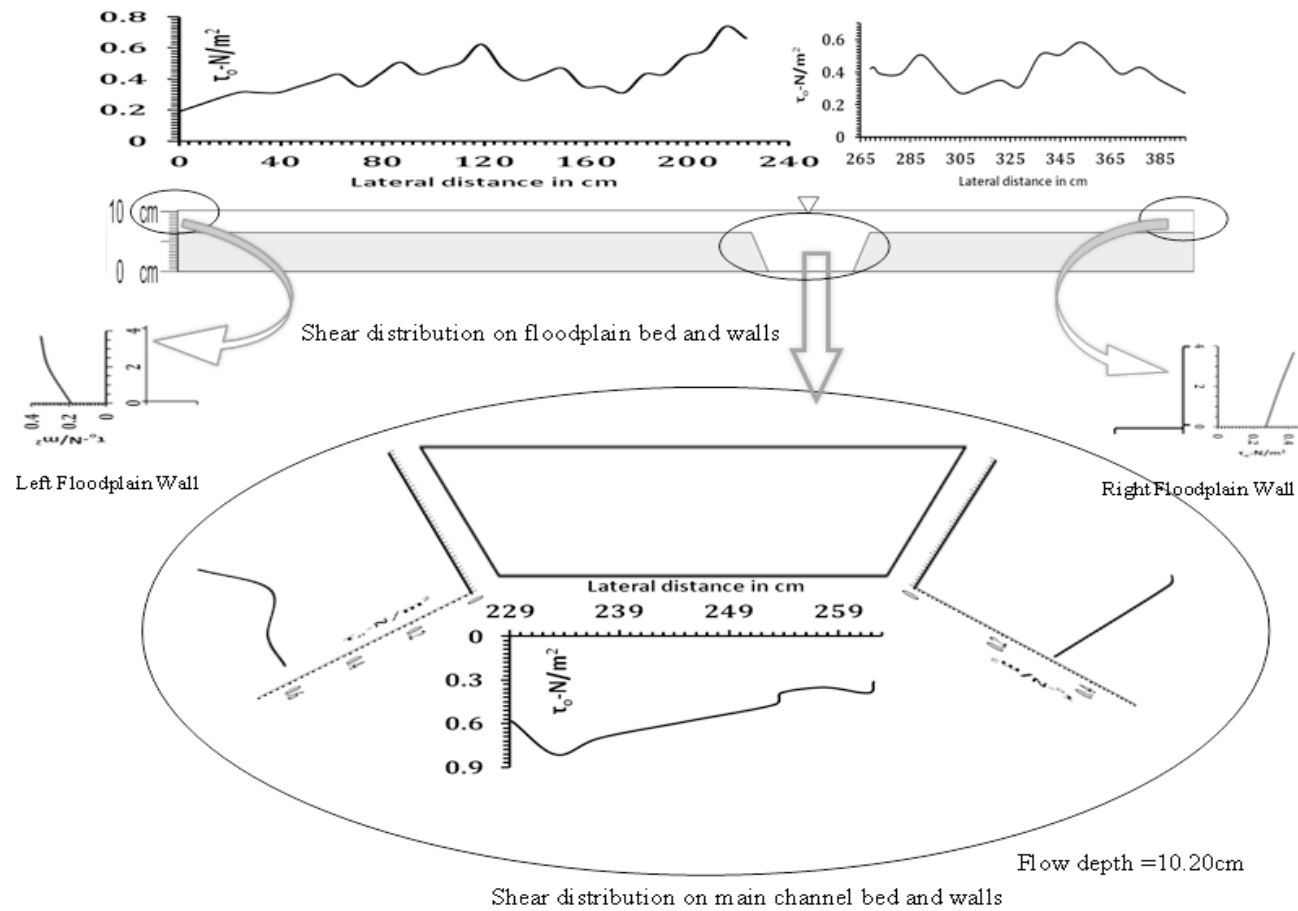


Fig.4-14(d) Shear stress distribution for overbank flow in meandering channel

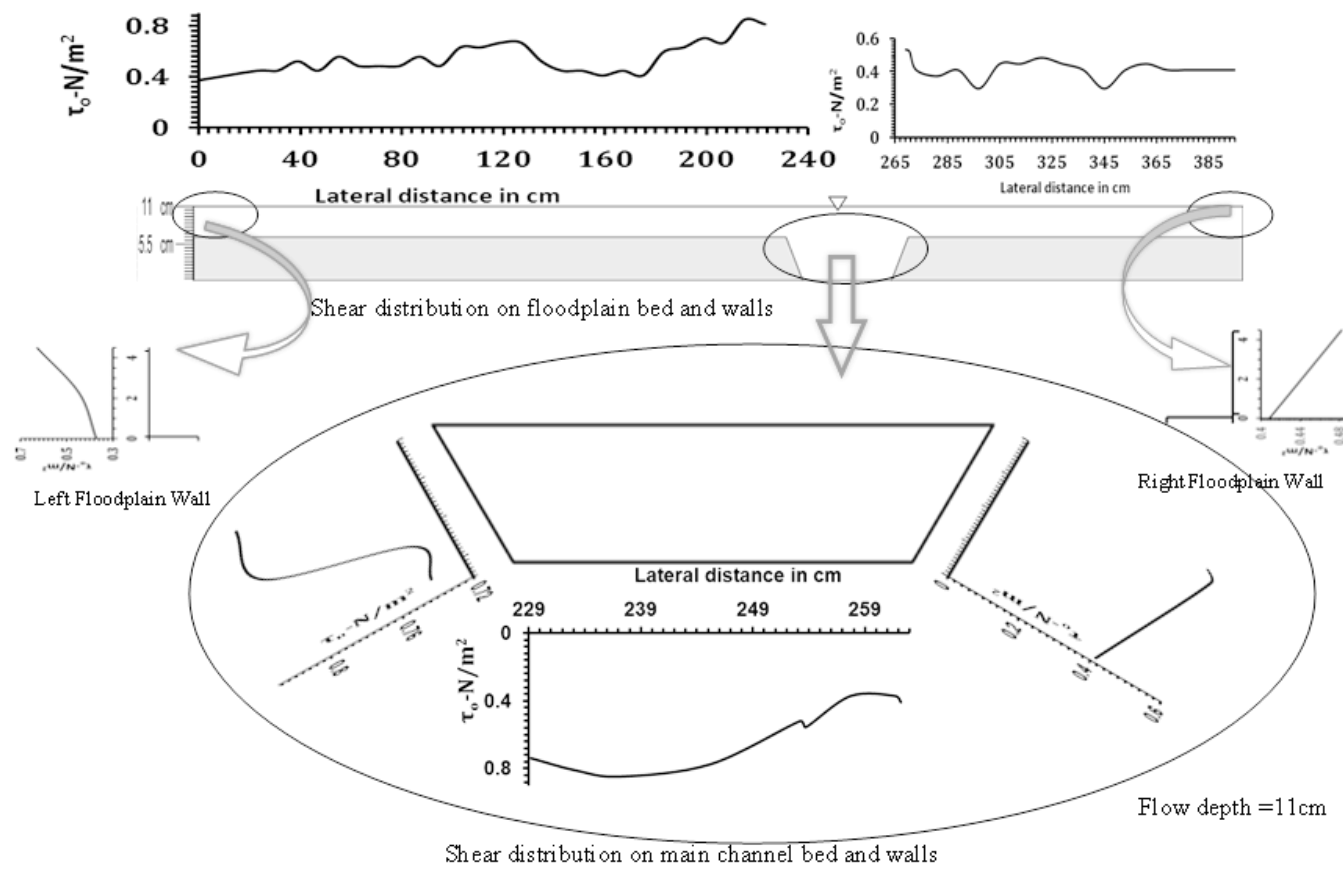


Fig.4-4 e Shear stress distribution for overbank flow in meandering channel

APPLICATION OF NUMERICAL TOOLS

5.1 INTRODUCTION

In the field of river hydraulics research in general and compound channels in particular the investigators have often taken recourse to a three-pronged strategy. In addition to the physical experiments on laboratory flumes mimicking river flows and the theoretical analysis of fluid dynamics governing the flow in any natural or artificial channels, a third approach namely the ‘Computational Fluid Dynamics’ (CFD) has lately been developed and pursued in the field of hydraulic research with the advent of modern high speed digital computers. As per Anderson, Jr. (1995), CFD does not replace experimental or theoretical studies; rather it nicely and synergistically complements the other two approaches as shown in Fig.5-1. Most physical models relating the fluid dynamics problem of open channel flow are basically expressed as differential equations whose solutions on a computer often involve numerical solution of complex mathematics.

So CFD is in essence nothing but a numerical tool that applies to solving complex differential and partial differential equations of fluid dynamics problem on high speed computers through various algorithms. In last quarter century or so lots of development have taken place in application of CFD to environmental flows resulting in emergence of a number of research codes as well as commercial packages for ready to use by different users.

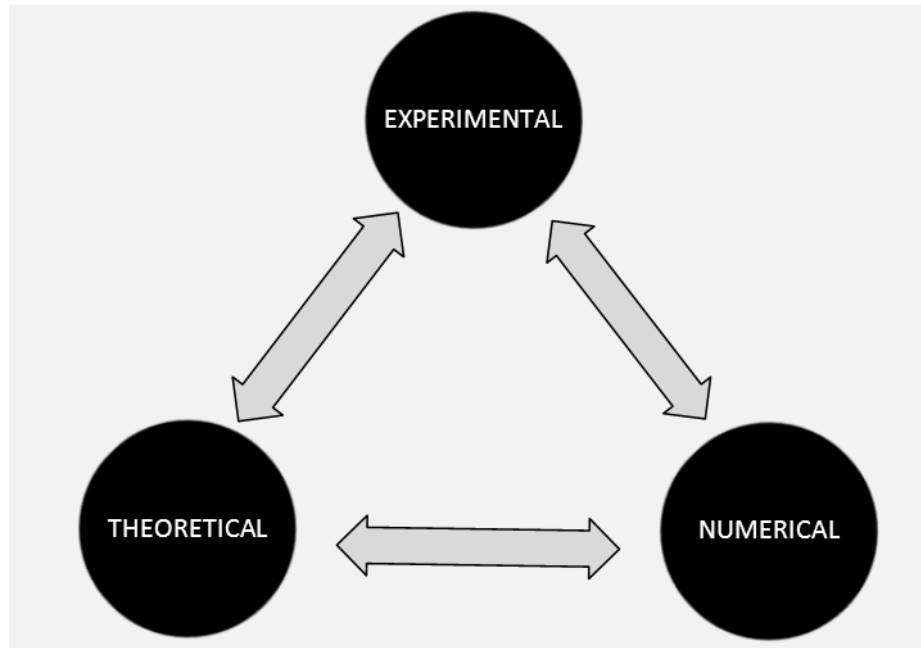


Fig.5-1 Three Dimensions of Research in River Hydraulics

The present research concerning straight and meandering compound channels with wide flood plains thus adopts application of some numerical tools to the problems at hand as a complementary study to the experimental research already undertaken. Two significant standard research tools viz. a 1D package ‘Conveyance Estimation System’(CES) developed by joint agency/DEFRA Research program on flood defense with contributions from the Scottish executive and the Northern Ireland Rivers Agency, HR Wallingford and the Environmental agency UK and widely recommended for use throughout Europe for reliable prediction of conveyance or discharge in flooded channels & streams and a 2D depth averaged hydrodynamic tool ‘CCHE2D’ developed by the National Center for Computational Hydro-science and Engineering (NCCHE), University of Mississippi, USA, are applied in the present research. This chapter gives a brief background for both the tools as well as deals in details about their application in simulation studies for the new experimental cases and some past cases from literature.

5.2 CONVEYANCE ESTIMATION SYSTEM

The Environment Agency for England and Wales identified the need to reduce the uncertainty associated with flood level prediction through incorporating the recent

research advances in estimating river and floodplain conveyance in response to the cry for a simpler, user friendly yet physics based approach instead of prevalent empirical based approaches as used to be done by applying Manning's or Chezy's formula. The new conveyance system has been developed taking into account the advances made in research in channel conveyance, the vast diversity in roughness of river and associated floodplains and finally understanding and quantifying the uncertainty due to methodology adopted and model inputs (Project Record W5A, 2001-04). This is now available as an open code capable of being incorporated into any one dimensional hydrodynamic modeling package e.g. HECRAS, HYDRO-1D, ISIS, MIKE11 etc. to improve the conveyance prediction for solution of the St Venant Equations. Also, it can serve as a tool for further educational/academic research across the universities and institutes.

Conveyance Estimation System was conceived and developed after certain shortcomings were pointed out in the existing 1D models such as ISIS, HECRAS, and MIKE11 in their methodology of estimating conveyance. The major drawbacks were demonstrated in expert paper of Knight (Scoping Study, 2001) and could be mentioned here briefly for some critical review. ISIS adopted mainly a divided channel method (DCM) approach which suffers from unphysical basis and poor quality output in case of overbank flow (ISIS V2.0, 2001). Almost a similar approach was adopted by HECRAS (HECRAS, 1998) where flow domain is subdivided on basis of uniform velocity coefficient and is usually done on basis of input cross-section, Manning's n value breakpoint as the basis of subdivision. Mainly both of above models are usually based on improper physics, overestimating floodplain and underestimating main channel conveyance. Mike11 (MIKE11 V3.11, 1995) adopted a modified form of DCM in its conveyance estimation approach in which bed resistance can be chosen on basis of Manning's M or Chezy's C where M is the Manning number ($=1/n$) which is equivalent to the Strickler coefficient. The Chezy's coefficient C is related to Manning's n (Cunge et al, 1980). Hence CES was developed to overcome these shortcomings by adopting the Reynolds-averaged Navier-Stokes (RANS) approach as the solution basis for estimation of conveyance. Compared to the previous 1D models, its outputs are diverse as it can generate a host of parameters such as lateral distribution of depth averaged velocity, boundary shear, friction velocity across the flow cross section

in addition to normal outputs such as flow, conveyance, Boussinesq's and Coriolis' coefficients etc.

The CES includes a component termed the 'Roughness Advisor', which provides advice on the surface friction or 'roughness', and another component termed the 'Conveyance Generator', which determines the channel capacity based on both this roughness and the channel morphology. In addition, the CES includes a third component, the 'Uncertainty Estimator', which provides some indication of the uncertainty associated with the conveyance calculation. The primary outputs from the CES components are:

- Roughness Advisor: roughness values
- Conveyance Generator: stage-conveyance relationship
- Uncertainty Estimator: upper and lower bands for the stage-conveyance relationship.

5.2.1. Development of the model for CES

Two important approaches e.g. The Energy loss approach (Ervine & Ellis, 1987; Shiono et al, 1999) and The Reynolds Averaged Navier-Stokes (RANS) Approach (Shiono & Knight, 1990; James & Wark, 1992; Ervine et al, 2000) were selected for further testing and subsequent adoption in the CES package. Both the approaches were then reviewed in terms of:

- The theoretical and physical basis of the method.
- Consideration of all energy losses.
- Representation of energy loss hierarchy with variation in water level/sinuosity e.g. changes in secondary current direction and structure.
- Previous testing of the method against physical model and real river data.
- Reliable and readily available calibration/empirical parameters.
- The ease of the method implementation for a range of channel types.
- The outputs i.e. discharge for a given water level (high priority), lateral velocity/bed shear stress distributions.

- The nature and number of roughness coefficients.
- Reach or cross-section analysis.

On basis of the above mentioned criteria, the RANS approach was found to be more suitable over the Energy loss approach and hence was adopted in the model.

5.2.1.1. Method description of RANS approach

This approach is based on the depth-integration of the RANS equations for flow in the streamwise direction. The basic form of the depth-averaged momentum equation for application to channel flow is (Shiono & Knight, 1988):

$$\underbrace{\rho g H \frac{dh}{dx}}_{(I)} - \underbrace{\beta' \tau_b}_{(II)} + \underbrace{\frac{\partial}{\partial y} (H \bar{\tau}_{yx})}_{(III)} = \frac{\partial}{\partial y} \left[\underbrace{H (\rho \overline{UV})_d}_{(IV)} \right] \quad (5.1)$$

where:

ρ = fluid density (kg/m³)

g = gravitational acceleration (m/s²)

H = local water depth normal to the bed (m)

h = water level (m)

x = streamwise direction parallel to the bed (m)

y = lateral distance across section (m)

U_d = depth-averaged streamwise velocity (m/s)

V_d = depth-averaged lateral velocity (m/s)

τ_b = bed shear stress (N/m²)

τ_{yx} = Reynolds stress (N/m²)

β' = coefficient for the influence of lateral bed slope on the bed shear stress

And the terms represent the:

(I) variation in hydrostatic pressure along the reach

(II) Boundary friction effects

(III) Turbulence due to shearing between the lateral layers

(IV) Turbulence due to secondary currents

The term β' is related to transverse bed slope S_y by the relation:

$$\beta' = (1 + S_y^2)^{\frac{1}{2}} \quad (5.2)$$

The bed shear stress can be expressed in terms of the shear velocity U_* (m/s) and hence the depth-averaged velocity and bed friction factor f as,

$$\tau_b = \rho U_*^2 = \rho \frac{f}{8} U_d^2 \quad (5.3)$$

The Reynolds' stress can be depth-averaged and expressed in terms of the eddy viscosity ε (m²/s) as,

$$\overline{\tau_{yx}} = \frac{1}{H} \int_0^H \tau_{yx} dz = \rho \varepsilon \frac{\partial U_d}{\partial y} \quad (5.4)$$

Substituting equations (5.3) and (5.4) into (5.1), approximating the friction slope ($\partial h / \partial x$) with the longitudinal bed slope, S , and implementing the eddy viscosity model,

$$\varepsilon = \lambda U_* H \quad (5.5)$$

where the depth ' H ' is some measure of the turbulence length scale and λ is the dimensionless eddy viscosity which accounts for the viscosity variation with depth, yields the SKM (Shiono & Knight, 1990),

$$\rho g H S - \frac{\rho f \beta' U_d^2}{8} + \frac{\partial}{\partial y} \left[\rho \lambda H^2 \left(\frac{f}{8} \right)^{\frac{1}{2}} U_d \frac{\partial U_d}{\partial y} \right] = \frac{\partial}{\partial y} [H (\rho \overline{UV})_d] \quad (5.6a)$$

Or solving for unit flow rate, q (m²/s) instead of depth-averaged velocity, U_d as advocated in previous research (Samuels, 1989) due to the strong continuity property of the q with variations in depth e.g. across a vertical face/step in an engineered channel cross-section the equation can be rewritten as

$$gHS - \frac{f\beta' q_x^2}{8H^2} + \frac{\partial}{\partial y} \left[\lambda H \left(\frac{f}{8} \right)^{1/2} q_x \frac{\partial}{\partial y} \left(\frac{q_x}{H} \right) \right] = \frac{\partial}{\partial y} \left[\frac{(q_x q_y)_d}{H} \right] \quad (5.6b)$$

Where the streamwise q_x and lateral q_y unit flow rates are defined as,

$$q_x = \frac{1}{H} \int_0^H u dz = HU_d \quad \text{and} \quad q_y = \frac{1}{H} \int_0^H v dz = HV_d \quad (5.7a, b)$$

Equation (5.6) can be solved analytically by dividing the cross-section into sub areas with specified boundary conditions. Alternatively, a numerical solution can be implemented whereby the channel cross-section is discretized (Fig.5-2) into a number of flow elements and finite difference/element approximations are substituted into the equation. The resulting system of equations is solved to find the local depth-averaged velocity within each element. The velocity distribution can thus be integrated to provide the total channel discharge.

However, a further difficulty is the unknown depth-averaged lateral velocity distribution V_d . Previously, two approaches have been examined:

(i) *Straight prismatic channels*

The SKM (Shiono & Knight, 1990) implements a secondary flow term, $\Gamma (= \rho(\overline{UV})_d)$, which is a calibration coefficient that varies laterally across the channel. It assumes different values for main channel and floodplain flows, and the value increases with increased relative depth, as the nature/direction of the secondary currents change.

(ii) *Meandering channels*

The Ervine *et al*, 2000 extends the SKM method to incorporate the secondary flow effects resulting from meandering channels. A coefficient C_{uv} , which relates the secondary currents to the depth mean velocity, is introduced such that,

$$\overline{UV} = C_{uv} U_d^2 \quad (5.8)$$

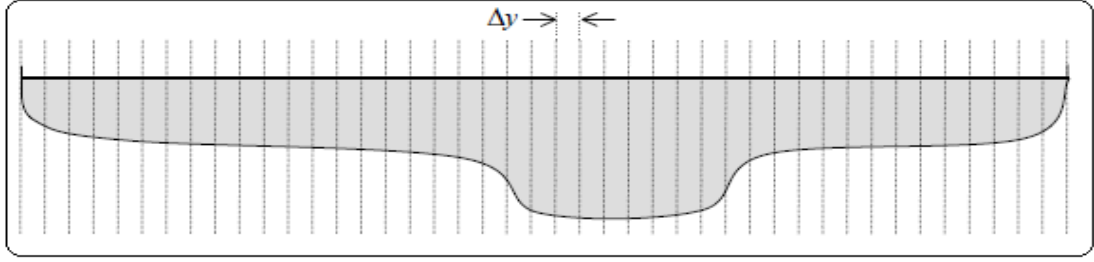


Fig.5-2 Channel Discretization for Solution of Depth-Integrated RANS

where C_{uv} attains a single value for a given cross-section and it is a function of the sinuosity, relative depth and relative roughness. The assumption is that the product of the local U and V velocities averaged over the depth, follow a similar profile to the streamwise depth-averaged velocity squared. The sinuosity and the secondary flow term for straight and meandering channels have been blended in equations (5.6 or 5.7) for use in Conveyance Generator equations built into CES in the following manners:

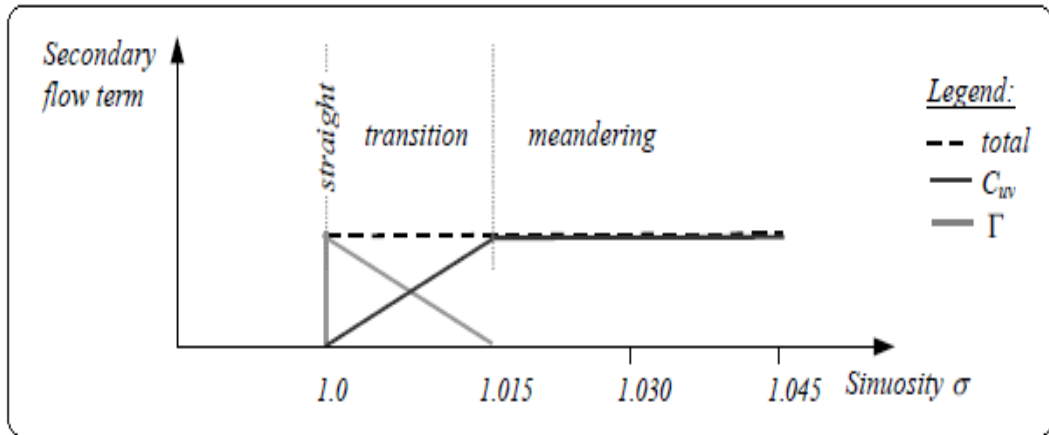


Fig.5- 1 Contributions from Secondary Flow Terms

The sinuosity, S_r , is defined here as the thalweg length over the valley length. To obtain a balance between $S_r = 1.0$ (equation 5.10) and $S_r > 1.015$ (equation 5.11), the contribution from the Γ term is linearly phased out (Fig.5-3) resulting in

$$-\frac{(1.015 - S_r)}{0.015} \Gamma - \frac{(S_r - 1.0)}{0.015} C_{uv} \frac{\partial}{\partial y} \left(\frac{q_x^2}{H} \right) = 0 \quad 1.0 \leq S_r \leq 1.015$$

$$-C_{uv} \frac{\partial}{\partial y} \left(\frac{q_x^2}{H} \right) = 0 \quad S_r > 1.015 \quad (5.9a, b)$$

Equation (5.6b) can thus be expressed for straight prismatic channels (Shiono & Knight, 1990) as

$$gHS - \frac{f\beta'q_x^2}{8H^2} + \frac{\partial}{\partial y} \left[\lambda H \left(\frac{f}{8} \right)^{1/2} q_x \frac{\partial}{\partial y} \left(\frac{q_x}{H} \right) \right] = \frac{(1.015 - S_r)}{0.015} \Gamma + \frac{(S_r - 1.0)}{0.015} C_{uv} \frac{\partial}{\partial y} \left(\frac{q_x^2}{H} \right) \quad (5.10)$$

and for meandering channels of sinuosity greater than 1.015 as

$$gHS - \frac{f\beta'q_x^2}{8H^2} + \frac{\partial}{\partial y} \left[\lambda H \left(\frac{f}{8} \right)^{1/2} q_x \frac{\partial}{\partial y} \left(\frac{q_x}{H} \right) \right] = C_{uv} \frac{\partial}{\partial y} \left[\frac{q_x^2}{H} \right] \quad (5.11)$$

Equation (5.10) is applicable for a sinuosity S_r of 1.0 for inbank flow and $1.0 < S_r < 1.015$ for overbank flow respectively in straight channels. Equation (5.11) is applicable for a sinuosity greater than 1.0 and greater than 1.015 for inbank and overbank flow in meandering channels respectively. The lateral unit flow rate distribution can then be integrated to find the total cross-section flow rate Q (m^3/s), and hence the total cross-section conveyance K (m^3/s), from

$$K = \frac{Q}{S_f^{1/2}} \approx \frac{\int q dy}{S^{1/2}} \quad (5.12)$$

where the reach-averaged longitudinal friction slope S_f is approximated by the reach averaged longitudinal bed slope S . Equations (5.10-5.11) can be expressed in more general form as

$$gHS_o - \frac{f\beta'q^2}{8H^2} + \frac{\partial}{\partial y} \left[\lambda H \left(\frac{f}{8} \right)^{1/2} q \frac{\partial}{\partial y} \left(\frac{q}{H} \right) \right] = c_1 \Gamma + c_2 C_{uv} \frac{\partial}{\partial y} \left[\frac{q^2}{H} \right] \quad (5.13)$$

The term q_x is replaced with q as mostly the unit flow rate is in streamwise direction. Equation (5.13) is a non-linear, non-homogeneous, and elliptic, second order partial differential equation and has been solved numerically in the Conveyance Generator. For this a one dimensional finite element method of solution well suited for solving elliptic equations has been selected. This involves discretizing the flow domain into a number of elements, and replacing the variable q with piecewise approximations,

usually polynomials termed ‘shape functions’. The result is a system of equations, which can be assigned boundary values and solved iteratively. For application in one-dimensional channel flow, the solution domain is the cross sectional area perpendicular to the flow direction. The domain is discretized through vertical slicing, generating fluid elements of width Δy . Each fluid element is in contact with the two adjacent elements, and the two elements situated at the cross-section edges are in contact with one other element and the boundary. For further details about these methods of solution reference can be made to DEFRA/EA (2003a, b; 2004/5).

5.2.1.2. Outline of Steps for Modeling through CES

The user has to use the steps as outlined below to run the software tool to obtain the results of simulation through CES.

First the roughness file named *.RAD File has to be created for the physical domain where the flow has to be simulated. For this the user needs to choose various roughness components comprising of vegetation, ground material and irregularity for all the three zones of the channel namely ;bed, bank and floodplain by selecting from the catalogue available for various morphotypes of vegetation, substrates for ground material and irregularity types inside the component ‘Roughness Advisor’ of CES.

- At this stage if there is some doubt about the actual value of roughness of the real vegetation , irregularity & substrates etc. the user can assign the lower and upper values for the assigned value so that CES accordingly computes the uncertainty band for the result outputs.
- After saving the RAD file, the Conveyance generator component needs to be activated for creating *.GEN file for where all general data for the physical domain such as name of reach, sinuosity, cross section details measurement (through lateral offsets and heights of various points on the cross section from bed to top of water surface) etc. are to be entered.
- Then all zones of the reach e.g. bed, bank & floodplains need to be assigned the roughness values as assigned previously through RAD file.
- By exercising the options available in advanced options tab in Conveyance Generator for various parameters e.g. no. of depth intervals, minimum depth

used in calculation, value of lateral eddy viscosity in the main channel, no. of vertical segments used in computation, relaxation parameter for convergence criteria, maximum no. of iterations and wall height multiplier etc. the user can vary the results of simulation so as to get the best possible outcome. Also there is a separate option of adopting Colebrook-White solver for experimental flumes where the temperature during the experiment has to be mentioned.

Finally the Conveyance Generator provides outputs for the whole cross-section, which are given at every depth, as below:

- total flow rate Q (m³/s)
- area A (m²)
- average velocity U_{av} (m/s)
- conveyance K (m³/s)
- Froude Number F_r ($=\frac{u}{\sqrt{gR}}$ and R = hydraulic mean depth or ratio of area to surface width)
- Reynolds Number Re [$=(uR_h)/\nu$ and R_h is the hydraulic radius]
- Coriolis' (or 'energy') coefficient α
- Boussinesq's (or 'momentum') coefficient β
- surface water width B (m).

and for each depth, the lateral variation of the following variables is also available.

- z co-ordinate (i.e. channel bed profile)
- unit flow q (m²/s)
- depth-averaged velocity U_d (m/s)
- unit conveyance k ($= K/m$) (m²/s)
- shear velocity U_* (m/s)
- bed shear stress τ (N/m²)
- bed friction f
- dimensionless eddy viscosity λ
- secondary flow term I'

5.3 CCHE2D MODEL

The CCHE modeling analysis system is an integrated system which is composed of a Graphical Users Interface (CCHE-GUI), a separate hydrodynamic numerical model (CCHE2D model) and a structured mesh generator (CCHE2D Mesh Generator).

- CCHE-GUI provides file management, run management, results visualization, and data reporting etc.
- CCHE2D Model is the numerical engine for hydrodynamic simulations. Presently the CCHE2D_EEM (Efficient-Element-Method-based) model is available.
- CCHE2D Mesh Generator is a necessary and useful tool for structured mesh generation in geometrically complex domains.

5.3.1. Governing Equations

The depth integrated two-dimensional equations are solved in CCHE2D model. The continuity equation and momentum equations in two dimensions neglecting the vertical variation of flow parameters can be written as

$$\text{Continuity Equation:} \quad \frac{\partial Z}{\partial t} + \frac{\partial(hu)}{\partial x} + \frac{\partial(hv)}{\partial y} = 0 \quad (5.14)$$

& Momentum Equations:

$$\frac{\partial u}{\partial t} + u \frac{\partial u}{\partial x} + v \frac{\partial u}{\partial y} = -g \frac{\partial Z}{\partial x} + \frac{1}{h} \left[\frac{\partial(h\tau_{xx})}{\partial x} + \frac{\partial(h\tau_{xy})}{\partial y} \right] - \frac{\tau_{bx}}{\rho h} + f_{cor}v \quad (5.15)$$

$$\frac{\partial v}{\partial t} + u \frac{\partial v}{\partial x} + v \frac{\partial v}{\partial y} = -g \frac{\partial Z}{\partial y} + \frac{1}{h} \left[\frac{\partial(h\tau_{yx})}{\partial x} + \frac{\partial(h\tau_{yy})}{\partial y} \right] - \frac{\tau_{by}}{\rho h} - f_{cor}u \quad (5.16)$$

where u and v are the depth-integrated velocity components in the x and y directions respectively; g is the gravitational acceleration; Z is the water surface elevation; ρ is water density; h is the local water depth; f_{Cor} is the Coriolis parameter; τ_{xx} , τ_{xy} , τ_{yx} , and τ_{yy} are the depth integrated Reynolds stresses; and τ_{bx} , τ_{by} are shear stresses on the bed surface.

5.3.2. Turbulence Closure

In Equations (5.15) and (5.16), the Reynolds stresses are approximated based on Boussinesq's assumption:

$$\tau_{xx} = 2\nu_t \frac{\partial u}{\partial x} \quad (5.17)$$

$$\tau_{xy} = \tau_{yx} = \nu_t \left(\frac{\partial u}{\partial y} + \frac{\partial v}{\partial x} \right) \quad (5.18)$$

$$\tau_{yy} = 2\nu_t \frac{\partial v}{\partial y} \quad (5.19)$$

where ν_t is the eddy viscosity.

5.3.2.1. Eddy Viscosity Model

There are two zero-equation eddy viscosity models adopted in the CCHE2D model.

The first one is the depth-integrated parabolic model, in which the eddy viscosity ν_t is calculated by the following formula:

$$\nu_t = \frac{A_{xy}}{6} \kappa U_* H \quad (5.20)$$

where A_{xy} is an adjustable coefficient of eddy viscosity, κ is the von Karman constant, and U_* the shear velocity. The second eddy viscosity model is the depth-integrated Mixing Length model. The eddy viscosity ν_t is calculated by the following equation.

$$\nu_t = \bar{l}^2 \sqrt{2 \left(\frac{\partial u}{\partial x} \right)^2 + 2 \left(\frac{\partial v}{\partial y} \right)^2 + 2 \left(\frac{\partial u}{\partial x} + \frac{\partial v}{\partial x} \right)^2 + \left(\frac{\partial \bar{U}}{\partial z} \right)^2} \quad (5.21a)$$

$$\bar{l} = \frac{1}{h} \int \kappa z \sqrt{\left(1 - \frac{z}{h} \right)} dz = \kappa h \int_0^1 \lambda \sqrt{1 - \lambda} d\lambda \approx 0.267 \kappa h \quad (5.21b)$$

$$\frac{\partial \bar{U}}{\partial z} = C_m \frac{U_*}{kh} \quad (5.21c)$$

where C_m is a coefficient with a value of 2.34375 so that Equation (5.21) will cover Equation (5.20) in the case of a uniform flow in which all the horizontal velocity gradients vanish.

5.3.2.2. Two-dimensional k - ε Model

In this model, differential equations are introduced for the turbulent kinetic energy k and the rate of dissipation of turbulent energy ε , where $k = \frac{1}{2} \overline{u_i' u_i'}$ and $\varepsilon = \mu_t \overline{\frac{\partial u_i'}{\partial x_j} \frac{\partial u_i'}{\partial x_j}}$.

The depth-integrated governing equations for k and ε are:

$$\frac{\partial k}{\partial t} + u \frac{\partial k}{\partial x} + v \frac{\partial k}{\partial y} - \frac{\partial}{\partial x} \left(\frac{\nu_t}{\sigma_k} \frac{\partial k}{\partial x} \right) - \frac{\partial}{\partial y} \left(\frac{\nu_t}{\sigma_k} \frac{\partial k}{\partial y} \right) = P - \varepsilon + P_{kV} \quad (5.22)$$

$$\frac{\partial \varepsilon}{\partial t} + u \frac{\partial \varepsilon}{\partial x} + v \frac{\partial \varepsilon}{\partial y} - \frac{\partial}{\partial x} \left(\frac{\nu_t}{\sigma_\varepsilon} \frac{\partial \varepsilon}{\partial x} \right) - \frac{\partial}{\partial y} \left(\frac{\nu_t}{\sigma_\varepsilon} \frac{\partial \varepsilon}{\partial y} \right) = c_{1\varepsilon} \frac{\varepsilon}{k} P - c_{2\varepsilon} \frac{\varepsilon^2}{k} + P_{\varepsilon V} \quad (5.23)$$

where
$$P = -\overline{u_i' u_{i,j}'} = \nu_t \left[2 \left(\frac{\partial u}{\partial x} \right)^2 + 2 \left(\frac{\partial v}{\partial y} \right)^2 + \left(\frac{\partial u}{\partial x} + \frac{\partial v}{\partial y} \right)^2 \right] \quad (5.24)$$

$$P_{kV} = C_k \frac{U_*^3}{h} \quad P_{\varepsilon V} = C_\varepsilon \frac{U_*^4}{h^2} \quad (5.25)$$

$$U_* = \sqrt{c_f (u^2 + v^2)} \quad (5.26)$$

$$C_k = \frac{1}{\sqrt{c_f}} \quad C_\varepsilon = 3.6 \frac{c_{2\varepsilon}}{c_f^{3/4}} \sqrt{c_\mu} \quad (5.27)$$

From the local values of k and ε , a local eddy viscosity can be evaluated as

$$\nu_t = \frac{c_\mu k^2}{\varepsilon} \quad (5.28)$$

In the above equations, the following values are used for the empirical constants:

$$c_\mu = 0.09, \quad c_{1\varepsilon} = 1.45, \quad c_{2\varepsilon} = 1.90, \quad \sigma_k = 1.0 \quad \& \quad \sigma_\varepsilon = 1.30$$

5.3.3. General Procedure

The numerical modeling based on solving the depth averaged Navier-Stokes equations is an initial-boundary value problem. It is necessary to provide initial conditions and the boundary conditions. The general procedure of a numerical simulation can be simply listed as follows:

- Mesh generation
- Specification of boundary condition
- Parameters setting
- Simulation
- Results visualization and interpretation

5.3.3.1. *Mesh Generation*

The mesh represents the computational domain. It should be prepared with utmost care and sufficient background knowledge in order to obtain a good simulation.

A good quality mesh meeting certain criteria is a prerequisite to any successful simulation. As per the CCHE2D v.3.0.user's manual (Zhang, 2009) the mesh must be built so as to meet the criteria as listed below:

- The interested zones have sufficient resolution;
- Transition between areas of different densities is smooth;
- Inlet(s) and outlet(s) should be sufficiently far away from the zones of interest;
- The mesh should be smooth and orthogonal as much as it allows.

For meeting the above and creating the mesh for the different physical domains the module 'CCHE-MESH' available in the package can be used by following a step by step procedure. Usually CCHE-MESH creates a structured mesh which consists of families of mesh lines with the property that members of a single family do not cross each other and cross each member of the other families only once. The mesh generation takes place in CCHE-MESH in two major steps. An algebraic mesh is generated first where a quick but crude initial mesh is created for further refinement and generation of a numerical mesh. Smoothness and orthogonality; the major two qualities are intermittently checked to evaluate the quality of mesh. For this purpose a mesh-evaluation table showing various parameters pertaining to mesh quality is available in the mesh module.

5.3.3.2. *Specification of boundary condition*

Boundary conditions are the user set values which govern or guide the flow in the simulated zone. It must be carefully selected representing the true physical behavior of the flow taking place. Mainly the inlet and outlet flow conditions of the domain are to

be set. Often the discharge entering the domain can be set as inlet flow boundary condition while the water surface level at the outlet of the domain is entered as the outlet boundary conditions. Additionally there is option of applying flow hydrograph or discharge hydrograph as inlet condition and rating curve or stage hydrograph as outlet boundary condition. However care must be exercised to mark the inlet and outlet boundaries sufficiently far away from the interested zones in the domain where simulated results are expected.

5.3.3.3. *Parameters setting*

There are a number of groups of parameters which must be then set after setting the initial and boundary conditions. They are termed as flow parameters and three groups of parameters are to be set viz. simulation parameters, bed roughness parameters and advanced parameters. Under the group of simulation parameter one has to choose the time step for each iteration and total simulation time thus fixing the time step, then one of the four turbulence closure options available and some other numerical parameters like wall slipness coefficient, method of iteration etc. Similarly in the bed roughness group there are a number of options to choose or specify the bed and wall roughness values such as Manning's n value or out of those from Wu & Wang (1999) or van Rajin (1989) formula as applicable to the case at hand. In the advanced group Coriolis force coefficient, gravitational acceleration, von Karman constant, and kinematic viscosity of fluid, with default values that suffice for most cases, are available. However the user can change them if found necessary.

5.3.3.4. *Simulation*

After specifying all initial conditions and boundary conditions, setting the flow parameters the model simulation can be started. For this 'run simulation' tab with a number of options such as steady flow, unsteady flows etc. are available and may be exercised depending on the user's need. Also multiple runs may be necessary with some changes in flow parameters to get the desired results as numerical simulation is often a trial and error process.

5.3.3.5. *Results visualization and interpretation*

After the simulation is run for the desired no. of time steps the console window inside the GUI of CCHE2D indicates that the simulation is successful and the flow final results are ready for use. There are a number of output variables such as water surface;

water depth; U & V velocity components (x & y components); U & V components of specific discharges; total specific discharge; X , Y components of shear stress; total shear stress; eddy viscosity (ε) and Froude no. (F_r) etc. Also if the user provides time interval to extract history results of simulation before setting up the simulation then CCHE2D can give history results at predetermined time intervals of 100 or 1000 time steps to analyse the progress of simulation in case an unsuccessful simulation. The results for different variables are then to be interpreted with proper care and sufficient expertise for practical use.

5.3.4. Channel Simulation Results

The overbank cases which were studied experimentally for straight compound channel as well as for meandering compound channel in Fluid mechanics and hydraulics laboratory of NIT, Rourkela were also simulated through both CES and CCHE2D in order to draw a comparative picture about the validity of the results obtained through numerical tools vis a vis the experimental observations. The typical overbank cases for NIT channels along with their physical flow parameters are shown in Table. 5-1. In addition to the application of the CES and CCHE2D models in NIT, Rourkela channels, two further studies were also taken up in this research work to predict the distribution of depth averaged velocity and boundary shear stress across their wetted perimeter to examine the suitability of these numerical tools in large scale flume and real river cases having wide flood plains similar to the geometrical conditions of the new experimental channels. Accordingly one large scale flume experiment from EPSRC-FCF series (Phase A-series1 Experiment) and a real river case i.e. the river Severn at Mont Ford Bridge site (Knight, 1989) were chosen for simulation. While the FCF series (Series A-1 Experiments) consists of smooth compound channel experiments (Details at Myers & Brennan, 1990) and have been widely used in past by various researchers (Ervine et al, 2000; Khatua, et al, 2012 etc.) for extensive study of their respective models, the latter case i.e. the River Severn at selected site has been extensively monitored for practical hydrometry and research purposes, providing a large body of accurate current metering data (Knight, 1989). It is a natural cross-section located in a straight reach with a cableway extending over the full width including the floodplains. The bankfull width and depth are 40 and 6.3 meters respectively. The total width, including the floodplains, is approximately 120m (Fig.5-10 shows the cross sectional geometry). No modeling studies of such large scale flume experiment or real river case having wide floodplains

in CCHE2D package could be found in literature. So in order to make this comparative study through both physical and numerical experiments, an exhaustive one, containing straight compound channels of width ratios $6.67 \leq \alpha < 12$ and meandering compound channel of $\alpha \approx 12$, all the four cases (two channels of NIT, Rourkela, one FCF channel and the River Severn site) were systematically studied in both CES and CCHE2D.

As regards simulation through CES, because of smooth main channel and floodplains of NIT channels, the flow cases for straight and meandering channels were simulated keeping the roughness value in main channel and floodplains in *.RAD file near to 0.01 (Manning's n value for smooth surface) by trial and error process until the back calculated value of n value outputs were equal to 0.01. Rest of the procedure for simulation was followed as outlined in section 5.2.1.2. Following a similar procedure the modeling for smooth FCF (A-1) channel and the river Severn site (CES v2.0 help manual, 2007) for the main channel and the floodplains were carried out. Thus the results for the distribution of depth averaged velocity and boundary shear across the cross section of compound sections for various overbank flow cases were extracted from CES. The same along with the comparative figures from CCHE2D results and experimental observations are shown and discussed later in this chapter.

For CHE2D, the computational mesh for both straight and meandering compound channels were created first with the help of CCHE-MESH. A number of trial meshes were created for both the domains keeping in view the objectives of simulation. Looking at the physical expanse of the flow domains and the physical discontinuity at the main channel and floodplain interface, a multi block boundary approach was planned in each case to first create the geometry of the domains. Each floodplain on either side of the main channel and the main channel itself totaled 3 nos. of blocks. In the very first step topographic database files containing the x , y & z (coordinates in space) dimensions of various defining points lying on the boundary of the channels were created. The multi block geometry was then created by joining the points sequentially. Thereafter an algebraic mesh was created for each block. The blocks were then joined appropriately to generate a multi block algebraic mesh for whole domain. From the algebraic mesh thus created, the numerical meshes were created by trial and error process by successively applying different options for numerical mesh generation viz. TTM mesh, RL mesh, RL adaptive mesh etc. In each case after generating the numerical mesh, the mesh was evaluated for its suitability regarding various mesh

evaluation criteria and a particular numerical mesh was adopted for simulation purpose only after achieving a satisfactory level of evaluation criteria. Thus many combinations were tried out even after running a simulation as the results were very much dependent upon the quality of the mesh as mentioned before. For brevity, the details for final mesh giving successful simulations for straight and meandering channel cases are only mentioned here. Two separate meshes were generated; one for simulating straight compound channel flow cases and the other for meandering channel cases. Two more meshes; one for FCF channel and another for the river Severn were also prepared to carry out the simulation. The physical dimensions for meshes for straight and meandering channels of NIT, Rourkela were taken as 1:1 i.e. the dimensions of length; breadth and height of the meshes were kept exactly same as in the experimental channels. The mesh for straight and meandering compound channels are shown in Figs.5-4 & 5-5 and Figs.5-6 & 5-7 respectively. For the FCF channel the mesh width was kept same as in original experiment i.e. 10m while the length of the computational mesh was chosen as 50m and the depth or height of the model remained same as in original. The bathymetry data for all the cases were prepared by analysing the cross sectional details, length of channels and bed slope and was used for interpolation so as to generate the test domains suitable for numerical analysis.

Table.5-1 Summary of Overbank Flow Cases in NIT Channels

Channel type	Run case ID	Discharge Q (liters/s)	Flow depth (H) (cm)	Relative depth (β)	Froude no. (F_r)	Reynolds no. (R_e)
(1)	(2)	(3)	(4)	(5)	(6)	(7)
Straight compound channel	SCO-01	13.543	7.3	0.110	0.507	39476
	SCO-02	17.482	7.5	0.133	0.555	45033
	SCO-03	36.396	8.8	0.261	0.508	52363
	SCO-04	53.546	10.1	0.356	0.372	47200
	SCO-05	60.282	10.5	0.381	0.364	48899
	SCO-06	106.181	11.5	0.435	0.505	77734
Meandering compound channel	MCO-01	17.074	8.06	0.194	0.220	19682
	MCO-02	27.617	8.55	0.240	0.283	27641
	MCO-03	47.245	9.5	0.316	0.340	38865
	MCO-04	55.393	10.2	0.363	0.410	52128
	MCO-05	80.667	11	0.410	0.443	63233
Note:- S-straight; C-compound; O-overbank and M-meandering.						

For the Severn model, a mesh mimicking the straight reach having length of 1km and cross section same as in Fig.5-10 was created for simulation. For FCF channel due to large physical width of 10m and to model the domain accurately, a five block boundary was chosen as shown (in Figs.5-8 & 5-9). However for the river Severn model a three block bounded geometry (Fig.5-11) sufficed. Here different roughness values for the bed roughness were assigned in the main channel and the floodplains as per the data available in literature (Knight, 1989; CES v2.0 help manual, 2007).

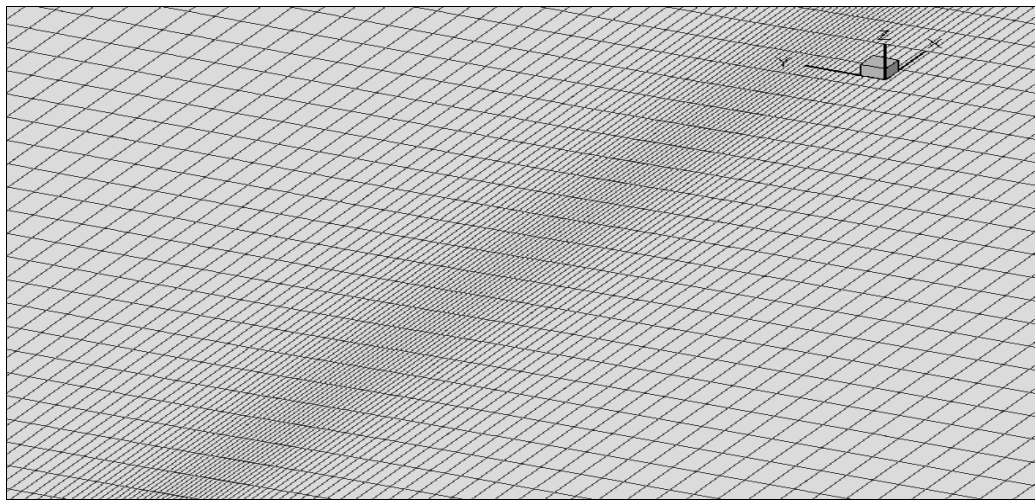


Fig.5- 4 Plan View of NIT Straight Compound Channel Mesh

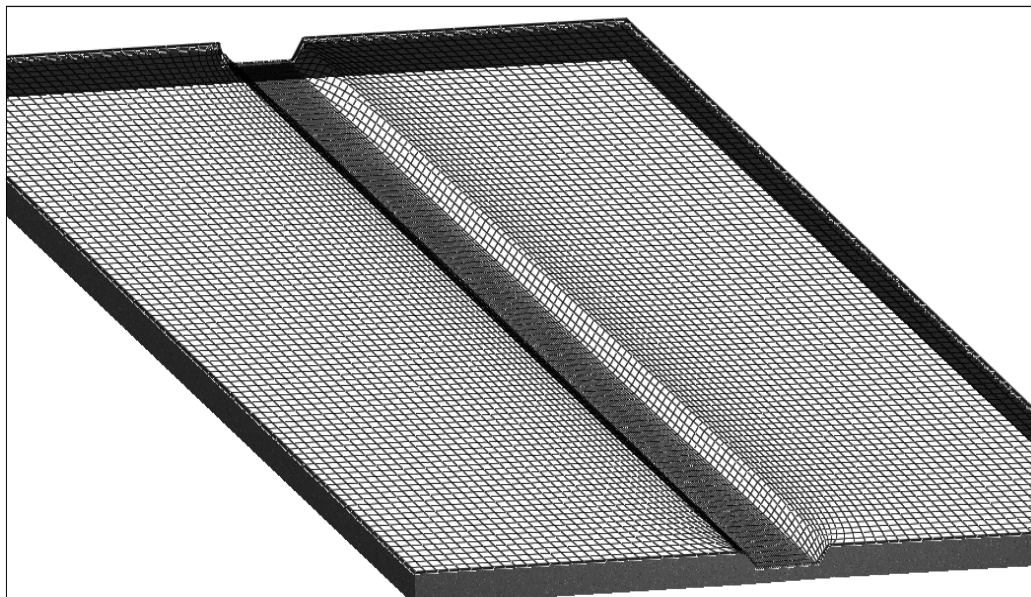


Fig.5-5 3D View of NIT Straight Compound Channel Mesh

In all cases the width of all blocks were chosen in such a manner so as to get sufficient resolution for the data to be extracted. Also the nos. of span wise gridlines were so chosen that a smooth transition in the mesh densities was achieved from the center of main channel to the floodplain ends resulting in gradual enlargement in spacing between two consecutive grid lines in outward spanwise direction. The salient features of the mesh for all the above cases along with other vital parameters of interest to the numerical analysis are given in the Tables.5-2 and 5-3.

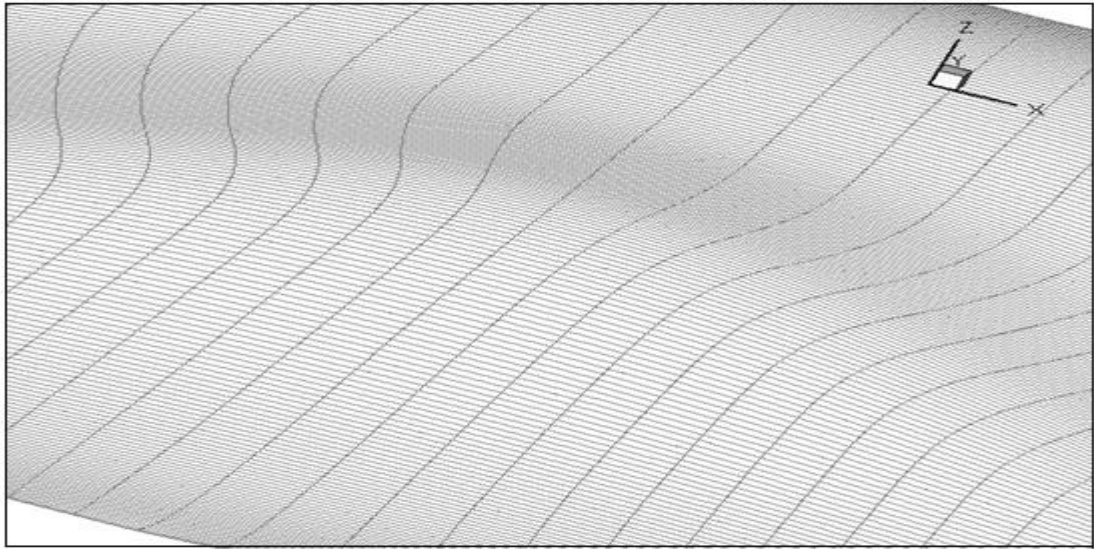


Fig.5-6 Plan View of NIT Meandering Compound Channel Mesh

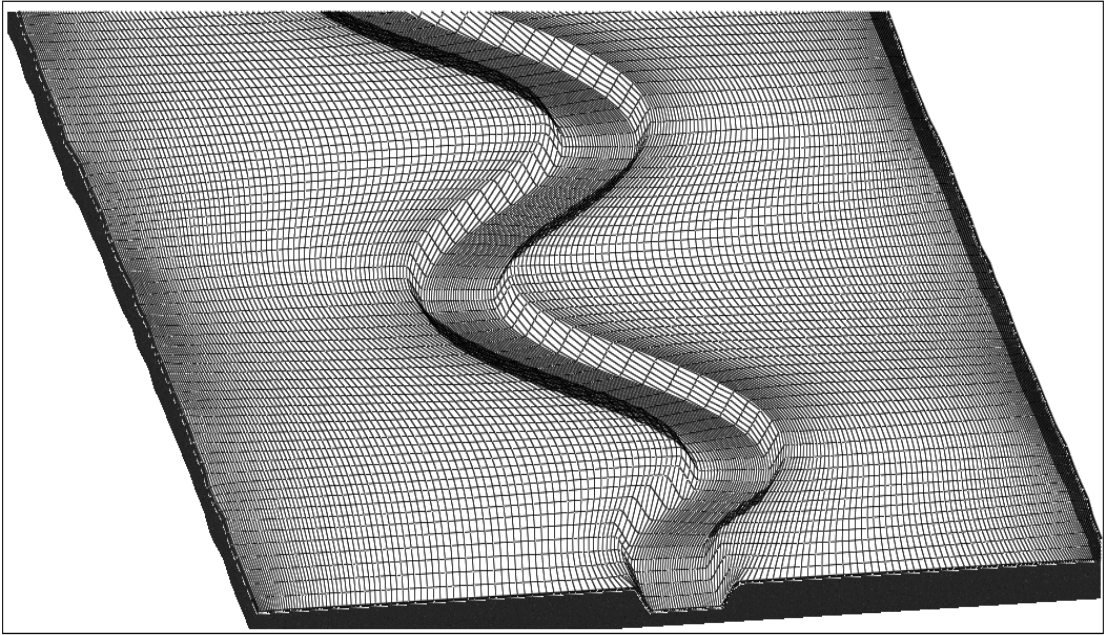


Fig.5-7 3D View of NIT Meandering Compound Channel Mesh

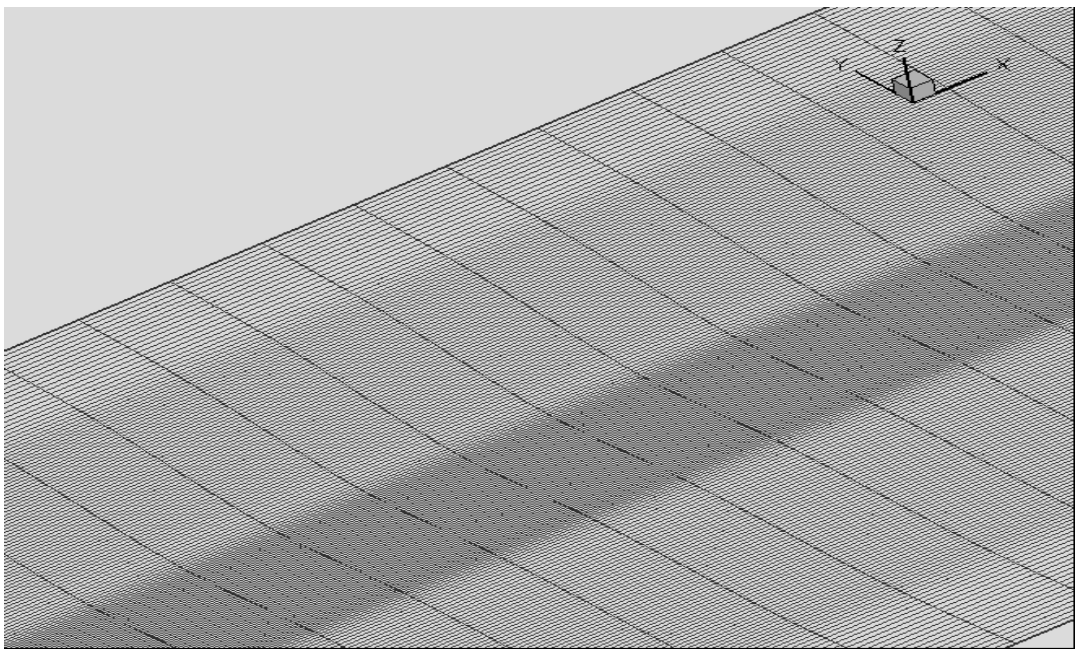


Fig.5-8 Plan View of FCFA-1 Channel Mesh

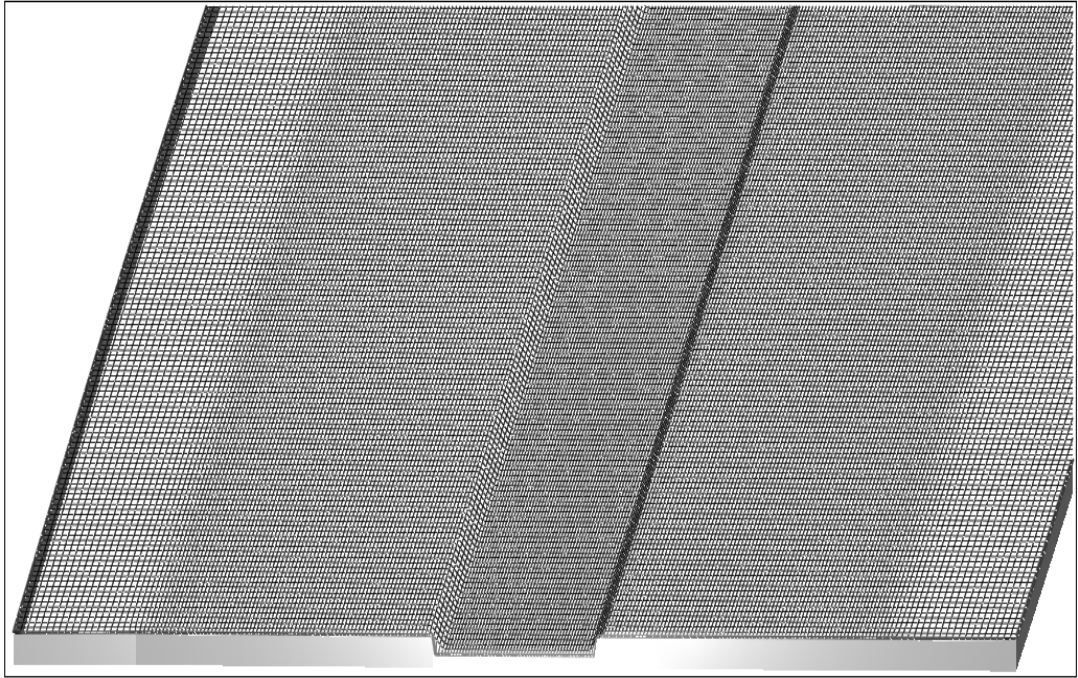


Fig.5-9 3D View of FCFA-1 Channel mesh

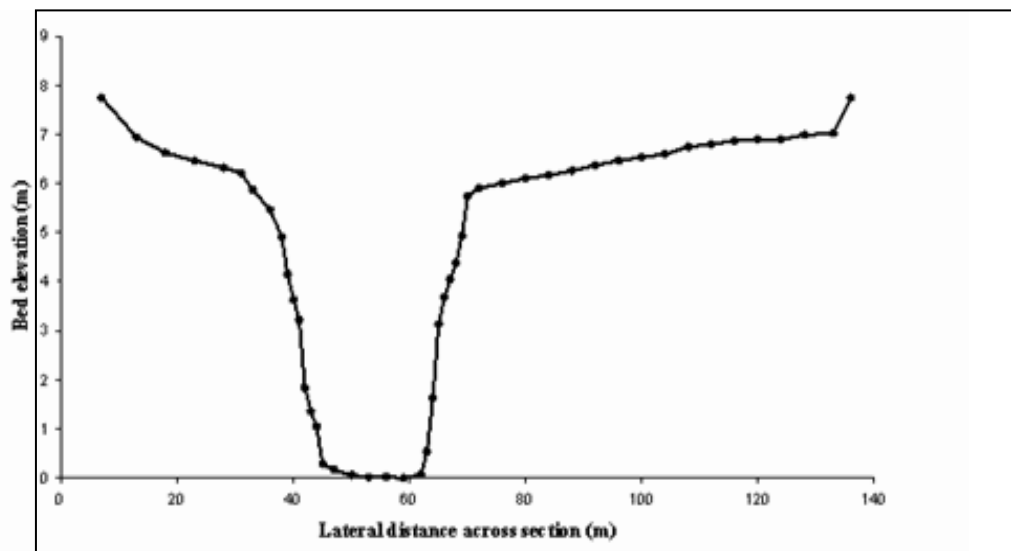


Fig.5-10 River Severn cross section-geometry at Mont ford bridge site.

(From CES v2.0 help manual, 2007)

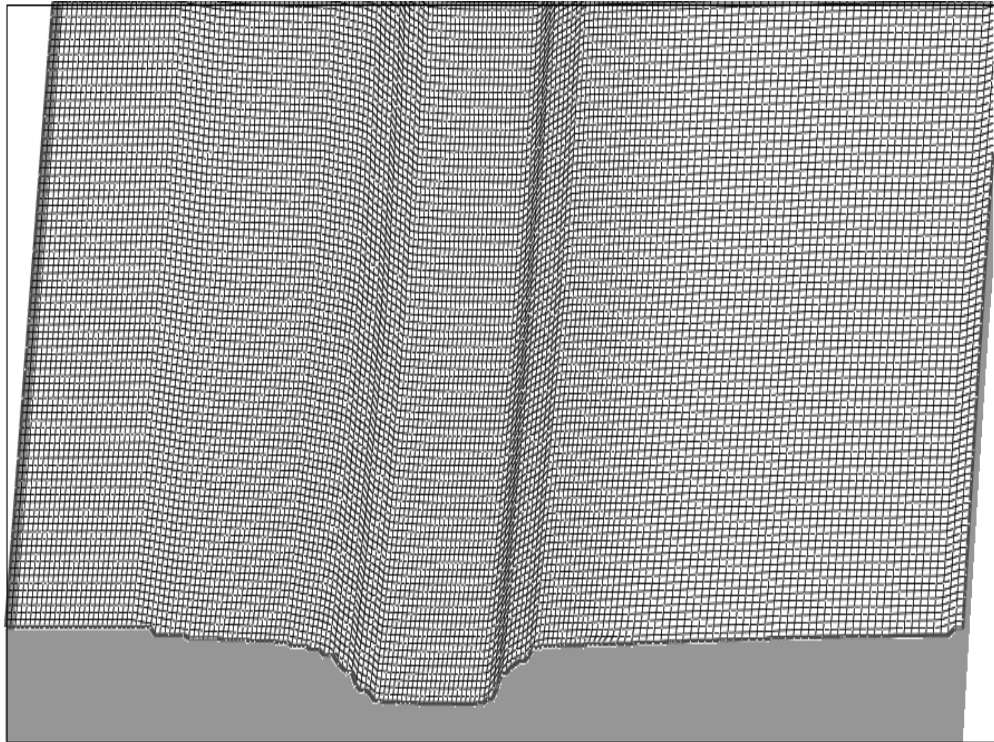


Fig.5-11 The Physical Model with Mesh for River Severn at Mont ford bridge site.

TABLE.5-2 Summary of Mesh Details for the Channels

Channel name	Grid lines in spanwise (I) direction	Grid lines in stream wise (J) direction	Total no. of elements	Average deviation from orthogonality (ADO)	Average Aspect ratio (AAR)	Cell length in I direction(Δy) in m		Cell length in J direction(Δx) in m	
						Min	Max	Min	Max
NIT Straight	206	60	12360	0.6254	11.5179	0.01227	0.03694	0.18407	0.18983
NIT Meander	208	80	16640	7.9100	7.5217	0.0054	0.03525	0.06861	0.24068
FCFA-1	256	150	38400	0.8568	9.800	0.02979	0.06938	0.36417	0.38601

The turbulence closure models were tried one by one in each case to run the simulations and finally the model which gave the best outputs in comparison with the respective experimental or measured values was accepted in each case. Similarly all other flow parameters including time steps, total simulation time etc. were adopted in each case by looking at the final results of simulation. In case of CCHE2D model the time steps were to be chosen so as to get a convergent solution. All these flow parameters for different cases are shown in Table.5-3.

Table.5-3 Flow Parameters Set in CCHE2D Numerical Analysis

Channel name	Time step (sec)	Simulation time (sec)	Total no. of time steps	Convergence	Turbulence model	Manning's n value	
						Main channel	floodplains
NIT Straight	0.01	100	10000	10	$k-\varepsilon$	0.01	0.01
NIT Meander	0.01	100	10000	10	Mixing length	0.01	0.01
FCFA-1	0.01	100	10000	10	$k-\varepsilon$	0.01	0.01
River Severn	0.01	250	25000	10	Smagorinski	0.032	0.04

Although in the final flow results several flow variables like water depth, depth averaged velocities, shear stress, specific discharge etc. in x & y (streamwise and spanwise) directions were available for different overbank flow depths in each channel cases, the depth averaged velocity U_d (x direction) and boundary shear stress (τ) results are presented here along with the results from respective CES outputs and experimentally observed values for the laboratory channels as well as the field data for the river Severn at Montford bridge site.

5.3.4.1. Depth averaged velocity results

The depth averaged velocity being an important flow variable in any compound channel or river flow analysis is first considered for comparison purpose in the present cases. In any 2dimensional flow analysis and particularly in the new cases of compound channels with high width ratio (α) values considered in this research work the predictive abilities of the models were put to test. So for all the overbank flow depths the depth averaged velocity data were extracted from CES outputs and CCHE2D and compared with their measured values. Figs.5-12 & 13 show depth averaged velocity values normalised with absolute maximum velocity value among all the three i.e.

Experimental, CES and CCHE2D respectively in case of Straight channels of NIT,Rourkela & FCFA-1 channel.

The figure 5-12(ii) relates to depth averaged velocity in NIT,Rourkela straight channel showing a comparison among experimental value and the simulated value through CES and CCHE2D. It is observed that significant difference between the experimental value and numerical values occur mainly at junction region. However both the predictions from CES and CCHE2D are seen to match well. The difference with experimental value is mainly due to complexities involved at low relative depth as the case relates to a β value of 0.133.

Fig.5-14 show the observed and CCHE2D simulated depth averaged velocity magnitudes directly for the the river Severn. Fig.5-15 shows the depth averaged velocity values for NIT,Meandering channel. For the river Severn only two data sets of depth averaged velocity values (at a flow depth of 6.918m and 6.45m are available in literature (CES v2.0 help manual,2007) for comparison with modeled values. Also as the same cases have been solved through CES and are available in its help manual, so only CCHE2D predicted values are shown here in Fig.5-14 for the two flow depths in the river Severn along with their gauged values.

From the straight channel cases it is seen that both CES and CCHE2D are good enough to predict the lateral distribution depth averaged velocity in wide trapezoidal compound channels having width ratio (α) equal to 6.67 as evident from validation results of FCFA-1 channel (for all 8 runs shown in Fig.5-13, i-viii). When applied the wide straight compound channel of NIT,Rourkela, it is seen that here CCHE2D and CES outputs are very well matched while mild deviation from the experimentally observed values can be noticed (Figs.5-12, i-vi). From the depth averaged velocity outputs for the wide meandering compound channel of NIT,Rourkela for all the five overbank cases shown in Figs.5-15 (i-v), it is observed that CCHE2D predictions are in very good agreement with their experimental values. The CES results matched well with CCHE2D and experimental values in case of higher overbank flow depths (Figs.5-15,iii-v). However some deviations at low overbank cases (Figs.5-15, i & ii) particularly in main channel region is noticed. In case of river Severn (in Figs.5-14, i & ii) also good agreement is noticed between the observed and simulated values of depth averaged velocity. The overall predictions from CCHE2D are very good while those from CES are satisfactory.

Thus it can be inferred from above that simulation studies through CCHE2D are able to predict lateral distribution of depth averaged velocity values quite satisfactorily over a range of straight compound channels consisting small scale flume, large scale flume and real river with wide floodplains ($6.67 \leq \alpha < 12$). Similarly the package is able to predict the velocity values even for a meandering compound channel with wide floodplains. CES is also quite useful in the present cases and hence both have good application in compound channel research.

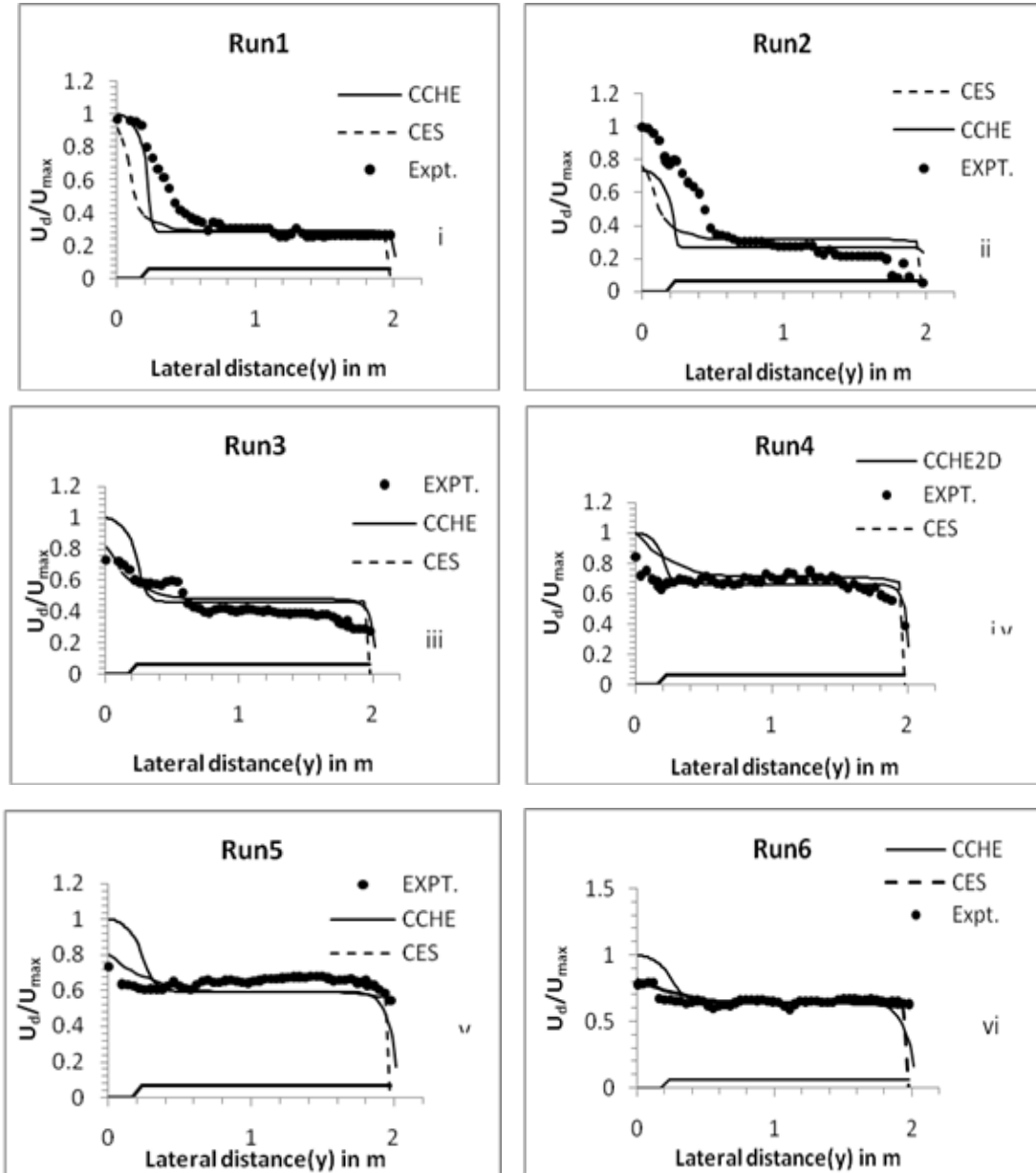


Fig.5- 12(i-vi) Depth Averaged velocity (U_d) normalized with U_{max} for NIT, Straight channel

5.3.4.2 *Boundary shear stress results*

The distribution of point boundary shear stress (τ) over the wetted perimeter of the whole compound section is next presented for all the cases. The same is normalised with maximum shear stress (τ_{max}) and is shown for all the straight channel cases first in Fig.5-16 for FCFA-1 channel; in Fig.5-17 for NIT,Rourkela straight channel and in Fig.5-18 for the meandering channel of NIT,Rourkela. As it is very difficult to collect boundary shear data in a flooded river, so the same is not available in literature for comparison for the river Severn case. Hence the CCHE2D boundary shear stress results for the river Severn could not be validated with field data. So the same is not shown here as the main aim of showing all velocity and boundary shear data from numerical simulation is to validate the CCHE2D for new complex domains like compound channels with high width ratio. The CCHE2D results for lateral distribution of boundary shear for straight channel cases are again shown to be in very good agreement with their observed values for FCFA-1 channel and also matched satisfactorily with experimental values in case of NIT straight channel. For FCFA-1 channel the CES results are even better than CCHE2D values as minor deviation of latter from the experimental values in case of main channel region is observed in a few runs e.g. runs 1,2 &4. In case of NIT,Rourkela Straight channel except in runs 1&2 i.e. for low overbank depths, good matching of all three viz. experimental values, CES & CCHE2D results is observed and hence CCHE2D values are once again validated in case of compound channel with high width ratio as in the present case. In Fig.5-18 (i-v) the boundary shear stress results for all the three i.e. experimental ,CES and CCHE2D values in NIT,Rourkela meandering channel case are shown.

The figure 5-16(i) relates to boundary shear in NIT,Rourkela straight channel showing a comparison among experimental value and the simulated value through CES and CCHE2D. It is observed that significant difference between the experimental value and numerical values occur mainly at junction region. However both the predictions from CES and CCHE2D are seen to match well. The difference with experimental value is mainly due to complexities involved at low relative depth as the case relates to a β value of 0.111.

The figure 5-17(iv) relates to boundary shear stress in FCF-series A straight channel showing a comparison among experimental value and the simulated value through CES and CCHE2D. The difference is mainly seen in main channel region and continued up

to the junction or interface of main channel and floodplain. The difference is an isolated one among the eight cases considered for the widest EPSRC channel. This comparative study was largely undertaken to know the general applicability of the two numerical tools viz. 1D-CES & 2D-CCHE2D package to a wide straight compound channel from the large scale EPSRC channels.

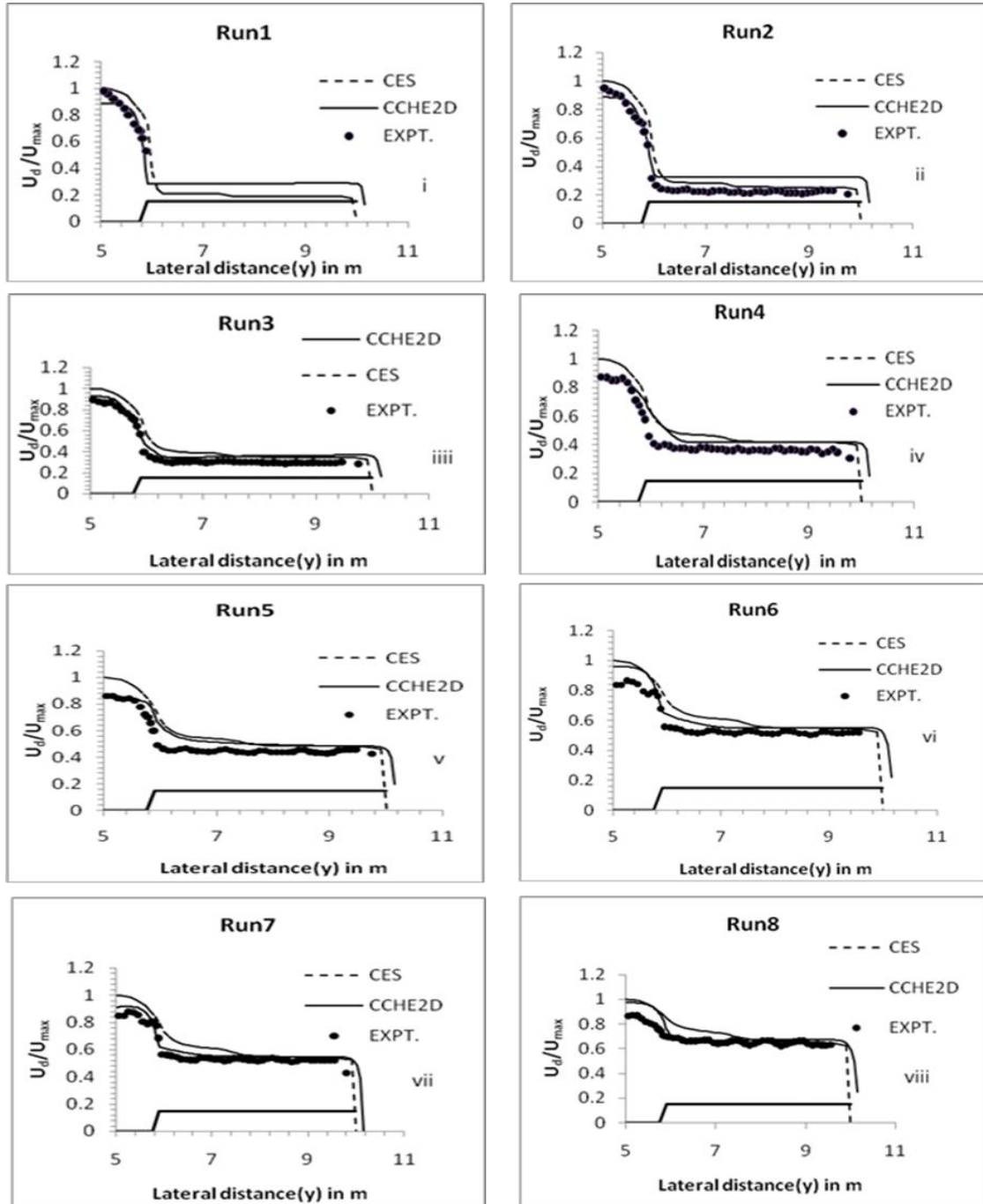


Fig.5- 13(i-viii) Depth averaged velocity normalized with U_{max} for FCFA-1 Channel

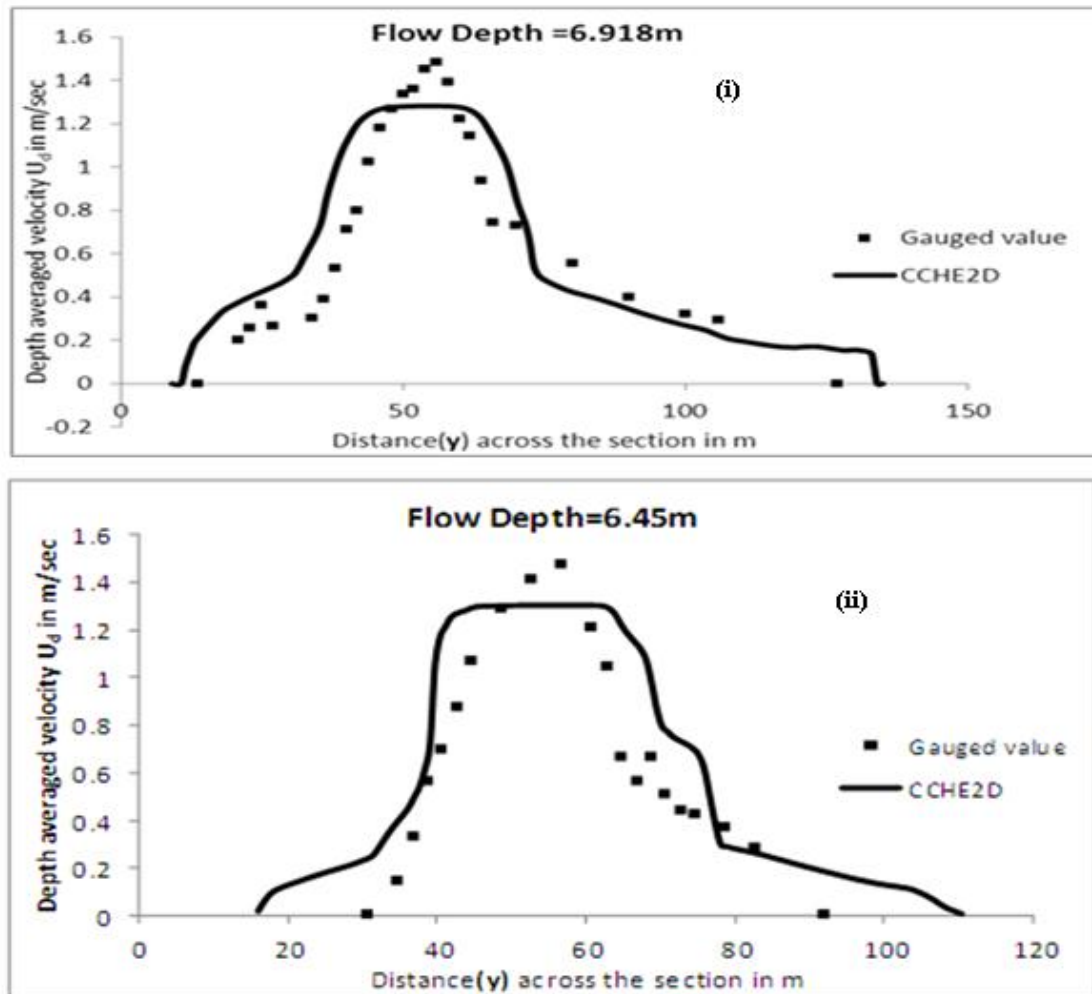
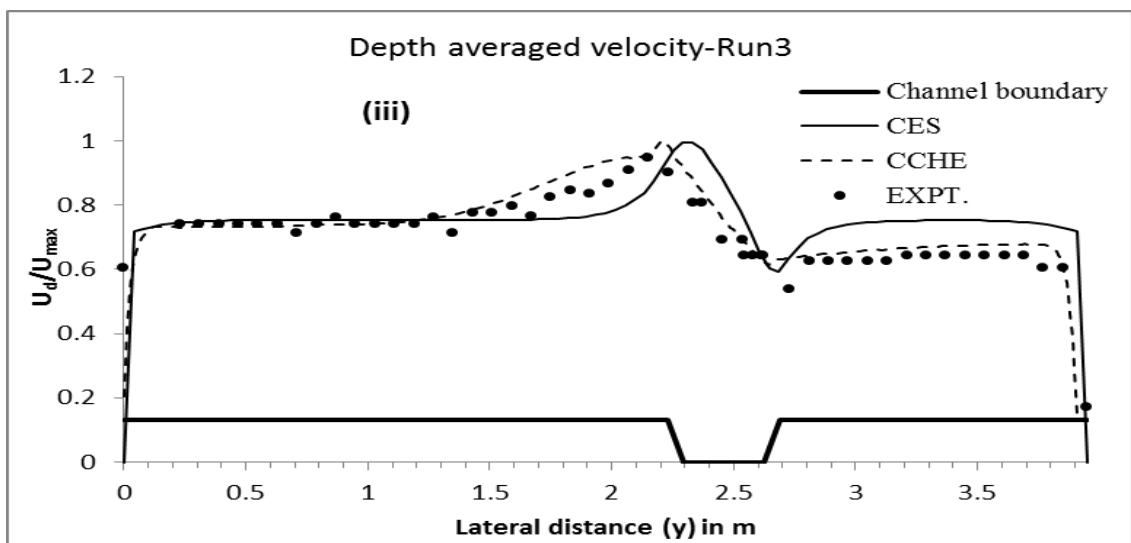
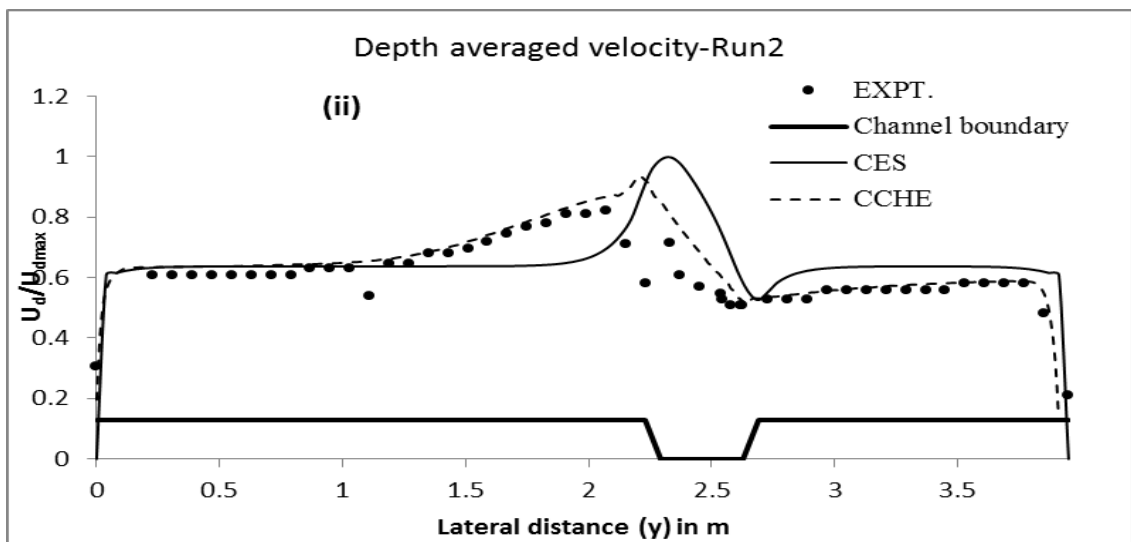
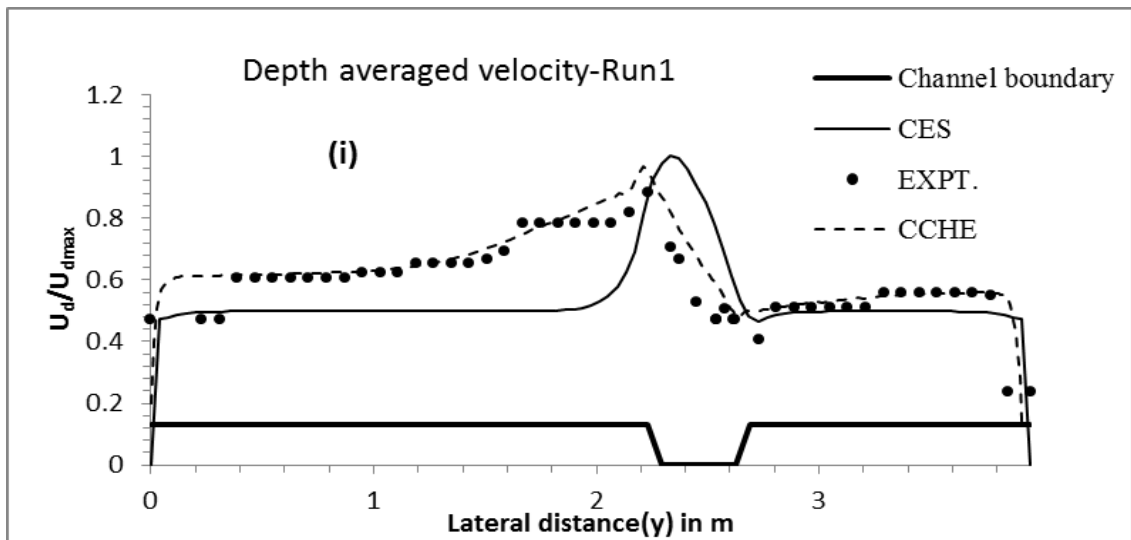


Fig.5- 14 (i & ii) Depth averaged velocity (U_d) prediction by CCHE2D for river Severn at Mont ford bridge site.



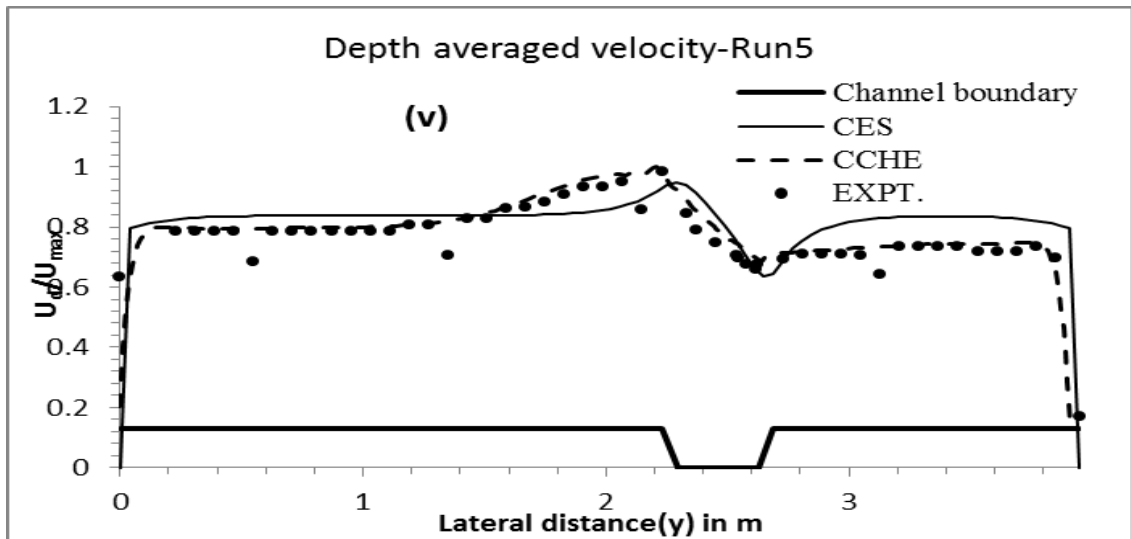
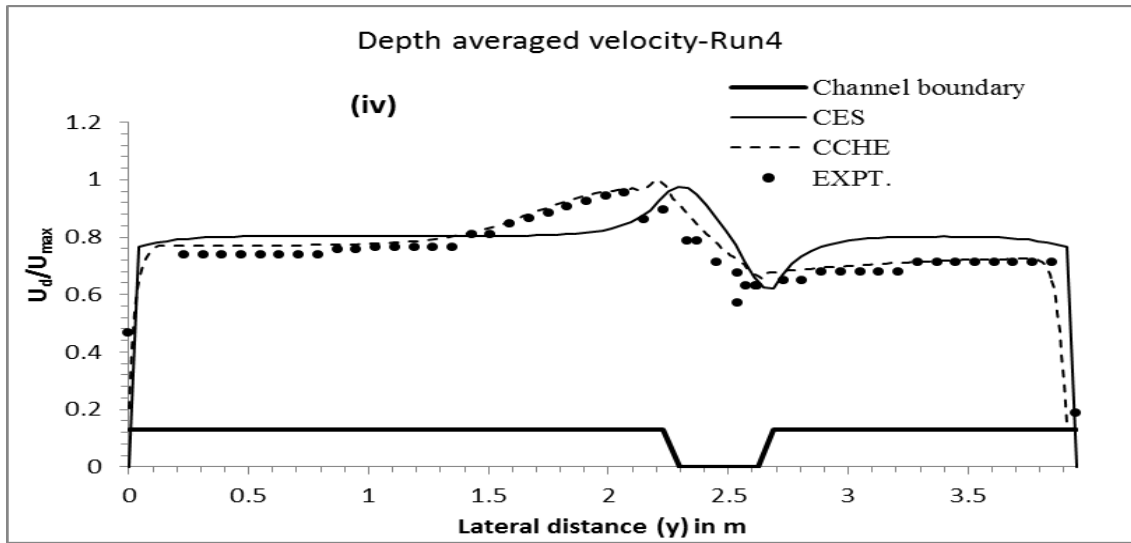


Fig.5- 15(i-v) Depth averaged velocity (U_d) normalized with U_{max} for NIT,
Meandering Channel

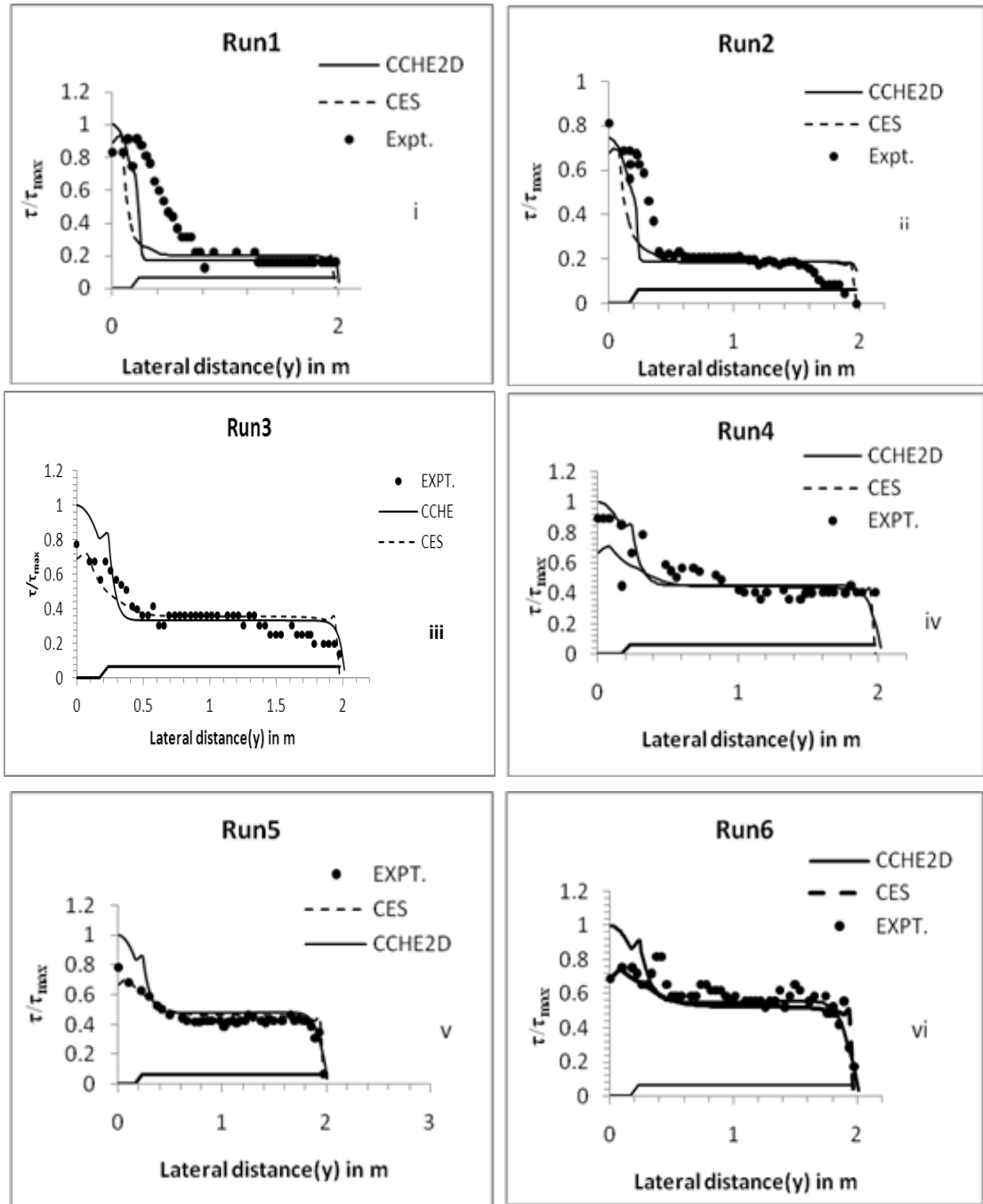


Fig.5- 16(i-vi) Boundary shear stress (τ) normalized with τ_{max} for NIT, Straight channel

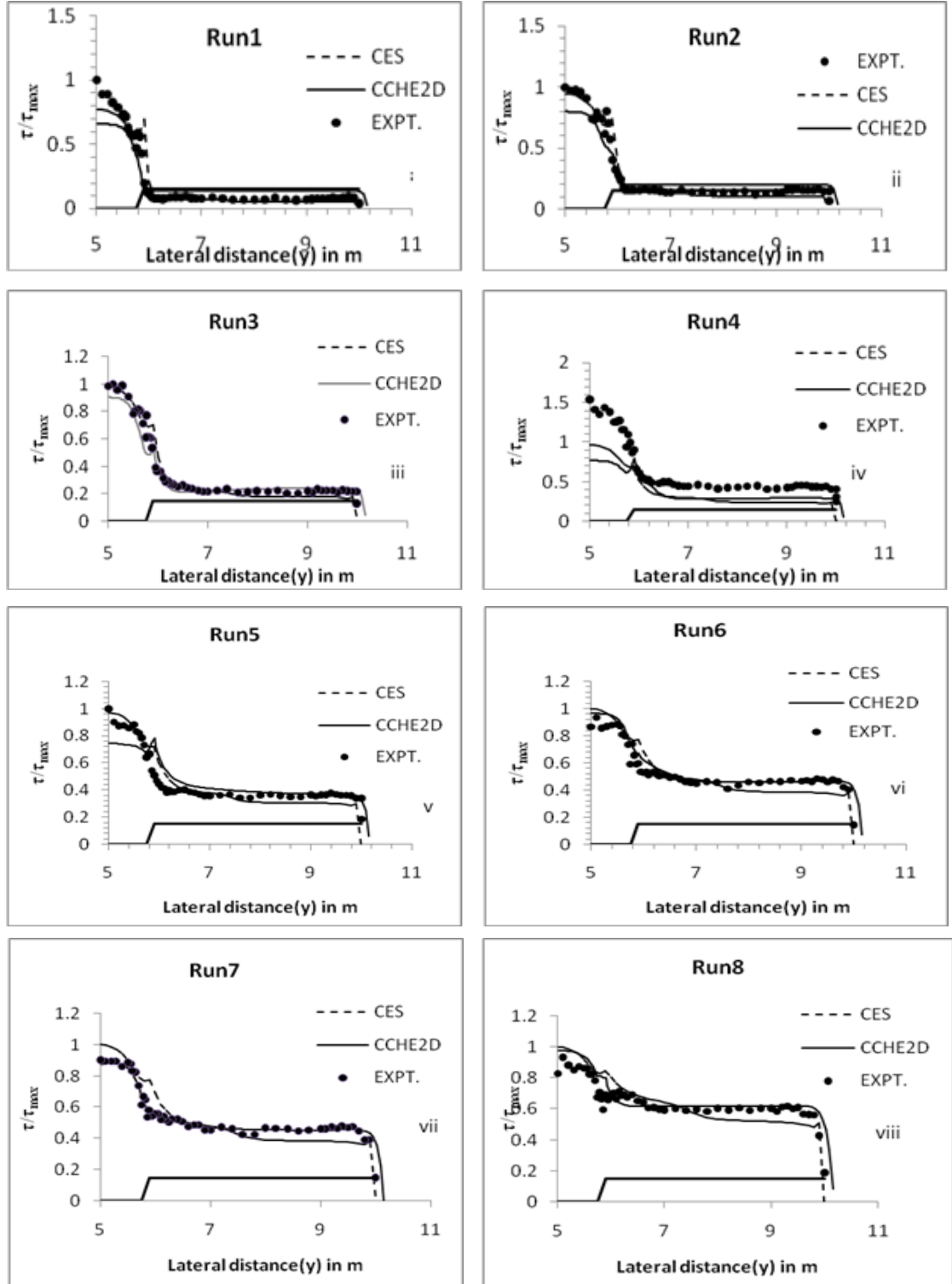


Fig.5- 17(i-viii) Boundary shear stress normalized with τ_{max} for FCFA-1 Channel

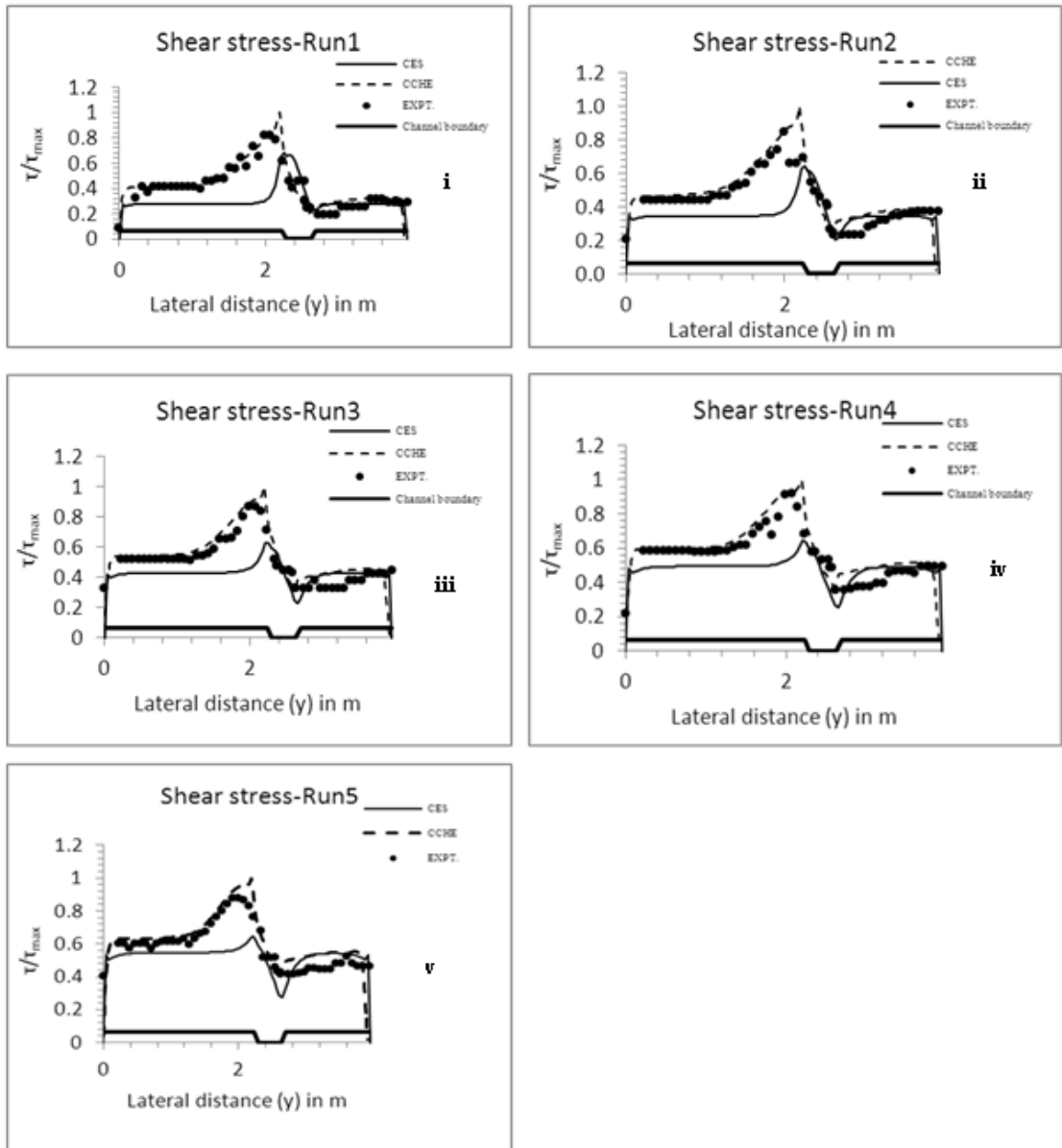


Fig.5- 18(i-v) Boundary shear stress (τ) normalized with τ_{max} for NIT, Meandering Channel

ANALYSIS AND DISCUSSION

6.1 GENERAL

The current section deals with the findings from the experiments conducted in the present straight and meandering compound channels. New models are developed for velocity distribution coefficients from the isovels shown in chapter 4 for both types of channels. The importance of accurate estimation of stage discharge relationship in any river or channel is underscored by many practical applications as any error in prediction might lead to economic damages or even loss of life (De Marchis and Napoli, 2008). Models have been developed separately for straight and meandering compound channels due to the disparate nature of the mechanisms associated with each type. On basis of the measured shear stress over the straight and meandering compound channels for different flow depths, separate model for each channel is presented by associating the sub sectional shear force with the corresponding flow area through exploring their functional relationship. Then stage discharge models are developed and analysed for straight compound channels of different width ratio range as well as for wide meandering compound channel.

6.2 VELOCITY DISTRIBUTION COEFFICIENTS

Accurate prediction of velocity distribution in channels is very important for flood studies and estimation of stage discharge curve in natural channels. Often for simplicity in river engineering practice the velocity is considered uniform and analysis is carried out considering energy or momentum approach. But any deviation from uniformity are usually accounted for by introduction of two correction factor namely, Kinetic energy correction coefficient (α) or simply energy coefficient {also termed as Coriolis' coefficient (Coriolis ,1877) and momentum correction coefficient (β) or simply momentum coefficient {also termed as Boussinesq coefficient (Boussinesq ,1836)}.The

former is applied when energy principle is adopted for computation while the latter is introduced in case of momentum approach for computation. Often in a simplified approach these coefficients are taken as unity particularly for simple prismatic channel sections. However when velocity distribution in a channel section in lateral and vertical direction are largely non-uniform, particularly in case of compound cross-sections then the assumption of value of α & β as unity no more holds good (Chow,1959;Choudhry,2008 etc.). The wide variations in velocity distributions as reported throughout literature has been known to be influenced by a host of factors e.g. cross sectional shape & complexity, alignment, depth of flow, channel slope and roughness etc. (French, 1987). For application in field it's really important to determine the numerical values of both coefficients with sufficient accuracy. Ignoring the effect of such variations often leads to considerable error in predicting flow behavior, stage discharge prediction, afflux studies and other related analysis in case of both natural and artificial rivers. Also there is a tendency to include some predefined values as reported in literature for energy coefficient (α) and momentum coefficient (β) by field engineers. As stated earlier in channels of simple geometry such approach works well but in channels of compound cross sections, where main channel carrying deeper and faster flow is flanked by one or two shallow berms or flood plains with shallow and slower flow, large variations in velocity magnitude both in lateral and vertical direction often necessitate an exact analysis to determine the numerical values of these coefficients.

Many researchers in past have studied the velocity distributions in compound channels and evaluated the energy and momentum coefficients. Notable among them are (Kolupaila, 1956; Blalock & Sturm, 1981; Al-Khatib & Gogus, 1999 and Seckin et al 2004). Kolupaila (1956) based on limited research at that point of time recommended average value of α as 1.75 and that of β as 1.25 for over flooded river valleys or channels flanked by floodplains. Seckin et al. (2004) based on their experimental results for a symmetrical rectangular compound channel of width ratio ($\alpha = 3.046$) and results of experiments conducted by Blalock & Sturm (1981) for an asymmetrical channel of width ratio value of 3.60 reported average values of α & β as 1.156 and 1.056 respectively. In both cases the main channels were of rectangular section. Similarly Al-Khatib & Gogus (1999) conducted a series of experiments on rectangular compound channel with width ratio 3.35 and reported values of α in range of 1.023-

1.063 & β in range of 1.005-1.034 under various flow and geometrical conditions. In each of these cases the models so presented were only validated through the data sets from which they had been developed. But seldom has any model been found applicable in a different channel or in other words the model has had general application.

The present research attempts to first develop models for α & β from experimental observations in straight and meandering compound channels and then validate them by applying for compound channel velocity distribution data of other researchers. Due to the presence of floodplains excessive momentum transfer usually takes place between deep main channel and shallow floodplains. This has been well reported in literature (Seckin, 2009; Knight & Demetriou, 1983; Knight & Hamed, 1984 and Sellin, 1964). On account of this momentum transfer the lateral distribution of velocity attains non uniformity in addition to natural non uniformity in velocity distribution between channel bed and free surface in vertical direction. This leads to different energy and momentum coefficients for compound channels as compared to single channels. Although FCF Phase A channel experiments were conducted for width ratio up to $\{\alpha\} = 6.67$ but no systematic estimation of α & β were reported for these channels in literature to the best knowledge of the author.

6.2.1 Estimation of velocity distribution coefficients (α & β)

From the velocity contours representing the variation of longitudinal velocities over the flow sections for various overbank flow conditions (varying β values) for both straight and meandering compound channel experiments (Figs.4-3, a-f, for straight compound channel & Figs.4-10, a-e, for meandering compound channel) the areas between successive isovels were first planimetered digitally and summed up to find total area of flow cross section by using a suitable graphic package. Any error from the true geometric area of cross section was distributed among all slices in a weighted average method. Then computations were performed to obtain the values of α & β for individual runs by using the standard expressions for them such as

$$\alpha = \frac{\int v^3 \Delta A}{V^3 A} = \frac{\sum v^3 \Delta A}{V^3 A} \quad (6.1)$$

$$\& \quad \beta = \frac{\int v^2 \Delta A}{V^2 A} = \frac{\sum v^2 \Delta A}{V^2 A} \quad (6.2)$$

Table 6-1 Values of Energy & Momentum coefficients for straight and meandering channels

CHANNEL	STRAIGHT COMPOUND			MEANDERING COMPOUND		
Sl.No.	Relative depth (β)	α	β	Relative depth (β)	α	β
1	0.110	2.093	1.385	0.194	1.194	1.067
2	0.133	1.965	1.321	0.240	1.099	1.033
3	0.261	1.261	1.083	0.316	1.073	1.017
4	0.356	1.045	1.016	0.363	1.050	1.013
5	0.381	1.028	1.010	0.410	1.035	1.008
6	0.435	1.037	1.013	xxx	xxx	xxx

where v is the point velocity measured in an elemental area ΔA of the whole cross sectional area A through which flow takes place and V is the cross sectional mean velocity found by dividing $\sum v \Delta A$ with A . The values of α & β thus estimated experimentally for both straight and meandering channels are tabulated in Table. 6-1. Although a value of 1.0 is normally adopted for both α & β for open channel flow cases, it is evident from Table.6-1 and Fig.6-1 that α & β values are quite different from a magnitude of 1.0 in case of compound channels of such high width ratio. It is also inferred that the energy coefficient and momentum coefficient are higher in a straight channel than those in a meandering channel of low sinuosity. Again at low relative depths the difference in α value of a straight channel case and that of a meandering channel is large & this also holds for β value and as the relative depth increases the difference diminishes. This is due to the fact that in compound meandering channel there is more intense mixing of velocity of different layers of fluid both in horizontal as well as in vertical direction than in a straight channel of similar dimensions. This lends some uniformity to the velocity magnitudes of different fluid particles in a meandering channel. Another discerning feature revealed from the Table.6-1 & Fig.6-1, is that in both straight and meandering channels nearly in all cases as the relative depth increases the velocity tends to get uniform over the section and α & β both approach unity.

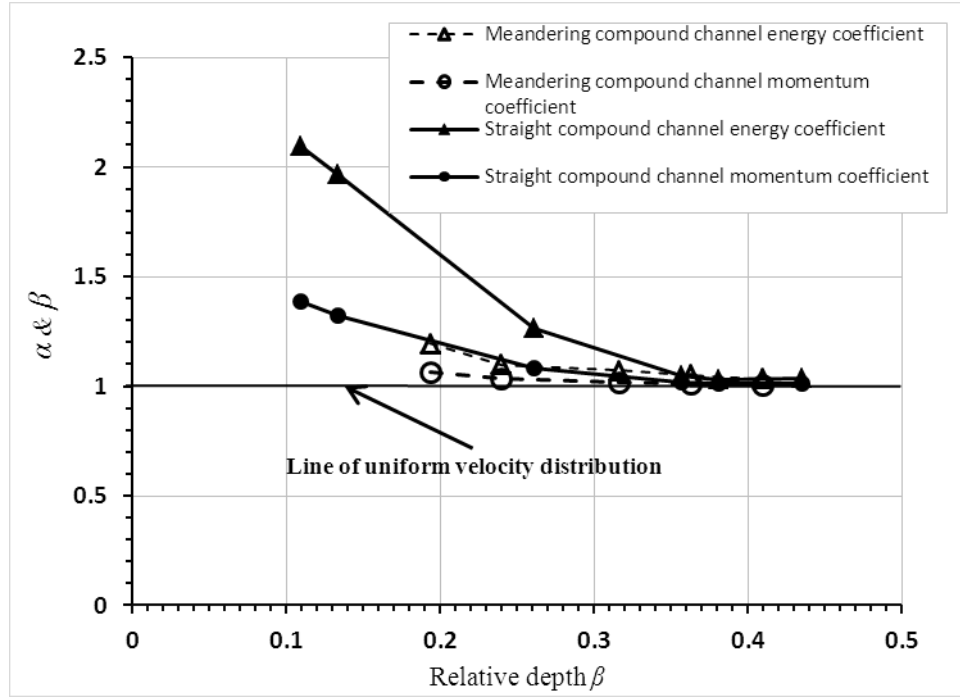


Fig.6-1 Deviation of α & β from unity in overbank flow cases

6.2.2 Model development for velocity distribution coefficients (α & β) in straight compound channel

Having computed the values of α & β for straight compound channel as shown in Table.6-1, a regression analysis was done to obtain mathematical relationships between the energy coefficient and relative depth as well as between the momentum coefficient and relative depth for straight compound channels. It is observed from such analysis (Figs.6-2 and 6-3) that both α & β are power functions of relative depth value β and the same can be expressed as

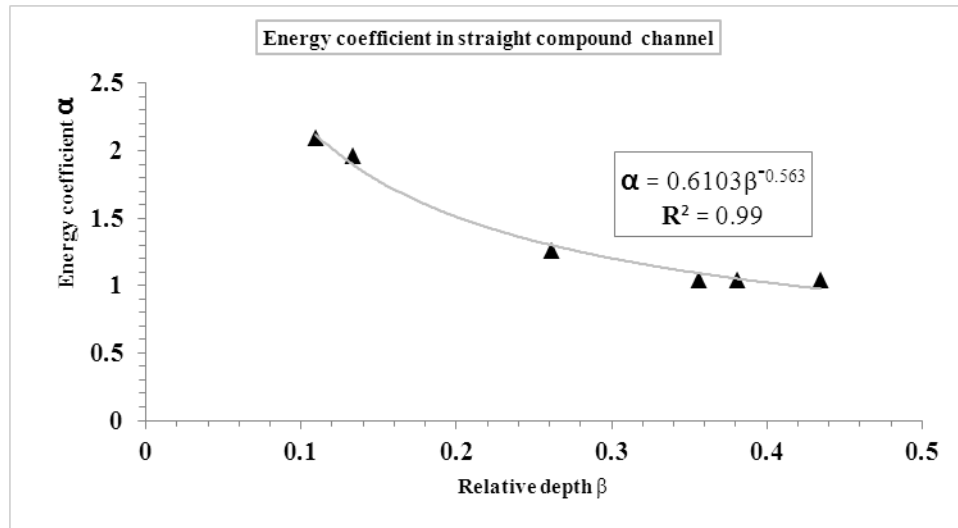


Fig.6- 2 Variation of α in straight compound channel

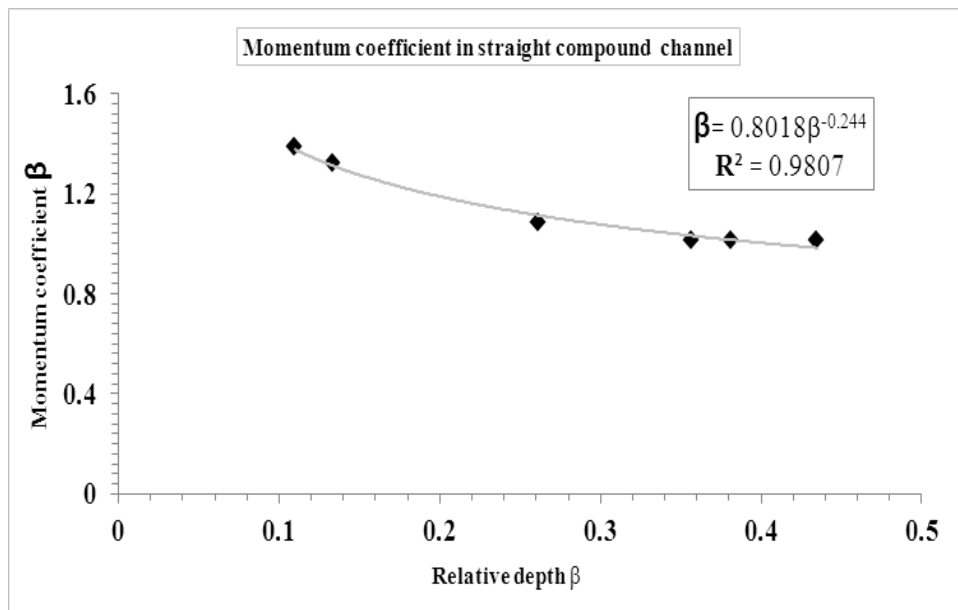


Fig.6- 3 Variation of β in straight compound channel

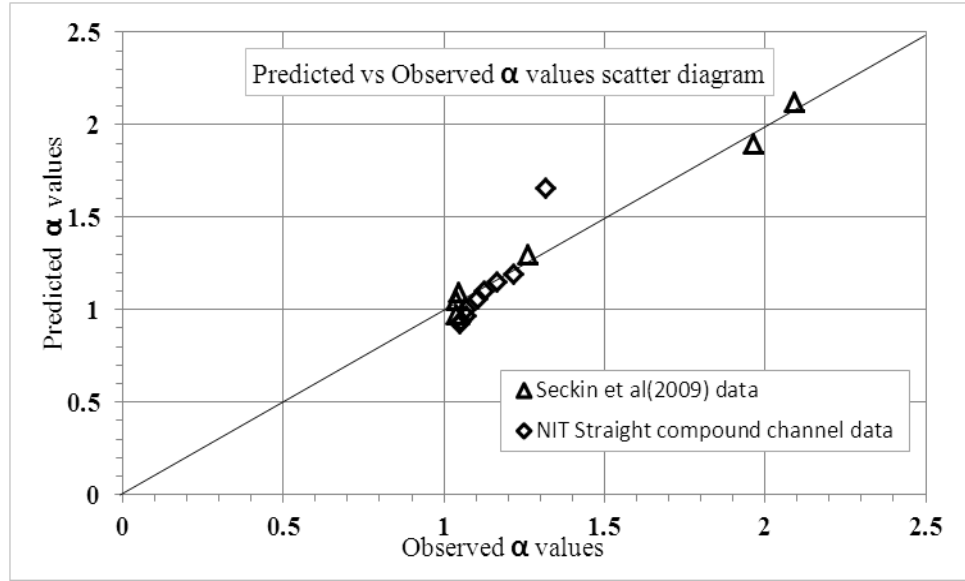


Fig.6- 4 Variation of Observed and Predicted value of α in straight compound channel

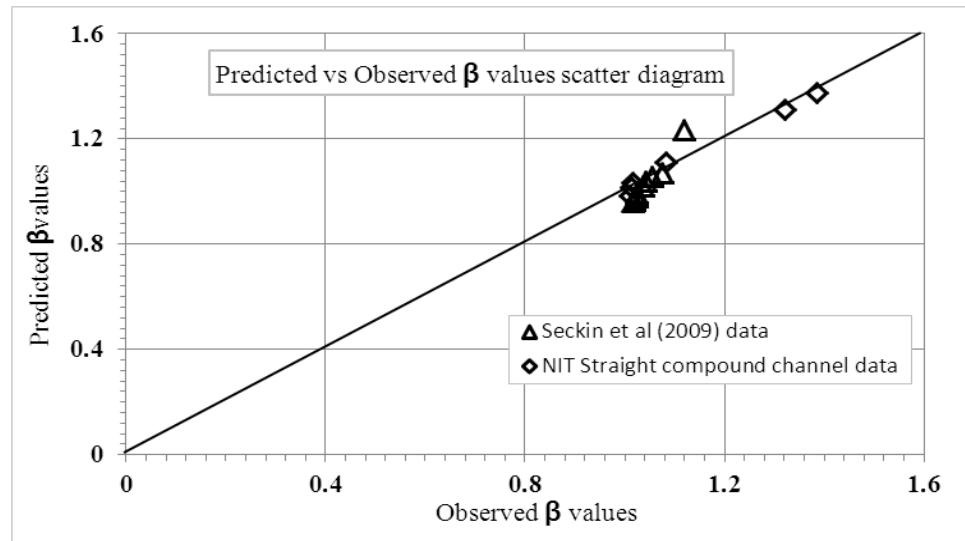


Fig.6-5 Variation of Observed and Predicted value of β in straight compound channel

$$\alpha = 0.6103\beta^{-0.563} \quad (6.3)$$

&
$$\beta = 0.8018\alpha^{-0.244} \quad (6.4)$$

Also the R^2 value is estimated as 0.99 and 0.98 for energy coefficient and momentum coefficient respectively which indicates a very good correlation for both the expressions i.e. for Equations (6.3) & (6.4). The models as developed for α & β are

then tested for their validity with the observed values of energy and momentum coefficients for present experimental runs in the NIT, Rourkela straight compound channel case and also with the observed α & β values reported for straight compound channel experimental runs of Seckin et al (2009). Figs. 6-4 & 6-5 show the scatter plots for predicted and observed α & β values respectively for both the above mentioned data sets. Both equations i.e. Eq.6.3 and Eq.6.4 are well suited for these data sets as is evident from Figs. 6-4 & 6-5 and both can be used to predict the values of energy and momentum coefficients in other straight compound channels under similar geometric and hydraulic conditions.

6.2.3 Model development for velocity distribution coefficients (α & β) in meandering compound channel

Similar steps were followed to obtain relationships between the energy coefficient and relative depth as well as between the momentum coefficient and relative depth for meandering compound channels. The regression analysis resulted in mathematical expressions for α & β with relative depth in case of a meandering compound channel.

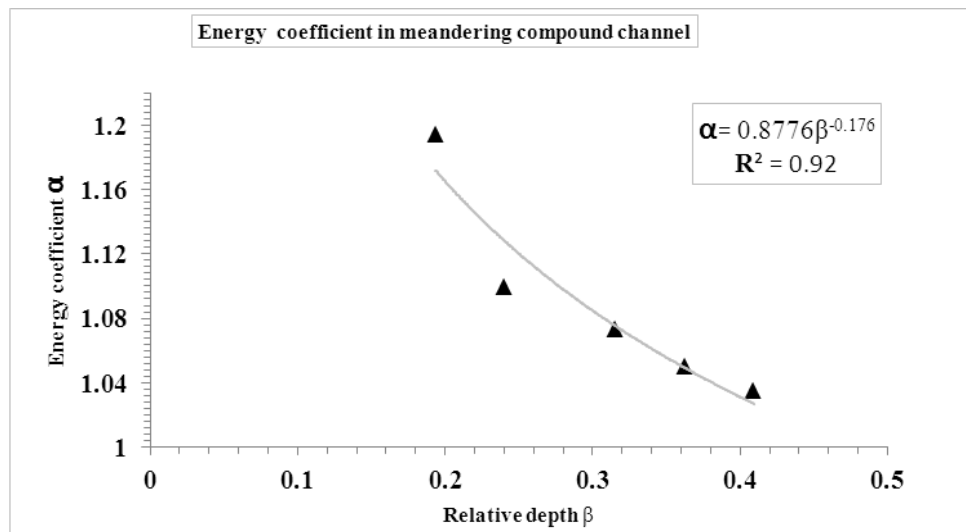


Fig.6- 6 Variation of α in meandering compound channel

Figs. 6-6 & 6-7 show that once again both energy and momentum are power functions of relative depth. The respective mathematical relation between α and β as well as between β and β can be written as

$$\alpha = 0.8776\beta^{-0.176} \quad (6.5)$$

&

$$\beta = 0.9409\beta^{-0.072} \quad (6.6)$$

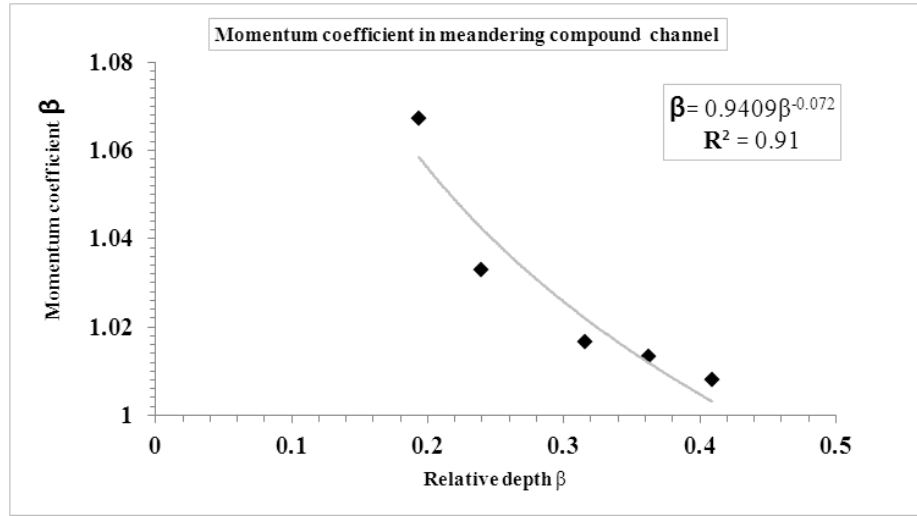


Fig.6- 7 Variation of β in straight compound channel.

the R^2 value is estimated as 0.92 and 0.91 for energy coefficient and momentum coefficient respectively. The models developed as in Eq.6.5 & Eq.6.6 are then tested for their validity with the present meandering channel experimental data and with the data computed from meandering channel experiments of Patra and Kar (2000).

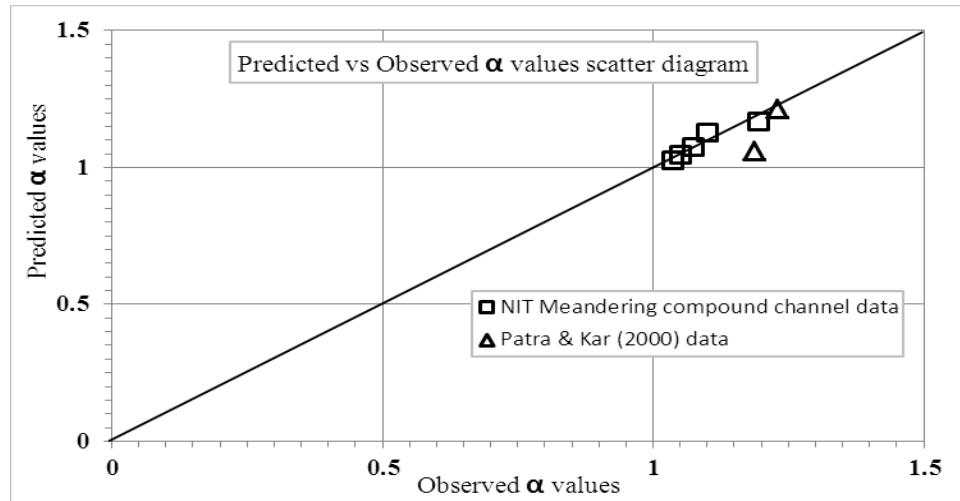


Fig.6-8 Variation of Observed and Predicted value of α in meandering compound channel

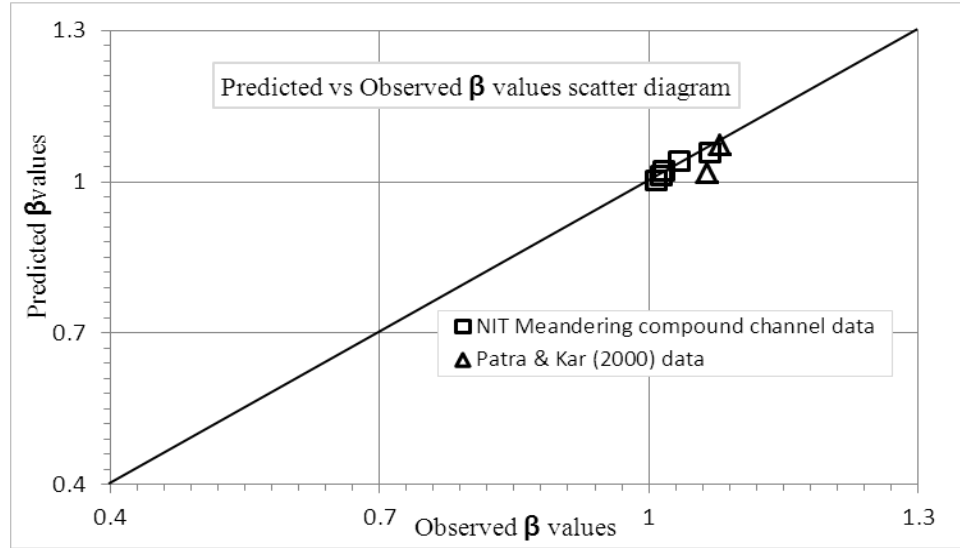


Fig.6-9 Variation of Observed and Predicted value of β in straight compound channel

Using these new models the values of α & β are computed for both the data sets and the scatter plots (Figs. 6-8 & 6-9) reveal good agreement between the predicted and observed values in case of both α & β .

6.2.4 Discussion

The above study regarding the energy and momentum coefficients in straight and meandering compound channels with wide floodplains reveal the following salient features.

- (a) The velocity distribution coefficients for meandering compound channel are found to be less as compared with those in straight compound channel cases. The meandering channel flow causes more mixing of fluid bringing more uniformity in velocity distributions as compared to the straight one.
- (b) New expressions for determining α & β in both straight and meandering compound channels for different over-bank flow depths are presented. The R^2 values for these developed expressions or mathematical models for straight and meandering cases are found to be in range of 0.99 and 0.91. Also it is seen that in all cases the relative depth β strongly influences the values of α & β both in straight and meandering compound channels.
- (c) The models developed seem to predict well the values of α & β for the channels of other investigators. This proves their adequacy.

6.3 DEVELOPMENT OF STAGE-DISCHARGE MODELS (STRAIGHT COMPOUND CHANNEL)

6.3.1 DEVELOPMENT OF METHOD (for α upto 6.67)

The numerical tools for flow modeling in rivers applied in chapter 5 are based on the mathematical equations governing the fluid flow. The CES uses the analytical SKM (Shiono & Knight, 1988, 1990) whereas the CCHE2D has been based on depth averaged form of continuity and momentum equations. However both the models require some empirical constants for a fruitful simulation. The SKM require three calibration coefficients viz. bed shear, eddy viscosity and secondary flow whereas CCHE2D has some turbulence closure schemes (as explained previously in chapter 5). Even other 1D software models such as HEC-RAS, SOBEK, and MIKE 11 etc. are based on one or other form of 'DCM' (Divided Channel Method) techniques for flow prediction in river engineering. Thus the basic mathematical models always form the cornerstones for development or up gradation of any software tools. The numerical tools such as the advanced 'CCHE2D' and other also require a number of skills in parameter settings etc. (as explained previously) on part of the ordinary user like field engineers for successful simulation. Thus the need of sound mathematical models capable of being directly used in field cannot be over emphasized.

Many attempts have been made in past to tackle the major issue of uncertainty in accurate prediction of stage discharge relationship for flow in a compound channel by analyzing the boundary shear, velocity and flow over various components of flow section e.g. main channel and floodplains. It is found from extensive research that in a compound channel momentum transfer, being mainly responsible for the non-uniformity in the boundary shear stress distribution (e.g. Myers and Elsayy 1975; Patra and Kar 2000 etc.) complicates the matter and impedes easy stage discharge modeling for such flow sections. The traditional discharge prediction methods for compound channels either use the Single-Channel Method (SCM) or the Divided-Channel Method (DCM). The DCM predicts better overall discharge as compared to SCM. Wormleaton et al. (1982) proposed an apparent shear stress ratio as the useful yardstick in selecting the best interfaces for flow division. Stephenson and Kolovopoulos (1990), Lambert and Myers (1998), Patra and Kar (2000), and Cassels et al. (2001) proposed zero shear interfaces that nullify the lateral momentum transfer.

Ackers (1992) proposed an empirically based correction to the DCM known as the Coherence Method (COHM). Prinos and Townsend (1984), Christodoulou (1992), and Huttof et al. (2008) parameterized the interface stress in terms of velocity of the main channel and floodplains or in terms of the channel dimensions. The resulting averaged flow velocities were determined from a rather complicated set of analytical equations (e.g. Bousmar and Zech 1999). The interaction phenomenon and the discharge assessment for compound sections were presented by many other researchers as well (e.g. Seckin 2004; Kejun Yang et al. 2007; Hin et. al. 2008). Failure of most subdivision methods were due to improper evaluation of the complicated interaction between the main channel and floodplain flows. Shiono and Knight (1991), and Van Prooijen et al. (2005) presented a continuum model that resolved the depth-averaged flow velocity as a function of the cross-channel coordinates. An attempt has been made here to propose an improved 1D model (Modified Divided Channel Method i.e. MDCM) especially for straight compound channels with wide floodplains by implementing a new boundary shear model in the revised DCM proposed by Khatua (2008) where the effects of lateral momentum transfer is taken care of by selecting the appropriate length of interaction between various zones of compound channel flow.

6.3.1.1 *The methodology*

Even though the full details of the said DCM technique are available in Khatua (2008), it is worth mentioning the same briefly here for providing a background to the current research being described. Looking at Fig.6-10, if the compound section is divided into subsections such as shown by drawing vertical interfacial lines splitting the whole section into one central main channel section and two symmetrical left and right floodplain sections and then normal vertical divided channel methods (VDM) are applied, it had been adequately shown that the discharge is either under predicted or over predicted (Wormleaton, et al. 1980; Huttof et al. 2008 etc.). So Khatua (2008) suggested instead quantifying the momentum transfer in terms of apparent shear force occurring at the interface in terms of an appropriate length of interface between the main channel and floodplain.

Wormleaton et. al. (1982) have shown that the total dragging force on the main channel due to floodplain at the interfaces must be equal to the accelerating force on floodplain due to the main channel. Therefore the wetted perimeter of the main channel needs to

be increased by a length (X_{mc}) suitably to take care of the net dragging force on the main channel. Similarly the wetted perimeter of the floodplain needs to be reduced by subtracting a suitable length of interface (X_{fp}) to account for the accelerating force on the floodplain due to the pulling of the main channel water.

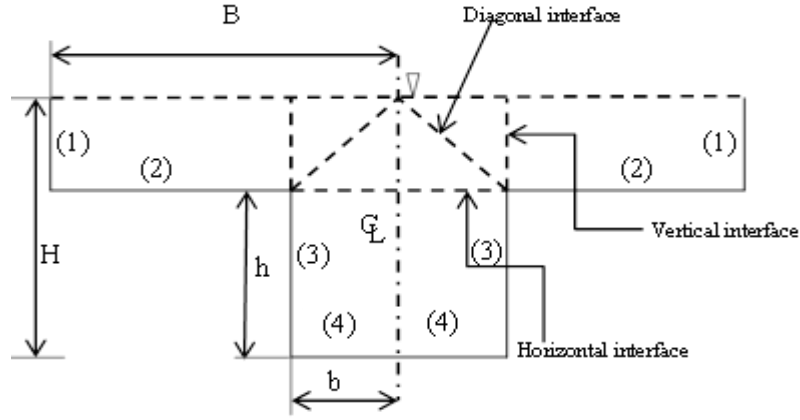


Fig.6-10 Common interfaces dividing a compound section into subsections

Net force at the assumed vertical interface should balance each other. The expressions for X_{mc} and X_{fp} can be written as

$$X_{mc} = P_{mc} \left[\frac{100}{(100 - \% S_{fp})} \frac{A_{mc}}{A} - 1 \right] \quad (6.7)$$

and

$$X_{fp} = P_{fp} \left[\frac{100}{\% S_{fp}} \left(\frac{A_{mc}}{A} - 1 \right) + 1 \right] \quad (6.8)$$

where P_{mc} and P_{fp} are the perimeter of main channel and flood plains; A_{mc} and A_{fp} are the area of main channel and flood plains respectively, A is the area of entire compound section and $\% S_{fp}$ is the percentage of shear force carried by the floodplains and found as $= [100 \times S_{fp} / (S_{fp} + S_{mc})]$ with S_{mc} being the shear force carried over main channel. Next, the discharge for main channel and floodplains are calculated using Manning's equation and added together to give over all discharge as

$$Q = \frac{\sqrt{S}}{n_{mc}} A_{mc}^{5/3} (P_{mc} + X_{mc})^{-2/3} + \frac{\sqrt{S}}{n_{fp}} A_{fp}^{5/3} (P_{fp} - X_{fp})^{-2/3} \quad (6.9)$$

where n_{mc} and n_{fp} are Manning's roughness coefficients for main channel and flood plains respectively and S is the bed slope of both main channel and floodplains and is taken same in one-dimensional approach.

By developing an appropriate expression relating the $\% S_{fp}$ with some easily identifiable physical parameters of the compound channel such as the depth of flow,

aspect ratio and width etc., Eq. (6.7 and 6.8) and hence Eq. (6.9) can be solved and the stage discharge relationship for the compound section can be easily found out.

6.3.1.2 *The boundary shear model (α upto 6.67)*

Various boundary elements comprising the wetted parameters are labeled as (1), (2), (3) and (4) in Fig.6-10. Label (1) denote the vertical wall(s) of floodplain of length $[(H - h)]$, where H = total depth of flow from main channel bed, h = depth of main channel. Label (2) denotes floodplain beds of length $(B - b)$, where $B = \frac{1}{2}$ (total width of compound channel), and $b = \frac{1}{2}$ (width or bed) of main channel represented by label (4). Shear stress distributions at each point of the wetted perimeter are numerically integrated over the respective sub-lengths of each boundary element (1), (2), (3), and (4) to obtain the respective boundary shear force per unit length for each element in the half section of the symmetric channel cross section. Twice the sum of the boundary shear forces for all the elements thus calculated in beds and walls of the compound channel gives the total shear force resisted in the whole compound section and is used as a divisor to calculate the shear force percentages carried by the boundary elements (1) through (4). Percentage of shear force carried by floodplains comprising elements (1) and (2) is represented as $\%S_{fp}$ and that for the main channel comprising elements (3) and (4) is represented as $\%S_{mc}$.

The parameter $\%S_{fp}$ needs to be evaluated accurately. Therefore, an analysis is also done to obtain a general expression for $\%S_{fp}$ for all types of compound channel geometry. Following the work of Knight and Demetriou (1983), Knight and Hamed (1984) proposed an equation for $\%S_{fp}$ for a compound channel section as

$$\%S_{fp} = 48(\alpha - 0.8)^{0.289}(2\beta)^m \quad (6.10a)$$

Equation (6.10a) is applicable for the channels having equal surface roughness in the floodplain and main channel. For non-homogeneous rough channels equation (6.10a) is improved by Knight and Hamed (1984) as

$$\%S_{fp} = 48(\alpha - 0.8)^{0.289}(2\beta)^m \{1 + 1.02\sqrt{\beta} \log \gamma\} \quad (6.10b)$$

where γ = the ratio of Manning's roughness of the floodplain (n_{fp}) to that for the main channel (n_{mc}). The exponent m is evaluated from the relation

$$m = 1/[0.75e^{0.38\alpha}] \quad (6.11)$$

Adequacy of equation (6.10) for smaller width ratio channels (α up to 4) has been shown by Knight and Hamed (1984) and Patra and Kar (2000). A regression analysis was also made by Khatua and Patra (2007) and they proposed an equation for $\%S_{fp}$ (adequate for compound channels of α up to 5.25) as

$$\%S_{fp} = 1.23 \beta^{0.1833} (38 \ln \alpha + 3.6262) \{1 + 1.02 \sqrt{\beta} \log \gamma\} \quad (6.12)$$

Interestingly, it is found that when both the above expressions are tested for FCF data having $\alpha = 6.67$, significant error in $\%S_{fp}$ is found [around 90% by equation (6.11) and 71% by equation (6.12)]. Fig.6-11 illustrates the results for FCF data obtained using equations (6.10) and (6.12) and its comparison with the observed values for $\alpha = 6.67$. The errors are found to increase with increase in the value of α . Furthermore, equations (6.10) and (6.12) estimate physically unrealistic values of $\%S_{fp}$, that is $\%S_{fp} > 100\%$ for a compound channel of $\alpha > 10$.

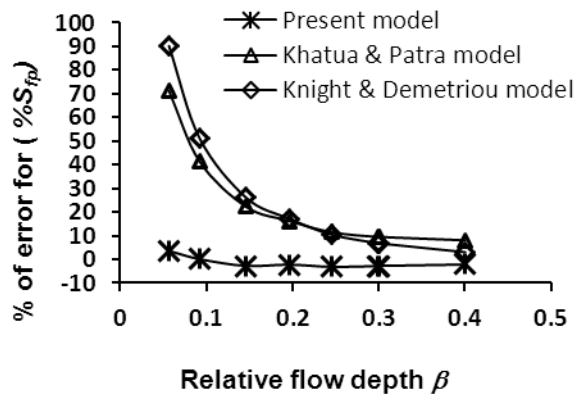


Fig.6-11 Variation of % error in estimation of $\%S_{fp}$ with β for the FCF channel having large width ratio (α)

For better understanding the boundary shear stress distribution, three series of compound channel data of Knight and Demetriou (1983), the data of experimental compound channel of NIT, Rourkela, India (Khatua, 2008) along with five series of

FCF phase-A channels (details of the data sets are given in Table.6-2) are studied. These compound channels have homogeneous roughness both in the main channel and floodplain subsections. Manning's n values for all these smooth surfaces are taken as 0.01.

In a simple open channel flow the boundary shear per unit length (SF) is generally assumed to be uniform and is expressed as $SF = \rho g A S$, where ρ is density of water and g is acceleration due to gravity. The parameters ρ , g and S are assumed constant for a given channel. Only the flow area (A) varies with flow depth. So it can be stated that SF is a function of A . The percentage of the area occupied by floodplain subsections obtained by vertical interfaces (Fig 6-10), $\%A_{fp} = 100 \times A_{fp} / A$. Then $\%S_{fp}$ ($100 \times S_{fp} / SF$) should be a function of $\%A_{fp}$. Due to the momentum transfer in a compound channel, it has been shown that S_{fp} doesn't vary linearly with A_{fp} (e.g. Knight and Hamed 1984; Patra and Kar 2000). Therefore, a functional relationship between $\%S_{fp}$ and $\%A_{fp}$ has been derived from a wide range of data sets from nine different types of compound channels with α ranging from 2.0 to 6.67 and β ranging from 0.1 to 0.5. Fig 6-12 shows the best fit curve and its equation is found as

$$\%S_{fp} = 4.1045(\%A_{fp})^{0.6917} \quad (6.13a)$$

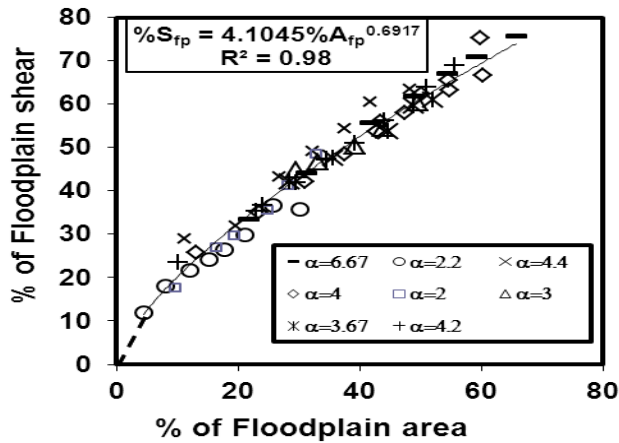


Fig.6-12 Variation of % of floodplain shear with % of area of floodplain

For rectangular channel and floodplains having homogeneous roughness (i.e same Manning's n value for both main channel and floodplain), equation (6.13a) can be expressed as

$$\%S_{fp} = 4.105 \left[\frac{100\beta(\alpha-1)}{1+\beta(\alpha-1)} \right]^{0.6917} \quad (6.13b)$$

For non-homogeneity in roughness values of floodplains and main channel the equation (6.13a) takes the form as equation (6.13c) using the relation from Knight & Hamed (1984);

$$\%S_{fp} = 4.1045(\%A_{fp})^{0.6917} \{1 + 1.02\sqrt{\beta} \log \gamma\} \quad (6.13c)$$

The variation between the calculated values of ($\%S_{fp}$) using equations (6.10), (6.12) and (6.13) and the corresponding observed values for all the nine types of channels are shown in Fig.6-13. The regression analysis (in Fig.6-12) also indicates high coefficients of determination ($R^2 = 0.98$) for equation (6.13). Fig.6-13 shows the comparative performance of the present model along with other models through a scatter plot and hence the accuracy of the developed model i.e. Equation (6.13) is verified.

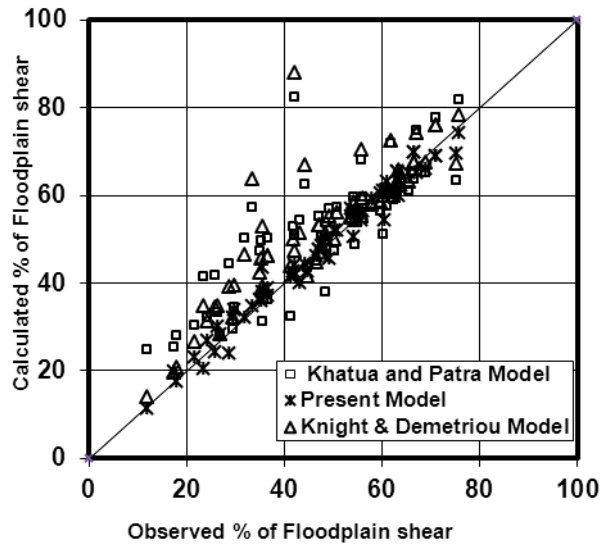


Fig.6-13 Scatter plot for observed and modeled value of $\%S_{fp}$

Further, the standard errors for the calculated values of $\%S_{fp}$ for all the data sets i.e. five data sets of FCF Phase-A(1,2,3,8 & 10), three data sets of Knight and Demetriou (1983) {K&D series) and one experimental channel data of Khatua (2008) are found to be the minimum for the present model and are shown in Fig. 6-14.

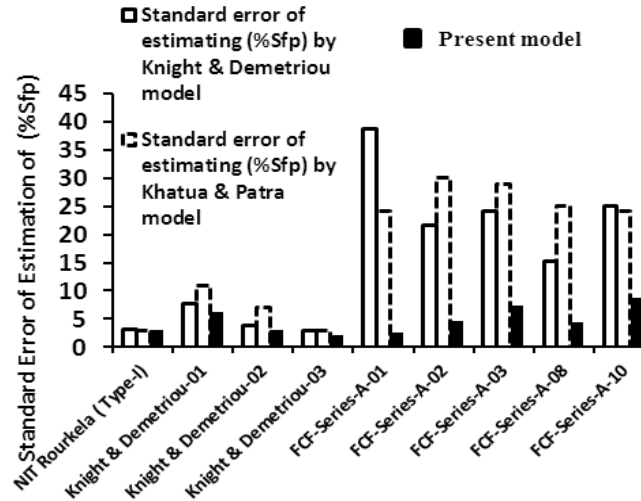


Fig.6-14 Standard error of estimation of $\%S_{fp}$ by various models.

6.3.1.3 Stage- Discharge Results

The discharge results obtained from six 1D approaches are compared with the MDCM. Among one-dimensional approaches, the Area Method (AM) by Stephenson and Kolovopoulos, 1990; two types of Vertical Division Methods (VDM-I and VDM-II); two types of horizontal division methods (HDM-I and HDM-II) and a Diagonal division Method (DDM) are considered in this work, where I stands for length of interface excluded in both the main channel and the floodplain wetted perimeters and II being used when the length of interface is included in the wetted perimeter of main channel only. The results are shown in Fig.6-15 (a-i) showing the performance of the MDCM. The standard errors for calculating discharge by MDCM are shown in Fig.6-16. It indicates values of 1.68 %, 4.59 % and 3.90 % for the (Khatua, 2008) experimental channel data, the data of Knight and Demetrious (1983) and the FCF series-A respectively. Considering all the 80 data points of all 9 types of channels considered, the overall mean standard error is the minimum (3.72%) for the proposed MDCM and the maximum (20.50%) for 'HDM-II' respectively among all the 1D approaches. The overall mean standard error further reduces to 3.18 % for wide compound channels, (i.e. $\alpha = 3.0, 3.67, 4.0, 4.2, 4.4$ and 6.67) in case of MDCM. The MDCM is also compared with the results obtained from the software package CES. It compares favorably with CES. This proves the adequacy of the proposed stage-discharge modeling for straight, smooth and symmetrical rectangular compound channels with wide floodplains.

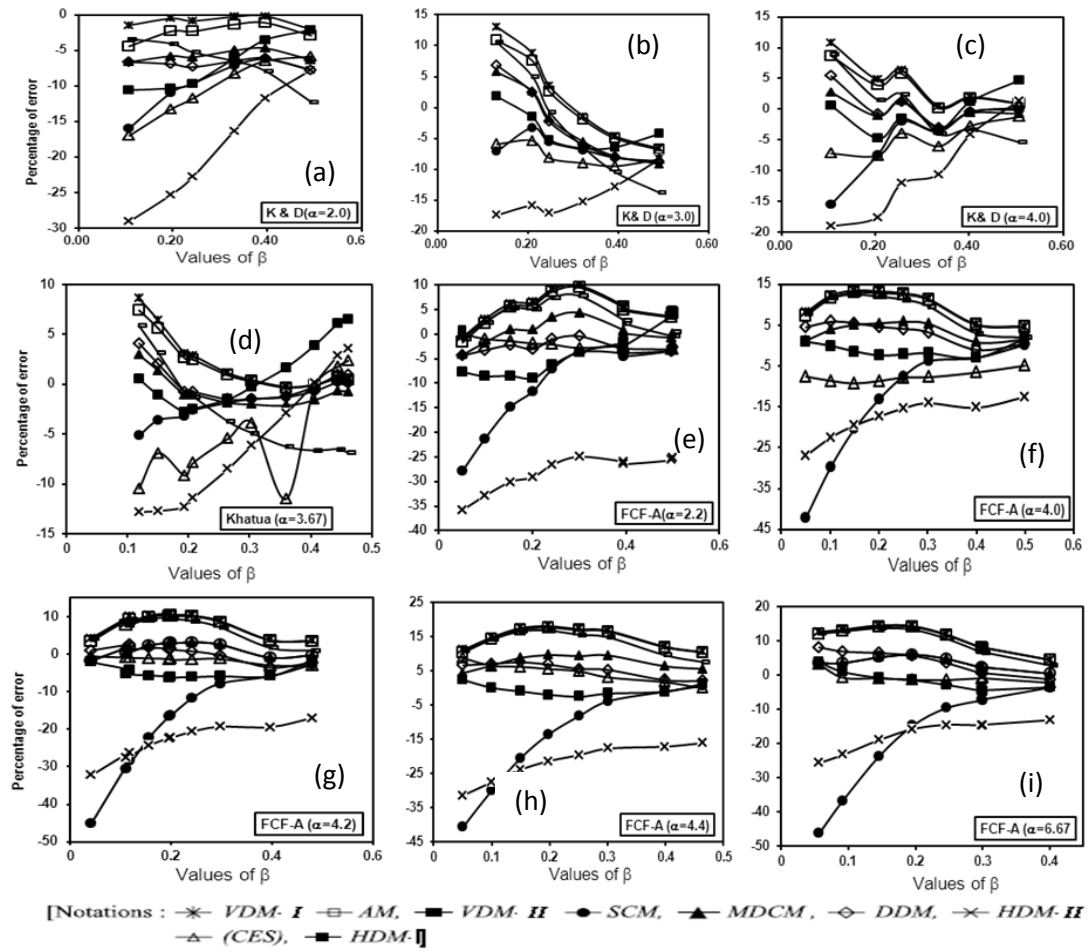


Fig.6-15 (a-i) Error percentages between calculated and observed discharges for the test channels of Knight and Demetriou 1983, Khatua (2008), and FCF-Phase-A channels

6.3.1.4 Practical Application of the MDCM

Discharge prediction approaches are also applied to river Batu (Hin et. al 2008) and river Main (e.g. Myers, & Lynness 1990; McGahey, Samuels and Knight 2007). Any method or approach to predict the stage-discharge relation must pass the test of satisfactorily performing in real world situation i.e. for field cases or for rivers .For this purpose two distinct cases, much publicized in literature are chosen to test the relevance of the developed method in real world application. As against the laboratory flume experiments, where the flow takes place under human control the same does not hold in case of rivers under flood. Both the cross section and roughness are much irregular in comparison with the laboratory flumes. So field data needs to be very carefully obtained and must undergo rigorous testing before being accepted for validation purpose. In view of this only river data published in well referred journals have been

considered here. The first one is an equatorial river named the Batu (Hin et. al 2008) flowing in Kuching, the capital city of Sarawak state, Malaysia. The other river is the River Main (Myers, & Lynness 1990; McGahey, Samuels and Knight 2007) which is located in County Antrim, Northern Ireland. It rises in the Antrim Plateau about 6km south-east of Ballymoney, County Antrim. The dimensions include a top width of 14m, a total width inclusive of floodplains of 27.3-30.4m, and bankfull depth ~0.9-1.0m.

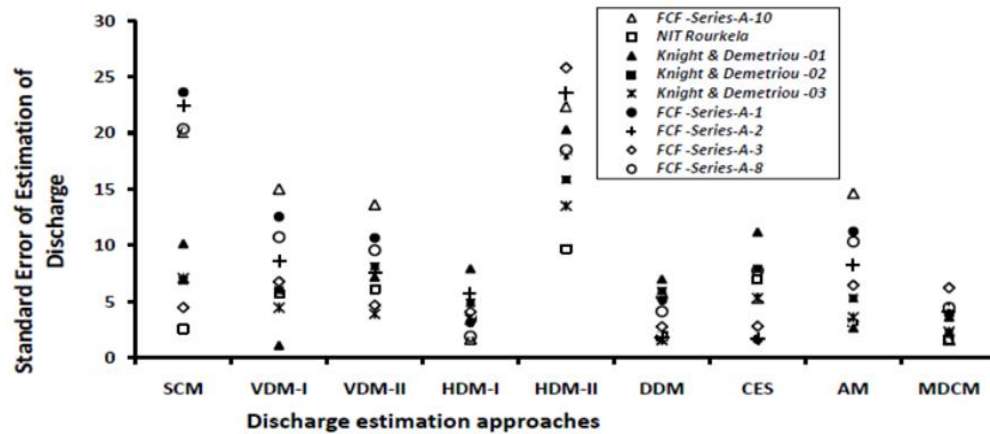


Fig.6-16 Standard error of estimation of discharge using different methods for different data sets.

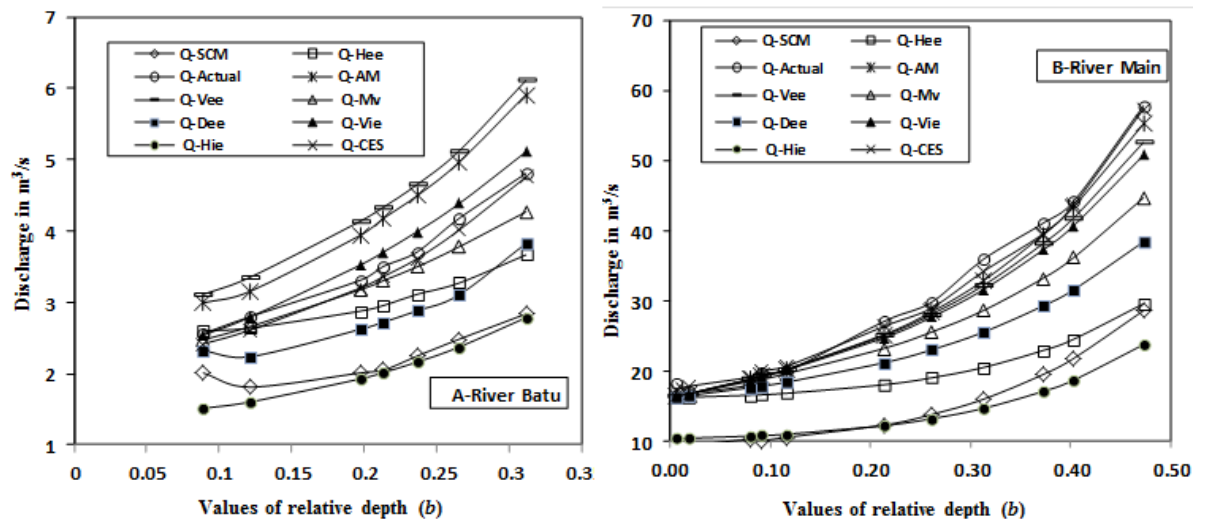


Fig.6- 17(A and B) Variation of predicted discharge for river data by different methods with relative overbank flow depth

Geometrical properties and surface conditions of these rivers are given in Table.A.1 and Figs.A-1 & A-2 (Appendix section). The rivers are almost straight and uniform in cross section at the present study area. Discharge results based on different methods for these rivers along with actual discharge are shown in Fig.6-17.

6.3.1.5 Discussion on MDCM

The distinguishing features of the developed MDCM can be summarised as below.

- ❖ Previous formulation for estimating $\%S_{fp}$ gives $\%S_{fp}$ more than 100 % when applied to a compound channel of higher width ratio ($\alpha \geq 10$). The present formulation is quite adequate for straight smooth compound channel having wide floodplains. It was derived for straight, smooth and symmetrical compound channels with wide flood plains up to α value equal to 6.67 and γ value of 1 and β value up to 0.5.
- ❖ MDCM is found to give satisfactory discharge results for both small scale and large scale experimental data. Considering all the data set, the standard error for MDCM is the minimum when compared to all other approaches and also it compares favorably with that estimated using CES.
- ❖ The improvement in the results obtained through MDCM illustrates that one-dimensional flow models used in river engineering can be quite easily extended to include effects due to lateral momentum transfer.
- ❖ The method is also found to give satisfactory results when applied to two sets of natural river data. However the method needs improvement for its general applicability.

6.3.2 Extended MDCM (EMDCM for $6.67 < \alpha < 12$)

6.3.2.1 The methodology

The MDCM thus developed for straight compound channels is shown to be applicable for the compound channels with floodplains having α value equal to 6.67 and γ value of 1 and β up to 0.5. In view of the present research, where the boundary shear is measured for straight compound channels with α value equal to 11.96; a new stage - discharge model is thus warranted where the applicability of the model can further be extended to still wider compound channels as compared to the previously developed one (MDCM), i.e. for $\alpha = 6.67$. So the present model will use the technique used in MDCM but with a new model for percentage shear force carried by floodplains ($\%S_{fp}$).

6.3.2.2 Development of boundary shear model (for $6.67 < \alpha < 12$)

Considering the present straight wide compound channel reported in this thesis ($\alpha \approx 12$) and the widest FCF channel (i.e. Series A-1 with α value of 6.67), a new regression

analysis is done to show the variation of $\%S_{fp}$ with $\%A_{fp}$ and the model for boundary shear percentage is obtained as

$$\%S_{fp} = 3.3254(\%A_{fp})^{0.7467} \quad (6.14)$$

Equation (6.14) has been obtained taking these two specific-standard data sets as these only correspond to compound channels with wide flood plains ($6.67 \leq \alpha \leq 11.96$) and R^2 value is obtained as ≈ 0.97 . Fig.6.18 shows the regression curve for the newly developed boundary shear model.

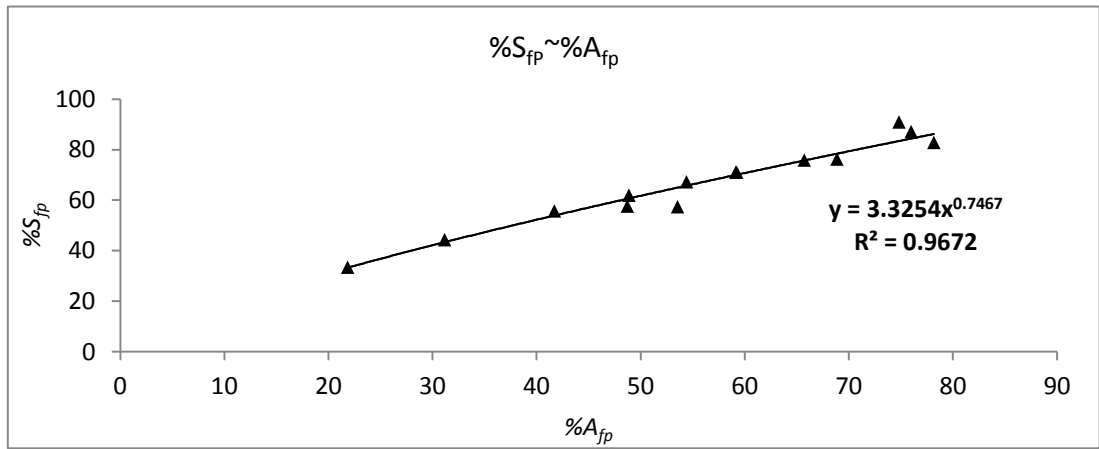


Fig.6-18 Regression curve for Shear force carried by flood plain with area of floodplain

For non-homogeneously roughened channel again the same factor suggested by Knight & Hamed (1984) is retained and for the present wide channel cases (6.14) is written as

$$\%S_{fp} = 3.3254(\%A_{fp})^{0.7467} \{1 + 1.02\sqrt{\beta} \log \gamma\} \quad (6.15)$$

In terms of non-dimensional parameters α, β, δ and s , where ' s ' is the value of side slope of trapezoidal main channel (1: s ::V:H) and δ is the aspect ratio of the main channel, the percentage of floodplain area can be simplified as

$$\%A_{fp} = \frac{\beta\alpha\delta - \beta(\delta + 2s)}{\beta\alpha\delta + (1 - \beta)(\delta + s)} \times 100 \quad (6.16)$$

For the trapezoidal main channel having side slope 1V:1H as in present case and rectangular flood plains, the value of $s = 1$ and the equation (6.16) reduces to

$$\%A_{fp} = \frac{\alpha\beta\delta - (2 + \delta)}{\alpha\beta\delta + (1 - \beta)(1 + \delta)} \times 100 \quad (6.17)$$

So from equations (6.14) and (6.17) shear force carried by floodplains can be expressed in terms of non-dimensional parameters defining the compound channel as

$$\%S_{fp} = 3.3254 \left[\frac{\alpha\beta\delta - (2 + \delta)}{\alpha\beta\delta + (1 - \beta)(1 + \delta)} \times 100 \right]^{0.7467} \quad (6.18)$$

For non-homogeneity in floodplain and main channel roughness, (6.18) is to be modified as

$$\%S_{fp} = 3.3254 \left[\frac{\alpha\beta\delta - (2 + \delta)}{\alpha\beta\delta + (1 - \beta)(1 + \delta)} \times 100 \right]^{0.7467} \left\{ 1 + 1.02\sqrt{\beta} \log \gamma \right\} \quad (6.19)$$

Equation (6.18) and (6.19) are alternative forms of equation (6.14) & (6.15) respectively and the former pair is to be used for all types of channels whereas latter pair is to be used in case of compound channels consisting the trapezoidal main channel and rectangular floodplains.

The percentage error in estimated shear carried by flood plains ($\%S_{fp}$) is the least when compared to previous models e.g. Khatua & Patra (2007) and Knight & Hamed (1984) for both NIT, Channel as well as for FCFA-1 Channel and are shown in Figs 6.19 (a & b).

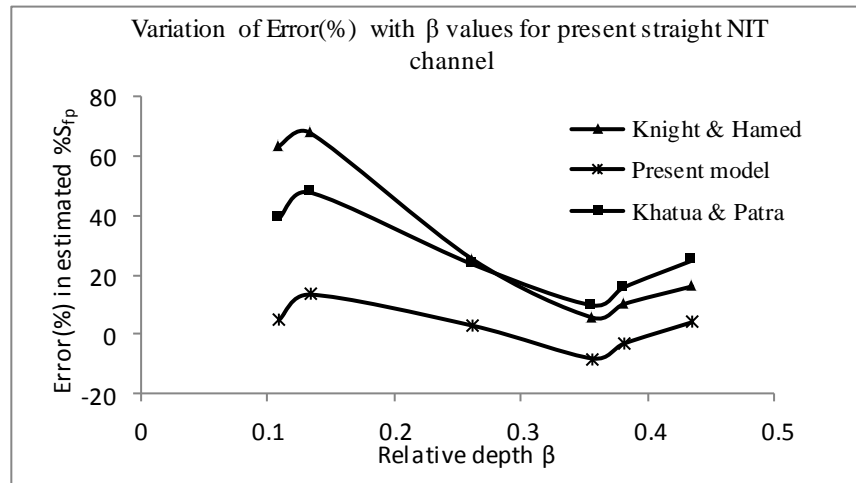


Fig.6-19(a) Comparison of models in Wide NIT Channel

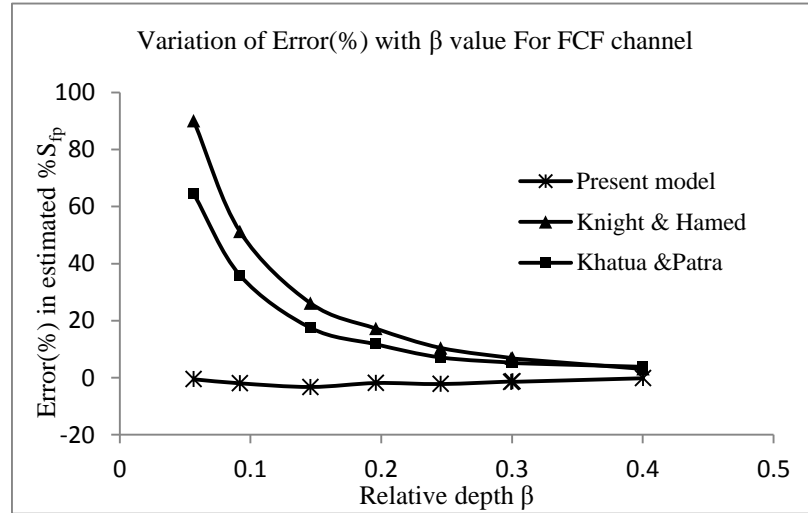


Fig.6- 19(b) Comparison of models in FCF A-1 Channel

6.3.2.3 Results and Discussion

Using the new method EMDCM, along with the single channel method, various conventional divided channel methods and the standard SKM Method of Shiono & Knight (1991) the discharge is estimated for the flow cases considered in NIT, Rourkela straight compound channel and FCFA-1 channel. The methods considered are Single channel method (SCM), Vertical division method (VDM), Diagonal division method (DDM), present method (EMDCM) and SKM of Shiono and Knight (1991). The percentage error in estimating the discharge is computed as before (in MDCM)

$$Error(\%) = 100 \left(\frac{Q_{calc} - Q_{act}}{Q_{act}} \right) \quad (6.20)$$

Where Q_{calc} is the estimated discharge and Q_{act} is actual discharge. Fig.6-20 and Fig.6-21 respectively show the comparison among various methods in the NIT channel and FCF channel cases. In Fig.6-20, for NIT channel EMDCM appears to be the best method whereas SCM method is least accurate among all methods. For FCF channel (in Fig.6-21) both EMDCM and SKM are among the best while again SCM method is least accurate as the error in discharge estimation is highest for the method.

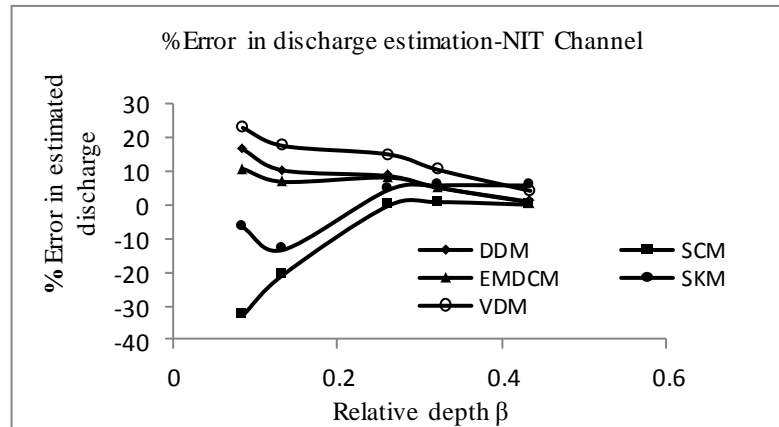


Fig.6- 20 Error percentage of discharge in Wide NIT Channel

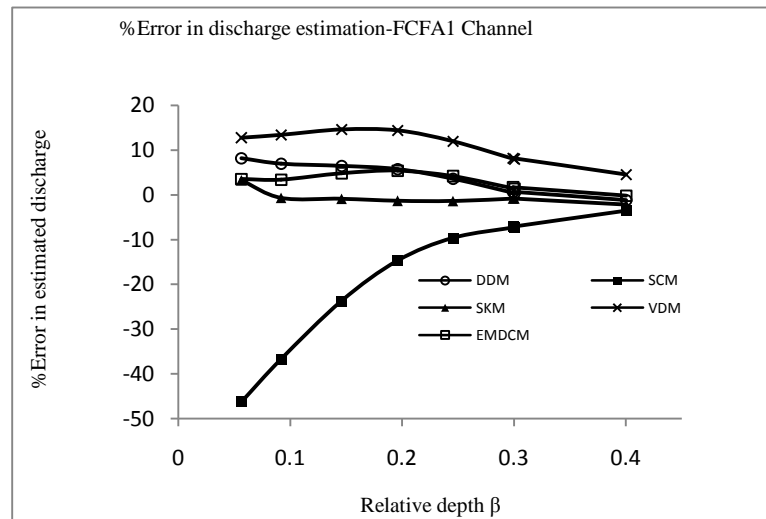


Fig.6- 21 Error percentage of discharge in FCF Channel

6.3.2.4 Practical Application of EMDCM

After applying the method EMDCM to the new experimental wide channel of NIT, Rourkela and the existing widest FCF channel, the same is tested for its suitability in a wide natural river data. For this published river data for river Batu (Hin et al, 2008) once again is considered in this work. The river Main considered previously is excluded here as its width ratio value is not in the range considered in the present approach. The previously considered other four standard methods are also applied to estimate discharge and the computed discharge values are then compared with actual discharge. Fig.6.22 shows the comparative picture and it is seen that EMDCM and SKM are again the best two methods in their ability to predict discharge in natural river. Fig.6.22

clearly establishes the fact that EMDCM can also be used to estimate discharge even in natural rivers having wide flood plains with width ratio in the range of 6.67-12.

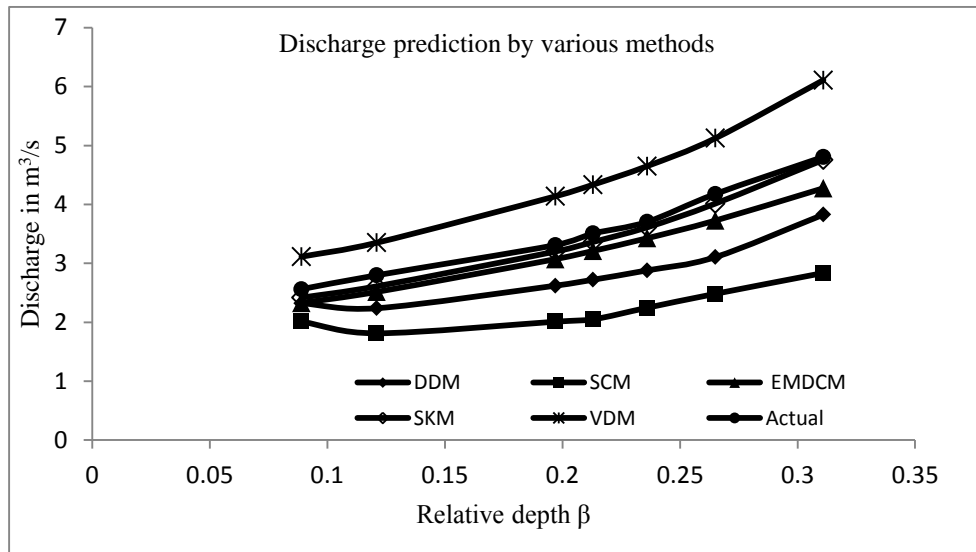


Fig.6- 22 Comparison of different methods for natural river data

6.3.3 DEVELOPMENT OF METHOD (For all ranges of α values)

6.3.3.1 Background

The models developed in previous sections, which are particularly applicable in the compound channels with predefined values of width ratio i.e. in the ranges of width ratios for which they have been developed are limited in their application. Those developed models are only capable of predicting total flow in the channel. However for general applicability, a model should also meet the requirement of predicting distribution of flow or sub section flow in compound channels (Knight & Shiono, 1996). So it is worthwhile to explore means to devise a new method which can have the potential of being applied for floodplains with all practical ranges of α value. It has been amply demonstrated by other researchers (e.g. Weber and Menéndez, 2004 etc.) that a method performing well in predicting the $H-Q$ relation for a particular channel might not be able to correctly assess the flow distribution between the various sub areas viz. flood plain and main channel zones. In this regard, in present section a new 1-D approach based on the experimental results from the present wide compound channel of NIT, Rourkela is attempted. The present work is extended albeit in a different way from the previous research work done in compound channels of different α values to predict stage discharge relationship i.e. for α up to 4 (Knight & Demetriou, 1983; Knight & Hamed, 1984), for α up to 5.25 (Khatua & Patra, 2007) and finally for α up to 6.67 (as in

MDCM of Khatua et al,2012) and up to 12 (EMDCM of Mohanty et al.2013) the details of which have already been provided in previous sections of this thesis as a prelude to the build-up for this new method. Using the method also the component discharges are estimated and compared with their observed values in case of several data series published in literature.

6.3.3.2 The methodology

In this section, an attempt is made to apply the Darcy- Weisbach equation to a straight compound channel incorporating the effect of momentum transfer between the main channel and floodplain and the distribution of zonal friction factors (f_z). The compound section can be decomposed as before into one main channel section and two symmetrical floodplain sections by drawing vertical lines at the junction of the main channel and the floodplains and writing the whole area of compound section as A , that of main channel as A_{mc} and that of floodplain sections as A_{fp} , from 1-D analysis the average shear stress (τ_z) (Knight, 2005, Knight & Shameseldin [Ed.], 2006) in any zone can be expressed as

$$\tau_z = \left(\frac{f_z}{8} \right) \rho U_z^2 \quad (6.21)$$

where, f_z is average Darcy's friction factor in a particular zone, ρ is water density and U_z is the average zonal velocity. For the floodplains we can write shear force S_{fp} carried by it per unit length perpendicular to the channel cross section as

$$S_{fp} = P_{fp} \tau_z \quad (6.22)$$

where P_{fp} is the floodplain wetted perimeter. From (6.21) & (6.22) one can find an expression for average flood plain velocity

$$U_{fp} = \sqrt{\frac{8S_{fp}}{P_{fp} f_{fp} \rho}} \quad (6.23)$$

Or in terms of percentage of shear force in floodplain area ($\%S_{fp}$), we can write above as

$$U_{fp} = \sqrt{\frac{\%S_{fp} gAS}{12.5P_{fp} f_{fp}}} \quad (6.24)$$

where subscript fp denotes respective terms used for floodplain. Similarly writing an expression for main channel region

$$U_{mc} = \sqrt{\frac{8S_{mc}}{P_{mc} f_{mc} \rho}} \quad (6.25)$$

Or in terms of percent of shear force carried by main channel ($\%S_{mc}$);

$$U_{mc} = \sqrt{\frac{\%S_{mc} gAS}{12.5P_{mc} f_{mc}}} \quad (6.26)$$

where subscript mc denotes respective terms in main channel region. For most of the channels normally the bed and wall roughness values are given in terms of Manning's roughness value, n . However Darcy's friction factor f , Manning's roughness value n and Chezy's ' C ' are related by the relation (Yen, 2002)

$$\sqrt{\frac{f}{8}} = \frac{n\sqrt{g}}{R^{1/6} K_n} = \frac{\sqrt{g}}{C} = \frac{\sqrt{gRS}}{U} \quad (6.27)$$

where R is hydraulic radius, S is bed slope, g is acceleration due to gravity and U is velocity. In SI Units $K_n = 1\text{m}^{1/2}/\text{s}$. So from (6.27) we can find ' f ' as

$$f = 8 \left(\frac{n\sqrt{g}}{R^{1/6}} \right)^2 \quad (6.28)$$

From (6.24) and (6.26) it is obvious that if S_{fp} and S_{mc} can be determined in any compound channel flow, then both U_{fp} and U_{mc} and hence the zonal discharge Q_{fp} and Q_{mc} as well as the total discharge Q can be found out.

6.3.3.3 Results and Discussion

Flow Estimation for Small Scale and Large Scale Data

The method so developed has been applied to a number of small scale and large scale data widely published in literature to estimate the stage-discharge relationship in addition to the present experimental data of NIT,Rourkela channel. Three (K&D

Series-1,2, & 3) data sets of Knight & Hamed (1984) and two (M-1,&2) data series of Myers (1987) which are small scale laboratory experimental data and five large scale data sets from EPSRC-FCF (FCF Phase A-1,2,3,8 &10) are selected to test the method for its validation. The overview of these experimental data is provided in Table 6-2. The above data series consisting both of small scale and large scale flume experiments have long served the purpose of being used as benchmark data series and so have been widely used by various researchers (e.g. Ervine et al.2000; Moreta and Martin-vide, 2010 etc.) in the field of compound channels to verify and validate their respective stage-discharge models. The width ratio α varies from 2 to 4 in case of K&D Series, is 4.89 in case of M-1 & 2 series and is from 2.2 to 6.67 in case of FCF-A series channels. Also some compound channels are rectangular and trapezoidal as evident from Table.6-2. While applying the method for discharge estimation, for calculating the shear force percentage carried by the floodplains for $\alpha \leq 6.67$, equation (6.13a) and for $\alpha \geq 6.67$, equation (6.14) has been chosen so as to correctly represent the shear percentage ($\%S_{fp}$) in terms of percentage of area occupied by floodplains ($\%A_{fp}$). The new method (NM) is pitted against some traditional methods such as single channel method (SCM), divided channel methods (DCMs) consisting of horizontal division methods with length of interface excluded and included for calculating main channel perimeter (HDM-I & HDM-II respectively), vertical division methods with similar variants (VDM-I & VDM-II respectively) and a diagonal division method with length of interface being excluded (DDM), and finally the (SKM) method of Shiono and Knight (1991). The discharge is estimated in each method and compared with actual discharge to find the percentage of error for each flow depth in each case as in equation (6.20). Figs.6-23(a-k) shows the result of the application of various discharge estimation models as enumerated above including the new method to the various data series. In Fig.6-23(a) it is seen that all methods at very low relative depths predict discharge with less error but as the β value grows the error (%) also grows for almost all methods though with varying degree. At β value of around 0.27 the error is maximum for all the methods considered and beyond this depth of flow the error in discharge estimation diminishes gradually. Even the SCM estimation beyond the β value of 0.27 is quite acceptable as error (%) lies within a range of 0.06-6.09 for higher depths of flow in the widest channel. It thus implies that a wide compound channel ($\alpha = 11.96$) behaves as a single channel at a much lesser relative depth value than 0.5 which has been the usual characteristic of other channels (Bhowmik & Demissie,1982).The different methods

either under predict or over predict the discharge for different channels under varying depths of flow as evident from Figs.6.23 (a-k) through the respective magnitudes of error percentage.

Table 6-2 Overview of Experimental and Natural river data considered for development and validation purpose of different stage discharge models

Authors	Series Name	Main channel type	Main channel side slope (<i>s</i>)	$\alpha = B/b$	Bed Slope (<i>S</i>)	Manning's roughness constant		Range of β values	Range of Discharge (<i>Q</i> in lit/s)
						Main Channel	Flood plains		
(a)Small Scale Flumes									
Knight & Demetriou(1984)	KD-1	Rect.	1V:0H	2	0.000966	0.01	0.01	0.1079-0.49265	5.2-17.1
	KD-2	Rect.	1V:0H	3	0.000966	0.01	0.01	0.13142-0.4906	5.0-23.4
	KD-3	Rect.	1V:0H	4	0.000966	0.01	0.01	0.1058-0.50586	4.9-29.4
Myers(1987)	M-1	Rect.	1V:0H	4.69	0.00093	0.01	0.01	0.18033-0.439	8.3-27.2
	M-2	Rect.	1V:0H	4.69	0.00037	0.01	0.01	0.0981-0.4764	3.1-21.1
Khatua (2008)	-----	Rect.	1V:0H	3.67	0.0019	0.01	0.01	0.118-0.461	8.726-39.071

Authors	Series Name	Main channel type	Main channel side slope (<i>s</i>)	$\alpha = B/b$	Bed Slope (<i>S</i>)	Manning's roughness constant		Range of β values	Range of Discharge (<i>Q</i> in lit/s)
						Main Channel	Flood plains		
(b) Large Scale Flumes									
Khatua et al(2012)	FCFA-1	Trapez.	1V:1H	6.67	0.001027	0.01	0.01	0.0565-0.40029	208.2-1014.5
	FCFA-2	Trapez.	1V:1H	4.2	0.001027	0.01	0.01	0.0414-0.47908	212.3-1114.2
	FCFA-3	Trapez.	1V:1H	2.2	0.001027	0.01	0.01	0.1314-0.50023	225.1-834.9
Knight and Shiono (1996)	FCFA-8	Rect	1V:0H	4	0.001027	0.01	0.01	0.0503-0.49955	185.8-1103.4
	FCFA-10	Trapez.	1V:2H	4.4	0.001027	0.01	0.01	0.05081-0.4637	236.8-1093.9
(c)River data									
Hin et al(2008)& Khatua et al(2012)	River Batu	Irregular	-----	4.64-7.3	0.0013-0.0016	0.075	0.3	0.089-0.311	2562.0-4808.0
Khatua et al(2012)	River Main	Irregular	-----	1.2-2.55	0.0029	0.03	0.06	0.00627-0.473	18344.0-57770.0
Knight(1989)	River Severn	Irregular	-----	3.8-8.52	0.000195	0.032	0.04	0.077-0.259	1810734-2871511

The positive and negative values are shown in figure 6.23(a) because for the wide straight experimental channel of NIT,Rourkela different methods studied in the thesis predict discharge with varying relative depths with different error percentages as can be seen in the figure. The methods SKM,SCM & HDM-II under predict the discharge whereas other methods over predict the discharge values especially up to β value of 0.27. However with depth ratio beyond 0.27 the methods usually over predict with mainly positive values.

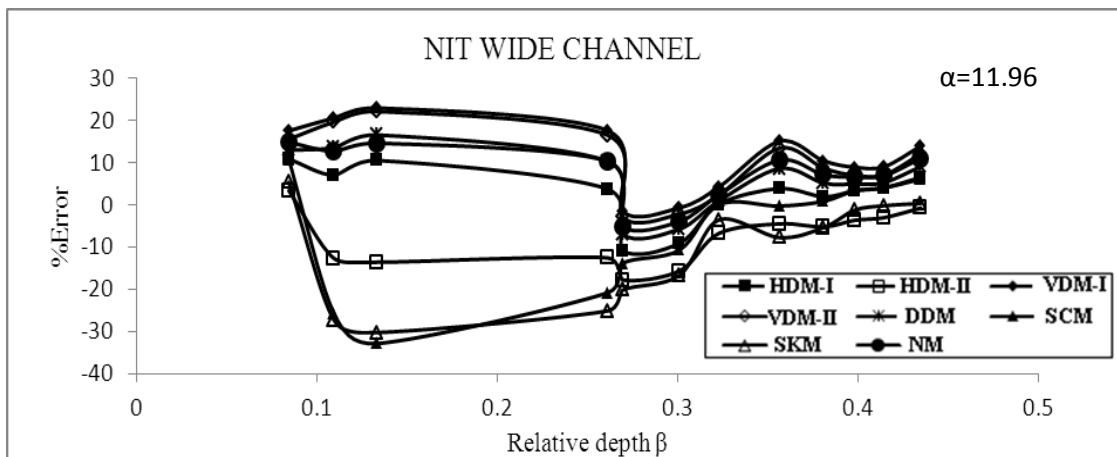


Fig.6-23(a) Error percentage in discharge estimation by various methods (NIT, Rourkela wide channel)

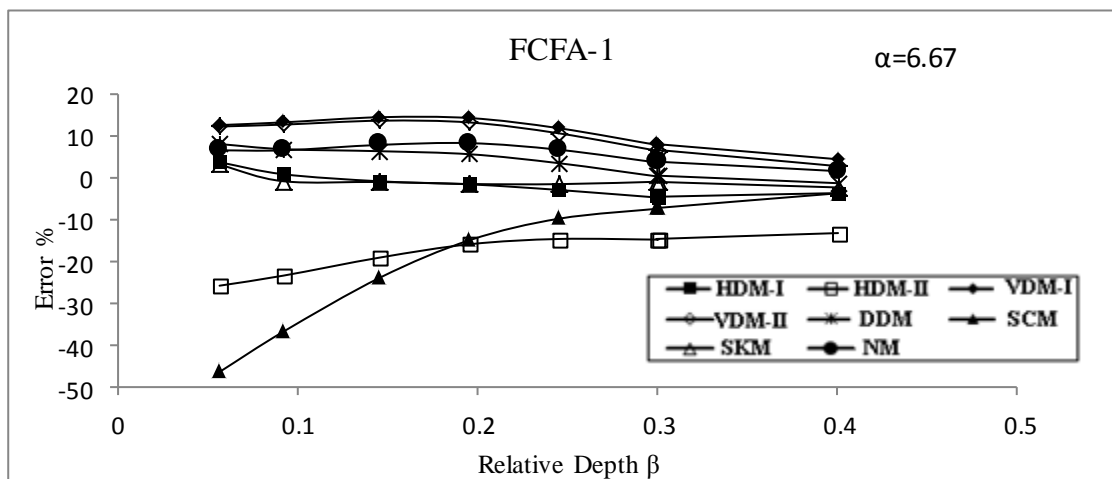


Fig.6-23(b) Error percentage in discharge estimation by various methods (FCF A-1 channel)

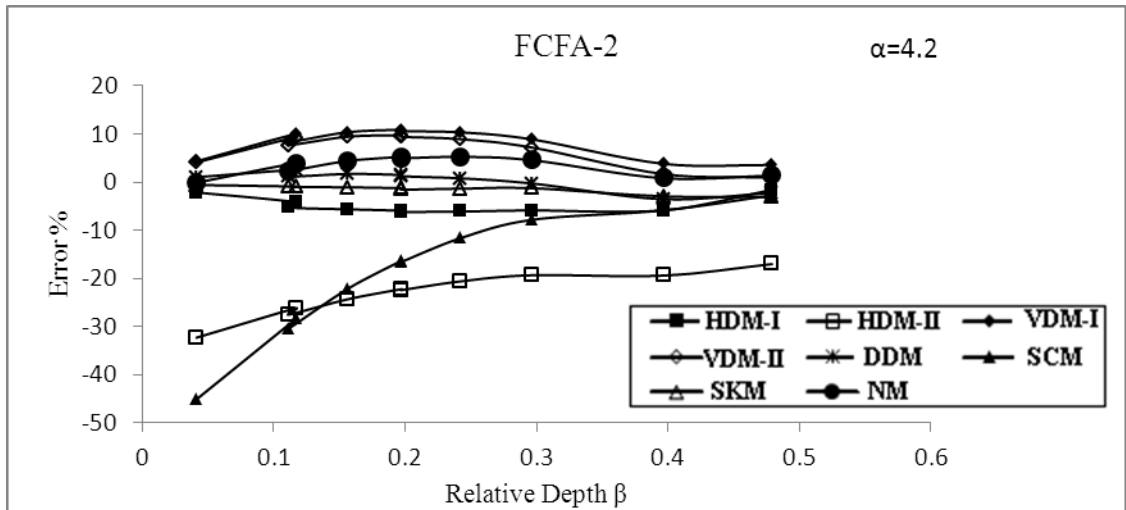


Fig.6-23(c) Error percentage in discharge estimation by various methods (FCF A-2 channel)

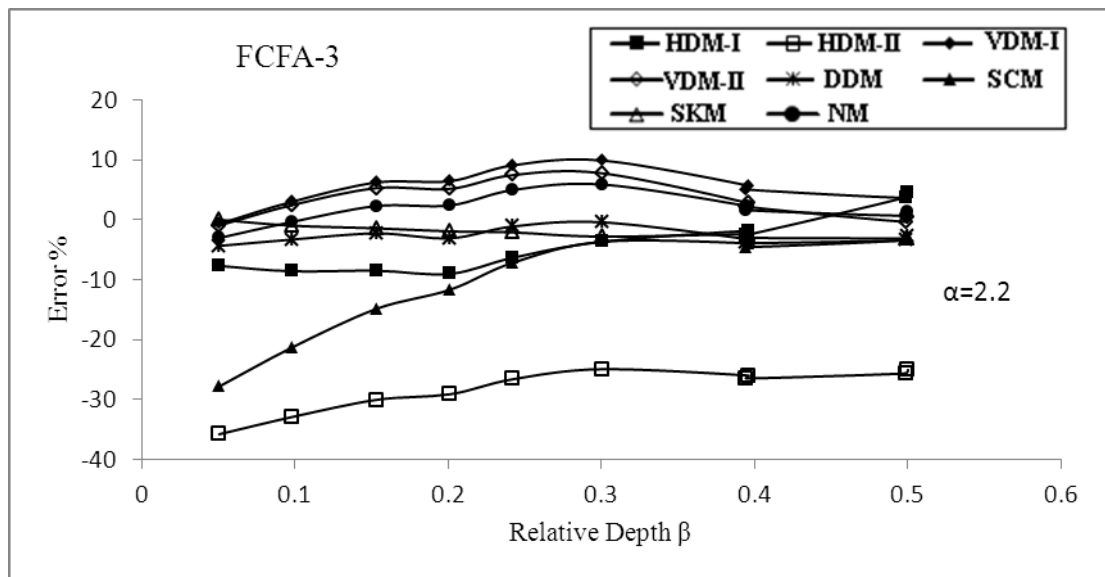


Fig.6-23(d) Error percentage in discharge estimation by various methods (FCF A-3 channel)

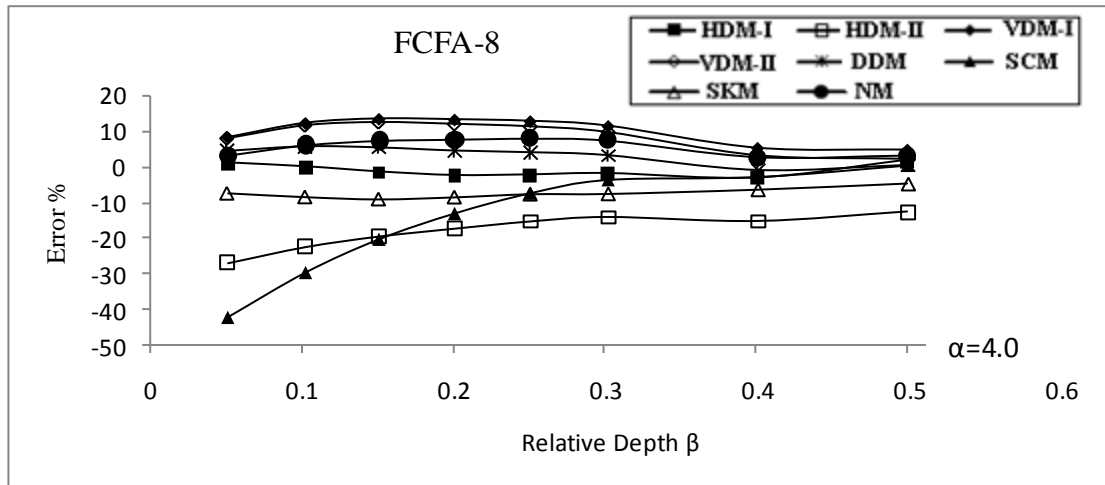


Fig.6-23(e) Error percentage in discharge estimation by various methods (FCF A-8 channel)

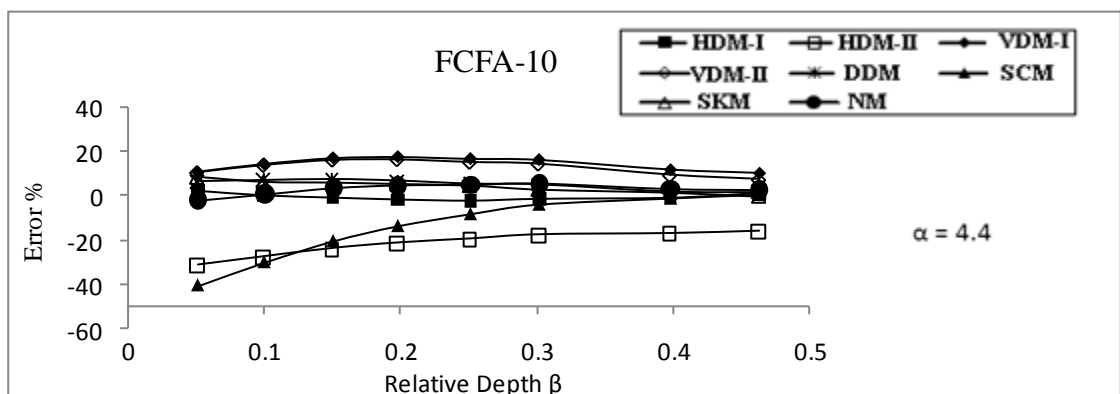


Fig.6-23(f) Error percentage in discharge estimation by various methods (FCF A-10 channel)

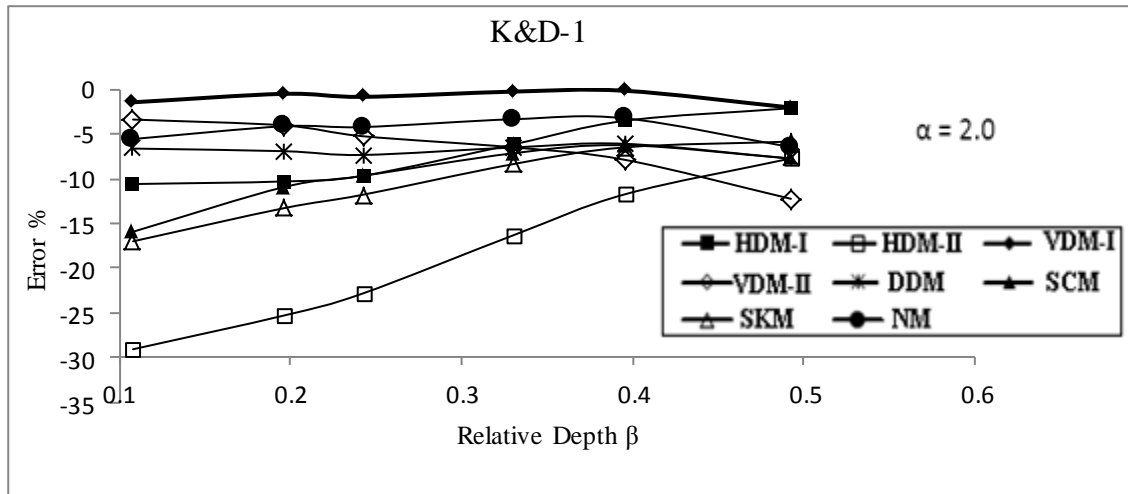


Fig.6-23(g) Error percentage in discharge estimation by various methods (K&D-1 channel)

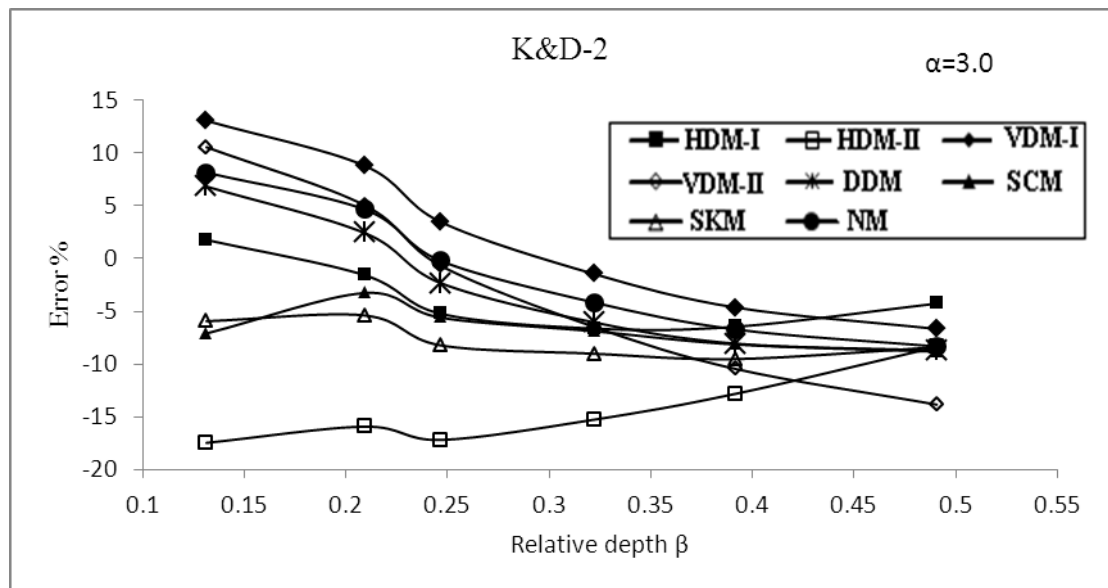
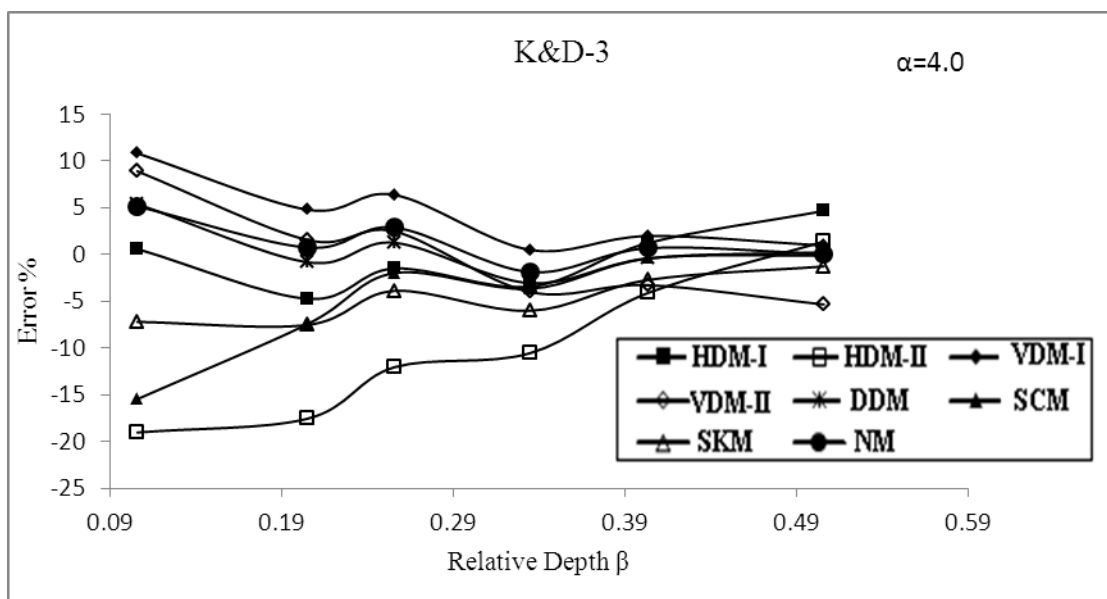


Fig.6-23(h) Error percentage in discharge estimation by various methods (K&D-2 channel)



6-23(a) Error percentage in discharge estimation by various methods (K&D-3channel)

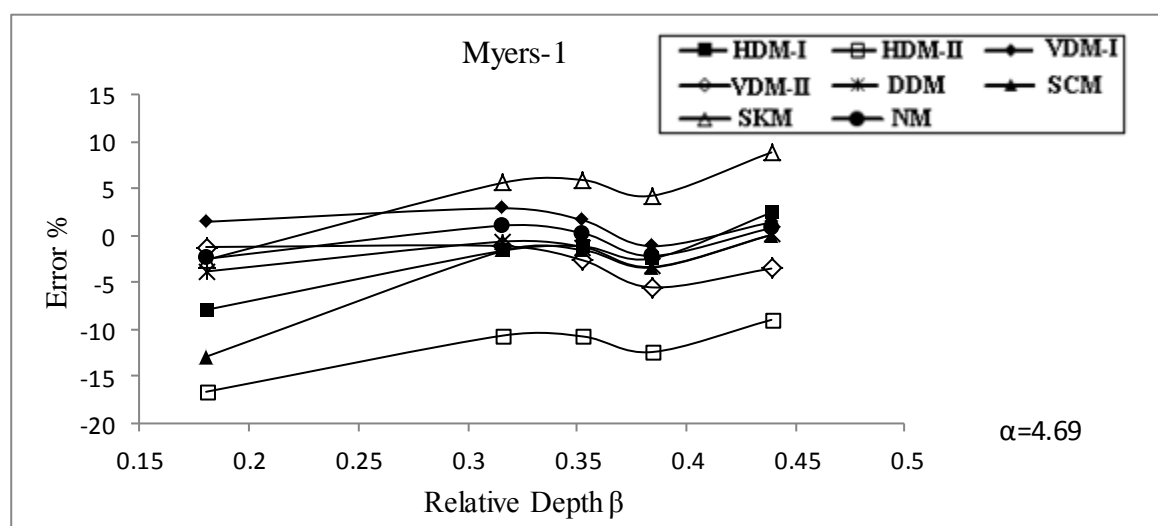


Fig.6-23(j) Error percentage in discharge estimation by various methods (M-1 channel)

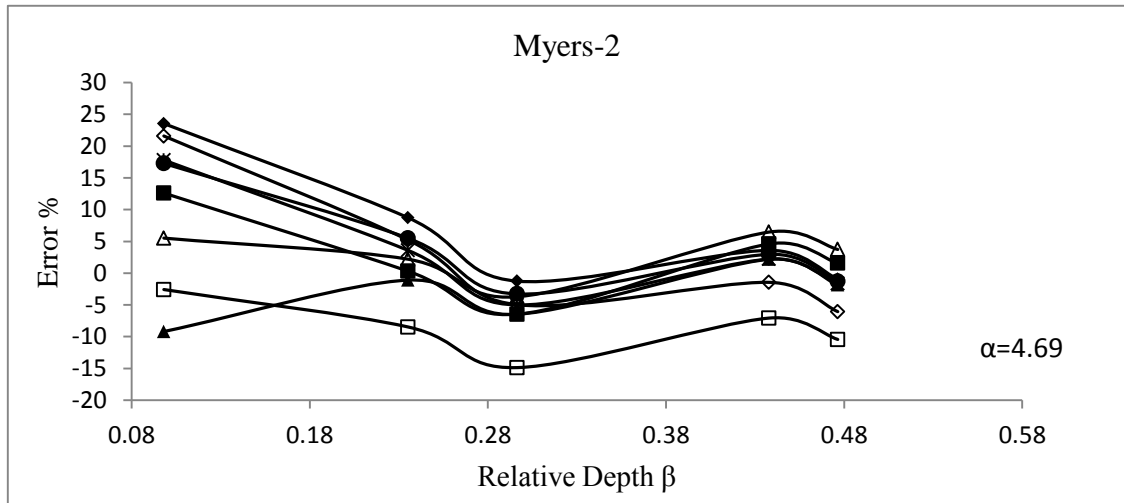


Fig.6-23(k) Error percentage in discharge estimation by various methods (M-2channel)

Table 6- 3 Series wise RMS value of error (%) for new method

SERIES	RMSE (%)
FCF1	6.2
FCF2	3.8
FCF3	3.0
FCF8	6.0
FCF10	3.8
KD1	4.6
KD2	6.1
KD3	2.6
M-1	1.6
M-2	8.4
NIT	9.7
River BATU	4.0
River MAIN	13.8
River SEVERN	7.5

Application to Field Data

In addition to the two previously described field cases e.g. the river Batu and the river Main, a third river data set from the river Severn at Montford Bridge site (in England),

is also used for validating the new stage discharge model. The Severn at Montford Bridge site has been extensively monitored for practical hydrometry and research purposes, providing a large body of accurate current metering data (Knight, 1989). It is a natural cross-section located in a straight reach with a cableway extending over the full width including the floodplains (Figs.A-3, a-c). The bank full width and depth are 40 and 6.3 meters respectively. The total width, including the floodplains, is approximately 120m and the reach-averaged longitudinal bed slope is 0.000195.

All the rivers have non-homogeneous roughness along their perimeter i.e. floodplain roughness coarser than that of main channel. So accordingly for calculating the shear force percentage carried by the floodplains for $\alpha \leq 6.67$ equation (6.13c) and for $\alpha \geq 6.67$ equation (6.15) have been used instead of (6.13a) and (6.14) respectively as used in case of the laboratory flumes having homogeneous roughness (same Manning's n value) in floodplain and main channel, so as to correctly predict the shear force percentage ($\%S_{fp}$) in terms of percentage of area occupied by floodplains ($\%A_{fp}$). Then after estimating the shear force the usual process of finding the discharge by new method as explained before is followed. All the other methods are also applied to these river data for comparison purpose. The Error (%) in estimation of discharge by various methods is shown in Figs.6.24 (a-c).

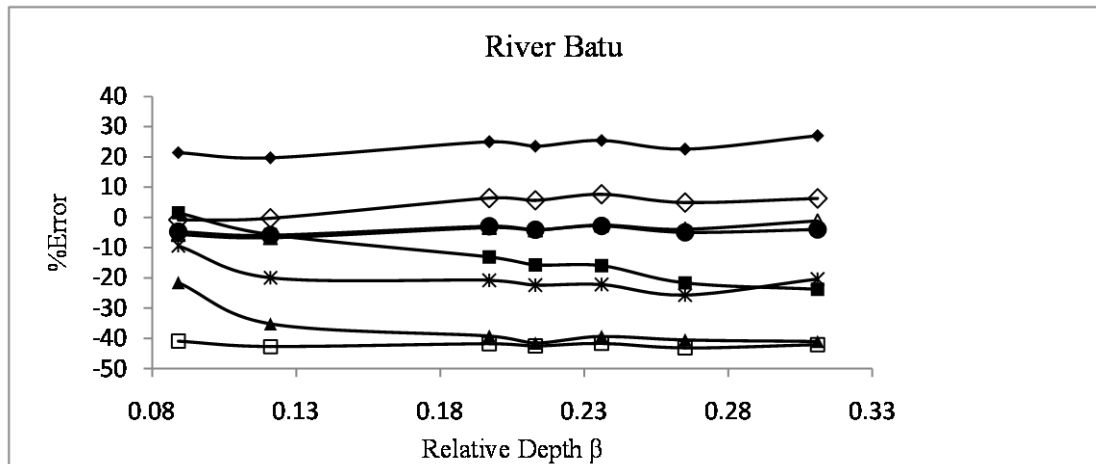


Fig.6-24(a) Error (%) in discharge estimation for the river Batu.

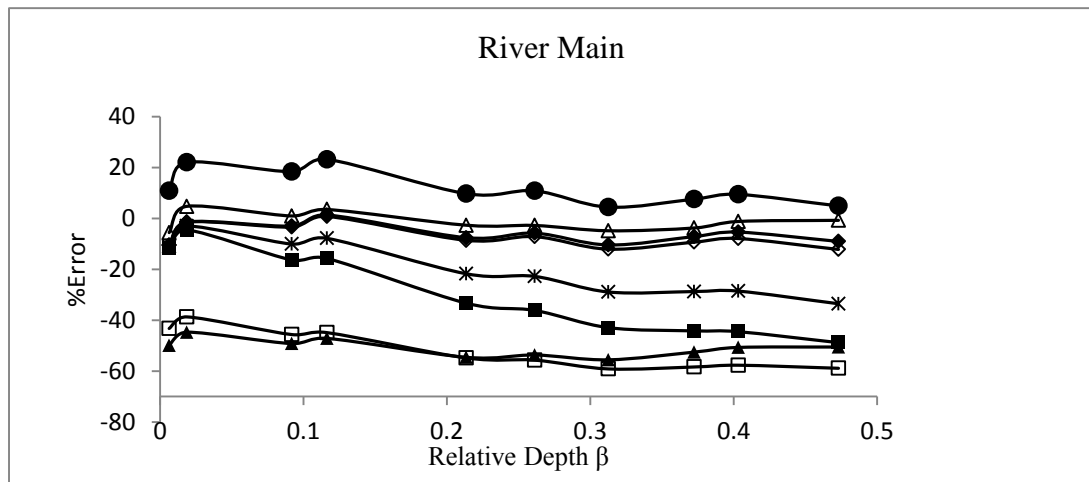


Fig.6-24(b) Error (%) in discharge estimation for the river Main

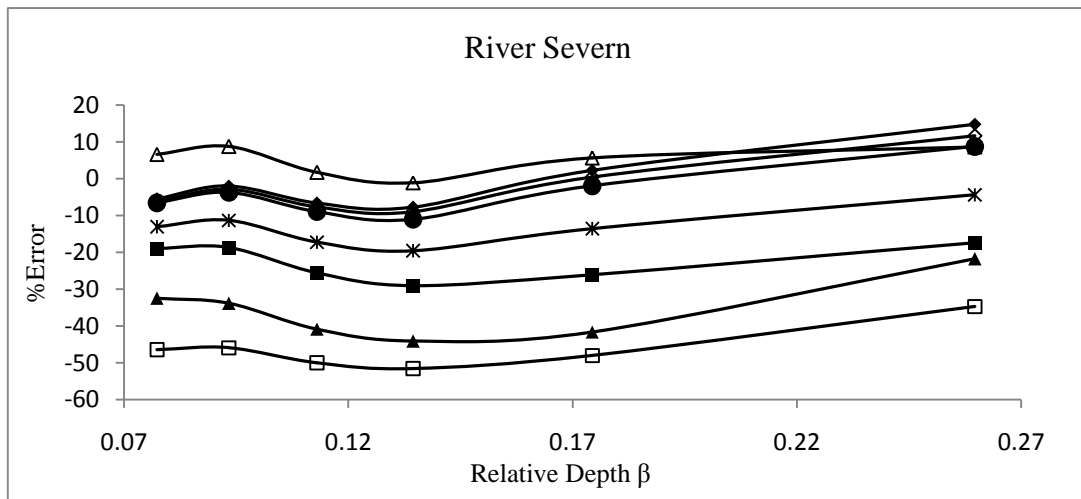
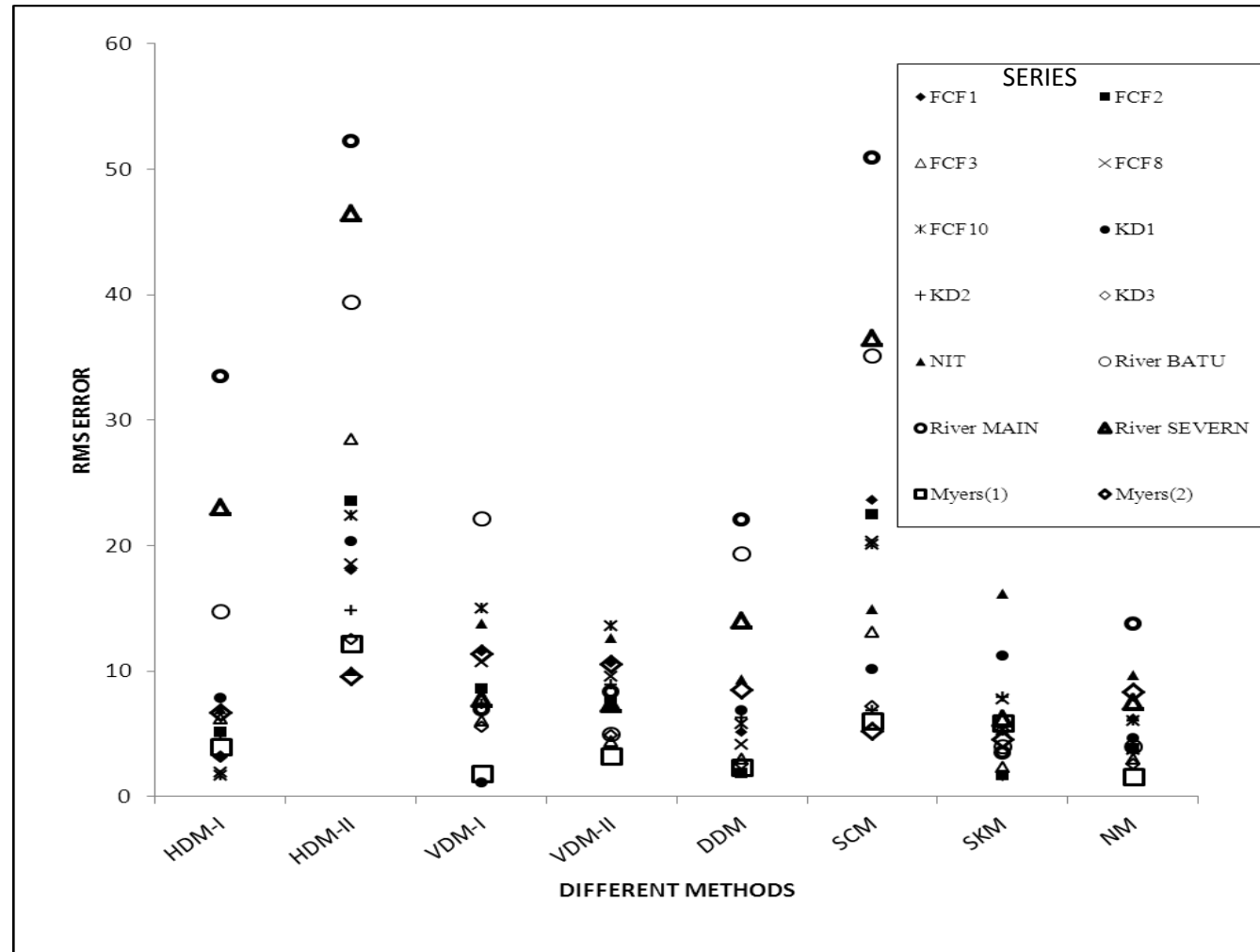


Fig.6-24(c) Error (%) in discharge estimation for the river Severn.

As evident in all three diagrams in Figs.6.24 (a-c) again the NM is among the best of the methods when predicting stage discharge in field application. In all the data series considered in this work, it is seen that methods sometimes over predict and sometimes under predict the discharge amount with varying relative depth there by resulting in positive and negative errors. So in order to make a comparison among all the methods regarding their performance in individual data series as well as their overall performance considering all 14 data sets, the root mean squared value of error (%) (RMSE) is computed. It is seen that both the horizontal methods (HDM-I & HDM-II), the diagonal method (DDM) and the new method (NM) give less error as compared to other methods for NIT channel only. For HDM-I, RMSE value is 6.94 and for NM it's

9.67. For FCF-A series (1, 2, 3, 8 and 10) channels the RMS values of the error (%) for NM are estimated to be 6.2, 3.78, 3.01, 5.99 and 3.75 respectively. Similarly considering the (KD-1, 2 &3) series channels the performance of NM is again very encouraging as the RMSE values are 4.6, 6.1 &2.6 respectively for the channels. Fig. 6-25 shows the performance of individual methods in a series wise manner whereas Fig.6-26 shows the overall performance of all the methods. As can be seen from Fig.6-26 the best three methods are NM, SKM and VDM-II whereas bottom ranking two methods are SCM and HDM-II. From the RMSE for overall performance shown in Fig.6-26, it is seen that RMS value of error percentage for NM, SKM and VDM-II are 7.31, 7.47 and 8.94 respectively whereas those for SCM, HDM-II, HDM-I, VDM-I and DDM are 24.79, 27.80, 13.10, 11.08 and 10.49 respectively.

Fig.6-25 Series wise RMSE value for the methods



The series wise RMS value of error percent for NM is given in Table 6.3. Thus Fig.6-25 along with Fig.6-26 adequately establishes the effectiveness of the NM in successfully predicting the stage-discharge relation under a widely varying range of geometric and hydraulic parameters encountered in straight compound channel.

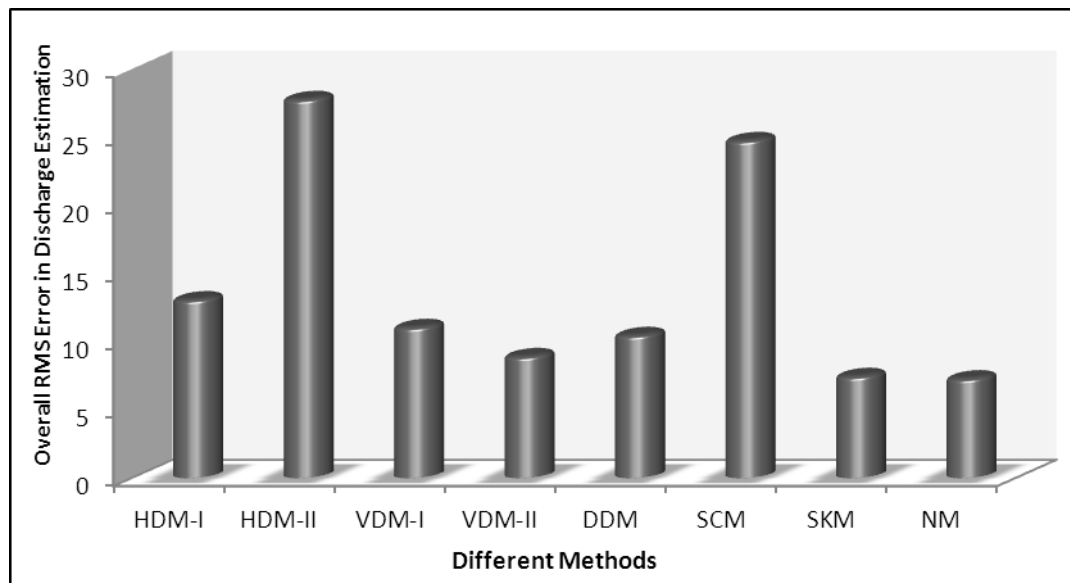


Fig.6- 26 Overall RMSE value for the methods.

Flow Distribution

It is a well-known fact that for a method to be considered successful, it must model accurately not only total discharge in the compound section, but also the component discharges in the deep section and floodplains. So accordingly the present method is tested in this regard by computing component discharges in floodplain and main channel zones by the procedure as outlined before. The component discharge data of FCF-A series channels, KD series channels and for river Batu are only available in literature to the best knowledge of author out of the data sets considered for discharge estimation presented before and so are only used here for validation of the NM. The observed and predicted main channel discharge percentages in terms of ratio of main channel discharge (Q_{mc}) to total discharge (Q) for the series considered are shown in the scatter plot given in Fig.6-27. It is evident from the diagram that the zonal discharge predictions are very close to their observed values.

The series wise RMSE value for discharge distribution is estimated and is shown in Fig.6-28. It is seen that in all the data series considered for the purpose, the present method can predict the flow distribution by estimating main channel discharge with RMS value of error less than 10% in each case and average RMSE value is 4.17% only.

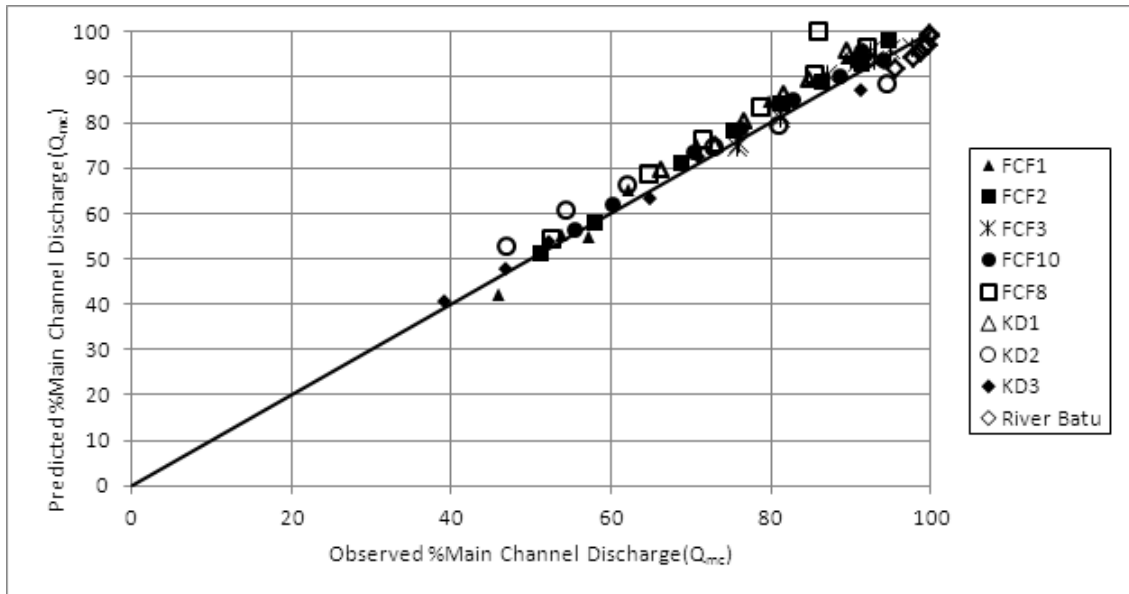


Fig.6-27 Scatter diagram for observed and modeled main channel discharge percentage for different data sets

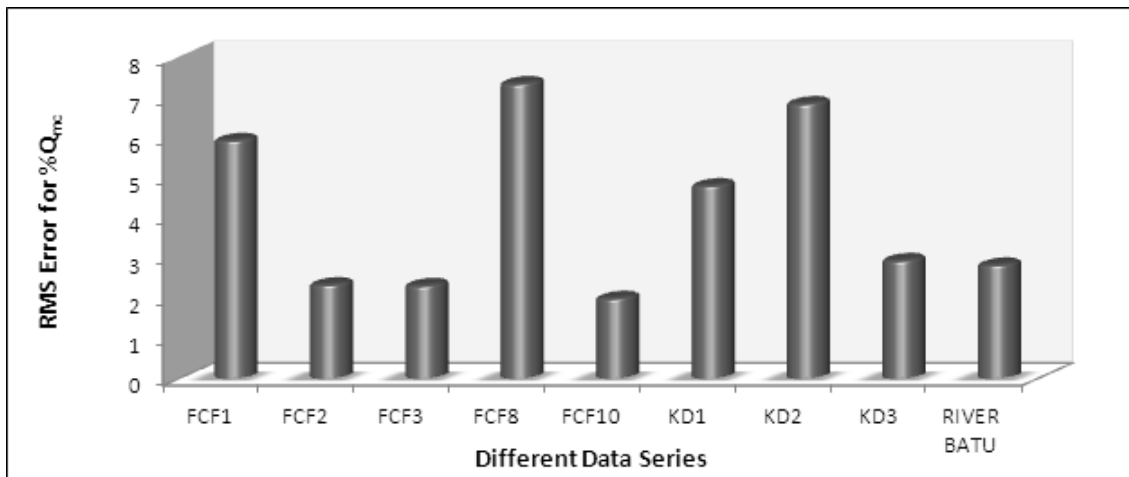


Fig.6-28 RMSE value for flow distribution by the New Method (NM)

Discussions

- (1) When different common approaches are applied to the present wide compound channel, it is found that the SKM method and SCM method give larger overall RMS error whereas Horizontal method (HDM-I) gives the best result. However a unique

feature is also noticed for SCM that beyond the β value of 0.27, the performance of SCM is quite acceptable. It thus implies that a wide compound channel behaves as a single channel at a much lesser relative depth value than 0.5 which has been the usual characteristic of less wide channels.

- (2) A new method is suggested based on zonal variation of friction factor (f) in the compound channel to predict total discharge carried by the whole section and component discharges carried by the floodplain and main channel.
- (3) The method is able to predict stage discharge relationship and component discharges for straight compound channels of different geometrical shapes and over a range of width ratios. This method is validated for its effectiveness over a wide range of published data series comprising small scale flumes, large scale flumes (FCF series) as well as some field data and is also compared with some other well established models for discharge estimation as regards their accuracy in predicting stage discharge relation.
- (4) The new method has very satisfactorily predicted the total discharge in all cases and is found to have the least overall RMSE value in discharge estimation among all the methods considered.
- (5) The method also is able to predict component discharges in a very satisfactory manner both for flume data series and river data series. The new method will be useful for discharge estimation in straight compound channels over a range of width ratios (α value in the range of 2 - 12).

6.4 DEVELOPMENT OF STAGE-DISCHARGE MODELS (MEANDERING COMPOUND CHANNEL)

6.4.1. Background

After devising models which can satisfactorily predict stage discharge ($H-Q$) in straight compound channel, attention is now turned to find a model which can take care of the issue in case of a meandering compound channels. The problem though is much more complex now as compared to a two stage straight channel. Many researchers in past namely, Ervine & Macleod (1999); McKeogh & Kiely (1991); Shiono & Muto (1998); Shiono et al. (1999); Sellin et al. (1993); Lambert & Sellin (2000); Ervine et al. (2000); Willet & Hardwick (1993); Greenhill & Sellin (1993); Patra & Kar

(2000);Knight (2005);Khatua & Patra (2007); Khatua (2008) and De Marchis & Napoli (2008) etc. have studied the problem in detail while attempting to develop models for predicting $H\sim Q$ relation in case of meandering compound channel. The sheer number of mechanisms involved in case of flow in a two stage meandering compound channel is so overwhelmingly large that any attempt to develop predictive methods based on the correlation of geometric and flow parameters will always be frustrated !(Willets & Hardwick,1993). Ervine et al. (2000) from studies done by Sellin et al. (1993) (pl.see Fig.6.29) summed up the mechanisms in a meandering compound channel as ,(a) The presence of a horizontal shear layer near the bankfull level in the crossover region (b) Bulk exchange of fluid taking place between the floodplain and main channel and making the flow highly 3-dimensional due to such mixing (c) As a result of the momentum exchange with floodplain flow in the crossover region, the channel flow enters the bend with a secondary circulation counter to that which is induced by the bend flow, and decays rapidly after each bend apex and (d) Water from the upstream floodplain plunging vigorously into the channel at the channel centerline producing strong secondary cells.

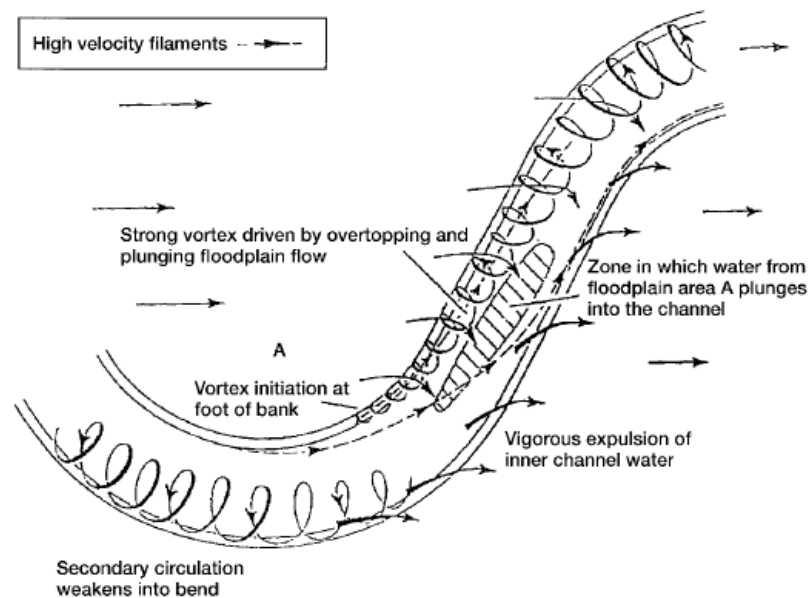


Fig.6-29 Flow Mechanisms in Compound Meandering Channels (Sellin et al. 1993)

Additionally there is a dearth of quality data sets comprising velocity; boundary shear stress etc. in case of compound meandering channels of both laboratories as well as of field cases i.e. rivers. Very few real data sets pertaining to field cases are available as collecting the velocity and boundary shear stress data in a meandering flooded river is not only difficult but dangerous also! Nevertheless scientists and researchers have made some flume experiments (involving meandering channels with various geometrical shapes) in laboratory environment for recording the hydraulic response of the channels to the flow phenomenon taking place. Willets & Hardwick, 1993 based on the experimental measurements conducted in a small laboratory meandering channel with various sinuosities concluded that inner channel sinuosity had a pronounced influence on the system conveyance in overbank flows due to large scale interaction between channel and floodplain flows. They also emphasized the need of a numerical model encompassing the principal mechanisms occurring in overbank flows in a meandering channel for an effective solution to the stage-discharge prediction problem. Greenhill & Sellin (1993) devised an empirical solution by using Manning's equation and a specialized DCM technique, which was successfully validated against the large scale data set of FCF channel (Series-B) and the data sets of some other research projects. Since for overbank flow the resistance to flow occurs due to various factors such as sinuosity, boundary friction, secondary flows, turbulence as well as flow expansion and contraction, so when discharge and hence depth increases all these factors contribute to overall resistance to flow in different measures (Knight, 2005). This obviously was the reason behind numerical studies undertaken to gain insights into the interrelation among various parameters (Rodi, 1980; Shiono & Muto, 1998; Rameshwaran et al., 1999; De Marchis & Napoli, 2008 etc.). De Marchis and Napoli (2008) based on their numerical experiments through a 3D finite-volume model solving RANS equations, conducted on a number of compound channels having identical cross-sectional area, roughness and bed slope but different planimetric patterns concluded that sinuosity is the main parameter to be accounted for in empirical formulae to assess the conveyance capacity of the meandering compound channels. In the present case a unique strategy is adopted where some meandering channel stage discharge data previously available in literature are once again numerically simulated in order to extract the boundary shear stress data. Then using these boundary shear stress data along with the meandering channel experimental data of NIT, Rourkela an empirical relation is found and is judiciously used for obtaining the $H \sim Q$ relation for meandering compound channel.

The method so developed is then validated against the large scale FCF data (Series-B) and the data sets of other researchers published in literature.

6.4.2. Methodology

The methodology adopted in case of the development of the model for straight compound channels by using the equations (6.13) & (6.14) as well as equations (6.24) & (6.26), is obviously not useful in case of meandering compound channels as the boundary shear stress carried by the floodplains are quite different in magnitude as compared to a straight compound channel of similar geometry due to the presence of additional mechanisms. This has also been corroborated by investigations of past researchers (Khatua,2008; Patra & Kar,2000 etc.). Also from the measurement of the boundary shear stress at the bend apex of a meandering compound channel, it is seen that total shear carried by the left floodplain is markedly higher than that carried by the right floodplain for a meandering main channel turning right (looking towards d/s end of the channel) and vice versa for a meandering main channel turning left. This variation needs to be accounted for while computing the average velocity U_z . Thus separate equations are used for finding the average velocity in left floodplain U_{lfp} and that in right floodplain U_{rfp} in line with equation (6.23 or 6.24) . Similarly by regression techniques two separate equations are determined, one each for the shear force carried by the total floodplain as $\%S_{fp}$ and for the left floodplain as $\%S_{lfp}$. By subtracting the $\%S_{lfp}$ from $\%S_{fp}$,the shear force carried by right floodplain $\%S_{rfp}$ can be found out and thus U_{lfp} and U_{rfp} . Finally as before in section 6.3.3.2, Q_{fp} and Q_{mc} as well as the total discharge Q can be found out for the whole meandering compound channel.

For determining shear percentages in different flow zones in terms of the respective floodplain areas, ideally a large number of shear data from flow cases in different channels are to be used for regression analysis. In literature only a few cases are available where one can find boundary shear stress variation with depth of flow in meandering compound channels. However many studies for meandering compound channels are reported in literature where stage-discharge data for different relative depths or depths of flow are available. So in order to extract reliable information on boundary shear stress for these flow cases, the method of numerical experiments is resorted to wherein the CES software tool is used for simulating flume experiments of the meandering channels considered in this study. CES tool is so chosen because it

estimated the percentage of shear force ($\%S_{fp}$) very close to the corresponding experimental values though the local shear is found to be under predicted at some points. Numerical simulation studies on meandering compound channels have been conducted in past by other researchers too to extract valuable information about the flow physics (De Marchis and Napoli, 2008). First of all each channel geometry is replicated in CES. Then the model is calibrated by assigning roughness values in main channel and floodplains and passing different depths of flow and then computing the discharge for the channel and equating the same with the reported stage-discharge curve from the literature. Thereafter the boundary shear stress value for each depth of flow is computed and hence the shear carried by floodplains and main channel is found out. Following this strategy, the boundary shear data is found out for all the flow cases considered in this research. For the present study the stage-discharge data from, large scale flume experiments of FCF (Series B) channel (Knight et al., 1992); the channel experiments of Shiono et al. (1999); the channel experiments of Willets & Hardwick, (1993) along with the present meandering channel of NIT, Rourkela experimental flume is considered. The shear stress data for FCF-Series B channel is reported in Knight et al. (1992) and so it could be extracted directly from the paper. For the other two studies apart from NIT channel, CES is used as explained before in chapter-5. On the basis of channel shape, bed slope and width ratio (α) Shiono et al. (1999) reported about flow experiments in 9 nos. of different channels with 98 stage-discharge data and Willet & Hardwick (1993) reported about flow experiments in 3 nos. of different channels with 51 stage-discharge data. All the channels considered in the development of the model are rigid and with wide floodplains ($7.27 \leq \alpha < 12$) having homogeneous roughness in main channel and floodplains. Table 6.4 shows the geometrical and hydraulic parameters of the data sets considered for the development of the shear force models in case of meandering compound channel. In view of the broad similarities in the selected channels' characteristics, it is expected that the study undertaken would result in a model which will be able to predict stage-discharge relation in meandering compound channels with wide floodplains rather satisfactorily.

6.4.3. The new boundary shear models

As all the boundary shear stress values are considered across the flow section at the bend apex with the particular meander bend turning right at the bend, so the shear carried by the left floodplain is much larger in comparison with that carried by the right

floodplain. Hence the regression analysis is done for the shear carried by the left floodplain and area of left floodplain data and the curve of best fit is shown in in Fig.6.30. Similarly the total shear carried by the whole floodplain is always an important parameter and so another regression analysis is done with floodplain shear and area of floodplain for all the cases and the best fit curve is shown in Fig.6.31.

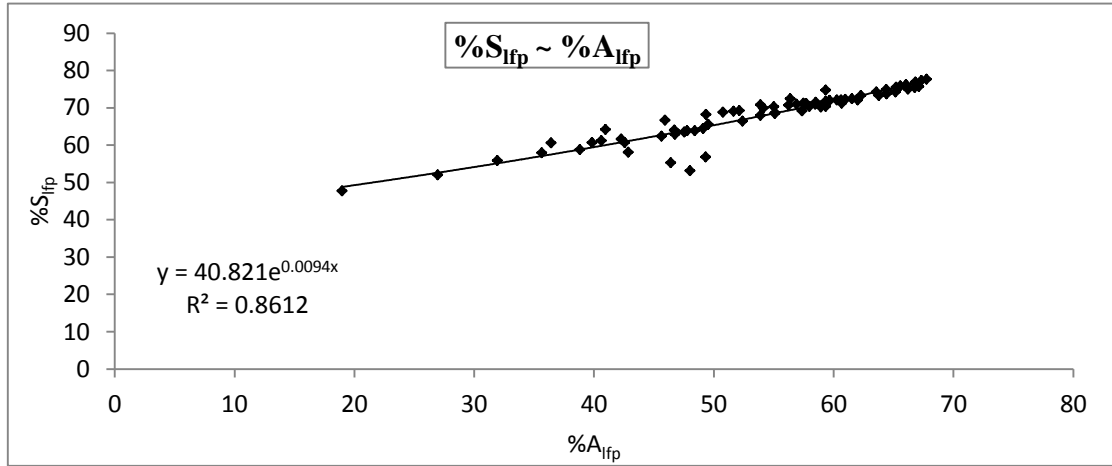


Fig.6- 30 Regression curve for percentage of Shear force carried by the left flood plain with percentage of area of left floodplain. (Meandering compound channels)

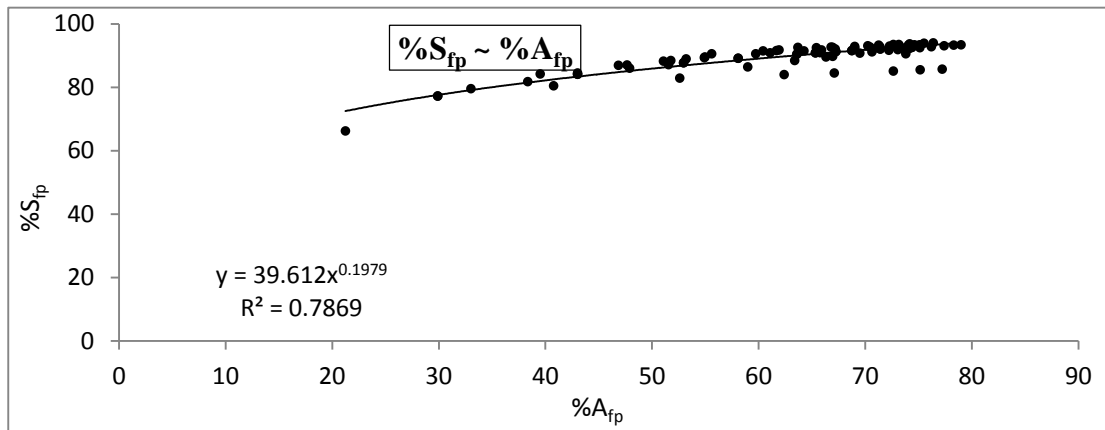


Fig.6- 31 Regression curve for percentage of Shear force carried by the flood plain with percentage of area of floodplain. (Meandering compound channels)

The equation for the best fit curve in case of shear in left floodplain ($\%S_{lfp}$) is an exponential relation and the same can be written as

$$\%S_{lfp} = 40.82e^{0.009(\%A_{lfp})} \quad (6.29)$$

with the R^2 value as 0.861.

However the equation for the best fit curve in case of shear carried by total floodplain ($\%S_{fp}$) is a power function of floodplain area of the compound channel and is described as

$$\%S_{fp} = 39.61(\%A_{fp})^{0.197} \quad (6.1)$$

with the R^2 value as 0.786.

As before for unequal roughness in floodplains and main channel the above equations (6.29) and (6.30) are to be modified with the extra term suggested by Knight and Hamed (1984). Using the above expressions i.e. equations (6.29) & (6.30) the shear carried by the respective zones of left floodplain and total floodplain are computed and then as explained before the discharge is computed for the different zones of flow section in the meandering compound channel. The zonal discharges can then be added to estimate the total discharge carried by the entire flow section. The error percentage in estimated discharge can then be found out by using equation (6.20) as before.

6.4.4. Results and Discussion

Fig.6.32 (i-v) shows the result of the application of the present method to various data series for discharge estimation through error (%) versus relative depth curves for all the series. For validation of the new stage discharge model, FCF-Series B data; all three data series of Willets & Hardwick, (1993) (W&H-1, 2 & 3); three data series of Shiono et al. (1999) (SAK-1, 2 & 3) and NIT data which are considered in the development of the shear force models (equation 6.29 & 6.30) have been used. Additionally the large scale data series of US Army Vicksburg, (1956) (US-1, 2, 3, 4 &5) have also been used for validation purpose. Figure 6-32(i) shows the application of the new method to large scale data sets of FCF-series-B channel; figure 6-32(ii) shows for the US Army Vicksburg (1956) data sets; figure 6-32(iii) shows the application of the method to Willet & Hardwick (1993) data sets; figure 6-32(iv) is for Shiono, Alromaiha & Knight (1999) data sets while figure 6-32(v) shows the validation of the method for the NIT,Rourkela meandering channel. The overview of all the data sets used for development and validation are provided in Table6.4 .The model is also applied to a natural river (The river Baitarani, Patra & Kar, 2000; Khatua et al., 2013; please see Fig.A-4 and TableA-2 for details of the geometric dimensions and surface conditions).

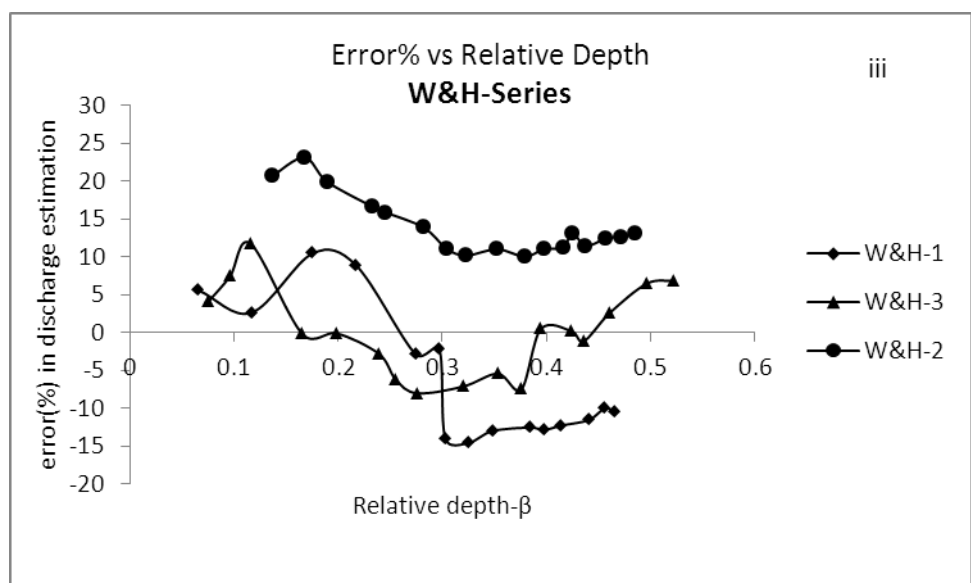
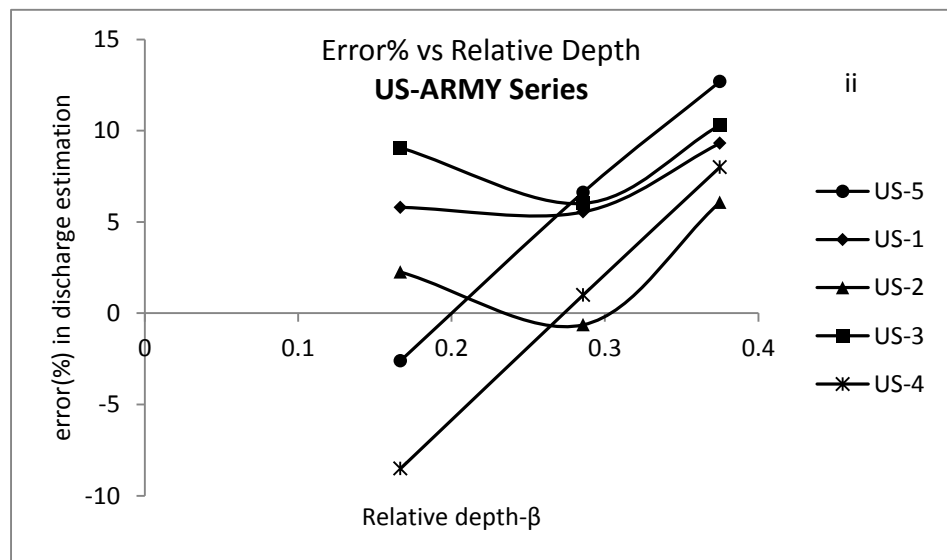
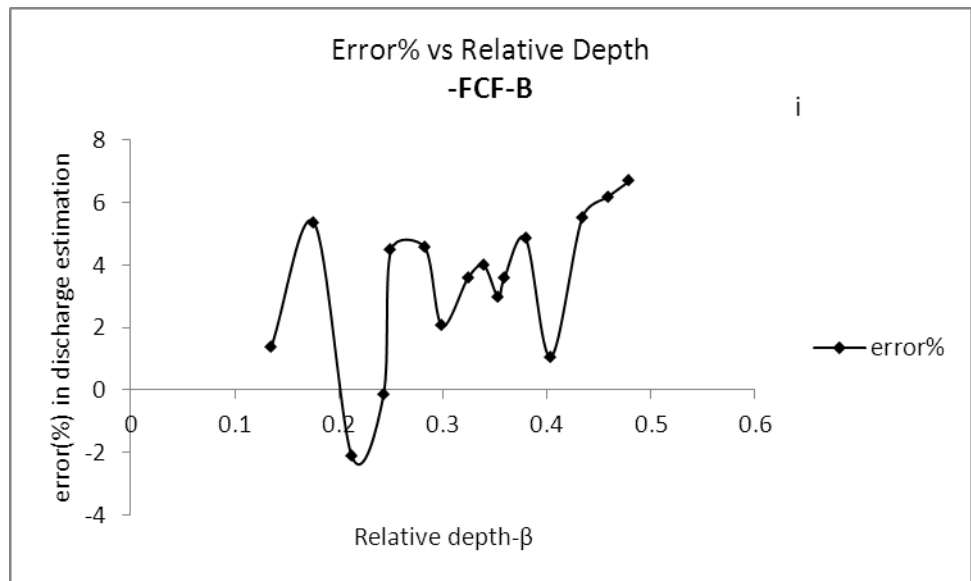
On careful examination it is found that the developed discharge model is very well validated for FCF-B data; US-1,2,3,4&5 data sets; W&H-1&3 data sets and SAK-2 data set with error (%) lying within $\pm 12\%$ and for other series also the error margin occasionally lies beyond such level.

The channels of Willets & Hardwick (1993) have moderate to very high sinuosity in the range of 1.2-2.03 and width ratio greater than 6.67. The model is giving very good result for W&H-1,3 channels whereas for W&H-2 channel the error in discharge estimation is found to be high at low overbank flow. This error though gradually diminishes with rise in flow depth in the channel. The model's performance regarding channels from FCF series and US Army (1956) series is very satisfactory as in each of these cases (sinuosity range 1.22-1.75 and width ratio range 11.11-30) the error percentage remain limited to $\pm 10\%$. The model's discharge prediction is satisfactory for low overbank depths in SAK-1 channel whereas its performance is good for SAK-3 channel in case of high overbank depths. The SAK-2 channel though is best validated through the model. The model is also found to provide reasonable result in case of present NIT, Rourkela channel at low to moderate overbank depths with minimal error percentage. The reason may be that in lower overbank depth momentum transfer is higher and at very high over bank depth the reversal of momentum transfer (from floodplain to main channel) occurs. In summary the error percentage for large scale data series of FCF-B is very small ($< 7\%$) and that for all 5 data sets of US Army, V'brg is within 12%. The same for all small scale flume tests are also very satisfactory with only stray cases giving high error in the vicinity of 20%.

Table 6- 4 Overview of Data sets used for development and validation of stage-discharge models for meandering compound channels.

Sl. no.	Authors / Research projects	Series Name	Main channel type	Main channel side slope (<i>s</i>)	$A = B/b$	Sinuosity S_r	Bed Slope (<i>S</i>) Floodplain /Main channel	Range of β values	Range of Discharge (<i>Q</i> in lit/s)
1	Willets & Hardwick (1993)	W&H-1	Trapez.	2.86V:1H	8.63	1.2	0.001/0.000833	0.066-0.465	1.81-24.9
2	-do-	W&H -2	Trapez.	2.86V:1H	8.63	1.41	0.001/0.00071	0.100-0.484	1.73-22.09
3	-do-	W&H -3	Trapez.	2.86V:1H	8.63	2.06	0.0006/0.00029	0.075-0.522	0.81-13.39
4	Shiono et al.,(1999)	SAK-1	Rect.	1V:0H	8.0	1.092	0.001/0.00092	0.121-0.499	3.07-30.350
5	-do-	SAK-2	Rect.	1V:0H	7.89	1.372	0.001/0.00073	0.087-0.494	3.07-29.450
6	-do-	SAK-3	Rect.	1V:0H	8.0	1.572	0.001/0.000637	0.121-0.474	2.64-24.835
7	-do-	SAK-4	Trapez.	1.14V:1H	7.27	1.372	0.0005/0.000364	0.128-0.645	2.124-32.755
8	-do-	SAK-5	Trapez.	1.14V:1H	7.27	1.372	0.001/0.000729	0.142-0.593	3.14-32.445
9	-do-	SAK-6	Trapez.	1.14V:1H	7.27	1.372	0.002/0.00146	0.061-0.503	3.14-27.47
10	-do-	SAK-7	Rect.	1V:0H	7.89	1.372	0.002/0.00146	0.139-0.434	2.571-20.493

Sl. no.	Authors / Research projects	Series Name	Main channel type	Main channel side slope (<i>s</i>)	$A = B/b$	Sinuosity S_r	Bed Slope (<i>S</i>) Floodplain /Main channel	Range of β values	Range of Discharge (<i>Q</i> in lit/s)
11	Shiono et al.,(1999)	SAK-8	Rect.	1V:0H	8.0	1.092	0.002/0.00183	0.077-0.433	2.31-27.976
11	Present experimental data	NITR	Trapez.	1V:1H	11.97	1.11	0.0011/0.00099	0.194-0.409	17.07-93.667
12	Sellin et al.,(1993)*	FCF-B	Trapez.	1V:1H	11.11	1.374	0.000996/0.000725	0.0565-0.400	117.355-1000
13	US Army, V'bg (1956)	USArmy-1	Trapez.	2V:1H	30	1.50	0.001/0.000667	0.167-0.375	103.639-440.327
14	-do-	USArmy-2	Trapez.	2V:1H	30	1.75	0.001/0.000571	0.167-0.375	96.277-419.655
15	-do-	USArmy-3	Trapez.	2V:1H	16	1.255	0.001/0.000797	0.167-0.375	60.314-250.604
16	-do-	USArmy-4	Trapez.	2V:1H	30	1.22	0.001/0.00082	0.167-0.375	91.180-438.911
17	-do-	USArmy-5	Trapez.	2V:1H	30	1.33	0.001/0.000752	0.167-0.375	87.782-433.247



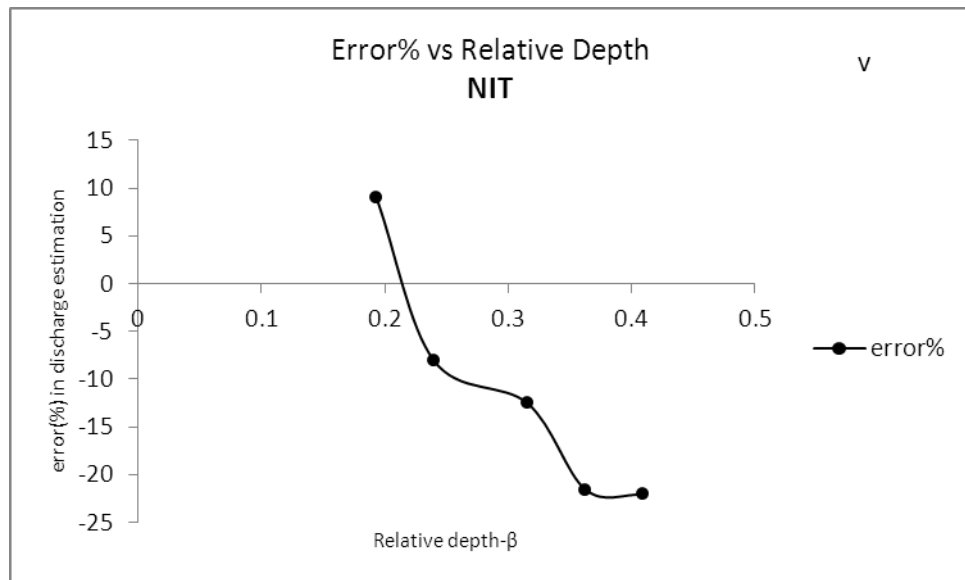
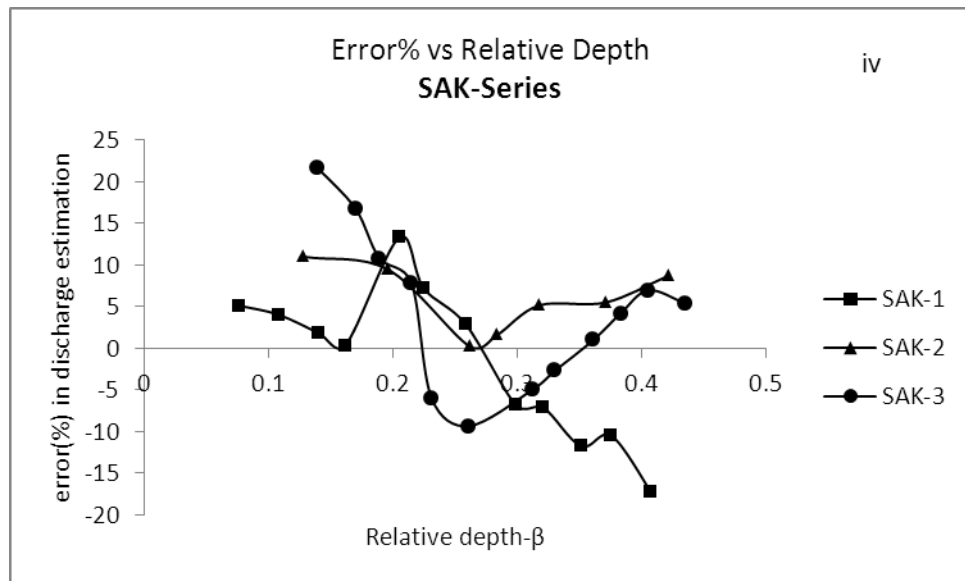


Fig-6.32 (i-v): Error (%) in discharge Estimation for different Data Series for meandering compound channels.

The flow in meandering compound channel is a very complex phenomenon involving a lots of mechanisms as outlined before in section 6.4.1 such as (a) The presence of a horizontal shear layer near the bankfull level in the crossover region (b) Bulk exchange of fluid taking place between the floodplain and main channel and making the flow highly 3-dimensional due to such mixing (c) As a result of the momentum exchange with floodplain flow in the crossover region, the channel flow enters the bend with a secondary circulation counter to that which is induced by the bend flow, and decays rapidly after each bend apex and (d) Water from the upstream floodplain plunging

vigorously into the channel at the channel centerline producing strong secondary cells. These of course render the task of finding a predictive model for discharge estimation in compound meandering channel cases a virtually impossible one. Against such a backdrop the performance of the model in the varieties of the cases considered can be stated satisfactory.

Fig.6.33 shows the scatter diagram for predicted and actual discharge for river Baitarani. It shows that the model has good potential of being used even in real life cases albeit with more refinement. For the use of the model in case of river Baitarani the appropriate variant of the shear force model for non-homogeneous compound channel i.e. in line with the modification suggested by Knight & Hamed (1984) is used in place of normal model developed in equation (6.29) and (6.30). The fact that the model is very best suited for meandering compound channels from two most scientifically controlled large scale extensive research projects; one each from USA (US Army series,1956) and UK(FCF-B, Sellin,1993) holds much promise for further research and refinement of the model.

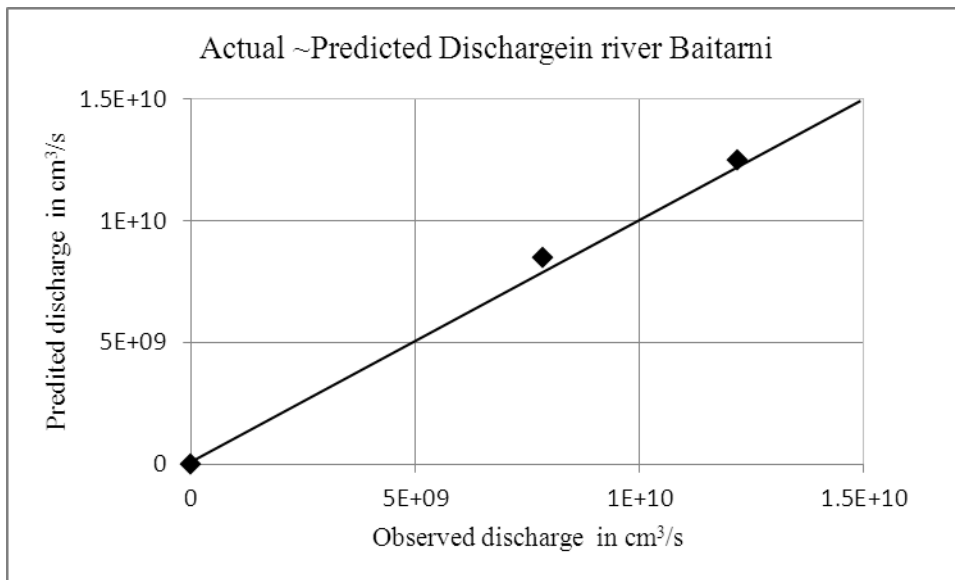


Fig-6.33: Scatter plot of predicted and actual discharge for river Baitarani (Patra&Kar, 2000)

CONCLUSIONS AND SCOPE FOR FUTURE WORK

7.1 CONCLUSIONS

The results of new experiments conducted in rigid straight and meandering compound channels with wide floodplains (having width ratio, $\alpha \approx 12$) have been reported in this thesis. The tests have been conducted under quasi uniform and subcritical flow conditions. Both the channels are of same main channel dimensions and same floodplain width. The straight compound channel has a trapezoidal main channel flanked by symmetric floodplains on either side while the meandering compound channel has its main channel aligned with a sine generated curve having cross over angle of 40° and sinuosity of 1.11. The primary or longitudinal velocity and depth averaged velocity along the mean valley direction at the test reaches for both the channels have been measured under a number of in bank and overbank flow conditions. The isovels drawn with the measured longitudinal velocity have been analysed. Point boundary shear stress along the wetted perimeter of both the channels has been measured and has been integrated over the respective subsections of the compound flow section to give sub sectional shear force percentages for both the channels. A 1D model (CES) and a 2D hydrodynamic model (CCHE2D) have also been applied to the new flume experiments as well as to a no. of cases reported in literature. On the basis of the analysis and results obtained the major conclusions can be enumerated as below:

- * New models for α & β relating with the relative depth of flow are developed for both straight and meandering compound channels. High values of coefficient of determination seem to suggest that the relative depth or depth ratio is a strong determinant for the velocity distribution coefficients. The models are also validated with data sets of present channels and those from flume experiments of previous researchers.
- * The depth averaged velocity distribution curves in overbank flow cases for straight compound channels also show the effect of momentum transfer between main channel flow and floodplain flow. The momentum transfer is more intense

at lower depth ratio values as compared to the higher ones. The phenomenon has lesser impact at higher flow as revealed from the velocity distribution curves. The depth averaged velocity distribution in meandering channel overbank cases reveals a similar trend as in straight channel overbank flow conditions except that the maximum depth averaged velocity magnitude is always observed over the inner side of the bend apex.

- * The 1D software package ‘Conveyance Estimation System’ is capable of predicting various flow features such as depth averaged velocity and boundary shear distribution across the flow cross sections of the present wide straight compound channel, large scale widest FCF A series channel and also of a natural river. However in case of the simulation studies conducted for present wide meandering compound channel, it is observed that the CES package under predicted the observed values in most cases.
- * The 2D hydrodynamic numerical tool ‘CCHE2D’ is applied to a number of wide compound channel cases such as both the present wide compound channels; the widest FCF A series channel and a natural river case for numerical validation studies. On basis of the results obtained, it is observed that ‘CCHE2D’ is quite capable in revealing important flow features like lateral distribution of depth averaged velocity and boundary shear stress across the whole compound section in such complex flow domains.
- * A new mathematical equation for sub sectional shear force percentage relating to the sub sectional flow area is obtained by conducting a regression analysis for floodplain shear force values of a large number data points from flume experiments including the large scale EPSRC-FCF A series channels, and small scale experiments of previous researchers. The equation seems to be well suited for compound channels having width ratio up to 6.67. Based on the above shear force model a new stage discharge model (MDCM) is then suggested for straight and smooth compound channels having width ratios up to 6.67. The model when tested for different experimental data sets and for real river data sets gives best predictions among a host of previous models of past researchers.
- * The measured boundary shear stress for the straight compound channel overbank cases is integrated over the wetted perimeter to obtain the subsection shear force per unit length in stream wise direction carried by different sub

sections of the compound channel flow section. The present shear force data then in combination with the shear data of the widest FCF A series channel is subjected to a further regression technique to give a second shear force model relating the shear force percentage carried by the floodplain with the percentage area occupied by the floodplains. The model shows that a nonlinear relationship exists between the two. The model is suggested for straight compound channels with α value lying between 6.67 and 12. Using the developed boundary shear model and applying the method employed in MDCM the stage discharge prediction method is extended (Extended Modified Divided Channel Method) to wider compound channel having width ratio in the range of ($6.67 < \alpha < 12$).

- * For devising a general method to predict stage discharge in straight compound channels having width ratios in all practical ranges, a new method based on zonal variation of Darcy's friction factor is suggested. The method is also able to predict zonal distribution of flow in straight compound channels. This approach is then tested over various small scale, large scale as well as some natural data sets reported in literature for prediction of both total flow and flow distribution in straight compound channels. The author's method is compared with some well known methods of past researchers to analyze their applicability with respect to a number of data sets as available in literature. From error analysis it is found out that the author's method is the best among all the competing models.
- * The boundary shear stress measured across the wetted perimeter of the present wide meandering compound channel for different flow depths reveal that the highest magnitude of resistance to the flow always occurs at the inner side of the bend. The total shear force carried by the floodplain lying on the concave side is always the largest among the sub section shear force values.
- * By regression analysis the mathematical models are developed relating the percentage shear force carried by respective zones with percentage area occupied by them in the total flow section for different flow zones in meandering compound channels.
- * A new model is also developed for stage discharge estimation in meandering compound channels. The model is then validated with a number of large scale experimental data sets comprising FCF Series B and US Army, Vicksburg,

Mississippi; small scale data sets of other researchers and the present wide compound channel. The model is also tested with available data of a natural river. Good agreement between the predicted and observed flow is observed in all the above cases.

7.2 SCOPE FOR FUTURE RESEARCH WORK

The present work leaves much room for further studies in the straight and meandering compound channels. Many aspects other than what has been incorporated in this thesis but could not be investigated due to the constraints of various natures may be pursued to widen our knowledge in compound channel research. Some suggestions in this regard may be as listed below:

- The work done in straight compound channels can be extended to compound channels with wide un-symmetrical floodplains.
- The equations developed may be improved by incorporating more data from channels of different geometries and sinuosity.
- Further investigation is required to study the flow properties and develop models for channels with different roughness in the sub-sections.
- The channels here are rigid. Further investigation for the flow processes may also be carried out for channels with mobile bed.
- The numerical simulations using standard software or using codes may be extended (3-D and other software) along with the experimental findings to enhance the understanding of the flow processes in compound channels for both straight and meandering reaches.
- The turbulence and flow structures in channels with such geometric and hydraulic conditions can be studied.

REFERENCES

1. Ackers, P. (1992). "Hydraulic Design of Two Stage Channels." *Proc. Inst. Civ. Eng., Waters. Maritime and Energy*, December, Paper No. 9988, 247-257.
2. Ackers, P. (1993a). "Stage-Discharge Functions for Two-Stage Channels." *The Impact of New Research*, *J. Inst. Water & Environmental Management*, 7(1), 52-61.
3. Ackers, P. (1993b). "Flow Formulae for Straight Two-Stage Channels", *J. Hydraul. Res.*, IAHR, 31 (4), 509-531.
4. Al-Khatib, I. A. and Gogus, M. (1999). "Momentum and Kinetic Energy Coefficients in Symmetrical Rectangular Compound Cross Section Flumes." *Tr. J. of Engineering and Environmental Science*, 23 (1999), 187- 197.
5. Al Amin, A., Khan, S. M. and Islam, A. (2013). "An Experimental Study of Shear Stress Distribution in a Compound Meandering Channel." *American Journal of Civil Engineering*, Science PG, 1(1), 1-5.
6. Anderson, Jr, J. D. (1995). "Computational Fluid Dynamics; The Basics with applications." McGraw- Hill Inc., New York, N.Y.
7. Atabay, S. A. and Knight, D.W., (2002). "The influence of floodplain width on the stage-discharge relationship for compound channels", *River Flow 2002, Proc. Int. Conf. on Fluvial Hydraulics*, Louvain-la-Neuve, Belgium, Sept., Vol. 1, 197-204.
8. Beaman, F. (2010). "Large Eddy Simulation of Open Channel Flows For Conveyance Estimation". Thesis submitted to the University of Nottingham for the degree of Doctor of Philosophy.
9. Bhowmik, N. G., and Demissie, M., "Carrying Capacity of Flood Plains," *J. Hydraul. Eng.*, ASCE, 108, No. HY3, Paper 16924, pp. 443-452.
10. Blalock, M. A., Sturm T. W. (1981). "Minimum specific energy in compound open channel." *J. Hydraul. Div.*, ASCE, 107, 699-717.
11. Bousmar, D. and Zech, Y. (1999). "Momentum transfer for practical flow computation in compound channels." *J. Hydraul. Eng.*, ASCE, 125(7), 696-706.
12. Boussinesq, J. (1877). "On the theory of flowing waters". *Mémoires & Œuvres de J. Boussinesq*, par divers savants de l'Académie des Sciences, Paris.

13. Cassels, J. B. C., Lambert, M. F., Myers, W. R. C. (2001). "Discharge Prediction in Straight Mobile Bed Compound Channels." *Proc. Inst. Civ. Eng., Waters. Maritime and Energy*, 148(3), 177–188.
14. Chang, H. H. (1983). "Energy Expenditure in Curved Open Channels." *J. Hydraul. Eng.*, ASCE, 109 (7), 1012-1022.
15. Chaudhry, M. H. (2008). "Open-Channel Flow" 2nd Edition, Springer, New York, USA.
16. Christodoulou, G. C. (1992). "Apparent Shear Stress in Smooth Compound Channels." *Water Res. Management*, 6(3), 235–247.
17. Chow, V. T. (1959). *Open-Channel Hydraulics*, McGraw-Hill Book Co. Inc., New York, N.Y.
18. Conveyance Estimation System v2.0 (2007) Wallingford Software, HR Wallingford OX10 8BAUK. <http://www.river-conveyance.net/download.asp>.
19. Coriolis, G. (1836). "On the backwater-curve equation and the corrections to be introduced to account for the difference of the velocities at different points on the same cross section." vol. 11, ser. 1, 314-335.
20. Cunge, J., Holly, F. and Verwey, A. (1980). "Practical Aspects of Computational River Hydraulics." Boston: Pitman.
21. da Silva, A.M.F. (1999) "Friction factor of meandering flows." *J. Hydraul. Eng.*, ASCE, 125 (7), 779-783.
22. da Silva, A. M. F., El-Tahawy, T., and Tape, W. D. (2006). "Variation of Flow Pattern with Sinuosity in Sine-Generated Meandering Streams." *J. Hydraul. Eng.*, 132 (10), 1003-1014.
23. DEFRA/EA, 2003a. Reducing Uncertainty in River Flood Conveyance, Interim Report2: Review of Methods for Estimating Conveyance, Project W5A- 057, HR Wallingford Ltd., United Kingdom.
24. DEFRA/EA, 2003b. Reducing Uncertainty in River Flood Conveyance, Roughness Review, Project W5A- 057, HR Wallingford Ltd., United Kingdom.
25. DEFRA/EA, 2004/5. Reducing Uncertainty in River Flood Conveyance, Interim Report3: Testing of Conveyance Methods in 1D River Models, Project W5A- 057, HR Wallingford Ltd., United Kingdom.
26. De Marchis M. and Napoli, E. (2008). "The effect of geometrical parameters on the discharge capacity of meandering compound channels". *Advances in Water Resources*, 31(12), 1662-1673.

27. Duan, J. G. (2004). "Simulation of Flow and Mass Dispersion in Meandering Channels." *J. Hydraul. Eng.*, ASCE, 130 (10), 964–976.
28. Ervine, D. A. and Ellis, J. (1987). "Experimental and Computational Aspects of Overbank Flood-Plain Flow." *Trans. Royl. Society Edinburgh, Series A*, Vol. 78, 315-325.
29. Ervine, D. A., Koopaei K. B. and Sellin R. H. J. (2000). "Two Dimensional Solution for Straight and Meandering Over-bank Flows." *J. Hydraul. Eng.*, ASCE, 126 (9), 653-669.
30. Ervine, D. A., Willetts, B. B., Sellin, R. H. J. and Lorena, M. (1993). "Factors Affecting Conveyance in Meandering Compound Flows." *J. Hydraul. Eng.*, ASCE, 119 (12), 383-1399.
31. French, R. H. (1987). *Open-Channel Hydraulics*. McGraw-Hill, Singapore. 2nd edition.
32. Ghosh, S. N. and Jena, S. B. (1971). "Boundary Shear Distribution in Open Channel Compound." *Proc. Inst. Civ. Eng.*, London, 49, 417-430.
33. Greenhill, R. K. and Sellin, R. H. J. (1993). "Development of a Simple Method to Predict Discharge in Compound Meandering Channels." *Proc. Inst. Civ. Eng., Water, Maritime and Energy*, 101, 37-44.
34. Ghosh, S. N. and Kar, S. K. (1975). "River Flood Plain Interaction and Distribution of Boundary Shear in a Meander Channel with Flood Plain." *Proc. of the Inst. of Civil Engineers*, London, Vol.59, Part 2, December.
35. Gyr, A. (2010). "The Meander Paradox—A Topological View." *Appl. Mech. Rev.*, 63(2):
36. Hannan, J. M. and Kandasamy, J. (2009). "Experience of 1D and 2D flood modelling in Australia - A guide to model selection based on channel and floodplain characteristics." Ch.33, *Flood Risk Management: Research and Practice*, Taylor and Francis group, CRC Press, London, 55-79.
37. HECRAS, 1998. *River Analysis System: Hydraulic Reference Manual Version 2.2*, U.S. Army Corps. of Engineers, Hydrologic Engineering Center, Davis.
38. Hin, I. S., Bessaih, N. *et. al.* (2008). "A study of hydraulic characteristics for flow in equatorial rivers." *Interl. J. River Basin Management*, IAHR, 6 (3), 213–223.

- 39.Huthoff, F., Roos, P. C., Augustijn, D. C. M. and Hulscher, S. J. M. H. (2008). "Interacting divided channel method for compound channel flow." *J. Hydraul. Eng.*, ASCE, 134(8), 1158–1165.
- 40.ISIS V2.0, 2001, Online Help Manual, Copyright HR Wallingford Ltd. / Halcrow.
- 41.James C. S. (1994). "Evaluation of Methods for Predicting Bend Loss in Meandering Channels." *J. Hydraul. Eng.*, ASCE, 120 (2).
- 42.James, C. S. and Wark, J. B. (1992). "Conveyance Estimation for Meandering Channels." Rep. SR 329, HR Wallingford, Wallingford, U.K. Dec.
- 43.Jing, H., Guo, Y., Li, C. and Zhang, J. (2009), "Three-dimensional numerical simulation of compound meandering open channel flow by the Reynolds stress model." *Int. J. Numer. Meth. Fluids*, 59, 927–943.
- 44.Johannesson, H. and Parker, G. (1989). "Velocity Distribution in Meandering Rivers." *J. Hydraul. Eng.*, ASCE, 115 (8), 1019-1039.
- 45.Kejun, Yang, Shuyou, Cao., Xingnian, Liu. (2007). "Flow Resistance and Its Prediction Methods in Compound Channels." Springer journal-Verlag.
- 46.Khatua,K.K,(2008) "Interaction of flow and estimation of discharge in two stage meandering compound channels", Thesis Presented to the National Institute of Technology, Rourkela, in partial fulfillments of the requirements for the Degree of Doctor of Philosophy
- 47.Khatua, K.K., Patra, K.C. (2007). "Boundary Shear Stress Distribution in Compound Open Channel Flow." *J. Hydraul. Eng.*, ISH, 12 (3), 39-55.
- 48.Khatua K.K, Patra K C, Mohanty, P.K. (2012). "Stage Discharge Prediction for Straight and Smooth Compound Channels with Wide Floodplains" *J. Hydraul. Eng.*, ASCE, 138 (1), 93-99.
- 49.Khatua, K.K.,Patra K.C. and Nayak,P. and Sahoo,N.(2013).“Stage-Discharge Prediction for Meandering Channels.” *International Journal of Computational Methods and Experimental Measurements*, Wit press Journal, UK, 1(1), 80–92.
- 50.Khatua, K.K., Patra, K.C. and Jha, R. (2010). "Apparent shear stress in compound channels." *J. Hydraul. Res.*, (ISH), 16 (3), 1-14, Special issue, Taylor & Francis, Dec.
- 51.Kiely, G. (1990). "Overbank Flow in Meandering Channels the Important Mechanisms." *Proceedings of the Institution Conference on River Flood Hydraulics*, W. R. White, ed., Wiley, Chichester, U.K., pp. 207–217.

52. Knight D. W. (1989). "River channels and floodplains." Final Report for Severn Trent Water Authority, Severn-Trent Water Authority, April, 1-100.
53. Knight D. W. (2005). "River flood hydraulics: theoretical issues and stage discharge relationships." River basin modelling for flood risk mitigation. Knight & Shamseldin [ed.], pp.301-334. Taylor & Francis/Balkema: The Netherlands, 616.
54. Knight D. W. and Demetriou J.D. (1983). "Floodplain and main channel flow interaction." *J. Hydraul. Eng.*, ASCE, 109(8), 1073–92.
55. Knight, D. W. and Hamed, M. E. (1984). "Boundary Shear in Symmetrical Compound Channels." *J. Hydraul. Eng.*, ASCE, Vol.110, Paper 19217, pp.1412-1430.
56. Knight, D.W., Al-Hamid, A. A. I. and Yuen, K. W. H. (1992). "Boundary shear in differentially roughened trapezoidal channels, In Hydraulic and Environmental Modelling: Estuarine and River Waters." (Eds R.A. Falconer, K. Shiono & R.G.S. Matthew), Ashgate Press, 3-14.
57. Knight, D.W., McGahey, C., Lamb, R. and Samuels, P.G. (2010). *Practical Channel Hydraulics*, Taylor and Francis Group, London, UK.
58. Knight, D.W. and Shamseldin, A. Y. (2005). "River basin modelling for flood risk mitigation." edited. Taylor & Francis/Balkema: The Netherlands, 616.
59. Knight, D. W., Yuan, Y. M. and Fares, Y. R. (1992). "Boundary shear in meandering channels." *Proceedings of the Institution Symposium on Hydraulic research in nature and laboratory*, Wuhan, China, Sept., Paper No.11017, Vol. 118, 151-159.
60. Kolupaila, S. (1956). "Methods of determination of the kinetic energy factor." *The Port Engnr*, Calcutta, India 5, 12-18.
61. Lambert, M. F. and Myers, W. R. (1998). "Estimating the Discharge Capacity in Straight Compound Channels." *Proc. Inst. Civ. Eng., Waters, Maritime and Energy*, 130, 84-94.
62. Langbein, W. B. and Leopold, L. B. (1966). "River meanders—Theory of minimum variance." U.S. Geological Survey, Paper, 422-H, 1–15.
63. Mc Keogh, E.J. and Kiley, G.K. (1989). "Experimental Study of Mechanism of Flood Flow in Meandering Channels." *Proceeding of 23rd IAHR congress*, IAHR, Ottawa, Canada, Vol. B, 491-498.

64. Me'tivier, F. and Gaudemer, Y. (1999). "Stability of output fluxes of large rivers in South and East Asia during the last 2 million years: implications on floodplain processes." *Basin Research*, 11, 293–303. © 1999 Blackwell Science Ltd.
65. MIKE11 V3.11, 1995, General Reference Manual, 1st-edition, Danish Hydraulic-Institute.
66. Moncho Esteve, I., Palau Salvador, G, Shiono, K, Muto, Y. (2010). "Turbulent structures in the flow through compound meandering channels." *Proceedings of Riverflow*, 1543-1550.
67. Moreta, P. J. M. & Martin-Vide, J. P. (2010). "Apparent friction coefficient in straight compound channels." *J. Hydraul. Res.*, IAHR, 48 (2), 169-177.
68. Morvan, H., Pender G., Wright N. G. and Ervine, D. A. (2003). "Three-Dimensional Hydrodynamics of Meandering Compound Channels." *Journal of hydrologic engineering* © asce / march/april 2003 / 99.
69. Myers, W.R.C. (1987). "Velocity and Discharge in Compound Channels." *J. Hydraul. Eng.*, ASCE, 113(6), 753-766.
70. Myers, W.R.C. and Brennan, E. K. (1990). "Flow resistance in compound channels." *J. Hydraul. Res.*, IAHR, 28(2), 157-155.
71. Myers, W. R. C. and Elsayy (1975). "Boundary Shear in Channel with Floodplain." *J. Hydraul. Eng.*, ASCE, 101(HY7), 933-946.
72. Myer, W. R. C. and Lyness, J. F. (1997). "Discharge Ratios in Smooth and Rough Compound Channels." *J. Hydraul. Eng.*, ASCE, 123 (3), 182-188.
73. Myer, W. R. C., Lyness, J. F. and Cassells, J. (2001). "Influence of Boundary Roughness on Velocity and Discharge in Compound River Channels," *J. Hydraul. Eng.*, ASCE, 39 (3).
74. Nalder, G. (1997). "Aspects of Flow in Meandering Channels." *Transactions of the Institution of Professional Engineers New Zealand: General Section*, 24 (1), 41-47.
75. Ozbek , T. and Cebe ,K. (2003). "Comparison of Methods for Predicting Discharge in Straight Compound Channels Using the Apparent Shear Stress Concepts." *Tr. Journal of Engineering and Environmental Science*, Tubitak, 101-109.
76. Pang, B. (1998). "River Flood Flow and its Energy Loss." *J. Hydraul. Eng.*, ASCE, 124 (2), 228-231.

77. Patel, V. C. (1965). "Calibration of the Preston tube and limitations on its use in pressure gradients." *Journal of Fluid Mech.*, Cambridge University Press, 23, 185-208
78. Patra, K. C. (2013). "Discharge assessment in meandering and straight compound channels." *J. Hydraul. Eng.*, ASCE, 139(2), 121-136.
79. Patra, K. C., Kar, S. K. (2000). "Flow interaction of Meandering River with Flood plains." *J. Hydraul. Eng.*, ASCE, 126(8), 593-603.
80. Patra, K. C., Kar, S. K. and Bhattacharya. A. K. (2004). "Flow and Velocity Distribution in Meandering Compound Channels." *J. Hydraul. Eng.*, ASCE, 130(5), 398-411.
81. Prinos, P. and Townsend, R. D. (1984). "Comparison of Methods of Predicting Discharge in Compound Open Channels." *Advances in Water Res.*, 7(12), 180–187.
82. Project Completion Report (Technical) (2010). Pilot and Demonstration Activity for Bangladesh: Field-Based Research on the Impacts of Climate Change on Bangladesh Rivers. Asian Development Bank.
83. Proust. S., Rivière. N., Bousmar. D., Paquier. A., Zech, Y. and Morel. R. (2006). "Flow in Compound Channel with Abrupt Floodplain Contraction." *J. Hydraul. Eng.*, ASCE, Vol. 132, No. 9, September 1.
84. Project Record W5A-057(2001-04). "Reducing Uncertainty in River Flood Conveyance, Conveyance Manual, Defra / Environment Agency Flood and Coastal Defence R&D Programme. HR Wallingford Ltd, Howbery Park, Wallingford, Oxon OX10 8BA.
85. Rajaratnam, N. and Ahmadi, R.M. (1979). "Interaction between Main Channel and Flood Plain Flows." *J. Hydraul. Div.*, ASCE, 105 (HY5), 573-588.
86. Rantz, S. E., and others. (1982). "Measurement and computation of channel flow." Water Supply Paper No. 2175. Vol. 1 and Vol. 5 of US Geological Survey, Washington D.C.
87. Rodi, W. (1979). "Turbulence Models and Their Application in Hydraulics," IAHR, State of Art Paper, IAHR section on Fundamental of Division II: experimental and mathematical fluid dynamics.
88. Samuels P. G. (1989). "Some Analytical Aspects of Depth Averaged Flow Models." *Intl. Conf. Hydraulic and Environmental Modelling of Coastal, Estuarine and River Water*, Bradford, England, Sept., 19-21.

- 89.Scoping Study, 2001, Scoping Study for Reducing Uncertainty in River Flood Conveyance, R&D Technical Report to DEFRA/Environment Agency, HR Wallingford Ltd. (Prepared by EP Evans, G Pender, PG Samuels, M Escarameia)
- 90.Seckin, G., Ardiclioglu, M., Seckin, N., Atabay, S. (2004). "An Experimental Investigation of Kinetic Energy and Momentum Correction Coefficients in Compound Channels." *Tech. J. Turk. Chamber Civil Engrs*, 15(4), 3323-3334.
- 91.Seckin, G., Ardiclioglu, M., Cagatay, H., Cobaner,M. and Yurtal, R.(2009). "Experimental investigation of kinetic energy and momentum correction coefficients in open channels." *Scientific Research and Essay*, 4 (5), 473-478.
- 92.Sellin, R. H. J. (1964). "A Laboratory Investigation into the Interaction between the Flow in the Channel of a River and that over its Floodplain." *Houllie Blanche*, Grenoble 7, p. 793-802.
- 93.Sellin, R. H. J., Ervine, D. A. and Willetts B. B. (1993). "Behavior of Meandering Two stage Channels." *Proc. Inst. Civ. Eng., Water, Maritime and Energy*, 101 (10106), 99-111.
- 94.Sin, K. S. (2010). "Methodology for Calculating Shear Stress In A Meandering Channel." MS Thesis submitted to Colorado State University Fort Collins, Colorado.
- 95.Shiono, K., Knight, D. W. (1988). "Refined Modelling and Turbulance Measurements." *Proceedings of 3rd International Symposium*, IAHR, Tokyo, Japan, July, 26-28.
- 96.Shiono, K. and Knight, D.W. (1990). "Turbulence measurements by LDA in complex open channel flows." *Proc. 5th Int. Symp. on Applications of Laser Techniques to Fluid Mechanics*, Lisbon, Portugal, July, Paper 3.5, 1-6.
- 97.Shiono, K., Muto, Y. (1998). "Complex flow mechanisms in compound meandering channels with overbank flow." *J. Fluid Mech.*, Cambridge University Press.UK, 376, 22-261.
98. Shiono, K., Muto, Y., Knight, D. W. and Hyde, A. F. L. (1999). "Energy Losses due to Secondary Flow and Turbulence in Meandering Channels with Overbank Flow." *J. Hydraul. Res.*, IAHR, 37 (5), 641-664.
- 99.Shiono, K. and Knight, D. W. (1991). "Turbulent open channel flows with variable depth across the channel." *J. Fluid Mech.*, 222, 617-46.

100. Shiono, K., Al-Romaih, J.S. and Knight, D.W. (1999). "Stage-Discharge Assessment in Compound Meandering Channels." *J. Hydraul. Eng.*, ASCE, 125(1), 66-77.
101. Soil Conservation Service (SCS). (1963). "Guide for selecting roughness coefficient 'n' values for channels." Washington, DC: USDA Soil Conservation Services.
102. Stephenson, D. and Kolovopoulos, P. (1990). "Effects of Momentum Transfer in Compound Channels." *J. Hydraul. Eng.*, ASCE, 116 (HY12), Paper No.25343, 1512-1522.
103. Stoesser, T., Ruether, N. and Olsen, N. (2010). "Calculation of primary and secondary flow and boundary shear stresses in a meandering channel." *Advances in Water Resources*, Volume 33, Issue 2, 158-170, ISSN 0309-1708,
104. Tang, X. and Knight, D.W. (2008). "Lateral Depth-Averaged Velocity Distributions and Bed Shear in Rectangular Compound Channels." *J. Hydraul. Eng.*, ASCE. 134 (9), 1337-1342.
105. Terrier, B. (2010). "Flow Characteristics in Straight Compound Channels with Vegetation along the Main Channel." Ph.D. thesis, Loughborough Univ, UK.
106. Thonon, I., Middelkoop, H. and van der Perk, M. (2007). "The influence of floodplain morphology and river workson spatial patterns of overbank deposition." *Netherlands Jr. of Geosc-Geologie en Mijnbouw* | 86 – 1 | 63 - 75 |.
107. Toebe, G.H. and Sooky, A.A. (1967). "Hydraulics of Meandering Rivers with Floodplains." *Journal of the waterways and Harbor Division, Proceedings of ASCE*, ASCE, 93 (WW2), 213-236.
108. Tominaga, A., Knight, D. W. (2004). "Numerical Evaluation of Secondary Flow Effects on Lateral Momentum Transfer in Overbank Flows." *River Flow-2004*, Taylor and Francis Group, London.
109. US Army Corps of Engineers. (1956). "Hydraulic capacity of meandering channels in straight floodways. Waterways Experiments Station, Vicksburg, Mississippi, Mar, 1956, Technical Memorandum 2-429.
110. Van Rijn, L. C. (1989). "Handbook: sediment transport by current and waves." Report H 461, Delft Hydraulics, the Netherlands.

111. Van Prooijen, B. C., Battjes, J. A., Uijttewaal, W. S. J, (2005). "Momentum exchange in straight uniform compound channel flow." *J. Hydraul. Eng.*, ASCE, 131(3), 175–183.
112. Wark, J. B. and James, C. S. (1994). "An Application of New Procedure for Estimating Discharge in Meandering Overbank Flows to Field Data." *2nd Intl. Conf. on River Flood Hydraulics*, 22-25, March, Published by John Wiley & Sons Ltd., 405-414.
113. Weber, J. F. and Menéndez. (2004). "An Performance of lateral velocity distribution models for compound channel sections." *River Flow 2004, Proc., Int. Conf. on Fluvial Hydraulics*, Balkema, Rotterdam, The Netherlands, Vol. I, 449–457.
114. Willetts, B. B. and Hardwick, R. I. (1993). "Stage Dependency for Over Bank Flow in Meandering Channels." *Proc. Inst. Civ. Eng., Water, Maritime and Energy*, March, 101, paper No.10049, 45-54.
115. Wormleaton, P. R., Allen, J. and Hadjipanós, P. (1982). "Discharge Assessment in Compound Channel Flow." *J. Hydraul. Eng.*, ASCE, 108(HY9), 975-994.
116. Wormleaton, and Hadjipanós, P. (1985). "Flow Distribution in Compound Channels." *J. Hydraul. Eng.*, ASCE, 111 (7), 1099-1104.
117. Wormleaton, P. R., Allen, J., Hadjipanós, P. (1980). "Apparent Shear Stresses in Compound Channel Flow." *Symp. of River Engg.*, IAHR, Delft, The Netherlands.
118. Wu, W. and Wang, S. S. Y. (1999). "Movable bed roughness in alluvial rivers." *J. Hydraul. Eng.*, ASCE, 125(12), 1309–1312.
119. Yen, B. C. (2002). "Open Channel Flow Resistance." *J. Hydraul. Eng.*, ASCE, 128(1), 20-39.
120. Yen, C. L. and Overton, D. E. (1973). "Shape Effects on Resistance in Floodplain Channels." *J. Hydraul. Div.*, ASCE, 99(1), 219-238.
121. Zarrati, A. R., Tamai, N. and Jin, Y. C. (2005). "Mathematical Modeling of Meandering Channels with a Generalized Depth Averaged Model." *J. Hydraul. Eng.*, ASCE, 131(6), 467-475.
122. Zhang, Y. (2009). "CCHE-GUI – Graphical Users Interface for NCCH Model User's Manual." NCCH, University of Mississippi, US.
<http://www.ncche.olemiss.edu/download>.

123. Zheleznyakov, G. V. (1965). "Relative deficit of mean velocity of unstable river flow: Kinematic effect in river beds with floodplains." *Proc. 14th Congress of IAHR*, Paris, France, 5, 144-148.

APPENDIX

Table A- 1 Geometrical Properties and Surface Conditions of River Batu
(Hin et al.2008) and River Main (Myers and Lynness, 1990)

River Batu			River Main		
Av. bank full depth= 1.544m Top width of main channel= 5.15m Bed slope of main channel= 0.0016 Surface condition of main channel =Large boulder Bed slope of left and right Floodplains= 0.0013 Surface condition of floodplain = Long vegetation Surface condition of side bank= Erodeable soil			Av. bank full depth= 0.95m Top width of main channel= 14.0m Surface condition of main channel = Coarse gravel Bed slope = 0.0029 Surface condition of floodplain = Heavy weed growth & sand Surface condition of side bank= Rip-rap		
Observed discharge (m ³ /s)	α	β	Observed discharge (m ³ /s)	α	β
4.81	7.30	0.311	17.02	1.20	0.007
4.17	6.68	0.265	18.04	1.21	0.019
3.70	6.46	0.236	18.34	1.30	0.080
3.50	6.12	0.213	19.86	1.42	0.092
3.31	5.94	0.197	19.97	1.46	0.116
2.79	5.08	0.121	27.06	1.89	0.214
2.56	4.64	0.089	29.79	2.07	0.261
*****	*****	*****	35.88	2.31	0.313
*****	*****	*****	41.05	2.49	0.373
*****	*****	*****	44.19	2.50	0.403
*****	*****	*****	57.77	2.55	0.473



Fig.A-1 Morphological cross-section of River Batu (Hin et al.2008)



Fig.A-2 The river Main in county Antrim, Northern Ireland
(CES V2.0, Help manual, 2007)



Fig.A- 3 The River Sever at Montford Bridge site (a) looking upstream from the right bank, (b) looking downstream from the cableway and (c) the cable way at the bridge (CES V2.0, Help manual, 2007)

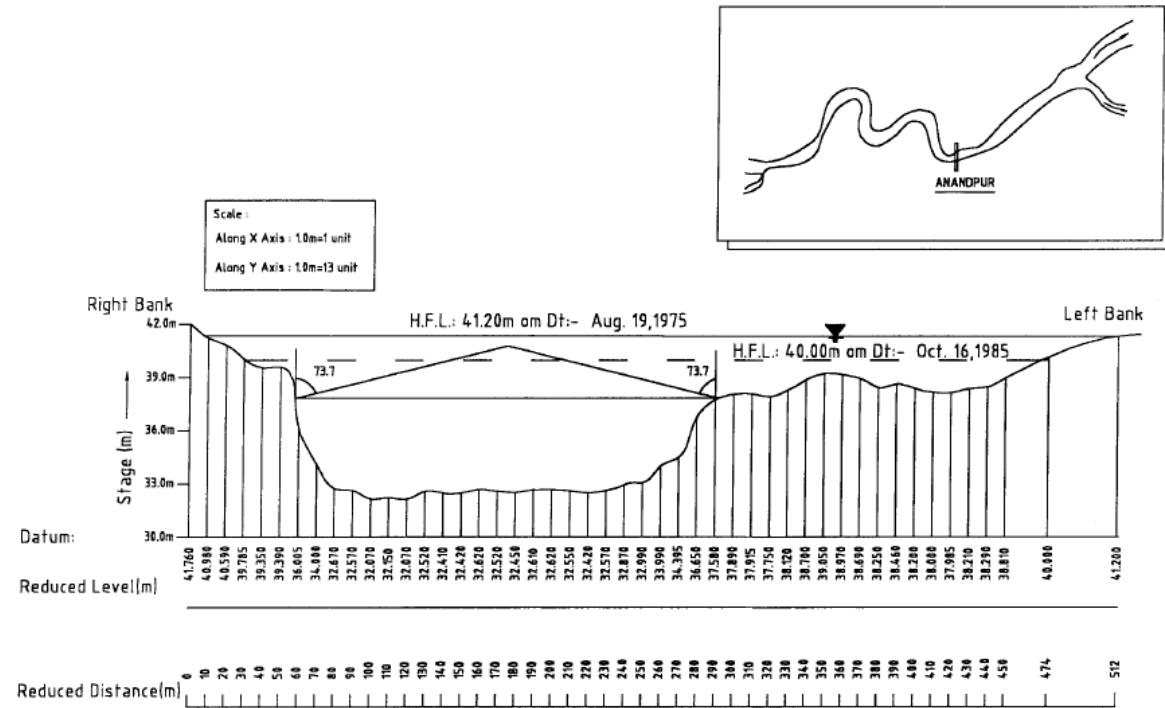


Fig. A- 4 Cross Section of River Baitarani at Anandapur Site, Orissa, India,
 Inset (Anandapur Site Showing Meandering Reach), Patra & Kar (2000)

Table A- 2 Geometrical and Surface condition details of river Baitarani
(Khatua et al.2013)

River Baitarani
<p>Av. Bank full Depth = 5.40m; Top width of main channel = 230m;</p> <p>Bed slope of main channel = 0.0011;</p> <p>Surface conditions of main channel = sandy surface;</p> <p>Bed slope of left and right floodplains = 0.0011</p> <p>Surface conditions of floodplain = grass vegetation;</p> <p>Surface conditions of side bank = Erodible soil</p>

PUBLICATIONS BASED ON PRESENT RESEARCH WORK

Journal Papers:

1. **Mohanty. P.K.**, and Khatua K.K. “Estimation of flow and its distribution in compound channels“. Journal of Hydrodynamics, Science Direct, Elsevier (in press 2013)
2. **Mohanty. P.K.**, Khatua K.K and Dash S. S. “Flow prediction in two stage wide compound Channels”, Journal of Hydraulic research, (ISH), Special issue , Taylor & Francis, (in press-2013)
3. **Mohanty. P.K.** and Dash., S.S. and Khatua K.K, (2013). "Flow Investigations in a Wide Meandering Compound Channel" International Journal of Hydraulic Engineering, Scientific & Academic Publishing, USA, issue1, vol 1, pp. 83-94, USA,
4. Saine S. Dash, K.K.Khatua, **P.K.Mohanty** (2013), “Factors influencing the prediction of resistance in a meandering channel”, International Journal of Scientific & Engineering Research ,Volume 4(5).
5. Khatua K.K, Patra K C, **Mohanty, P.K.**, Sahu., M. (2013). “Selection of interface for discharge prediction in a compound channel flow” International Journal of Sustainable Development and Planning, Wit press Journal, UK, Vol. 8(2), 214–230.
6. Khatua K.K, Patra K C, **Mohanty, P.K.**, (2012). “Stage Discharge Prediction for Straight and Smooth Compound Channels with Wide Floodplains” Journal of Hydraul Engg, ASCE, Vol. 138(1), pp 93-99.
7. Khatua K.K, Patra K C, and **Mohanty P K**,(2011).“Apparent Shear Stress and Boundary Shear Distribution in a Compound Channel Flow”, Computational Methods and Experimental Measurements, Volume XV, 2011, pp 215-228, Wessex Institute Press Trans., The New Forest, UK.
8. Khatua K.K, Patra K C, and **Mohanty P. K.** (2010). “Wall shear distribution in meandering channels.” *Institution of Engineers India (IEI), India.*

Conference Proceedings:

1. “Sinuosity dependencies in boundary shear distribution modeling for meandering compound channels”. Presented and published in Proceedings of ninth International Conference on Hydro-Science and Engineering by IAHR and IIT Madras, (ICHE 2010), 2 – 5, August 2010.
2. “Apparent shear stress and boundary shear stress distribution in compound channels of higher width ratio” Presented and published in Int. Conf. in Advances in Fluid Mechanics, September, 2010, AFM-2010, Portugal, Lisbon.
3. “Investigation on shear layer in compound channels”. Presented and published in Proceedings of National conference Hydro-2011, December, 2011, at VNIT, Surat, India.
4. “Energy and Momentum coefficients in a compound channel flow with wide floodplains” Presented and published in Int. Conf. in Advances in Fluid Mechanics, AFM-2012, 26 - 28 June, 2012. Split, Croatia.
5. “Flow prediction in two stage wide compound Channels.” Presented and published in Hydro-2012, December, at IIT Bombay.
6. “Evaluation of Roughness Coefficients for Open Channel Flow” Presented and published in International Conference Hydro-Vision, July 23-26, 2013, Colorado, USA.

Communicated For Publication in Journals:

- “Flow modeling in two stage compound meandering channels”-Manuscript is under review with J. Hydraul. of Engg. ASCE.
- “Prediction of velocity distribution coefficients in wide compound channels”. Paper being reviewed by WIT press journal.
- “Improved modeling of apparent shear stress ratio in two stage compound channels.” Paper being reviewed by Journal of Hydraulic research. IAHR.

BRIEF BIO-DATA OF THE AUTHOR

TITLE: **MOHANTY**
NAME: **PRABIR KUMAR**
DATE OF BIRTH: First January, 1968
Marital Status: Married

DETAILED ACADEMIC QUALIFICATIONS:

Sl. No.	Degree/ Certificate	Division/ Grade	Year	University/Board
1	HSC Exam.	First division	1983	Board of Secondary Education, Orissa
2	I. Sc.	First division	1985	Ravenshaw College, Cuttack. Utkal University
3	B.Sc.(Civil Engg.)	First division	1989	University College of Engineering (Now VSSUT, Burla), Burla, Orissa
4	M.Sc. (Engg.) (Hydraulics & Irrigation Engg.)	69% MARKS	1992	University College of Engineering (Now VSSUT, Burla), Burla, Orissa
5	MBA (HR& Finance)	First division	2008	Sambalpur University, Orissa, INDIA
6.	Doctorate (Ph.D.)	-----	Continuing- ---	National Institute of Technology, Rourkela, India

PROFESSIONAL CAREER:

Position	Durations
Field Engineer in a private company	One year(July1989-June1990)
Asst. Director(Stipendiary Engineer) with Deptt. Of Water Res. Govt. of Orissa.	15/03/1993-31/08/1995
Lecturer in Civil Engg. in E.T.E.& T. Department .Govt. of Odisha	Continuing since 01/09/1995
Research experience	7years
QUALIFICATION IN NET/GATE: Qualified in GATE (Graduate Aptitude Test in Engineering) 1990 with a Valid score and completed Master's programme with Scholarship.	

Permanent Address: **C/o Sri R.N.MOHANTY**

**Plot#994/2819, Samanatarapur,
Old Town, BHUBANESWAR,
District-KHURDA,
ODISHA, INDIA-751002**